



Università degli Studi di Padova

DIPARTIMENTO DI FISICA E ASTRONOMIA "GALILEO GALILEI"

Corso di Laurea Magistrale in Fisica

TESI DI LAUREA MAGISTRALE

Dark Matter in Supersymmetric theories

Relatore:

Prof. Paride Paradisi

Correlatore:

Dott. Eugenio Del Nobile

Candidato:

Valentino Ramponi

Contents

Introduction	5
1 Experimental evidences of Dark Matter	7
1.1 Experimental evidences at galactic scales	7
1.2 Evidences at galaxy cluster scale	9
1.3 Evidences at cosmological scale	10
1.4 Dark Matter characteristics	12
1.5 Dark matter candidates	12
2 Boltzmann equation and relic density	17
2.1 Boltzmann equation for the standard case	17
2.2 Thermally averaged cross-section	21
2.3 Co-annihilations	24
3 Supersymmetry and Dark Matter	29
3.1 Why Supersymmetry	29
3.2 Basics of SUSY	31
3.3 The Minimal Supersymmetric Standard Model	33
3.4 R -parity	36
3.5 DM in the MSSM	37
4 Dark Matter Phenomenology in the MSSM	43
4.1 Direct detection of DM	43
4.1.1 Elastic scattering cross-section in the MSSM	45
4.2 Pure Bino LSP	52
4.2.1 Pure Bino LSP with co-annihilations	56
4.3 Pure Higgsino LSP	58
4.4 Pure Wino LSP	65
4.5 Well-Tempering	69
4.6 Well-Tempered Bino/Higgsino	70
4.7 Well-Tempered Bino/Wino	77
Conclusions	85
A	87
A.1 Approximate solution for the Boltzmann equation	87
A.2 Non-relativistic approximate solution for the thermal average of σv	88
A.3 Thermal average of $\sigma_{\text{eff}} v$	91
B MSSM Feynman rules	95
C Matrix diagonalization	101

D	105
D.1 Velocity integral	105
D.2 Effective Lagrangian for neutralino-quark interaction	107
D.3 Non-relativistic expansion of scattering amplitudes	109
E	111
E.1 Kinematical quantities	111
E.2 Majorana fermions and Feynman rules	113
E.3 Pure Bino LSP annihilation cross-section	115
E.4 Pure Wino LSP annihilation and co-annihilation cross-sections	118
E.5 Pure Higgsino LSP annihilation and co-annihilation cross-sections	133

Introduction

There is today an overwhelming experimental evidence, on different astrophysical scales, that the Universe contains much more matter than what can be detected by electromagnetic interactions. This non-visible amount of matter is called Dark Matter (DM). During the last century many attempts were made to understand the nature of DM, which remains one of most important open issues in modern Physics. The identity of DM has important implications in many branches of Physics. For instance, in Astrophysics and Cosmology its nature has an impact on the evolution of the Universe and plays a fundamental role in structure formation. Furthermore, in Particle Physics DM can provide empirical evidence of the existence of a new particle.

In the course of the last century, many alternatives have been proposed as DM candidates. To date, some of these proposals have been nearly ruled out, such as the possibility that dark matter is due to compact objects formed by ordinary matter. Instead, other hypotheses have had a remarkable success in the past few years, such as the proposal that DM is made of a new kind of particle (or more than one) interacting with ordinary matter through unknown interactions. Within the various particle DM models, there are different mechanisms of DM production in the early Universe. One of the most successful mechanisms is thermal production, where the DM is assumed to be in thermal equilibrium with the primordial plasma until its co-moving density “freezes out” due to the expansion of the universe. In particular, with this mechanism, a particle with a mass at the electroweak scale and interactions with ordinary matter of comparable strength to the electroweak force, has a relic abundance in agreement with experiments. This is the so-called “WIMP miracle”, with WIMP standing for weakly-interacting massive particle.

The various DM candidates proposed by different theories are tested with a variety of experimental searches. For instance, i) direct searches try to detect DM particles while they are passing through the Earth, ii) indirect searches detect and analyse the putative products of DM annihilations in today’s Universe, and iii) collider searches look for signals of DM production in high-energy processes. There are many theoretical models featuring a particle DM candidate. Some of them were constructed specifically to address the DM problem, while in others the DM candidate is a natural prediction of the theory. Among the most compelling models of the latter type are supersymmetric theories. Supersymmetry –a symmetry which relates bosonic and fermionic degrees of freedom– provides one of the most famous solutions to the long-standing “hierarchy problem”, which is related to the presence of an elementary scalar in the Standard Model (SM), i.e. the Higgs boson. The most studied scenario is the minimal supersymmetric standard model (MSSM), the supersymmetric extension of the SM with the minimal particle content. In this model, each SM boson (fermion) has a fermionic (bosonic) counterpart with the same quantum numbers, called superpartner. A natural solution of the “hierarchy problem” would require these particles to lie below the TeV scale, which makes the Large Hadron Collider (LHC) the ideal place where to look for them. Therefore, the lack of evidence of any superpartner at the LHC challenges the capability of the MSSM to solve the “hierarchy problem”. Yet, the MSSM still provides a successful DM candidate.

The aim of this thesis is the analysis of supersymmetric DM candidates in the framework of the MSSM. We focus on the possibility that DM is made of neutralinos. These are a mixture of Bino, Wino and Higgsino which are the superpartners of the electrically and color neutral SM bosons. In particular we consider the scenario discussed by N. Arkani-Hamed, A. Delgado and G.F. Giudice in their work "The Well-Tempered Neutralino" [11]. At first we study three cases

where the DM candidate is a pure Bino, Wino or Higgsino. Then, we consider two other setups where the DM candidate is a mixture of Bino, Wino, and Higgsino with relative fractions tuned to reproduce the observed DM density. For this reason these DM candidates are referred to as “Well-Tempered” neutralino. We compute the relic abundance both numerically and, when it is possible, also analytically. This quantity is determined solving the Boltzmann equation, and strongly depends on the annihilation cross-section of the DM candidate. In our analysis, we also account for “co-annihilations”, in which case the standard methods to solve approximately the Boltzmann equation fail. This situation occurs when the DM candidate is the lightest state of a multiplet of nearly mass degenerate particles. In this case, the relic abundance is not determined only by the annihilation cross-section of the DM candidate, but also by the annihilation of heavier particles in this multiplet which, eventually, will decay into the lightest one.

We further constrain each scenario imposing the powerful constraints from the most recent direct detection experiments. In the MSSM, but also in many other models, the DM scattering cross-section with nucleons can be separated into spin-dependent (SD) and spin-independent (SI) contributions. Therefore, we compute the SD and SI neutralino-nucleon scattering cross-section both numerically and analytically, comparing the obtained results with the bounds provided by the LUX [7],[6], XENON100 [10], PANDAX [64] and PICO-60 [8] experiments. This analysis provides an update of the results presented in our reference work of N. Arkani-Hamed, A. Delgado and G.F. Giudice. In order to monitor the relative size of the SI and SD contributions, we consider them separately, as customarily done by the experimental collaborations. In the cases where these contributions are both important, we recast the experimental analyses to account for both interactions. We compare our analytical results with numerical computations performed with `micrOmegas` 4.2.5 [21], a code for the computation of quantities such as the DM relic density and its direct/indirect detection rates.

The thesis is organized as follows: in Chapter 1 we review the compelling evidences for DM on different astrophysical scales. Then, we summarize what is actually known about DM, listing its main features. Also, we briefly review the arguments in favour of the “WIMP miracle” and we list the most relevant particle DM candidates. In Chapter 2 we review the formalism of the Boltzmann equation, which governs the statistical behavior of thermodynamic systems. First, we present a solution for the classical case of two annihilating particles of the same mass, then, we solve the Boltzmann equation for the case of co-annihilations. In Chapter 3 we summarize the basic concepts of Supersymmetry, starting from the original motivations that led to its introduction, then we specialize to the R-parity conserving MSSM, providing its particle content and mass spectrum. In Chapter 4, after a brief review of the theory of direct detection, we analyse the phenomenology of the “Well-Tempered” neutralino scenario, discussing both the DM relic density and the constraints from direct detection experiments. At last, we summarize our conclusions and possible future prospects.

In the appendices some detailed calculations are collected. In particular, in appendix A we derive the relic density solving the Boltzmann equation both in the standard and in the co-annihilation cases. In appendix B we list some useful Feynman rules in the MSSM. In appendix C we provide an analytical diagonalization of the neutralino mass matrix which is valid in the Well-Tempered neutralino scenario. In appendix D we derive the effective interaction terms between neutralinos and quarks, giving also the non-relativistic expansion of the scattering amplitudes. In appendix E, after providing the conventions for Majorana fermions and some useful formulae, we perform approximate calculations of the relevant annihilation cross sections.

Chapter 1

Experimental evidences of Dark Matter

At the present time, the experimental evidences, show that the DM constitutes about the 25% of the total mass-energy content of the Universe, while the ordinary matter makes up only the 5%. The remaining 70% is due to Dark Energy (DE) [42].

Now we briefly analyse the various experimental evidences of DM, at different scales.

1.1 Experimental evidences at galactic scales

Galaxies can be regarded as the building blocks of the Universe. They have a mass range from about $10^9 M_\odot$ to about $10^{13} M_\odot$ ¹ [42].

They can be of three basic types: spiral, elliptical or irregular [29]. For what concern the spiral type, the most convincing evidence of DM, comes from the observation of the rotational curves of the galaxies. Roughly speaking these are graphs of circular velocities of stars and gases as function of the distance, R , from the barycenter of the galaxy. These circular velocities, $v_c(R)$, solely are measured in visible light or exploiting radio emission [19]. Following Newtonian mechanics we have that

$$v_c(R) = \sqrt{\frac{G_N M(R)}{R}}, \quad (1.1)$$

where, as usual $G_N = 6.6738 \times 10^{-11} \text{ N m}^2 \text{ kg}^{-2}$ [60] is the Newton gravitational constant, and for a system with spherical symmetry, $M(R)$ is define as

$$M(R) \equiv 4\pi \int_0^R \rho(r) r^2 dr, \quad (1.2)$$

where $\rho(r)$ is the mass density.

What we would expect if only ordinary matter is present, is that $v_c(R)$ first rises (due to the fact that when increasing the radius more mass is included) and then, when all visible mass ends, it decreases as

$$v_c(R) = \sqrt{\frac{G_N M_{\text{tot}}}{R}}. \quad (1.3)$$

However what we observe is a radically different pattern. After the expected initial rise, $v_c(R)$ does not fall as $1/\sqrt{R}$. In fact as we can see from Fig. 1.1 the rotational curve shows a quite flat behaviour ($v_c(R) \simeq \text{constant}$), which continues well beyond the visible edge of the galaxy disk.

Under the assumption of spherical mass distribution, we can invert the observed rotational curve to determine the mass density profile of the galaxy. Equating the Poisson's equation

¹ $M_\odot = 1.988 \times 10^{30} \text{ kg}$ is the solar mass, from Ref. [60].

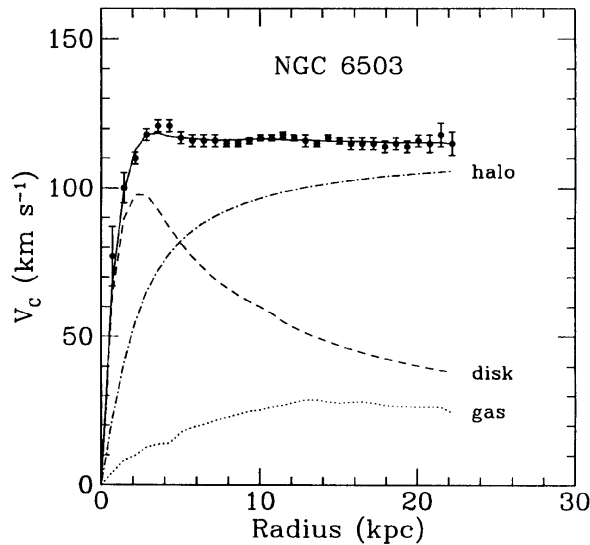


Figure 1.1: Galactic rotation curve for NGC 6503. In the figure are showed also the relative contributions respectively from visible disk, gases and DM halo. As we can see far from the center of the galaxy the DM contribution causes an unexpected flat behaviour (from Ref. [41]).

$\nabla^2\phi = 4\pi G_N\rho(R)$, where $\phi = -\frac{G_N M(R)}{r}$ is the gravitational potential, with the divergence of the centripetal acceleration, $a_c(r) = v_c(R)^2/R$, we can derive that [20]

$$4\pi G_N\rho(R) = 2\frac{v_c(R)}{R}\frac{\partial v_c(R)}{\partial R} + \left(\frac{v_c(R)}{R}\right)^2. \quad (1.4)$$

For a constant value of $v_c(R)$ Eq. (1.4) tell us that $\rho(R) \propto 1/R^2$ which, using Eq. (1.2), gives $M(R) \propto R$ [19]. This peculiar mass behaviour is a strong hint in favour to the existence of dark, i.e. non-visible, halo which encapsulates the entire visible disk of the galaxy. The most interesting objects in the study of rotational curves are the Low-Surface-Brightness (LSB) galaxies. These are probably DM dominated and hence the stellar population gives only a small contribution to the observed rotational curves [20]. From the observation of the rotational curves of several galaxies, the mass of the dark halo is thought to be between 3 to 10 times the mass of the luminous matter.

Elliptical and irregular galaxies have not an order orbital motion, thus the study of rotational curves becomes difficult [29]. To prove the existence of DM for this type of galaxies is possible to use the gravitational lensing. This method exploits a fundamental result of general relativity, which states that a gravitational field distorts the path travelled by the light. Thus the shapes of distant objects, such as stars or galaxies, are deformed by the presence of a foreground mass density [31]. For instance, measuring the entity of the distortion produced by an elliptical galaxy we are able to infer its mass density. Comparing this deduced mass density with the one obtained using the mean value of the mass-to-light ratio, $\langle M/L \rangle$, we can observe that the mass deduced using the gravitational lensing is more than the one derived using $\langle M/L \rangle$; this suggests the presence of an amount of non-visible mass, i.e. DM.

For what concern the problem of how DM is distributed into the galaxy, the observations lead to a general consensus about its distribution at large radii, which is quite a spherical halo that encapsulates the visible disk of the galaxy [42]. However there is still a debate about the DM profile in the innermost region of the galaxies, it is unclear if they present a cuspy or a shallow flat distribution [19].

1.2 Evidences at galaxy cluster scale

Most of the galaxies are not distributed in the space randomly, in fact they tend to form clumps called cluster. Studying the velocity dispersions of the galaxies in the Coma cluster F.Zwicky, in 1933 gave the first insight about the presence of DM [65].

One of the most important methods to estimate the amount of mass in a cluster, which was used also by Zwicky and collaborators, consist in measuring the radial velocities of galaxies within a cluster, and then apply the virial theorem. This theorem states that for a stable system bounded by the gravitational force, the time average of the total kinetic energy, $\langle E_k \rangle$, and the time average of the total potential energy, $\langle U \rangle$, are related by [44]

$$2\langle E_k \rangle = -\langle U \rangle. \quad (1.5)$$

Thus assuming that the cluster is a stable system, measuring the velocities, and hence the time average of the total kinetic energy, exploiting the virial theorem we can infer the total mass density in the cluster .

In his paper Zwicky assumed that Coma cluster contained 1000 galaxies. He estimated the physical size of the cluster to have a radius of about 2×10^6 light-Yr. Observing a mean velocity dispersion of 700 km/s he obtained a value for the mass of the cluster of about $4.5 \times 10^{13} M_\odot$, which corresponded to an average galaxy mass of $8.5 \times 10^{10} M_\odot$. Then assuming an average galaxy luminosity of about $8.5 \times 10^7 L_\odot$, he found a very high mass-to-light ratio, $\langle M/L \rangle$, of about $500 M_\odot / L_\odot$ ² [65]. Nowadays taking into account the fact that Coma cluster contain also an invisible halo of hot gases, (fact that was not known from Zwicky and his collaborators), what is find is that the total amount of baryonic mass is a factor of about ~ 6 too small to explain the high dispersion velocities of galaxies into the cluster [44].

Other estimations of the cluster's mass exploiting the virial theorem, was performed by Schmit studying the Virgo cluster. In his work Schmit found an average mass for galaxies of about $2 \times 10^{11} M_\odot$ a value much higher than the one find at the galactic scale by Hubble, $\sim 10^9 M_\odot$ [18].

Another way to determine the mass of a cluster comes from the study of the X-ray emission of hot gases, which traces their distribution. Assuming that the cluster is a stable system and denoting with $P(R)$ the pressure, with $\rho(R)$ the density and with $a(R)$ the gravitational acceleration of the gases at a distance, R , from the barycenter of the cluster, the equation of the hydrostatic equilibrium states that

$$\frac{dP(R)}{dR} = -a(R)\rho(R). \quad (1.6)$$

Using the equation of state of an ideal gas

$$P(R)V(R) = Nk_B T(R), \quad (1.7)$$

where k_B is the Boltzmann constant, Eq. (1.6) can be rewritten in term of the gas temperature, $T(R)$, as [19]

$$\frac{d \log \rho(R)}{d \log R} + \frac{d \log T(R)}{d \log R} = -\frac{R}{T(R)} \left(\frac{\mu m_p}{k_B} \right) a(R), \quad (1.8)$$

where m_p is the proton mass and μ is the average molecular weight of the gases. Knowing that $a(R) = \frac{M(R)G_N}{R^2}$ we find that the mass of the cluster, within a radius R , is given by

$$M(R) = -\left(\frac{d \log \rho(R)}{d \log R} + \frac{d \log T(R)}{d \log R} \right) \left(\frac{k_B}{\mu m_p} \right) \frac{T(R)R}{G_N}. \quad (1.9)$$

Thus, under the assumption that outside the core of the cluster the temperature is roughly constant, and that we know the power law of the density profile of the gas, measuring the temperature $T(R)$ we can estimate the total amount of mass in the cluster [19]. Vice versa if we state that $M(R)$ is the total mass of baryonic matter, using Eq. (1.9), we find a temperature

² $L_\odot = 3.828 \times 10^{26} W$, is the solar luminosity, from Ref. [60]

$T(R)$ much lower than the observed one. This suggest the presence of a substantial amount of non-emitting matter i.e. DM.

As for elliptical/irregular galaxies also for cluster another method to estimate their mass is achieved by the use of the gravitational lensing.

1.3 Evidences at cosmological scale

Basing upon the observations discussed above we are not able to exactly estimate the total amount of DM in the Universe. However this information can be extrapolate analyzing the Cosmic Microwave Background (CMB) [42]. The small matter density inhomogeneities set up during the inflation era are considered the seeds that led to the formation of the large structures of the Universe i.e. cluster, galaxies, stars [29]. This inhomogeneities can be related to the temperature anisotropies of the CMB. Thus the study of the entity of this anisotropies allow us to infer how much matter (baryonic and non-baryonic) is present in the Universe [31]. Usually these temperature anisotropies, $\delta T/T$, are expanded in spherical harmonics base

$$\frac{\delta T}{T} = \sum_{\ell=2}^{+\infty} \sum_{m=-\ell}^{+\ell} a_{\ell m} Y_{\ell m}(\Theta, \phi). \quad (1.10)$$

where $Y_{\ell m}(\Theta, \phi)$ are spherical harmonics. The coefficients $a_{\ell m}$ have a variance C_ℓ which, under the assumption of Gaussian temperature fluctuations, is given by [19]

$$C_\ell \equiv \langle |a_{\ell m}|^2 \rangle \equiv \frac{1}{2\ell + 1} \sum_{m=-\ell}^{+\ell} |a_{\ell m}|^2. \quad (1.11)$$

The way to extrapolate informations from the measure of the parameters $\delta T/T$ and C_ℓ , given by the CMB anisotropies map Fig. 1.3, is the method of the likelihood function. This function is defined as the probability that an experiment gives the same results as the ones given by a theory [31]. Substantially once we have the likelihood function we are able to extrapolate the parameters of the theory. These are the values, in the parameter space, which maximize the likelihood function.

One of the most important missions launched to map and analyzing the CMB is Planck [3].

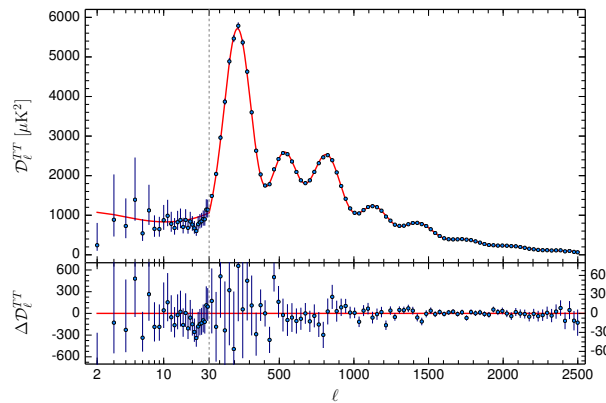


Figure 1.2: The CMB power spectrum. The plot shows $\mathcal{D}_\ell = \ell(\ell + 1)\mathcal{C}_\ell/(2\pi)$ as a function of the multipole ℓ , (from Ref. [4]).

Following the method of the likelihood, the analysis of the Planck data gives the results [3]

$$\Omega_B h^2 = 0.02227 \pm 0.00020, \quad \Omega_M h^2 = 0.1413 \pm 0.0011 \quad (1.12)$$

where $\Omega_B \equiv \rho_B/\rho_c$, $\Omega_M \equiv \rho_M/\rho_c$ and ρ_B , ρ_M , ρ_c are respectively the baryon matter density, the total matter density and the critical density.³ Thus the amount of DM in the Universe from Planck data analysis is [3]

$$\Omega_{DM}h^2 = \Omega_Mh^2 - \Omega_Bh^2 = 0.1184 \pm 0.0012. \quad (1.13)$$

From these results is evident that the dominant part of the matter in the Universe has a non-baryonic nature. Note that the value of Ω_B is consistent with the range set by the Big Bang Nucleosynthesis (BBN) analysis, which is [19]

$$0.018 < \Omega_Bh^2 < 0.023. \quad (1.14)$$

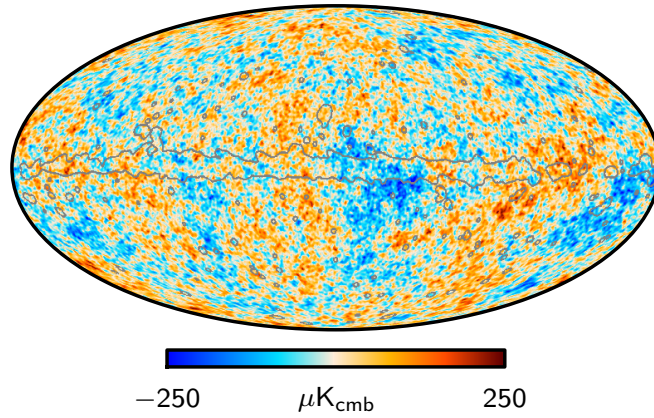


Figure 1.3: CMB temperature map obtained from the Planck 2015 observations, (from Ref. [4]).

³ $\rho_c = \frac{3H_0}{8\pi G_N} = 1.87847 \times 10^{-29}h^2 \text{ g cm}^{-3}$, where $H_0 = 100h \text{ km s}^{-1} \text{ Mpc}^{-1}$ is the Hubble constant, from Ref. [60]

1.4 Dark Matter characteristics

Here we provide a list of the principal characteristics which DM is supposed to have.

- DM as ordinary matter has attractive gravitational interaction. In fact evidences about DM arise from the observations of the gravitational effects which it has on visible matter. About other type of fundamental interactions we have no data [42]. For this reason many attempt was made to explain the evidences for DM as probes of departures from the law of gravity. One of the most successful model of this type, is a modification of the Newtonian dynamics called MOND (Modified Newtonian Dynamics). In MOND the force is $\vec{F} = \mu(a)m\vec{a}$, where the parameter $\mu(a)$ deviates from unity only for small accelerations [38]. This model explain very well the flatness of the rotational curves of the galaxies, without assuming the presence of DM, but fails in the explanation of evidences of DM at larger scales. Another model of this type is the TeVeS [13], which is a relativistically invariant theory that yields MOND in the non-relativistic weak-field limit.
- DM is stable or has a lifetime $\tau_{\text{DM}} \gg t_{\text{U}}$ where $t_{\text{U}} = 13.796 \pm 0.029 \text{ Gyr}$ [3], is the age of the Universe.
- There are no observations of the interactions between DM and light i.e. electromagnetic interaction. This means that DM has very small, or zero, electromagnetic interaction.
- An important consequence of a non interaction with light, is that DM is dissipation-less i.e. it cannot cool radiating photons as baryons do during the galaxy formation [42]. This is consistent with the existence of such extended dark haloes. Conversely visible matter dissipates energy emitting photons, which causes its collapse through the center of the galaxy, forming a disk [42].
- DM is a thermal relic, and can be Cold or Warm, it cannot be a Hot thermal relic [42]. A thermal relic is Cold if at the freeze-out (i.e. when it goes out of the thermal equilibrium with the cosmic plasma), it is non-relativistic, $m_{\text{DM}} \gg T_{\text{fo}}$, where m_{DM} is the mass of DM and T_{fo} is the freeze-out temperature. Conversely, a thermal relic is Hot when at the freeze-out it is relativistic, $m_{\text{DM}} < T_{\text{fo}}$. As last a thermal relic is Warm if at the freeze-out is becoming non-relativistic. The reasons why DM cannot be Hot but only Cold or Warm rely on the fact that the presence of DM is fundamental for the formation of the structures in the early Universe. With Hot DM the matter density inhomogeneities would led first to the formation of super-cluster and then, via fragmentation, to the other substructures, the sequence stops with the formation of galaxies. This is in disagreement with the observations of the Universe. On contrary with Cold DM, the matter density inhomogeneities led to the formation of smaller structures as first, which then aggregate forming more larger structures such as galaxies, cluster and super-cluster. This is in good agreement with the observed Universe. With Warm DM hypothesis there are much less substructures then in the Cold DM case, but this model still represents quite well our Universe [42].
- DM is assumed to have a very weak self-interactions i.e. DM is collision-less. If the interactions between DM particles are too efficient, many small scale structures would be erased [42].

1.5 Dark matter candidates

From the late 1980s the idea that the bulk of DM consisted of one or more unknown elementary particles started to be a very interesting hypothesis. As the various alternatives were ruled out by observations, this hypothesis became the leading paradigm for the DM issue [18].

Here we list some of the leading particle DM candidates. All the following proposals come from theories which were not proposed to resolve the DM problem, but their main prospectives

were to provide solutions to others SM's issues. The coincidence that two completely different problems can be resolved within a unique theory is a strong hint about the validity of that theory.

Because much of this thesis will be devote to the analysis of WIMPs, and in particular of neutralinos as DM candidates, we start with a brief review of the WIMP "miracle"; then we will go on listing the major DM candidates.

The WIMP "miracle"

The expression WIMP "miracle" (WIMP is the acronym for Weakly Interactive Massive Particle) refers to the fact that particles with electroweak scale masses and weak interaction coupling constant, naturally give rise to a thermal relic density which is similar to the observed one for DM. This suggests that thermal relic WIMPs give a natural solution to the DM problem [55]. As we will see in the next sections thermal relics are those relics produced via "decoupling" or "freeze-out" from a condition of thermal equilibrium with the primordial thermal plasma. In particular when the interaction rate Γ , that change the number of particles, is larger than the expansion rate of the Universe H , where H is the Hubble constant, the thermal equilibrium is maintained [42]. The freeze-out is set up when $\Gamma \approx H$, and the involved species goes out from the equilibrium.

For non-relativistic particles with mass m_χ , the equilibrium number density n can be approximate as

$$n \simeq (m_\chi T)^{3/2} e^{-m_\chi/T}, \quad (1.15)$$

where T is the equilibrium temperature. The interaction rate can be approximate as $\Gamma = n\langle\sigma v\rangle \simeq n\sigma_0$, where σ_0 indicates the leading term of the expansion of the thermal average of the annihilation cross-section, σ , times particles relative velocity, v , i.e. $\langle\sigma v\rangle$. Furthermore when the Universe is radiation dominated, H can be approximate as $H \simeq T^2/M_{\text{Pl}}^4$. Thus supposing that the decoupling occurs when the Universe is radiation dominated we can rewrite the freeze-out condition as

$$n_{\text{fo}} \simeq \frac{T_{\text{fo}}^2}{M_{\text{Pl}}\sigma_0}, \quad (1.16)$$

that using the above expression for n , can be recast as

$$\frac{m_\chi^3 e^{-x_{\text{fo}}}}{x_{\text{fo}}^{3/2}} \simeq \frac{m_\chi^2}{x_{\text{fo}}^2 M_{\text{Pl}}\sigma_0}, \quad (1.17)$$

where we have defined $x \equiv m_\chi/T$.

Inserting a typical electroweak expression for σ_0 such as $\sigma_0 \simeq G_{\text{F}}^2 m_\chi^2$, where $G_{\text{F}} = 1.166 \times 10^{-5} \text{ GeV}^{-2}$ [60] is the Fermi constant, and an electroweak scale value for $m_\chi \sim 10^2 \text{ GeV}$, what we find is $x_{\text{f.o.}} \sim 20$ [62].

The relic density is roughly given by

$$\Omega_\chi = \frac{m_\chi n(T_0)}{\rho_c}, \quad (1.18)$$

where $T_0 = 2.7255 \text{ K} \sim 10^{-4} \text{ eV}$ [60] is the today temperature. Furthermore for a Universe with constant entropy, the quantity Ta is constant, where as usual a denote the expansion parameter of the Universe; thus we have that

$$\frac{n(T_0)}{T_0^3} = \frac{n(T_{\text{fo}})}{T_{\text{fo}}^3}, \quad (1.19)$$

note that this relation is a consequence of the fact that after the decoupling the number of particles of a specific species remains constant or, in other words, the density number, n , scales as a^{-3} .

Now substituting Eq. (1.19) into Eq. (1.18), we have that

$$\Omega_\chi = \frac{m_\chi T_0^3}{\rho_c T_{\text{fo}}} \left(\frac{n(T_{\text{fo}})}{T_{\text{fo}}} \right)^2 = \frac{T_0^3}{\rho_c M_{\text{Pl}}} \frac{x_{\text{fo}}}{\sigma_0}, \quad (1.20)$$

⁴ $M_{\text{Pl}} = 1.22 \times 10^{19} \text{ GeV}^2/c^2$ is the Planck mass, from Ref. [60]

where we used Eq. (1.16). Putting the numerical value of the constants in the above equation we find [62],

$$\frac{\Omega_X}{0.2} \simeq \frac{x_{f_0} 10^{-8} \text{ GeV}^{-2}}{20 \sigma_0}, \quad (1.21)$$

hence to fit the right DM relic density the value of the annihilation cross-section has to be about $\sigma_0 \sim 10^{-8} \text{ GeV}^{-2}$, which is of the order of a typical weak process. Hence the expression WIMP "miracle" can be rephrase as: if a stable WIMP exist, then it naturally has a relic density consistent with the one of DM [40].

Sometimes Eq. (1.21) is written in terms of the average cross-section times velocity, $\langle\sigma v\rangle$. So for $v \sim c/3$, which is implied by the assumption $x_{f_0} \sim 20$, we have [62]

$$\langle\sigma v\rangle \sim 10^{-8} \text{ GeV}^{-2} \times 10^{10} \frac{\text{cm}}{\text{s}} = 3 \times 10^{-26} \frac{\text{cm}^3}{\text{s}}. \quad (1.22)$$

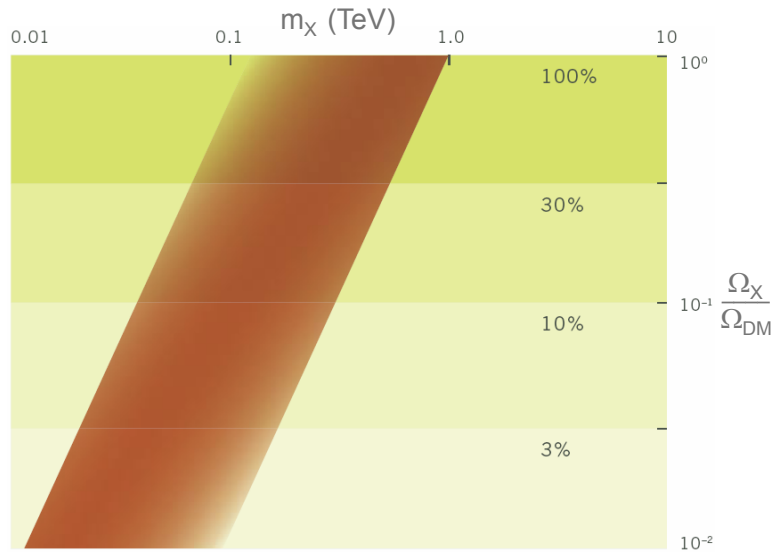


Figure 1.4: The plot shows a band of natural mass values for the DM candidate X . Ω_X is the relic density of the DM candidate while $\Omega_{DM} \simeq 0.23$. We can see that the major contribute to DM is given by a particle with a mass in the range $m_X \simeq 100 \text{ GeV} - 1 \text{ TeV}$, while for example a candidate with a mass in the range $10 - 100 \text{ GeV}$ can make up only the 3% of the DM density (from Ref. [40]).

Supersymmetric candidates

Many frameworks of R -parity conserving supersymmetry, provide a natural DM candidate, which is called the Lightest Supersymmetric Particle (LSP). This particle has to be a stable (R -parity symmetry prevents its decay into SM particles), electrically neutral particle. Depending on the particular model chosen, the most famous candidates are

- *Gravitinos* \tilde{G} , which are spin 3/2 fermions, super-partners of the gravitons. In some supersymmetric models they can be the LSP. However, with only gravitational interaction, they are very difficult to observe [19]. Note that they are not WIMPs.
- *Neutralinos* $\tilde{\chi}_1, \tilde{\chi}_2, \tilde{\chi}_3, \tilde{\chi}_4$, which are spin 1/2 fermions, that generally are an admixture of $\tilde{B}, \tilde{W}_3, \tilde{H}_u, \tilde{H}_d$. These are respectively the fermionic superpartners of the SM B hypercharge gauge boson, W_3 $SU(2)_L$ gauge boson, and H_u, H_d scalar Higgs doublets. In particular in models where the LSP is a neutralino, the lightest one, $\tilde{\chi}_1$, provides a good WIMP candidate. This thesis will be focus on this DM candidate.

Kaluza-Klein

The idea about the existence of extra spatial dimensions was first developed by Kaluza and Klein in 1920's. The newest model based upon their idea is called universal extra dimensions (UED). In UED all particles (fields) propagates in flat, compact extra dimensions of size $R \sim 10^{-18}\text{m}$ or smaller [40]. A general feature of this models is that all particles, which propagate in the extra dimensions, have their momentum quantized in units of $p^2 \sim 1/R^2$ [19]. This implies that for each particle exists an infinite set of Fourier modes called Kaluza-Klein (KK) states. For us, in 1 + 3-dimensions, these states appear as series of particles of mass $m_n = n/R$, where n denotes the mode number [40]. Note that the various KK states share the same quantum numbers.

The simplest UED (minimal UED) model has one extra dimension compactified on a circle of radius R , and it is completely determined by two parameters, m_h , the mass of the SM Higgs scalar, and the size R . This model preserve also a discrete symmetry called KK-parity, which prevents the decay of the lightest KK particle (LKP). This imply that, if the LKP is also electrically neutral, it can be a possible DM candidate. Typically this particle is B^1 , the level 1 partner of the hypercharge gauge boson B .

SuperWIMPs

Basing upon the WIMP "miracle" may appear that the DM candidates must have weak interactions to naturally fit the right relic density. This is not actually true. In fact exist some models in which the DM candidate has different interactions from the weak one, but still has the correct relic density [40].

An example of this are superWIMPs. In this scenario the DM candidate has the desired relic density, but it has an interaction much weaker than the weak one.

This model provides also an example of non-thermal DM. In fact superWIMPs particles are produced via WIMPs particles late decay. First, in the early Universe, WIMPs freeze-out from the thermal bath, then they decay into superWIMPs which form the today DM. Assuming that in every WIMP decay is produced one superWIMP, the relic density is given by [40]

$$\Omega_{\text{sWIMP}} = \frac{m_{\text{sWIMP}}}{m_{\text{WIMP}}} \Omega_{\text{WIMP}}, \quad (1.23)$$

and if $m_{\text{sWIMP}} \sim m_{\text{WIMP}}$ the WIMP "miracle" argument implies that Ω_{sWIMP} quite reproduces the amount of DM.

Sterile neutrinos

The problem to explain the neutrinos masses can be resolve introducing in the SM right-handed neutrinos. Thank to this neutrinos can acquire mass via the standard Higgs mechanism. In order to have an invariant neutrions's mass term, under the SM gauge symmetries, the right-handed neutrinos must have no SM gauge interactions i.e. they are sterile.

The relic density of sterile neutrinos depends on their masses and their mixing angles. To reproduce the correct DM relic density these parameters must have well define small values which are not justify by any independent theoretical argument. Hence sterile neutrinos do not naturally give the right relic density [40].

Axions

Quantum chromodynamics (QCD) is a successful theory which describes the strong force experienced by gluons and quarks. One of the feature of this theory is the fact that the QCD Lagrangian contains the following pseudo-scalar term [18]

$$\mathcal{L}_{\text{CP-QCD}} = \Theta \frac{g_3^2}{32\pi^2} \text{Tr}\{G^{\mu\nu} \tilde{G}_{\mu\nu}\}, \quad (1.24)$$

where g_3 is the strong coupling constant, and with $\tilde{G}_{\mu\nu}$ we denoted the dual of the gluons field strength tensor.⁵ Θ is a parameter related to the phase of the QCD vacuum.

If Θ is of order of unity, then larger CP violating effects would affect the theory. However to be consistent with the experimental bound imposed by the non-observation of the electric dipole moment, d_e , of the neutron, ($d_e < 2.9 \times 10^{-26} \text{ e cm}$ [40]), Θ has to be smaller than $\sim 10^{-10}$ [18]. So the essence of the strong CP problem is to ask why the value of Θ has to be so small. In 1977 R.Peccei and H.Quinn proposed an elegant solution to the problem. Their idea was based on the introduction of a new global $U(1)$ symmetry, which when it is spontaneously broken, the parameter Θ is naturally driven to zero. Later F.Wilczek and S.Weinberg, basing on the fact that the new $U(1)$ symmetry is a global one, stated that its spontaneous break implies the existence of a Nambu-Goldstone boson, which was called axion. It is important to note that, despite the fact that the axion comes from the breaking of a global symmetry, it has a small mass due to the $U(1)$ chiral anomaly. Its mass can be approximate as $m_a \sim g_3^2/f_{\text{PQ}}$ where f_{PQ} is the energy scale of the $U(1)$ symmetry breaking. The facts that axions are electrically neutral and massive stable particles, make them good candidates for the DM problem.

Beyond these few candidates there are many other proposals, motivate by other reasons. Some of them come from relaxing some DM characteristics such as self-interactions, electrical neutrality or non-dissipative behaviour. Some example are models of Self Interacting DM (SIDM), millicherge DM or double disk DM [42].

Others candidates come from the attempts to resolve the DM problem without introducing new particles, such as MACHOs (Massive Astrophysical Compact Halo Objects). These massive objects are supposed to be so faintly luminous to prevent their detection. Hence the probes of their existence can be tested only exploiting their gravitational effects, in particular using the gravitational lensing.

⁵ $\tilde{G}_{\mu\nu} = \epsilon_{\mu\nu\alpha\beta}G^{\alpha\beta}$, where $\epsilon_{\mu\nu\alpha\beta}$ is the total antisymmetric tensor in four dimension

Chapter 2

Boltzmann equation and relic density

For much of its history, most of the constituents of the Universe were in thermal equilibrium. However to reproduce the observed Universe there have been a number of very notable departures from the primordial thermal equilibrium. These departures from the thermal equilibrium have led to important relics, such as the thermal DM.

As we said in the previous Chapter thermal relics are produced via interaction with thermal bath, reach the equilibrium with this bath and then “freeze-out” when their interaction rate are lower than the rate of the expansion of the Universe [42]. In particular the evolution of systems which are decoupling from the thermal equilibrium is governed by the Boltzmann equation which describes the statistical behaviour of a thermodynamic system [31]. In this Chapter we will review the solution of the Boltzmann equation in the standard case and for the case of co-annihilations. We follow refs [31], [43], [33].

2.1 Boltzmann equation for the standard case

The Boltzmann equation can be schematically written as [31]

$$\frac{df(x, p)}{dt} = \mathbf{C}[f], \quad (2.1)$$

where $f(x, p)$ is the phase space distribution function which in principle depends on the four-momentum p^μ , on the coordinate four vector x^μ and on the temperature T . The term $\mathbf{C}[f]$ is called the collisional term and, in principle, is a functional of the phase space distribution function and it describes the interactions between the various particles. Assuming a flat Universe, which is defined by the FRW (Friedmann-Robertson-Walker) metric

$$g_{\mu\nu} = \begin{pmatrix} 1 & 0 & 0 & 0 \\ 0 & -a^2(t) & 0 & 0 \\ 0 & 0 & -a^2(t) & 0 \\ 0 & 0 & 0 & -a^2(t) \end{pmatrix} \quad (2.2)$$

where $a(t)$ is the expansion parameter of the Universe, the above Boltzmann equation can be rewritten as [31]

$$\frac{\partial f}{\partial t} + \frac{p}{E} \frac{p^i}{a} \frac{\partial f}{\partial x^i} - \frac{p^2}{E} H \frac{\partial f}{\partial E} = \mathbf{C}[f] \quad (2.3)$$

where $H \equiv \dot{a}(t)/a(t)$ is the Hubble constant.

Assuming that we are interested in the change of species called 1, with four-momentum p_1 ,

the collisional term for $2 \leftrightarrow 2$ annihilation processes is equal to [31]

$$\begin{aligned} \mathbf{C}[f(\vec{p}_1)] &= \frac{1}{E_1} \int \frac{d^3 p_2}{(2\pi)^3 2E_2} \int \frac{d^3 p_3}{(2\pi)^3 2E_3} \int \frac{d^3 p_4}{(2\pi)^3 2E_4} \\ &\quad (2\pi)^4 \delta^4(p_1 + p_2 - p_3 - p_4) \sum_{\text{spins}} |\mathcal{M}|^2 \\ &\quad \{f_3 f_4 [1 \pm f_1][1 \pm f_2] - f_1 f_2 [1 \pm f_3][1 \pm f_4]\} \end{aligned} \quad (2.4)$$

where we have assumed that species 1 annihilates with species 2 producing species 3 and 4 and that also the inverse process is possible, namely $1 + 2 \leftrightarrow 3 + 4$. Considering the collisional term starting from the last line we see that the rate of producing the species 1 is proportional to the distribution functions, f_3 and f_4 . Similarly the annihilation rate of species 1 is proportional to f_1 and f_2 . The $[1 \pm f]$ terms, with plus sign for bosons and minus sign for fermions, represent the Bose enhancement and Pauli blocking factors. In particular if, for example, species 1 already exist the processes, that produce more type-1 particles would be more favoured if 1 is a boson, while they would be disfavoured if species 1 is a fermion. The Dirac delta assure the four momentum conservation. The quantity $|\mathcal{M}|^2$ is the square amplitude of the process which is determined from the theoretical model considered.

The Boltzmann equation given in Eq. (2.3), can be re-expressed in terms of the number density n , which is a more desirable form when we have to evaluate relic densities. Integrating both side of the Eq. (2.3) over the phase space volume $gd^3p/(2\pi)^3$, where g counts the internal degrees of freedom of the species of interest, and using the definitions respectively of the density number

$$n = \int dn \equiv g \int \frac{d^3 p}{(2\pi)^3} f(p, T) \quad (2.5)$$

and of the velocity components

$$v^i \equiv \frac{g}{n} \int \frac{d^3 p}{(2\pi)^3} \frac{p \hat{p}^i}{E} f(p), \quad (2.6)$$

we obtain that the Boltzmann equation becomes

$$\frac{\partial n}{\partial t} + 3Hn = \int g \frac{d^3 p}{(2\pi)^3 2E} \mathbf{C}[f]. \quad (2.7)$$

The above equation is an integro-differential equation and its solution need the solution of the Boltzmann equations for the other species involved in the process. Nevertheless this difficult can be overcome assuming some approximations. As first we will assume that the kinetic equilibrium will be maintained. As a consequence the departures from the thermal equilibrium will be determined by chemical decoupling [42]. Furthermore we will assume that the scattering processes, which tend to enforce the kinetic equilibrium, take place so rapidly that the distribution functions for the various species take the general Fermi/Dirac or Bose/Einstein form,

$$f_{\text{BE}}(E, t) = \frac{1}{e^{\frac{E-\mu}{T}} - 1} \quad (2.8)$$

$$f_{\text{FD}}(E, t) = \frac{1}{e^{\frac{E-\mu}{T}} + 1} \quad (2.9)$$

where μ represent the chemical potential when the species are in equilibrium, but in general it is a perturbation function which depends on the temperature, $\mu(T)$. We will be interested in systems at temperatures T smaller than the quantity $E - \mu$. In this limit the above distribution functions reduce to

$$f(E, T) \rightarrow e^{-\frac{E-\mu}{T}}. \quad (2.10)$$

Note that with these approximations we can safely neglect the Pauli blocking/Bose enhancement factors in Eq. (2.4), so

$$\begin{aligned} &\{f_3 f_4 [1 \pm f_1][1 \pm f_2] - f_1 f_2 [1 \pm f_3][1 \pm f_4]\} \\ &\rightarrow e^{-\frac{(E_1+E_2)}{T}} \left\{ e^{\frac{(\mu_1+\mu_2)}{T}} - e^{\frac{(\mu_3+\mu_4)}{T}} \right\}. \end{aligned} \quad (2.11)$$

where we made use of the energy conservation, $E_1 + E_2 = E_3 + E_4$. Therefore the number density of species i is given by

$$n_i = g_i e^{\frac{\mu_i}{T}} \int \frac{d^3 p}{(2\pi)^3} e^{-\frac{E_i}{T}} \quad (2.12)$$

where we have used the definition given in Eq. (2.5). The equilibrium number density of species i is define as [31]

$$n_i^{(0)} \equiv g_i \int \frac{d^3 p}{(2\pi)^3} e^{-\frac{E_i}{T}}. \quad (2.13)$$

Note that if the species of interest is non-relativistic i.e. $m_i \gg T$, Eq. (2.13) gives

$$n_i^{(0)} = \left(\frac{m_i T}{2\pi} \right)^{3/2} e^{-\frac{m_i}{T}}, \quad (2.14)$$

while, if we refer to a relativistic species i.e. $m_i \ll T$, the result would be

$$n_i^{(0)} = g_i \frac{T^3}{\pi^2}. \quad (2.15)$$

Thanks to the definition in Eq. (2.13), the perturbation factor, $e^{\frac{\mu_i}{T}}$, can be re-express as the ratio $n_i/n_i^{(0)}$, and so the last factor in (2.11) becomes

$$\left(e^{\frac{(\mu_1+\mu_2)}{T}} - e^{\frac{(\mu_3+\mu_4)}{T}} \right) = \left(\frac{n_3 n_4}{n_3^{(0)} n_4^{(0)}} - \frac{n_1 n_2}{n_1^{(0)} n_2^{(0)}} \right). \quad (2.16)$$

Using this result the r.h.s. of Eq. (2.7) becomes

$$\begin{aligned} \sum_{\text{spins}} \int \frac{d^3 p_1}{(2\pi)^3 2E_1} \int \frac{d^3 p_2}{(2\pi)^3 2E_2} e^{-\frac{(E_1+E_2)}{T}} \left\{ \int \frac{d^3 p_3}{(2\pi)^3 2E_3} \right. \\ \left. \frac{d^3 p_4}{(2\pi)^3 2E_4} (2\pi)^4 \delta^4(p_1 + p_2 - p_3 - p_4) |\mathcal{M}|^2 \right\} \left(\frac{n_3 n_4}{n_3^{(0)} n_4^{(0)}} - \frac{n_1 n_2}{n_1^{(0)} n_2^{(0)}} \right) \end{aligned} \quad (2.17)$$

where we used the collisional term given in Eq. (2.4). This expression can be further simplify exploiting the definition of the cross-section σ [61], obtaining that

$$g_1 g_2 \int \frac{d^3 p_1}{(2\pi)^3} \frac{d^3 p_2}{(2\pi)^3} \sigma v_M e^{-\frac{E_1}{T}} e^{-\frac{E_2}{T}} \left(\frac{n_3 n_4}{n_3^{(0)} n_4^{(0)}} - \frac{n_1 n_2}{n_1^{(0)} n_2^{(0)}} \right). \quad (2.18)$$

where v_M is the Møller velocity, which is defined as [43]

$$v_M = \frac{\sqrt{(p_1 \cdot p_2)^2 - m_1^2 m_2^2}}{E_1 E_2} \equiv \frac{F}{E_1 E_2} \quad (2.19)$$

and with \cdot we mean the Lorentz four-dimensional scalar product. Knowing that the thermal average of cross-section times velocity is defined as

$$\langle \sigma v_M \rangle \equiv \frac{\int \frac{d^3 p_1}{(2\pi)^3} \frac{d^3 p_2}{(2\pi)^3} g_1 g_2 \sigma v_M e^{-\frac{E_1}{T}} e^{-\frac{E_2}{T}}}{n_1^{(0)} n_2^{(0)}} \quad (2.20)$$

we can finally rewrite the Boltzmann equation in its standard form

$$\frac{\partial n_1}{\partial t} + 3H n_1 = n_1^{(0)} n_2^{(0)} \langle \sigma v_M \rangle \left(\frac{n_3 n_4}{n_3^{(0)} n_4^{(0)}} - \frac{n_1 n_2}{n_1^{(0)} n_2^{(0)}} \right). \quad (2.21)$$

Assuming that after their production species 3 and 4 go quickly in equilibrium with the thermal background i.e. $n_3 = n_3^{(0)}$, $n_4 = n_4^{(0)}$, and that species 1 and 2 have the same mass $m_1 = m_2 \equiv m$ (which implies that $n_1 = n_2 \equiv n$, $n_1^{(0)} = n_2^{(0)} \equiv n^{(0)}$), Eq. (2.21) becomes

$$\frac{\partial n}{\partial t} + 3Hn = \langle \sigma v_M \rangle \left[(n^{(0)})^2 - n^2 \right]. \quad (2.22)$$

In order to resolve Eq. (2.22) a useful way is to rewrite it scaling out the effect of the expansion of the Universe using the variable [31]

$$Y \equiv \frac{n}{s}, \quad (2.23)$$

where s is the entropy density which is equal to [51]

$$s = \frac{2\pi^2}{45} g_{*s} T^3 \quad (2.24)$$

and the quantity g_{*s} is defined as [51]

$$g_{*s} \equiv \sum_{\text{bosons}} g_b \left(\frac{T_b}{T} \right)^3 + \frac{7}{8} \sum_{\text{fermions}} g_f \left(\frac{T_f}{T} \right)^3. \quad (2.25)$$

In both the above equations T is the photons temperature, which defines the common temperature of the species in equilibrium with the thermal bath. Therefore using the variable defined in Eq. (2.23) the Boltzmann equation read as

$$\frac{\partial Y}{\partial t} = -s \langle \sigma v_M \rangle \{ Y^2 - (Y^{(0)})^2 \}. \quad (2.26)$$

Since $\langle \sigma v_M \rangle$ usually, depends explicitly upon temperature, T , rather than time, t , it is useful to introduce the variable

$$x \equiv \frac{m}{T}. \quad (2.27)$$

This variable can be connected with the time t knowing that in a flat Universe the Hubble constant is equal to [51]

$$H = \sqrt{\frac{8\pi G}{3} \frac{\pi^2}{30} g_* T^2} = \sqrt{\frac{4}{45} \frac{\pi^3 g_*}{M_{\text{Pl}}^2} T^2} \approx 1,66 \sqrt{g_*} \frac{T}{M_{\text{Pl}}} \quad (2.28)$$

and the fact that in the radiation-dominated era¹ we have that $a(t) \propto \sqrt{t}$ thus [51]

$$t = \frac{1}{2H} = \sqrt{\frac{45}{16\pi^3 g_*} \frac{M_{\text{Pl}}^2}{T^2}} \approx 0.301 g_*^{-1/2} \frac{M_{\text{Pl}}}{T} = 0.301 g_*^{-1/2} \frac{M_{\text{Pl}}}{m^2} x^2, \quad (2.29)$$

where in both the above equations g_* is defined as [51]

$$g_* \equiv \sum_{\text{bosons}} g_b \left(\frac{T_b}{T} \right)^4 + \frac{7}{8} \sum_{\text{fermions}} g_f \left(\frac{T_f}{T} \right)^4. \quad (2.30)$$

Therefore using Eq. (2.29) we can recast Eq. (2.26) as

$$\frac{\partial Y}{\partial x} = -\frac{\langle \sigma v_M \rangle s}{Hx} \{ Y^2 - (Y^{(0)})^2 \}. \quad (2.31)$$

The Boltzmann equation given in Eq. (2.31) is a particular form of Riccati equation [51], for which there are no general analytic solutions. Approximate solutions to it are given in Appendix

¹The assumption of a radiative Universe is consistent with the fact that all the freeze-out processes which we are interested occur much earlier than the matter-dominated era.

A; here we recall the later time solution which would be useful to find the relic abundance. Thus for $x \rightarrow \infty$ Eq. (2.31) has as approximate solution

$$Y_\infty = \sqrt{\frac{45}{\pi}} \frac{g_*^{1/2}}{g_{*s}} \frac{1}{m M_{\text{Pl}} J(x_{\text{fo}})}, \quad (2.32)$$

where $J(x_{\text{fo}})$ is defined as

$$J(x_{\text{fo}}) \equiv \int_{x_{\text{fo}}}^{\infty} \frac{\langle \sigma v_{\text{M}} \rangle}{x^2} dx \quad (2.33)$$

and x_{fo} is defined at the "freeze-out" temperature T_{fo} . Now because we have assumed that the species under interest is non-relativistic, its present density is simply given by $\rho = mn = m s_0 Y_\infty$, where s_0 is the present entropy density. Usually the relic density is defined as $\Omega \equiv \rho/\rho_c$ where ρ_c is the critical density. So we have that the relic density is given by [45]:

$$\Omega h^2 = \frac{1.07 \cdot 10^9}{M_{\text{Pl}} J(x_{\text{fo}})} \frac{g_*^{1/2}}{g_{*s}} \text{GeV}^{-1} \quad (2.34)$$

where h is the Hubble parameter defined as $h = H_0/100 \text{ Km s}^{-1} \text{ Mpc}^{-1}$.² The "freeze-out" temperature T_{fo} and in particular x_{fo} is given by the iterative solution [45], [19], [51]

$$x_{\text{fo}} \simeq \ln \left[\frac{0.038c(c+2)g M_{\text{Pl}} m \langle \sigma v_{\text{M}} \rangle}{g_{*s}^{1/2} x_{\text{fo}}^{1/2}} \right]. \quad (2.35)$$

where c is a constant of order of unity. The principal steps to arrive to this approximate solution are given in Appendix A.

Here we have implicitly made an important approximation. We assumed that g_* and g_{*s} , remain constant during all the evolution of the species considered; this approximation is in general not correct, in fact as we can see from Eq. (2.30) and Eq. (2.25) g_* and g_{*s} depend on the ratio between the species temperatures, T_i , and the one of the thermal bath, T . Relaxing this approximation it can be demonstrated [43] that the relic density formula given in Eq. (2.34) is modified as

$$\Omega h^2 = \frac{1.07 \cdot 10^9}{M_{\text{Pl}} \overline{g_{\text{tot}}} J(x_{\text{fo}})} \text{GeV}^{-1} \quad (2.36)$$

where $\overline{g_{\text{tot}}}$ denote the mean value of the quantity g_{tot} which is equal to [43]

$$g_{\text{tot}} = \frac{g_{*s}(T)}{\sqrt{g_*(T)}} \left[1 + \frac{1}{3} \frac{d \ln h_c(T)}{d \ln T} \right]. \quad (2.37)$$

where $h_c(T)$ is defined as

$$h_c(T) = \sum_{i \text{ coup}} g_i \quad (2.38)$$

which is the sum of all degrees of freedom of the species in equilibrium at temperature T .

2.2 Thermally averaged cross-section

The physic which determines the relic density is contained in the thermal average of annihilation cross-section times velocity, $\langle \sigma v_{\text{M}} \rangle$. This is, usually, computed by expanding the cross-section at low velocity, or equivalently, expanding it in the total kinetic energy per unit of mass. Following [43] here we give an expansion formula for the thermal average in the non-relativistic regime assuming $m_1 = m_2 \equiv m$. We start observing that the product $v_{\text{M}} n_1 n_2$ is invariant under Lorentz transformations; in fact its definition is such that, the invariant interaction rate per unit of volume and unit of time can be written as

$$\frac{dN}{dV dt} = \sigma v_{\text{M}} n_1 n_2 \quad (2.39)$$

² $H_0 \simeq 67.3 \text{ Km s}^{-1} \text{ Mpc}^{-1}$ [60] is the present value of the Hubble constant.

where σ is the invariant annihilation cross-section. In our case, the densities n_1 , n_2 and the Møller velocity v_M refer to a generic cosmic co-moving frame. In particular, from Eq. (2.19), the Møller velocity in terms of the velocities of the incoming particles, \vec{v}_1 and \vec{v}_2 , reads [43]

$$v_M = \sqrt{(\vec{v}_1 - \vec{v}_2)^2 - (\vec{v}_1 \times \vec{v}_2)^2} \quad (2.40)$$

Now the question is what relationship there is between the thermal averages $\langle \sigma v_M \rangle$, $\langle \sigma v_{\text{lab}} \rangle^{\text{lab}}$ and $\langle \sigma v_{\text{cm}} \rangle^{\text{cm}}$, where the first average is taken relatively to the generic cosmic co-moving frame, the second in the laboratory frame (the frame where particle 1 is at rest), and the third in the center-of-mass frame. Exploiting the Lorentz invariance of the ratio dn_i/E_i [43] and the Lorentz invariance of the factor $v_M dn_1 dn_2$ we have that

$$v'_M dn'_1 dn'_2 = v_M \frac{E_1 E_2}{E'_1 E'_2} dn_1 dn_2 \quad (2.41)$$

from which we get

$$v_M = v'_M \frac{1 - (\vec{v}_1 \cdot \vec{v}_2)}{1 - (\vec{v}'_1 \cdot \vec{v}'_2)} \quad (2.42)$$

where the quantities with a prime refer to a different frame. In the case where the primed system is the laboratory frame, e.g. the rest frame of particle 1, or the center-of-mass frame, the Møller velocity v'_M coincides with the relative velocity v_{lab} or v_{cm} respectively, see Eq. (2.40). Thus using Eq. (2.42) we get that

$$v_M = v_{\text{lab}}(1 - \vec{v}_1 \cdot \vec{v}_2) \quad (2.43)$$

for the laboratory frame, while in the center-of-mass frame we have that

$$v_M = v_{\text{cm}} \frac{E_{\text{cm}}^2}{E_1 E_2} = v_{\text{cm}} \frac{1}{2} \left[1 - \vec{v}_1 \cdot \vec{v}_2 + \frac{m^2}{E_1 E_2} \right] \quad (2.44)$$

where we have used the fact that for particles of equal mass, m , the invariant Mandelstam variable s is $s = 4E_{\text{cm}}^2$, and E_{cm} is the energy of particles in the center-of-mass frame, remember that they have equal masses.

The relation between the thermal average of cross-section times velocity in the primed system, which is defined as

$$\langle \sigma v'_M \rangle' = \frac{\int \sigma v'_M dn'_1 dn'_2}{\int dn'_1 dn'_2}, \quad (2.45)$$

with $\langle \sigma v_M \rangle$ in the generic cosmic co-moving frame, which defined in the same way without a prime, can be obtained by noticing that the numerator is Lorentz invariant while the denominator changes under Lorentz transformations. Thus we have that

$$\langle \sigma v_M \rangle = \langle \sigma v'_M \rangle' \frac{\int dn'_1 dn'_2}{\int dn_1 dn_2}. \quad (2.46)$$

To find the ratio $\frac{\int dn'_1 dn'_2}{\int dn_1 dn_2}$ we consider the invariance of the quantity $v_M dn_1 dn_2$ rewritten as

$$\frac{v_M}{v'_M} dn_1 dn_2 = dn'_1 dn'_2. \quad (2.47)$$

Integrating both sides of the last equation and dividing by $\int dn_1 dn_2$ we get

$$\frac{\int v_M/v'_M dn_1 dn_2}{\int dn_1 dn_2} = \frac{\int dn'_1 dn'_2}{\int dn_1 dn_2} = \left\langle \frac{v_M}{v'_M} \right\rangle. \quad (2.48)$$

Substituting this result into Eq. (2.46) we obtain the relation between $\langle \sigma v_M \rangle$ and $\langle \sigma v'_M \rangle'$

$$\langle \sigma v_M \rangle = \langle \sigma v'_M \rangle' \left\langle \frac{v_M}{v'_M} \right\rangle. \quad (2.49)$$

Using Eqs. (2.43) for the laboratory frame, we have

$$\begin{aligned} \left\langle \frac{v_M}{v_{\text{lab}}} \right\rangle &= \langle 1 - \vec{v}_1 \cdot \vec{v}_2 \rangle \\ &= 1 - \frac{\int_0^\infty g_1 \frac{|\vec{p}_1|^3}{E_1} f_1 \frac{d|\vec{p}_1|}{(2\pi)^3} \int_0^\infty g_2 \frac{|\vec{p}_2|^3}{E_2} f_2 \frac{d|\vec{p}_2|}{(2\pi)^3} \int \hat{p}_1^i d\Omega_1 \int \hat{p}_2^i d\Omega_2}{\int dn_1 dn_2} = 1 \end{aligned} \quad (2.50)$$

where we have used Eq. (2.6) for velocities and the fact that $\int \hat{p}^i d\Omega = 0$, p^i is the 3-momentum vector. For the center-of-mass frame using Eq. (2.44) we have

$$\begin{aligned} \left\langle \frac{v_M}{v_{\text{cm}}} \right\rangle &= \frac{1}{2} \left\langle 1 - \vec{v}_1 \cdot \vec{v}_2 + \frac{m^2}{E_1 E_2} \right\rangle \\ &= \frac{1}{2} \left[1 + \left\langle \frac{m^2}{E_1 E_2} \right\rangle \right] \end{aligned} \quad (2.51)$$

where we used the result given in Eq. (2.50). Thus we finally obtain the relation

$$\langle \sigma v_M \rangle = \langle \sigma v_{\text{lab}} \rangle^{\text{lab}} = \frac{1}{2} \left[1 + \left\langle \frac{m^2}{E_1 E_2} \right\rangle \right] \langle \sigma v_{\text{cm}} \rangle^{\text{cm}}. \quad (2.52)$$

Note that the factor $\left\langle \frac{v_M}{v_{\text{cm}}} \right\rangle$ varies from 1/2 for a highly relativistic species to 1 for a fully non-relativistic one. Therefore in the non-relativistic limit we have that

$$\langle \sigma v_M \rangle = \langle \sigma v_{\text{lab}} \rangle^{\text{lab}} \approx \langle \sigma v_{\text{cm}} \rangle^{\text{cm}}. \quad (2.53)$$

Thus, thanks to this result, we can perform the calculation of the thermal average, in the non-relativistic limit, referring indifferently to $\langle \sigma v_{\text{lab}} \rangle^{\text{lab}}$ or $\langle \sigma v_{\text{cm}} \rangle^{\text{cm}}$ instead of $\langle \sigma v_M \rangle$.

We choose to perform our calculations in the laboratory frame. We can expand σv_{lab} in terms of the total kinetic energy per unit of mass in the laboratory frame, that for particles with same mass is equal to [43]

$$\begin{aligned} \epsilon &= \frac{(E_{1\text{lab}} - m) + (E_{2\text{lab}} - m)}{2m} \\ &= \frac{E_{2\text{lab}} - m}{2m}. \end{aligned} \quad (2.54)$$

The Taylor expansion of σv_{lab} in powers of ϵ is defined as [43]

$$\begin{aligned} \sigma v_{\text{lab}} &= \sum_{n=0}^{\infty} \frac{1}{n!} \left. \frac{\partial^n \sigma v_{\text{lab}}}{\partial \epsilon^n} \right|_{\epsilon=0} \epsilon^n \\ &\equiv \sum_{n=0}^{\infty} \frac{a^{(n)}}{n!} \epsilon^n \end{aligned} \quad (2.55)$$

and the thermal average of σv_{lab} with the Maxwell-Boltzmann approximation reads as

$$\langle \sigma v_{\text{lab}} \rangle^{\text{lab}} = \frac{\int \sigma v_{\text{lab}} e^{-E_1/T} e^{-E_2/T} d^3 p_1 d^3 p_2}{\int e^{-E_1/T} e^{-E_2/T} d^3 p_1 d^3 p_2}. \quad (2.56)$$

From this equation and using the expansion given in Eq. (2.55), we obtain that $\langle \sigma v_{\text{lab}} \rangle^{\text{lab}}$ in powers of $1/x$ in the non-relativistic limit is equal to

$$\begin{aligned} \langle \sigma v_{\text{lab}} \rangle_{\text{n.r.}}^{\text{lab}} &= \sum_{n=0}^{\infty} \frac{a^{(n)}}{n!} \frac{1}{x^n} \frac{(2n+1)!!}{2^n} \\ &= a^{(0)} + \frac{3}{2} \frac{a^{(1)}}{x} + \frac{15}{8} \frac{a^{(2)}}{x^2} + \mathcal{O}\left(\frac{1}{x^3}\right). \end{aligned} \quad (2.57)$$

where the subscript n.r. means non-relativistic and in Appendix A we perform the detailed calculation to obtain this result from Eq. (2.56). Substituting this expansion into the definition of $J(x_{\text{fo}})$, Eq. (2.33), we obtain that

$$J(x_{\text{fo}}) = \left(a^{(0)} + \frac{3}{4} \frac{a^{(1)}}{x_{\text{fo}}} \right) \frac{1}{x_{\text{fo}}} + \mathcal{O} \left(\frac{1}{x_{\text{fo}}^3} \right) \quad (2.58)$$

and the relic density formula becomes

$$\Omega h^2 = \frac{1.07 \cdot 10^9 x_{\text{fo}}}{\bar{g}_{\text{tot}} M_{Pl} (a^{(0)} + (3 a^{(1)})/(4 x_{\text{fo}}))} \text{GeV}^{-1}. \quad (2.59)$$

Furthermore substituting the expansion in Eq. (2.57) into Eq. (2.35) we find that x_{fo} is equal to

$$x_{\text{fo}} \simeq \ln \left(0.038c(c+2)gM_{Pl}m a^{(0)} \right) - \frac{1}{2} \ln \left(g_{*s} \ln \left(0.038c(c+2)gM_{Pl}m a^{(0)} \right) \right) \quad (2.60)$$

Many authors expand the quantity σv_{lab} in powers of the relative velocity v_{lab} . Noting that in the non relativistic limit we have

$$\epsilon \simeq \frac{v_{\text{lab}}^2}{4}, \quad (2.61)$$

the expansion of σv_{lab} in terms of v_{lab} read as

$$\sigma v_{\text{lab}} = \sum_{n=0}^{\infty} \frac{a^{(n)}}{n!} \epsilon^n = \sum_{n=0}^{\infty} \frac{a^{(n)}}{n!} \frac{v_{\text{lab}}^{2n}}{4^n} \equiv \sum_{n=0}^{\infty} \frac{b^{(n)}}{n!} v_{\text{lab}}^{2n} \quad (2.62)$$

where the coefficients $a^{(n)}$ and $b^{(n)}$ are related by

$$b^{(n)} = \frac{a^{(n)}}{4^n}. \quad (2.63)$$

In particular the above result for the relic density change as [42], [19]

$$\Omega h^2 = \frac{1.07 \cdot 10^9 x_{\text{fo}}}{\bar{g}_{\text{tot}} M_{Pl} (a^{(0)} + 3 b^{(1)}/x_{\text{fo}})} \text{GeV}^{-1} \quad (2.64)$$

2.3 Co-annihilations

There are exception where the standard solution of the Boltzmann equation given above fails. One of these exceptions occurs when the lightest particle is nearly mass degenerate with a set of other particles. When this is the case the present relic density of the lightest particle would not be determined only by its annihilation processes but also by the annihilation processes between the slightly heavier particles, which will later decay into the lightest one [45]. Following ref [33], we consider a system formed by N nearly degenerate species, X_i , with $i = 1, \dots, N$, with g_i internal degrees of freedom, and masses m_i ; we assume that the label i runs from the lightest to the heaviest particle, $m_1 < m_2 < \dots < m_N$, and also that the lightest one is a stable particle. The latter requirement can be satisfied assuming that X_1 carries a multiplicatively conserved quantum number which prevent its decay. Note that this quantum number must be the same for all the particles in the set. For example if X_i are supersymmetric particles this quantum conserved number is provided by R-parity which prevents the decay of the lightest supersymmetric particle into SM particles as we will see in the next Chapter. For the system under consideration, the reactions which can change the X_i number densities are

$$X_i X_j \leftrightarrow ll' \quad (2.65)$$

$$X_i l \leftrightarrow X_j l' \quad (2.66)$$

$$X_i \leftrightarrow X_j ll'. \quad (2.67)$$

As in the last section we assume that the l species are relativistic and in (LTE) with the plasma and for this reason, sometimes, we refer to them just as cosmic thermal background. Note that reactions such as $X_i X_j \leftrightarrow X_k l$ and $X_i l \leftrightarrow l' l''$ are forbidden by the assumed symmetry. Also note that, as long as reactions of type (2.67) take place at a reasonable rate, we expect that at the present time all the X_i particles have decayed into the lightest one. The relic abundance of the generic X_i species is determined by a system of N Boltzmann equations such as

$$\begin{aligned} \frac{dn_i}{dt} + 3Hn_i = & - \sum_{j=1}^N \langle \sigma_{ij} v_{ij} \rangle (n_i n_j - n_i^{(0)} n_j^{(0)}) \\ & - \sum_{\substack{j=1 \\ j \neq i}}^N [\langle \sigma'_{lij} v_{ij} \rangle (n_i n_l - n_i^{(0)} n_l^{(0)}) - \langle \sigma'_{l'ij} v_{ij} \rangle (n_j n_l - n_j^{(0)} n_l^{(0)})] \\ & - \sum_{\substack{j=1 \\ j \neq i}}^N [\Gamma_{ij} (n_i - n_i^{(0)}) - \Gamma_{ij} (n_j - n_j^{(0)})] \end{aligned} \quad (2.68)$$

where v_{ij} is the Møller velocity of i, j particles.

The first term on the right-hand side describes $X_i X_j$ annihilations, whose total cross-section is

$$\sigma_{ij} = \sum_{l'} \sigma(X_i X_j \rightarrow ll'). \quad (2.69)$$

The second term describes $X_i \rightarrow X_j$ conversions by scattering with the thermal background, while the last term accounts for X_i decays. Note the relative minus sign for the inverse scattering and production processes. Following Eq. (2.20) we can define the thermal average cross-section of a generic annihilation process as

$$\langle \sigma_{ij} v_{ij} \rangle = \frac{\int \frac{d^3 p_i}{(2\pi)^3} \int \frac{d^3 p_j}{(2\pi)^3} \sigma_{ij} v_{ij} f_i f_j}{\int \frac{d^3 p_i}{(2\pi)^3} \int \frac{d^3 p_j}{(2\pi)^3} f_i f_j} \quad (2.70)$$

where, as usual, f_i is the phase space distribution function, and as in the previous sections we will assume the Maxwell-Boltzmann approximation that sets $f_i = e^{-\frac{E_i}{T}}$. Since all the X_i which remains after the "freeze-out" will decay into X_1 , the relevant quantity is the total number density of all the X_i species, namely

$$n = \sum_{i=1}^N n_i. \quad (2.71)$$

Summing Eq. (2.68) over i from 1 to N , we get an evolution equation for the total number density n

$$\frac{dn}{dt} + 3Hn = - \sum_{i,j=1}^N \langle \sigma_{ij} v_{ij} \rangle (n_i n_j - n_i^{(0)} n_j^{(0)}) \quad (2.72)$$

where the scattering and decay terms cancel in the sum.

Here, as in the previous section, we will assume that the scattering processes, with the cosmic background, take place at rate which is faster than the rate of the annihilation ones and of the expansion rate of the Universe. As we said before this fact enforces the kinematical equilibrium, so the perturbation of the distribution function, during the freeze-out, would be carried by a single function of the temperature $\mu_i(T)$ [43]. Note that the assumption of a nearly mass degeneracy between the species X_i implies that they decouple from the thermal bath at the same epoch. This allows us to assume that the $\mu_i(T)$ would be nearly the same for every species i.e. $\mu_1 \approx \mu_2 \approx \dots \approx \mu_N$. Thus using Eq. (2.12) and Eq. (2.13) for the density numbers n_i and $n_i^{(0)}$, we have that the following approximation holds [45]

$$\frac{n_i}{n} \approx \frac{n_i^{(0)}}{n^{(0)}}. \quad (2.73)$$

where n and $n^{(0)}$ are respectively the total number density and the total number density at the equilibrium. Note that if the annihilation cross-sections, σ_{ij} , are not radically different from those of scattering processes, σ'_{il} , the assumption that the latter occur more rapidly than the former ones is well satisfied. In fact the annihilation rate is about [45]

$$n_i n_j \sigma_{ij} \sim T^3 m_i^{\frac{3}{2}} m_j^{\frac{3}{2}} \sigma_{ij} e^{-\frac{m_i+m_j}{T}} \quad (2.74)$$

while the scattering rate is about

$$n_i n_l \sigma'_{il} \sim T^{\frac{9}{2}} m_i^{\frac{3}{2}} \sigma'_{il} e^{-\frac{m_i}{T}}. \quad (2.75)$$

where we have used the results given in Eq. (2.14) and Eq. (2.15) and the fact that the species l is assumed to be relativistic. From this results we can see that the scattering rates are larger by a factor $\frac{n_l}{n_j} \sim \left(\frac{T}{m_j}\right)^{3/2} e^{m_j/T}$.

In order to recast Eq. (2.72) in a more suitable form it is convenient to define

$$\begin{aligned} r_i &\equiv \frac{n_i^0}{n^0} = \frac{\left(\frac{T}{2\pi}\right) g_i m_i^{\frac{3}{2}} e^{-\frac{m_i}{T}}}{\left(\frac{T}{2\pi}\right) \sum_{i=1}^N g_i m_i^{\frac{3}{2}} e^{-\frac{m_i}{T}}} \\ &= \frac{g_i (\Delta_i + 1)^{\frac{3}{2}} e^{-x \Delta_i}}{g_{\text{eff}}} \end{aligned} \quad (2.76)$$

where we have used Eq. (2.14) and the quantities Δ_i , x and g_{eff} are respectively defined as

$$\Delta_i \equiv \frac{m_i - m_1}{m_1}, \quad x \equiv \frac{m_1}{T}, \quad g_{\text{eff}} \equiv \sum_{i=1}^N g_i (\Delta_i + 1)^{\frac{3}{2}} e^{-x \Delta_i}.$$

With the definition in Eq. (2.76) we can rewrite the the right-hand side of Eq. (2.72) as

$$\begin{aligned} \sum_{i,j=1}^N \langle \sigma_{ij} v_{ij} \rangle (n_i n_j - n_i^{(0)} n_j^{(0)}) &= \sum_{i,j=1}^N \langle \sigma_{ij} v_{ij} \rangle r_i r_j (n^2 - (n^{(0)})^2) \\ &= \langle \sigma_{\text{eff}} v \rangle (n^2 - (n^{(0)})^2) \end{aligned} \quad (2.77)$$

where we have redefined

$$\sum_{i,j=1}^N \langle \sigma_{ij} v_{ij} \rangle r_i r_j \equiv \langle \sigma_{\text{eff}} v \rangle \quad (2.78)$$

Therefore the Boltzmann equation for the total number density n becomes [33], [45]

$$\frac{dn}{dt} + 3Hn = -\langle \sigma_{\text{eff}} v \rangle (n^2 - (n^{(0)})^2). \quad (2.79)$$

This equation has the same form as the one in the standard case, given in Eq. (2.22), and so it can be resolved with the same methods. In particular the relic density formula will be the same as in Eq. (2.34) with $J(x_{\text{fo}})$ redefined as

$$J(x_{\text{fo}}) \equiv \int_{x_{\text{fo}}}^{\infty} \frac{\langle \sigma_{\text{eff}} v \rangle}{x^2} dx. \quad (2.80)$$

Note that the exponential term, $e^{-x \Delta_i}$ in Eq. (2.76), regulates the effectiveness of the various co-annihilation processes. In fact if

$$\Delta_i \gg \frac{1}{x} \quad (2.81)$$

we have that the particular process becomes less important because $r_i \rightarrow 0$ and the contribution of terms like $\langle \sigma_{ij} v_{ij} \rangle r_i r_j$ in Eq. (2.78) are negligible. Thus we can state that the co-annihilations

processes are of fundamental importance in the evaluation of the relic abundance of species X_1 if

$$\Delta_i \lesssim \frac{1}{x}. \quad (2.82)$$

For what concern the thermal average of $\sigma_{ij}v_{ij}$ also in the case of co-annihilations we have that the relation given in Eq. (2.73) holds,

$$\langle \sigma_{ij}v_{ij} \rangle = \langle \sigma_{ij}v_{ij}^{\text{lab}} \rangle^{\text{lab}}. \quad (2.83)$$

The quantity $\sigma_{ij}v_{ij}^{\text{lab}}$, as in the previous section, can be expanded as

$$\sigma_{ij}v_{ij}^{\text{lab}} = \sum_{n=0}^{\infty} \frac{a_{ij}^{(n)}}{n!} \epsilon_{ij}^n \quad (2.84)$$

where ϵ_{ij} is the total kinetic energy per unit of mass of particles X_i and X_j in the laboratory frame i.e. the rest frame of species i , which is equal to

$$\epsilon_{ij} = \frac{(E_{i\text{lab}} - m_i) + (E_{j\text{lab}} - m_j)}{m_i + m_j} = \frac{E_{j\text{lab}} - m_j}{m_i + m_j} \quad (2.85)$$

Following the same procedure of the standard case given in Appendix A we have that

$$\langle \sigma_{ij}v_{ij}^{\text{lab}} \rangle_{\text{n.r.}}^{\text{lab}} = \sum_{n=0}^{\infty} \frac{a_{ij}^{(n)}}{n!} \frac{1}{x^n (1 + \Delta_i)^n} \frac{(2n+1)!!}{2^n}. \quad (2.86)$$

Using this result and the definition in Eq. (2.78), we can define the quantities [45]

$$I_{0\text{eff}} \equiv \frac{x_{\text{fo}}}{a_{11}^{(0)}} \sum_{i,j=1}^N \int_{x_{\text{fo}}}^{\infty} \frac{a_{ij}^{(0)} g_i g_j (\Delta_i + 1)^{\frac{3}{2}} (\Delta_j + 1)^{\frac{3}{2}} e^{-x\Delta_i} e^{-x\Delta_j}}{x^2 g_{\text{eff}}^2} \quad (2.87)$$

$$I_{1\text{eff}} \equiv \frac{x_{\text{fo}}^2}{a_{11}^{(1)}} \sum_{i,j=1}^N \int_{x_{\text{fo}}}^{\infty} \frac{a_{ij}^{(1)} g_i g_j (\Delta_i + 1)^{\frac{3}{2}} (\Delta_j + 1)^{\frac{3}{2}} e^{-x\Delta_i} e^{-x\Delta_j}}{x^3 (1 + \Delta_i) g_{\text{eff}}^2} \quad (2.88)$$

With these formulae we can approximate the integral given in Eq. (2.80) as

$$J(x_{\text{fo}}) \simeq \left(a_{11}^{(0)} I_{0\text{eff}} + \frac{3}{2} I_{1\text{eff}} \frac{a_{11}^{(1)}}{x_{\text{fo}}} \right) \frac{1}{x_{\text{fo}}}, \quad (2.89)$$

which replaced in the relic density formula gives

$$\Omega h^2 = \frac{1.07 \cdot 10^9 x_{\text{fo}}}{\bar{g}_{\text{eff}} M_{\text{Pl}} (a_{11}^{(0)} I_{0\text{eff}} + 3/2 a_{11}^{(1)} I_{1\text{eff}}/x_{\text{fo}})} \text{GeV}^{-1}. \quad (2.90)$$

In the case of co-annihilation the x_{fo} is given by

$$x_{\text{fo}} \simeq \ln \left[\frac{0.038c(c+2)g_{\text{eff}}M_{\text{Pl}}m_1 \langle \sigma_{\text{eff}}v_{\text{M}} \rangle}{g_{*s}^{1/2} x_{\text{fo}}^{1/2}} \right]. \quad (2.91)$$

where we have used Eq. (2.35).

To conclude this Chapter we note that there are situations where the thermal average of σv , both in the standard case that in the co-annihilations one, is poorly approximate by the expansions given above. For example if the annihilation process occurs near a resonance the expansion of the cross-section is inappropriate, because the propagator in the amplitude leads to derivatives with alternating signs [43]. For this reason we give an exact formula for $\langle \sigma_{\text{eff}}v \rangle$ which is computed in the Appendix A. The exact formula is

$$\langle \sigma_{\text{eff}}v \rangle = \frac{\int_0^{\infty} dp_{\text{eff}} p_{\text{eff}}^2 W_{\text{eff}} K_1\left(\frac{\sqrt{s}}{T}\right)}{m_1^4 T \left[\sum_i \frac{g_i}{g_1} \frac{m_i^2}{m_1^2} K_2\left(\frac{m_i}{T}\right) \right]^2}. \quad (2.92)$$

where W_{eff} and p_{eff} are respectively defined in Appendix A, and $K_1(x)$, $K_2(x)$ are the Bessel function respectively of the first and second kind [1].

Chapter 3

Supersymmetry and Dark Matter

In this Chapter we briefly review the more important features of a supersymmetric theory, following, principally, refs. [54] and [5]. In particular we start recalling the more important theoretical motivation which lead to the introduction of supersymmetry (SUSY), namely the "hierarchy problem". After that we will give the basic bricks to construct a supersymmetric theory and then we will specialize on the R -parity conserving minimal supersymmetric standard model (MSSM), giving its particle content with a particular attention to neutralinos, which constitute the DM candidates considered in this thesis.

3.1 Why Supersymmetry

The Standard Model (SM) of particles, provided with an adequate extension to explain the origins of neutrino's masses, is a remarkably successful theory, which is able to explain the phenomenology of elementary particles, from an energy scale of few eV to about 10^2 GeV. So, one, may wonder why we need to go beyond the SM, introducing, for example, an intricate formalism such as the supersymmetric one. The motivation to this relies on the fact that the SM is affected by some theoretical problems [5].

One of these issues is the, so called, "hierarchy problem". This problem is related to a rather high sensitivity of SM Higgs potential and, in particular of the Higgs mass parameter, to the high energy scale.

The SM Higgs potential is defined as [5]

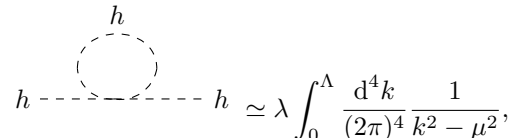
$$V_H = \mu^2 \phi^\dagger \phi + \frac{\lambda}{4} (\phi^\dagger \phi)^2 \quad (3.1)$$

where, $\phi \equiv \begin{pmatrix} \phi^+ \\ \phi^0 \end{pmatrix}$, is the $SU(2)_L$ Higgs doublet, while λ and μ are respectively the self-interaction coupling constant and the Higgs mass parameter. To spontaneously break the electroweak symmetry, the Higgs field must acquire a non-vanishing vacuum expectation value (VEV), which is defined as $\langle \phi \rangle_0 \equiv v/\sqrt{2}$; note that this is possible if and only if $\lambda > 0$ and $\mu^2 < 0$.

From measurements regarding the proprieties of the weak interaction, the VEV is known to be about [5]

$$\sqrt{\frac{2\mu^2}{\lambda}} = \frac{v}{\sqrt{2}} \approx 174 \text{ GeV}. \quad (3.2)$$

The "hierarchy problem" arise when we include high order corrections to the μ parameter. For example, at the one loop, the self-interaction term gives the diagram [5]


$$h \text{ --- } \text{loop} \text{ --- } h \simeq \lambda \int_0^\Lambda \frac{d^4 k}{(2\pi)^4} \frac{1}{k^2 - \mu^2}, \quad (3.3)$$

3.2 Basics of SUSY

As we said in the previous section, SUSY transformations turn bosons into fermions and vice versa, see Eq. (3.6). Thus, changing the spin of the field from integer to semi-integer and vice versa, they act directly on the representation of a given field under the Poincarè algebra. This suggest that SUSY must be a space-time symmetry.

The question if and how is possible to extend the Poincarè algebra in order to include also SUSY transformations, is a non trivial issue. From the Coleman-Mandula theorem [28], any new conserved operator, other than the already present four-momentum vector P_μ and the anti-symmetric angular-momentum tensor $M_{\mu\nu}$, can have only a trivial character or, in other words, it must be a Lorentz scalar. Adding more conserved operators with non-trivial Lorentz transformations would lead to a restriction of the possible kinematical configurations in a scattering process [5]. Nevertheless the Coleman-Mandula theorem does not take into account the possibility that the new operator could be a spinor. In fact the Haag-Lopuszanski-Sohnius [46] extension theorem state that using both commutative and anti-commutative generators, the Poincarè algebra can be extended in a non-trivial way, leading to the more general supersymmetric algebra.

Thus the generator of a SUSY transformation, Q , has a spinor character. Note that because spinors are intrinsically complex objects, also Q^\dagger must be a SUSY generator [54]. In principle we can add more spinorial generators, but in this thesis we refer only to a model with only two SUSY generators, namely Q and Q^\dagger . In light of this the components of the SUSY generators, Q_a and Q_b^\dagger must satisfied both commutation and anti-commutation relations, which are [54]

$$\{Q_a, Q_b^\dagger\} = -2\sigma_{ab}^\mu P_\mu \quad (3.9a)$$

$$\{Q_a, Q_b\} = \{Q_a^\dagger, Q_b^\dagger\} = 0 \quad (3.9b)$$

$$[Q_a, P_\mu] = [Q_b^\dagger, P_\mu] = 0, \quad (3.9c)$$

where P_μ is the 4-dimensional conserved momentum vector. Note that the appearance of P_μ in the first relation is consistent with the fact that it transforms like a 1-spin object under Lorentz transformations, while Q and Q^\dagger transforms as 1/2-spin objects [54].

As we know in a generic quantum field theory every field must belong to an irreducible representation of the Poincarè algebra. Within the SUSY algebra the irreducible representations are called supermultiplets.

Because SUSY generators turn bosons into fermions and vice versa, every supermultiplet must contains both fermionic and bosonic states. Following [54] we can show that every supermultiplet must contain the same number of bosonic and fermionic d.o.f. Defining S as the spin angular momentum operator, the operator $(-1)^{2S}$ has eigenvalues respectively

$$(-1)^{2S} |f\rangle = (-1) |f\rangle, \quad (-1)^{2S} |b\rangle = (+1) |b\rangle, \quad (3.10)$$

where f denotes a fermionic state and b a bosonic one. Using Eqs. (3.6) it is straightforward to show that

$$\{(-1)^{2S}, Q_a\} = 0. \quad (3.11)$$

Furthermore, given a supermultiplet we can consider a subspace of states $|i\rangle$ which, tanks to relations (3.9), all have the same eigenvalue of the 4-momentum operator P_μ . This assures that any combinations of Q and Q^\dagger cannot change the 4-momentum of the states $|i\rangle$ and so we have a completeness relation within their subspace, $\sum_i |i\rangle \langle i|$.

Now taking the trace over all $|i\rangle$ of the operator $(-1)^{2S} P_\mu$ we have

$$-2\sigma_{ab}^\mu \sum_i \langle i| (-1)^{2S} P_\mu |i\rangle = \sum_i \langle i| (-1)^{2S} Q_a Q_b^\dagger |i\rangle + \sum_i \langle i| (-1)^{2S} Q_b^\dagger Q_a |i\rangle \quad (3.12)$$

where we used Eqs. (3.9). Now inserting the completeness relation in the second term of the

above expression we find

$$\begin{aligned} -2\sigma_{ab}^\mu \sum_i \langle i | (-1)^{2S} P_\mu | i \rangle &= \sum_i \langle i | (-1)^{2S} Q_a Q_b^\dagger | i \rangle + \sum_i \sum_j \langle i | (-1)^{2S} Q_b^\dagger | j \rangle \langle j | Q_a | i \rangle \\ &= \sum_i \langle i | (-1)^{2S} Q_a Q_b^\dagger | i \rangle + \sum_j \langle j | Q_a (-1)^{2S} Q_b^\dagger | j \rangle \end{aligned} \quad (3.13)$$

and using Eq. (3.11) we get

$$-2\sigma_{ab}^\mu \sum_i \langle i | (-1)^{2S} P_\mu | i \rangle = \sum_i \langle i | (-1)^{2S} Q_a Q_b^\dagger | i \rangle - \sum_j \langle j | (-1)^{2S} Q_a Q_b^\dagger | j \rangle = 0. \quad (3.14)$$

Knowing that every $|i\rangle$ state has the same 4-momentum p_μ and taking into account relations (3.10), the previous result can be rewritten as

$$p_\mu \text{Tr}\{(-1)^{2S}\} = p_\mu (n_b - n_f) = 0 \quad (3.15)$$

which, if $p_\mu \neq 0$, implies that $n_b = n_f$, where n_b and n_f denote respectively the number of bosonic and fermionic d.o.f.

SUSY algebra, given in Eq. (3.9), implies that Q commutes also with $P_\mu P^\mu \equiv P^2$. Thus within the same supermultiplet the bosonic d.o.f. and the fermionic ones must have the same P^2 eigenvalue and therefore they have the same mass.

Furthermore the generators of gauge transformations commute with the SUSY generators Q and Q^\dagger . Therefore all the particles in a given supermultiplet must be in the same representation of the gauge group [54]

The type of supermultiplets which compare in a renormalizable SUSY theory are called chiral and vector supermultiplets.

Chiral supermultiplets are the supersymmetric generalization of spinors field and they are composed by a Weyl spinor ψ_i with an associated scalar complex field, ϕ_i and a further scalar complex auxiliary field F_i , which does not propagate and so it cannot represent any particle. The associated non-interacting supersymmetric Lagrangian is [58]

$$\mathcal{L}_{\text{Chiral}} = \partial_\mu \phi_i^\dagger \partial^\mu \phi_i + i\psi_i^\dagger \bar{\sigma}^\mu \partial_\mu \psi_i + F_i^\dagger F_i \quad (3.16)$$

where the index i indicates all gauge and/or flavor d.o.f., and as usual the sum over repeated indices is understood. The auxiliary field is added to maintain the equality between bosonic and fermionic d.o.f. both on-shell and off-shell. In fact as we can check [47], from the equations of motion we note that F_i has no free components while ϕ_i , as a complex scalar field, has 2 free components and so the total number of bosonic d.o.f., on-shell, is $n_b = 2$. A Weyl spinor, on-shell, has 2 free components, which lead to a total number of fermionic d.o.f. $n_f = 2$. Thus on-shell the relation $n_b = n_f$ holds.

Conversely off-shell a Weyl spinor has 4 free components while a scalar complex field still has 2 free components and so without the field F_i there would be a mismatch between n_f and n_b . The fact that the field F_i , without the constraint provided by the equations of motion has 2 free components, implies that its introduction will restore the relation $n_f = n_b$ also off-shell, where $n_f = 4$ and $n_b = 4$. Moreover the introduction of the field F_i , provided with the appropriate SUSY transformations, will assure that the SUSY algebra closes both on-shell and off-shell [54].

Vector supermultiplets are the supersymmetrization of the gauge boson fields. They contain a vector field A_μ^a , an associated Weyl spinor, λ^a , called gaugino and an auxiliary real scalar field D^a which is introduced for the same reasons which lead to the introduction of F_i . All these fields belong to the adjoint representation of the associated gauge group. A sample of their Lagrangian is [58]

$$\mathcal{L}_{\text{Vector}} = -\frac{1}{4} F_{\mu\nu}^a F^{a\mu\nu} + i\lambda^{\dagger a} \bar{\sigma}^\mu D_\mu \lambda^a + \frac{1}{2} D^a D^a \quad (3.17)$$

where the sum over repeated a is understood. $F_{\mu\nu}^a = \partial_\mu A_\nu^a - \partial_\nu A_\mu^a + gf^{abc}A_\mu^b A_\nu^c$ is the field strength and $D_\mu \lambda^a = \partial_\mu \lambda^a + g_a f^{abc} A_\mu^b \lambda^c$ is the covariant derivative where g_a is the gauge coupling constant², and the f^{abc} s are the structure constants.

As usual to make the chiral Lagrangian (3.16) gauge invariant we have to promote the ordinary derivative to a covariant one $\partial_\mu \rightarrow D_\mu$ which for chiral fields is defined as $D_\mu \psi_i = \partial_\mu \psi_i + ig_a T_{ij}^a A_\mu^a \psi_j$, where T_{ij}^a are the generators of the gauge group and the same definition holds also for ϕ_i . After that combining the Lagrangians (3.16), (3.17), we can write the SUSY Lagrangian as

$$\begin{aligned} \mathcal{L}_{\text{Free}}^{\text{SUSY}} = & D_\mu \phi_i^\dagger D^\mu \phi_i + i\psi_i^\dagger \bar{\sigma}^\mu D_\mu \psi_i + F_i^\dagger F_i - \frac{1}{4} F_{\mu\nu}^a F^{a\mu\nu} + i\lambda^{\dagger a} \bar{\sigma}^\mu D_\mu \lambda^a \\ & + \frac{1}{2} D^a D^a + (\sqrt{2}g(\phi_i^\dagger T_{ij}^a \psi_j)\lambda^a + h.c.) + g_a(\phi_i^\dagger T_{ij}^a \phi_j) D^a \end{aligned} \quad (3.18)$$

where the last 3 terms come from the necessity to consider all the possible supersymmetric, renormalizable and gauge invariant interactions. However in a realistic theory there are also mass and non-gauge interactions³. It is possible to show [54], that the most general, renormalizable interaction Lagrangian which is also gauge and supersymmetric invariant, can be written as

$$\mathcal{L}_{\text{Int}}^{\text{SUSY}} = \left(-\frac{1}{2} W_{ij}^a \psi_i \psi_j + W_i F_i \right) + h.c. \quad (3.19)$$

where W_{ij} and W_i turn out to be respectively

$$W_{ij} = \frac{\delta^2 W}{\delta \phi^i \delta \phi^j} \quad W_i = \frac{\delta W}{\delta \phi^i}. \quad (3.20)$$

The functional W is called superpotential and its form is completely determined by the requirement that the Lagrangian (3.19) must be supersymmetric invariant

$$W = \frac{1}{2} M_{ij} \phi_i \phi_j + \frac{1}{3!} y_{ijk} \phi_i \phi_j \phi_k. \quad (3.21)$$

Note that just because the mass dimension of (3.19) must be $[\mathcal{L}_{\text{int}}] = 4$, we have that the superpotential has $[W] = 3$ and thus the matrix M_{ij} has $[M_{ij}] = 1$ while the Yukawa-like couplings have $[y_{ijk}] = 0$. It is important to note that treating the scalar fields ϕ_i as complex variables, the superpotential Eq. (3.21), is a holomorphic function [54]. This fact will have a fundamental consequence as we will see below. To finish we note that the auxiliary fields F_i and D^a , via their equations of motion, can be rewritten in terms of the scalars ϕ_i . In fact using the total supersymmetric Lagrangian

$$\mathcal{L}_{\text{Tot}}^{\text{SUSY}} = \mathcal{L}_{\text{Free}}^{\text{SUSY}} + \mathcal{L}_{\text{Int}}^{\text{SUSY}} \quad (3.22)$$

the equations of motion for F_i and D^a turn out to be

$$F_i = -W_i \quad D^a = -g_a(\phi_i^\dagger T_{ij}^a \phi_j), \quad (3.23)$$

and consequently we can eliminate them in favour of ϕ_i 's, obtaining a SUSY Lagrangian containing only scalars, ϕ_i , Weyl fermions, ψ_i , gauge vectors, A_μ^a , and gauginos, λ^a .

3.3 The Minimal Supersymmetric Standard Model

The Minimal Supersymmetric Standard Model is the supersymmetric version of the SM, with the minimal particle content [58]. First of all to promote the SM to a supersymmetric theory we need to define all the superpartners of the fields present in the SM Lagrangian. In other words

²Here the index a has not to be summed, it labels only the gauge group.

³It does not mean that these interaction terms are not gauge invariant, it means that the interaction terms do not come from covariant derivatives.

we have to define all the supermultiplets remembering that the partners and the associated superpartners transform in the same way under the SM gauge group $SU(3)_c \times SU(2)_L \times U(1)_Y$.

For what concerns leptons and quarks we have to take into account that their left-handed and right-handed parts transform differently under the SM gauge group. For this reason they must be member of different chiral supermultiplets. Thus the left-handed leptons form chiral supermultiplets (one for each family generation) with their scalar superpartners which are called left-handed sleptons. The same holds for the left-handed quarks, where their superpartners are called left-handed squarks. For what concerns the right-handed fermions we follow the convention used in [54], where, instead to take them explicitly, are used their conjugate versions. Also here to each right-handed leptons/quarks is associated a right-handed sleptons/squarks which together form chiral supermultiplets. In such a manner the MSSM chiral sector is defined in terms of only left-handed fields.

The SM gauge vector bosons are put, with their gauginos superpartners, into vector supermultiplets. So the $SU(2)_L$ gauge bosons, W^\pm and W^0 , have their fermionic superpartner which are called winos and are indicated as \tilde{W}^\pm and \tilde{W}^0 . The definition of \tilde{W}^\pm follows directly from the one for W^\pm gauge boson [5], and so we have

$$\tilde{W}^\pm \equiv \frac{\tilde{W}^1 \mp i\tilde{W}^2}{\sqrt{2}}, \quad (3.24)$$

where \tilde{W}^1 and \tilde{W}^2 are the superpartners respectively of W^1 and W^2 gauge bosons. The fermionic superpartner of B , the $U(1)_Y$ gauge boson, is called bino and it is indicated as \tilde{B} . It is worth to note that \tilde{B} and \tilde{W}^0 can be mixed to form the superpartners of the Z^0 boson and of the photon, γ , which are called zino, \tilde{Z}^0 , and photino, $\tilde{\gamma}$. As last gluinos, \tilde{g} , are the fermionic superpartners of the gluons, g , and also them, they are an $SU(3)_c$ octet.

The Higgs sector can be supersymmetrize putting the SM Higgs doublet, $H_u \equiv \begin{pmatrix} H_u^+ \\ H_u^0 \end{pmatrix}$, in a chiral supermultiplet with the corresponding fermionic superpartner $\tilde{H}_u \equiv \begin{pmatrix} \tilde{H}_u^+ \\ \tilde{H}_u^0 \end{pmatrix}$, called Higgsino. Unfortunately in a SUSY theory this is not enough.

In the SM we can give mass to down type quarks via the Higgs field H_u . In order to give mass also to up type quarks, in the SM, we use the definition[58]

$$\hat{H}_u \equiv i\sigma_2 H_u^* = \begin{pmatrix} H_u^{0*} \\ -H_u^- \end{pmatrix}. \quad (3.25)$$

This recipe does not work in a SUSY theory, for two reasons. First, recalling what we said above, the superpotential must be an holomorphic function of its fields and so it cannot contains their complex conjugate versions. Second, if there is only one chiral supermultiplets the MSSM would suffer of a gauge anomaly. In the SM this anomaly cancels among the contributions of various fermions. The condition for anomaly cancellation is [47]

$$\text{Tr}\{T_3^2 Y\} = \text{Tr}\{Y^3\} = 0 \quad (3.26)$$

where T_3 is the diagonal (usually the third) generator of the $SU(2)_L$ algebra while Y are the $U(1)_Y$ hypercharges. Using the hypercharge values given in Tab. (3.1), it is straightforwardly to check that in SM this relation holds. Now the introduction of a new fermion with $Y_u = 1/2$, namely the higgsino \tilde{H}_u , definitely spoils the relation in (3.26), restoring the anomaly[47]. This can be cancelled again introducing a new Higgs doublet, which is define as $H_d \equiv \begin{pmatrix} H_d^0 \\ H_d^- \end{pmatrix}$ with an opposite hypercharge, $Y_d = -1/2$. This new Higgs field forms a supermultiplet with its higgsino superpartner define as $\tilde{H}_d \equiv \begin{pmatrix} \tilde{H}_d^0 \\ \tilde{H}_d^- \end{pmatrix}$. Thus, in this manner, the relation (3.26) is restored, because of the cancellation between Y_u and Y_d . Note that H_d can be used also to give mass to up type quarks, preventing the use of complex conjugate fields in the superpotential. All the particle content of the MSSM is depicted in Tab. (3.1)

Names		Fields		$(SU(3)_c, SU(2)_L, Y)$
quarks	squarks	$Q \equiv \begin{pmatrix} u_L \\ d_L \end{pmatrix}$	$\tilde{Q} \equiv \begin{pmatrix} \tilde{u}_L \\ \tilde{d}_L \end{pmatrix}$	$(\mathbf{3}, \mathbf{2}, \frac{1}{6})$
		u_R^\dagger	\tilde{u}_R^*	$(\bar{\mathbf{3}}, \mathbf{1}, -\frac{2}{3})$
		d_R^\dagger	\tilde{d}_R^*	$(\bar{\mathbf{3}}, \mathbf{1}, \frac{1}{3})$
leptons	sleptons	$L \equiv \begin{pmatrix} \nu_L \\ e_L \end{pmatrix}$	$\tilde{L} \equiv \begin{pmatrix} \tilde{\nu}_L \\ \tilde{e}_L \end{pmatrix}$	$(\mathbf{1}, \mathbf{2}, -\frac{1}{2})$
		e_R^\dagger	\tilde{e}_R^*	$(\mathbf{1}, \mathbf{1}, 1)$
Higgs	higgsinos	$H_u \equiv \begin{pmatrix} H_u^+ \\ H_u^0 \end{pmatrix}$	$\tilde{H}_u \equiv \begin{pmatrix} \tilde{H}_u^+ \\ \tilde{H}_u^0 \end{pmatrix}$	$(\mathbf{1}, \mathbf{2}, \frac{1}{2})$
		$H_d \equiv \begin{pmatrix} H_d^0 \\ H_d^- \end{pmatrix}$	$\tilde{H}_d \equiv \begin{pmatrix} \tilde{H}_d^0 \\ \tilde{H}_d^- \end{pmatrix}$	$(\mathbf{1}, \mathbf{2}, -\frac{1}{2})$
gluons	gluinos	g	\tilde{g}	$(\mathbf{8}, \mathbf{1}, 0)$
Wbosons	winos	$W^\pm \quad W^0$	$\tilde{W}^\pm \quad \tilde{W}^0$	$(\mathbf{1}, \mathbf{3}, 0)$
Bboson	bino	B	\tilde{B}	$(\mathbf{1}, \mathbf{1}, 0)$

Table 3.1: In the table are summarized all the particles of the MSSM model. The convention used for the hypercharge assignment is $Q = T_3 + Y$ where Q is the electric charge normalized with the electronic one and with T_3 we denote the component of the diagonal generator of the $SU(2)_L$ group.

Now that we know the particle content of the MSSM the other thing that we need to specified is the superpotential. For the MSSM it is defined as [5]

$$W_{\text{MSSM}} = y_u^{ij} \tilde{u}^{*i} \tilde{Q}^j \cdot H_u - y_d^{ij} \tilde{d}^{*i} \tilde{Q}^j \cdot H_d - y_e^{ij} \tilde{e}^{*i} \tilde{Q}^j \cdot H_d + \mu H_u \cdot H_d \quad (3.27)$$

where the indices i, j run over family generations and we have suppressed the color indices. The (\cdot) means the $SU(2)_L$ invariant product of doublets i.e. $H_u \cdot H_d \equiv \epsilon_{\alpha\beta} H_u^\alpha H_d^\beta$ where $\epsilon_{\alpha\beta}$ is the total anti-symmetric tensor in two dimensions. The parameters y_u, y_d, y_e are Yukawa 3×3 matrices in family space and in particular they are exactly the same Yukawa matrices which enter in the SM. In fact, as we can see from Eq. (3.21), when the Higgs fields H_u and H_d respectively acquire VEVs these couplings provide the masses to quarks and leptons. On contrary the μ parameter is a new one and it has nothing to do with the μ mass parameter of the SM Higgs scalar potential given in Eq. (3.1).

As we mentioned before, in an unbroken SUSY framework all the members of the same supermultiplet must have the same mass. In the MSSM this would imply, for example, that selectrons would have the same mass of the electrons, $m_{\tilde{e}} = m_e \simeq 0.511 \text{ MeV}$ [60], and this would made them easily detectable. The fact that no one of the superpartners of the SM particles have been detected, suggests that at the electroweak energy scale SUSY must be a broken symmetry. Roughly speaking there are two way to break a symmetry, the first is by introducing terms which spoil the symmetry explicitly while the second is by spontaneously breaking it, as it happens to the electroweak symmetry in the SM [5]. Here we adopt the first approach, taking into account only the effects of an unknown breaking mechanism which is assumed to operate at some high energy scale.

However there is another subtle point with the SUSY breaking issue. The SUSY braking parameters must be *soft* terms, which means that their coupling parameters must have positive mass dimension [54]. The motivation to this requirement is related to the "hierarchy problem". As we can see from Eq. (3.8) to resolve (at any radiative order) the problem of the quadratic divergence, the equality between the coupling constants must holds i.e. $\lambda_b = g_f^2$. If the SUSY breaking terms contain coupling constants of null-mass dimension, the radiative corrections due to these non-*soft* terms would make the equality between λ_b and g_f^2 no longer valid and the quadratically divergence will be restored [5]. So we require that the breaking terms have to be *soft*, because we want that SUSY still resolves the "hierarchy problem".

The requirement that the relation (3.8) still be resolved, implies that the corrections due to the *soft* terms to μ^2 , have to be proportional to $\ln(\Lambda/m_{soft}^2)$ [54]. By dimensional analysis this corrections have the form [5]

$$\delta\mu^2 \simeq m_{soft}^2 \ln(\Lambda/m_{soft}^2) \quad (3.28)$$

where m_{soft} is the typical energy scale of SUSY breaking terms. From this result we can also argue that, to ensure that SUSY still provides a solution to the "hierarchy problem", m_{soft} must not be much greater than a few TeV.

For these reasons to provide a phenomenologically viable model we have to introduce in the unbroken MSSM Lagrangian (3.22) a *soft* Lagrangian, having care to write only those *soft* terms which do not break the MSSM gauge symmetry, $SU(3)_c \times SU(2)_L \times U(1)_Y$. For the MSSM the general \mathcal{L}_{soft} is [54].

$$\begin{aligned} \mathcal{L}_{soft} = & -\frac{1}{2}(M_3\tilde{g}\tilde{g} + M_2\tilde{W}^0\tilde{W}^0 + M_1\tilde{B}\tilde{B} + h.c.) - M_2\tilde{W}^+\tilde{W}^- \\ & - (a_u\tilde{u}^*\tilde{Q} \cdot H_u - a_d\tilde{d}^*\tilde{Q} \cdot H_d - a_e\tilde{e}^*\tilde{L} \cdot H_d + h.c.) \\ & - m_{\tilde{Q}}^2\tilde{Q}^\dagger \cdot \tilde{Q} - m_{\tilde{L}}^2\tilde{L}^\dagger \cdot \tilde{L} - m_{\tilde{e}}^2\tilde{e}^*\tilde{e} - m_{\tilde{u}}^2\tilde{u}^*\tilde{u} - m_{\tilde{d}}^2\tilde{d}^*\tilde{d} \\ & - m_{H_u}^2H_u^\dagger \cdot H_u - m_{H_d}^2H_d^\dagger \cdot H_d - (bH_u \cdot H_d + h.c.), \end{aligned} \quad (3.29)$$

where we have suppressed all the flavor and color indices. The constants M_1 , M_2 and M_3 have a mass dimension of one and are called respectively bino, wino and gluino mass parameters. The constants a_u , a_d , a_e and $m_{\tilde{Q}}$, $m_{\tilde{L}}$, $m_{\tilde{e}}$, $m_{\tilde{u}}$, $m_{\tilde{d}}$ are 3×3 matrices in the families space and they have a mass dimension of one. It is worth to remark that in order to resolve the "hierarchy problem", we must have that

$$\begin{aligned} M_1, M_2, M_3, a_u, a_d, a_e & \sim m_{soft} \\ m_{\tilde{Q}}^2, m_{\tilde{L}}^2, m_{\tilde{e}}^2, m_{\tilde{u}}^2, m_{\tilde{d}}^2, m_{H_u}^2, m_{H_d}^2, b & \sim m_{soft}^2. \end{aligned}$$

3.4 R -parity

The MSSM superpotential given in Eq. (3.21) is not the most general one. In fact, in principle, we can also introduce the renormalizable and gauge invariant terms [54]

$$W_{\Delta L, \Delta B} = \frac{1}{2}\lambda_{ijk}\tilde{L}_i\tilde{L}_j\tilde{e}_k^* + \lambda'_{ijk}\tilde{L}_i\tilde{Q}_j\tilde{d}_k^* + \mu'\tilde{L}_i \cdot H_u + \frac{1}{2}\lambda''_{ijk}\tilde{u}_i^*\tilde{d}_j^*\tilde{d}_k^*. \quad (3.30)$$

Assign to the sfermions the same Baryon, B , and Lepton, L , numbers of the relative fermionic partners, we have that $B = +1/3$ and $L = 0$ for \tilde{Q}_i and \tilde{d}_i , $B = -1/3$ and $L = 0$ for \tilde{u}_i^* and \tilde{d}_i^* , while $L = 1$ and $B = 0$ for \tilde{L}_i and $L = -1$ and $B = 0$ for \tilde{e}_i^* . Therefore as we can see the first three terms in the Lagrangian (3.30) violate the total Lepton number by a unit, $\Delta L = 1$, while the last term violates the Baryon number by a unit, $\Delta B = 1$.

At the present time we have no experimental evidences of processes, between SM particles, which violate B and L . Furthermore if λ' and λ'' are both different from zero there would be the chance to have a proton lifetime extremely short. For example a process like $p \rightarrow \pi^0 e^+$, mediated by a squarks with a mass of about 1 TeV, would lead to a proton lifetime of a small fraction of a second [54].

So, to neglect terms as those given in Eq. (3.30), the most simple possibility would be to take L and B exactly conserved. However we know that L and B are violated by non-perturbative electroweak effects [5]. So neither B nor L can be taken as exact symmetries. Therefore a new symmetry is needed to prevent the presence of terms such as the ones in (3.30). This new symmetry is called R -parity and it is defined as [54]

$$R = (-1)^{3(B-L)+2S} \quad (3.31)$$

where S is the spin operator. From the Baryon and Lepton number assignments given above, it is easily to see that each SM particles have $R = +1$ while each superpartners have $R = -1$.

The R -parity conservation requirement has the consequence that the possible interaction terms which we can write, must have an even number of odd-particles i.e. particles with odd R -parity. As a consequence the terms in (3.30) are forbidden.

From a phenomenological point of view, R -parity conservation has three important consequences [5]

- The lightest odd-particle, which is called the lightest supersymmetric particle (LSP), is absolutely stable. Furthermore if it is also electrically neutral it can provide a viable DM candidate [37].
- Every odd-particle, more massive than the LSP, must eventually decay into an odd number of, less massive, odd-particles.
- Conversely when the odd-particles are created, for example in collider experiments, they must be produced in an even number.

3.5 DM in the MSSM

One of the more interesting feature of a R -parity conserving SUSY models, is that they naturally provide a DM candidate. Following ref. [37] now we briefly analyse, within the R -parity conserving MSSM, every odd-particle as DM candidate, giving the motivations which prevent or favour this possibility.

We start considering a charged un-colored particle such as charged sleptons. The possibility that the masses of the sleptons lays in the right range to give a relic density consistent with the one given in Eq. (1.13), is ruled out by the failure in the searches of anomalous heavy protons. In particular this result leads to the conclusion that a generic charged odd-particle cannot be the LSP. So also charged winos and/or charged higgsinos cannot form the today DM.

The other possibility is provided by squarks. Due to strong interaction they tend to form new hadrons. So if at least one of these hadrons is stable then the associated squark can be the LSP. Charged hadrons can be ruled out as every other charged odd-particles invoking the failure in the searches of heavy protons. For what concern neutral hadrons, the question is more complicated. However in quite all SUSY models squarks are heavier than sleptons and so there is no possible squark LSP. Another possibility, a neutral one, is provided by gluinos. Also them tend to form new hadrons, but as for squarks also gluinos, in many SUSY models, are more massive than the other gauginos and so they do not provide a good LSP i.e. a good DM candidate. Sneutrinos for long time have been considered as good DM candidate, but today we know that their calculated scattering cross-section with nucleons is much more larger than the limits found by direct detection experiments [19] and so they are ruled out.

What remains in the odd-sector of MSSM are the two neutral gauginos, namely the \tilde{B} and the \tilde{W}^0 , and the neutral components of the higgsinos doublets, namely \tilde{H}_u^0 and \tilde{H}_d^0 . Against them there are no such strong arguments, both experimental and theoretical, as the previous ones. Thus, in principle, every one of them can provide a good DM candidate. More in detail because of electroweak symmetry breaking (EWSB) they tend to mix with each other forming four mass eigenstates called neutralinos. So the less massive of them, in many SUSY models, can be regarded as the LSP and so it provides a viable DM candidate [49].

As we just said the mixing between \tilde{B} , \tilde{W}^0 , \tilde{H}_u^0 and \tilde{H}_d^0 is a direct consequence of EWSB. In the MSSM the breaking of the gauge group $SU(2)_L \times U(1)_Y$ is more complicated than in the SM, because of the presence of two Higgs doublets [54].

We briefly summarize the EWSB in the MSSM context. The MSSM scalar Higgs potential,

it can be written as [5]

$$\begin{aligned}
V_{\text{Higgs}} = & (|\mu|^2 + m_{H_u}^2) \left(|H_u^+|^2 + |H_u^0|^2 \right) + (|\mu|^2 + m_{H_d}^2) \left(|H_d^-|^2 + |H_d^0|^2 \right) \\
& + [b (H_u^+ H_d^- - H_u^0 H_d^0) + h.c.] + \frac{(g^2 + g'^2)}{8} \left(|H_u^+|^2 + |H_u^0|^2 - |H_d^0|^2 - |H_d^-|^2 \right)^2 \\
& + \frac{g^2}{2} \left| H_u^+ H_d^{0\dagger} + H_u^0 H_d^{-\dagger} \right|^2
\end{aligned} \tag{3.32}$$

where g and g' are respectively the $SU(2)_L$ and $U(1)_Y$ coupling constants. Exploiting the $SU(2)_L$ symmetry we can rotate one of the two Higgs doublets in order to obtain that its charged component is setted to zero at the minimum of the Higgs potential, so for instance we can take $H_u^+ = 0$ at the minimum. Furthermore the requirement that $\partial V_{\text{Higgs}} / \partial H_u^+ = 0$, at the minimum, implies that also $H_d^- = 0$. As a consequence we can safely take $H_u^+ = H_d^- = 0$, so the Higgs potential is simplify as

$$\begin{aligned}
V_{\text{Higgs}} = & (|\mu|^2 + m_{H_u}^2) |H_u^0|^2 + (|\mu|^2 + m_{H_d}^2) |H_d^0|^2 - (b H_u^0 H_d^0 + h.c.) \\
& + \frac{(g^2 + g'^2)}{8} (|H_u^0|^2 - |H_d^0|^2)^2
\end{aligned} \tag{3.33}$$

Redefining the phases of H_u^0 and H_d^0 it is possible to reabsorb any phase in b and thus we can regarding to it as a real positive quantity. Furthermore, exploiting the $U(1)_Y$ gauge symmetry, we can transform the fields H_u^0 and H_d^0 in order to have two real and positive VEVs, namely $\langle H_u^0 \rangle \geq 0$ and $\langle H_d^0 \rangle \geq 0$. Also we take to be satisfied all the necessary conditions to have $\langle H_u^0 \rangle \neq 0$ and $\langle H_d^0 \rangle \neq 0$, given in ref. [54].

From the covariant derivative of the Higgs fields we can find that the VEVs are related to the masses of W^\pm and Z^0 bosons by the relations [5]

$$m_{Z^0}^2 = \frac{1}{2} (g^2 + g'^2) (v_u^2 + v_d^2) = \frac{1}{2} (g^2 + g'^2) v^2 \tag{3.34a}$$

$$m_W^2 = \frac{1}{2} g^2 (v_u^2 + v_d^2) = \frac{1}{2} g^2 v^2 \tag{3.34b}$$

where we have redefined $\langle H_u^0 \rangle \equiv v_u$, $\langle H_d^0 \rangle \equiv v_d$ and v is the SM Higgs VEV given in Eq. (3.2).

Instead to take v_u and v_d as new parameters, what is traditionally used is their ratio, which is defined as

$$\tan \beta \equiv \frac{v_u}{v_d}. \tag{3.35}$$

Note that, just because $v_u > 0$ and $v_d > 0$, the definition above implies that $0 \leq \beta \leq \pi/2$.

To the two complex $SU(2)$ -doublet Higgs scalar fields correspond eight real d.o.f. As we know after the EWSB three of them become the longitudinal modes of the massive gauge bosons W^\pm and Z^0 . To the remaining five real d.o.f. correspond five Higgs mass eigenstates which are two CP -even neutral fields h_0 and H_0 , one CP -odd neutral field A_0 , and two charge fields H^\pm . The masses of these Higgs fields are given by [54]

$$\begin{aligned}
m_{A_0}^2 &= 2|\mu|^2 + m_{H_u}^2 + m_{H_d}^2 \\
m_{h_0}^2 &= \frac{1}{2} \left(m_{A_0}^2 + m_{Z^0}^2 - \sqrt{(m_{A_0}^2 - m_{Z^0}^2)^2 + 4m_{Z^0}^2 m_{A_0}^2 \sin^2 2\beta} \right) \\
m_{H_0}^2 &= \frac{1}{2} \left(m_{A_0}^2 + m_{Z^0}^2 + \sqrt{(m_{A_0}^2 - m_{Z^0}^2)^2 + 4m_{Z^0}^2 m_{A_0}^2 \sin^2 2\beta} \right) \\
m_{H^\pm}^2 &= m_{A_0}^2 + m_W^2.
\end{aligned} \tag{3.36}$$

Using these results we can define the mixing angle, α , between h_0 and H_0 , as [54]

$$\frac{\sin 2\alpha}{\sin 2\beta} = - \left(\frac{m_{H_0}^2 + m_{h_0}^2}{m_{H_0}^2 - m_{h_0}^2} \right), \quad \tan 2\alpha = \left(\frac{m_{A_0}^2 + m_{h_0}^2}{m_{A_0}^2 - m_{h_0}^2} \right), \tag{3.37}$$

which is traditionally defined to be a negative quantity, and so we have that $-\pi/2 < \alpha < 0$.

Returning now to neutralinos we refer to them with $\tilde{\chi}_i$ ($i = 1, \dots, 4$) with the convention that the index i runs from the lightest to the heavier one, i.e. from $\tilde{\chi}_1$ to $\tilde{\chi}_4$; note that with this convention $\tilde{\chi}_1$ denote the LSP. The possible mass terms for neutralinos come from the mass Lagrangian [48]

$$\begin{aligned} \mathcal{L}_{\text{Neutralino}} = & + \frac{g}{\sqrt{2}} v_u \tilde{H}_u^0 \tilde{W}^0 - \frac{g'}{\sqrt{2}} v_u \tilde{H}_u^0 \tilde{B} - \frac{g}{\sqrt{2}} v_d \tilde{H}_d^0 \tilde{W}^0 + \frac{g'}{\sqrt{2}} v_d \tilde{H}_d^0 \tilde{B} \\ & + \frac{\mu}{2} (\tilde{H}_u^0 \tilde{H}_d^0 + \tilde{H}_d^0 \tilde{H}_u^0) - \frac{M_1}{2} \tilde{B} \tilde{B} - \frac{M_2}{2} \tilde{W}^0 \tilde{W}^0 + h.c. \end{aligned} \quad (3.38)$$

In the gauge eigenstates basis we can define

$$\tilde{\psi}^0 \equiv \begin{pmatrix} \tilde{B} \\ \tilde{W}^0 \\ \tilde{H}_d^0 \\ \tilde{H}_u^0 \end{pmatrix}, \quad (3.39)$$

and so, with this definition, the Lagrangian (3.38) can be re-expressed as

$$\mathcal{L}_{\text{Neutralino}} = -\frac{1}{2} (\tilde{\psi}^0)^\text{T} M_{\tilde{\psi}^0} \tilde{\psi}^0 + h.c., \quad (3.40)$$

where $M_{\tilde{\psi}^0}$ is a symmetric matrix defined as

$$\begin{aligned} M_{\tilde{\psi}^0} & \equiv \begin{pmatrix} M_1 & 0 & -g' v_d / \sqrt{2} & g' v_u / \sqrt{2} \\ 0 & M_2 & g v_d / \sqrt{2} & -g v_u / \sqrt{2} \\ -g' v_d / \sqrt{2} & g v_d / \sqrt{2} & 0 & -\mu \\ g' v_u / \sqrt{2} & -g v_u / \sqrt{2} & -\mu & 0 \end{pmatrix} \\ & = \begin{pmatrix} M_1 & 0 & -c_\beta s_W m_{Z^0} & s_\beta s_W m_{Z^0} \\ 0 & M_2 & c_\beta c_W m_{Z^0} & -s_\beta c_W m_{Z^0} \\ -c_\beta s_W m_{Z^0} & c_\beta c_W m_{Z^0} & 0 & -\mu \\ s_\beta s_W m_{Z^0} & -s_\beta c_W m_{Z^0} & -\mu & 0 \end{pmatrix} \end{aligned} \quad (3.41)$$

where in the second equality we have made use of the relations given in Eqs. (3.34), and that $g/g' = \tan \theta_W$. We have also introduced the short expressions $c_\beta \equiv \cos \beta$, $s_\beta \equiv \sin \beta$, $c_W \equiv \cos \theta_W$, and $s_W \equiv \sin \theta_W$. This matrix can be diagonalized by the use of an unitary matrix N , such that [48]

$$N^* M_{\tilde{\psi}^0} N^{-1} = M_{\tilde{\chi}^0} \equiv \begin{pmatrix} m_{\chi_1} & 0 & 0 & 0 \\ 0 & m_{\chi_2} & 0 & 0 \\ 0 & 0 & m_{\chi_3} & 0 \\ 0 & 0 & 0 & m_{\chi_4} \end{pmatrix} \quad (3.42)$$

where the eigenvalues m_{χ_i} are real and positive. The mass eigenstates i.e. neutralinos, are given by

$$\tilde{\chi}_i = N_{ij} \tilde{\psi}_j^0 \quad i, j = 1, \dots, 4 \quad (3.43)$$

It is worth to note that the parameters M_1, M_2 and μ , in principle, can have arbitrary phases. However redefining the phases of \tilde{B} and \tilde{W}^0 we can take M_1 and M_2 to be both real and positive. On contrary the phase of μ cannot be reabsorb in this manner, because we have already redefined the phases of \tilde{H}_u^0 and \tilde{H}_d^0 to take the parameter b real and positive. However, in order to avoid CP violation effects, we can safely take μ as real [54]. Note that the sign of μ is still undetermined.

Using Eq. (3.43) the LSP is determined by [49]

$$\tilde{\chi}_1 = N_{11} \tilde{B} + N_{12} \tilde{W}^0 + N_{13} \tilde{H}_d^0 + N_{14} \tilde{H}_u^0 \quad (3.44)$$

Two useful parameters which define the LSP neutralino composition, is the gaugino fraction, f_g and the higgsino fraction, $f_{\tilde{h}}$, which are defined as [49]

$$f_g = |N_{11}|^2 + |N_{12}|^2 \quad (3.45)$$

$$f_{\tilde{h}} = |N_{13}|^2 + |N_{14}|^2. \quad (3.46)$$

Thus if $f_g < 0.5$ ($f_{\tilde{h}} > 0.5$) the LSP is primarily a higgsino. Conversely if $f_g > 0.5$ ($f_{\tilde{h}} < 0.5$) it is primarily a gaugino. From the matrix $M_{\tilde{\psi}_0}$ we can see that the neutralino masses and mixing angles depend upon four parameters, namely M_1, M_2, μ and β .

The complete expressions for the neutralinos eigenvalues are given in ref. [12]. In this thesis we specialized in a limit where the electroweak breaking effects are regarded as small perturbations to the neutralino mass matrix [54], thus we assume that

$$m_{Z^0}, m_W \ll |M_1 - \mu|, |M_2 - \mu|. \quad (3.47)$$

Assuming for example that $M_1 < M_2 \ll |\mu|$, the four neutralinos masses are given by [54]

$$m_{\tilde{\chi}_1} \simeq M_1 - \frac{m_{Z^0}^2 s_W^2 (M_1 + \mu \sin(2\beta))}{\mu^2 - M_1^2} \quad (3.48a)$$

$$m_{\tilde{\chi}_2} \simeq M_2 - \frac{m_{Z^0}^2 s_W^2 (M_2 + \mu \sin(2\beta))}{\mu^2 - M_2^2} \quad (3.48b)$$

$$m_{\tilde{\chi}_3} \simeq |\mu| + \frac{m_{Z^0}^2 (\text{sgn}(\mu) - \sin(2\beta)) (\mu + M_1 c_W^2 + M_2 s_W^2)}{2(\mu + M_1)(\mu + M_2)} \quad (3.48c)$$

$$m_{\tilde{\chi}_4} \simeq |\mu| + \frac{m_{Z^0}^2 (\text{sgn}(\mu) + \sin(2\beta)) (\mu - M_1 c_W^2 - M_2 s_W^2)}{2(\mu - M_1)(\mu - M_2)}. \quad (3.48d)$$

For later purpose we give also the analytic expressions of the ratios N_{ik}/N_{i1} (with $k \neq 1$) between the mixing matrix elements [12]

$$\frac{N_{i2}}{N_{i1}} = -\frac{1}{t_W} \frac{M_1 - m_{\chi_i}}{M_2 - m_{\chi_i}} \quad (3.49a)$$

$$\frac{N_{i3}}{N_{i1}} = \frac{\mu (M_2 - m_{\chi_i}) (M_1 - m_{\chi_i}) - m_{Z^0}^2 \sin \beta \cos \beta [(M_1 - M_2) c_W^2 + M_2 - m_{\chi_i}]}{m_{Z^0} (M_2 - m_{\chi_i}) s_W (-\mu \cos \beta + m_{\chi_i})} \quad (3.49b)$$

$$\frac{N_{i4}}{N_{i1}} = \frac{m_{\chi_i} (M_2 - m_{\chi_i}) (M_1 - m_{\chi_i}) - m_{Z^0}^2 \cos^2 \beta [(M_1 - M_2) c_W^2 + M_2 - m_{\chi_i}]}{m_{Z^0} (M_2 - m_{\chi_i}) s_W (-\mu \cos \beta + m_{\chi_i})}. \quad (3.49c)$$

Now we move more step forward analyzing the charginos mass spectrum. These mass eigenstate are mixing between the charged winos \tilde{W}^\pm and the charged higgsinos $\tilde{H}_u^\pm, \tilde{H}_d^\pm$. Their mass terms in the MSSM Lagrangian are

$$\mathcal{L}_{\text{Chargino}} = -M_2 \tilde{W}^+ \tilde{W}^- + \mu \tilde{H}_u^+ \tilde{H}_d^- - g v_u \tilde{H}_u^+ \tilde{W}^- - g v_d \tilde{H}_d^- \tilde{W}^+ + h.c. \quad (3.50)$$

As we done for neutralinos also here is convenient to define the two gauge eigenstate [5]

$$\tilde{\psi}^+ \equiv \begin{pmatrix} \tilde{W}^+ \\ \tilde{H}_u^+ \end{pmatrix} \quad \tilde{\psi}^- \equiv \begin{pmatrix} \tilde{W}^- \\ \tilde{H}_d^- \end{pmatrix} \quad (3.51)$$

and consequently the Lagrangian (3.50) becomes

$$\mathcal{L}_{\text{Chargino}} = -\frac{1}{2} (\tilde{\psi}^+)^T X^T \tilde{\psi}^- - \frac{1}{2} (\tilde{\psi}^-)^T X \tilde{\psi}^+ + h.c. \quad (3.52)$$

where the matrix X is defined as

$$X \equiv \begin{pmatrix} M_2 & 2g v_u \\ 2g v_u & \mu \end{pmatrix} = \begin{pmatrix} M_2 & \sqrt{2} s_\beta m_W \\ \sqrt{2} c_\beta m_W & \mu \end{pmatrix} \quad (3.53)$$

This 2-dimensional matrix can be diagonalized by a bi-unitary transformation, namely

$$U^* X V^{-1} = M_{\tilde{\chi}^\pm} \equiv \begin{pmatrix} m_{\tilde{\chi}_1^\pm} & 0 \\ 0 & m_{\tilde{\chi}_2^\pm} \end{pmatrix}. \quad (3.54)$$

Thus the mass eigenstates are

$$\tilde{\chi}^+ = V \tilde{\psi}^+ \quad (3.55a)$$

$$\tilde{\chi}^- = U \tilde{\psi}^- \quad (3.55b)$$

where $\tilde{\chi}^+ \equiv \begin{pmatrix} \tilde{\chi}_1^+ \\ \tilde{\chi}_2^+ \end{pmatrix}$ and $\tilde{\chi}^- \equiv \begin{pmatrix} \tilde{\chi}_1^- \\ \tilde{\chi}_2^- \end{pmatrix}$.

Also here we take the limit where the electroweak effects are regarded as small perturbations, see Eq. (3.47). In this limit the eigenvalues are approximately given by [54]

$$m_{\tilde{\chi}_1^\pm} \simeq M_2 - \frac{m_W^2 (M_2 + \mu \sin(2\beta))}{\mu^2 - M_2^2} \quad (3.56a)$$

$$m_{\tilde{\chi}_2^\pm} \simeq |\mu| + \frac{m_W^2 \text{sgn}(\mu) (\mu + M_2 \sin(2\beta))}{\mu^2 - M_2^2} \quad (3.56b)$$

where we have assume that $M_2 \ll |\mu|$

Comparing Eqs. (3.48) and Eqs. (3.56), we can argue that, under our assumption that $M_1 < M_2 \ll |\mu|$, $m_{\tilde{\chi}_1^\pm}$ is nearly equal to $m_{\tilde{\chi}_2^\pm}$. Thus depending on the assumptions made upon the value of M_1, M_2 and $|\mu|$ it is possible to have a LSP, $\tilde{\chi}_1$, nearly degenerate with the lightest charginos, $\tilde{\chi}_1^\pm$. This fact has extraordinarily consequences. In fact co-annihilation effects among these particles, can be determinant in favouring, or not, some LSP configurations as DM candidate.

For later purpose we give also the square squark mass matrices. For the up-type squarks it is given by [5]

$$M_{\tilde{u}}^2 = \begin{pmatrix} m_Q^2 + m_{q_u}^2 + \Delta_{\tilde{u}L} & m_{q_u} (a_u - \mu \cotan \beta) \\ m_{q_u} (a_u - \mu \cotan \beta) & m_{\tilde{u}}^2 + m_{q_u}^2 + \Delta_{\tilde{u}R} \end{pmatrix} \quad (3.57)$$

where the quantities $\Delta_{\tilde{u}L}$ and $\Delta_{\tilde{u}R}$ are respectively defined as

$$\Delta_{\tilde{u}L} \equiv \left(\frac{1}{2} - \frac{2}{3} s_W^2 \right) m_{Z^0}^2 \cos 2\beta, \quad \Delta_{\tilde{u}R} \equiv -\frac{2}{3} m_{Z^0}^2 s_W^2 \cos 2\beta. \quad (3.58)$$

For the down-type squarks the matrix is

$$M_{\tilde{d}}^2 = \begin{pmatrix} m_Q^2 + m_{q_d}^2 + \Delta_{\tilde{d}L} & m_{q_d} (a_d - \mu \tan \beta) \\ m_{q_d} (a_d - \mu \tan \beta) & m_{\tilde{d}}^2 + m_{q_d}^2 + \Delta_{\tilde{d}R} \end{pmatrix} \quad (3.59)$$

where here $\Delta_{\tilde{d}L}$ and $\Delta_{\tilde{d}R}$ are respectively defined as

$$\Delta_{\tilde{d}L} \equiv \left(-\frac{1}{2} + \frac{1}{3} s_W^2 \right) m_{Z^0}^2 \cos 2\beta, \quad \Delta_{\tilde{d}R} \equiv \frac{1}{3} m_{Z^0}^2 s_W^2 \cos 2\beta. \quad (3.60)$$

Note the appearance of the masses of the associated quarks m_{q_u}, m_{q_d} and of the soft-parameters given in Eq. (3.29), a_u, a_d . The orthogonal matrices which diagonalized the above square mass matrices can be defined as [34]

$$U_{\tilde{q}_i} \equiv \begin{pmatrix} \cos \theta_{\tilde{q}}^i & \sin \theta_{\tilde{q}}^i \\ -\sin \theta_{\tilde{q}}^i & \cos \theta_{\tilde{q}}^i \end{pmatrix} \equiv \begin{pmatrix} \eta_{11}^i & \eta_{12}^i \\ \eta_{21}^i & \eta_{22}^i \end{pmatrix} \quad (3.61)$$

where $i = 1$ for up-type squarks while $i = 2$ for down-type squarks. The mixing angle $\theta_{\tilde{q}}^i$ is given by [32]

$$\sin 2\theta_{\tilde{q}}^i = 2\eta_{11}^i \eta_{12}^i = \frac{2m_{q_i} (a_i - \mu (\tan \beta)^{(-1)^i})}{m_{\tilde{q}_{1i}}^2 - m_{\tilde{q}_{2i}}^2} \quad (3.62)$$

Note that when $m_Q^2, m_{\tilde{u}}^2, m_{\tilde{d}}^2 \gg a_u, a_d, \mu$ the matrices $M_{\tilde{u}}^2$ and $M_{\tilde{d}}^2$ are nearly diagonal and as a consequence $\eta_{11}^i = \eta_{22}^i \rightarrow 1$ and $\eta_{12}^i = -\eta_{21}^i \rightarrow 0$.

Chapter 4

Dark Matter Phenomenology in the MSSM

In this Chapter we will analyse LSP neutralinos as DM candidates. As first, we will explore the limiting cases where the LSP is a pure Bino, a pure Higgsino, or a pure Wino; after that we will analyse two LSP configurations, called Well-Tempered neutralino [11], which are particular admixtures of the pure states just listed. Every proposal will be compared with the experimental limits provided by direct detection experiments. In particular we will take into account the direct detection experimental bounds provided by LUX-2016 [7], PICO-60 [8] and XENON100 [10] for the spin-dependent interaction and by LUX-2016 [6] and PANDAX-2016 [64] for the spin-independent one.

The numerical analysis, both for relic density calculation and for neutralino-nucleon scattering cross-section, is performed using the program `micrOmegas 4.2.5` [21]. We start by reviewing direct detection theory, focusing on its application in the MSSM.

4.1 Direct detection of DM

One of the most important experimental evidences of particle DM would be provided by the direct detection of these particles, while they are passing through the Earth [49]. The idea at the base of these searches, is the detection of nuclear recoil energies due to nuclei-WIMP (neutralinos in a SUSY context) elastic scattering processes. The major issue with these experiments is due to the low scattering cross-section of DM on ordinary matter which makes these processes difficult to observe. Furthermore the nuclear recoil energies, that have to be measured, are small. In fact, because the DM particles in our system are moved by the same gravitational potential which acts on the Sun, it is naturally to assume that they have a rotational velocity similar to the one of the stars in the neighbourhood of the Sun i.e. of the Local Standard of Rest (LSR) [23], which, relative to the Galactic rest frame, is about $v_0 \approx 220$ km/s [57]. This value of the velocity, implies that for a neutralino mass from 10 GeV to 1 TeV the typical nuclear recoil energies are from 1 keV to 100 keV [53]. From an experimental point of view these rather small energies imply that the direct detection signals can be easily confused with the background, and so they have to be finely distinguished from it. In order to alleviate this problem the detectors are placed underground so as to eliminate, as much as possible, the background signal [14]. Note also that this small values of the velocities and the energies transferred, in the scattering processes, allow us to take into account the non-relativistic limit.

Typically in direct detection experiments, what is measure is the number of events, R , per day per Kg of detector, as a function of the energy deposited in it, Q ,

$$dR = \frac{\rho_{\text{DM}}}{m_{\tilde{\chi}} m_N} v f(\vec{v}) \frac{d\sigma(q)}{dq^2} dq^2 d^3v \quad (4.1)$$

where ρ_{DM} is the DM local density, which we take within $0.3 \text{ GeV/cm}^3 \lesssim \rho_{\text{DM}} \lesssim 0.7 \text{ GeV/cm}^3$ [19], $m_{\tilde{\chi}}$ is the neutralino mass, m_N is the nuclear mass, \vec{v} the DM velocity relative to the

detector frame, and $f(\vec{v})$ is a velocity distribution function¹. The vector \vec{v} is the DM velocity relative to the laboratory frame, which in terms of the DM velocity in the galactic frame \vec{v}_G read as,

$$\vec{v} = \vec{v}_G - \vec{v}_E, \quad (4.2)$$

where \vec{v}_E is the Earth velocity relative to the galactic rest frame. Note the presence of the DM-nucleus elastic scattering cross-section, $\sigma(q)$, which depends on the modulus of the three-dimensional momentum transferred, q , that, in the non-relativistic limit, is equal to

$$q^2 = 2m_r^2 v^2 (1 - \cos \theta) \quad (4.3)$$

where $m_r \equiv (m_{\tilde{\chi}} m_N)/(m_{\tilde{\chi}} + m_N)$ is the reduced mass between the neutralino and the nucleus, and θ is the angle, in the CoM frame, between the momentum of the incoming neutralino and the momentum of outgoing one. Using Eq. (4.3) we can find that the energy deposited in the detector, is

$$Q = \frac{q^2}{2m_N} = \frac{m_r^2 v^2}{m_N} (1 - \cos \theta). \quad (4.4)$$

Note that both Eq. (4.3) and Eq. (4.4) are valid in the non-relativistic limit. Now we can defined the the elastic scattering cross-section at zero momentum transferred as [49]

$$\frac{d\sigma(q)}{dq^2} \equiv \frac{\sigma_0}{4v^2 m_r^2} F^2(Q) \quad (4.5)$$

where the entire q dependence of $\sigma(q)$ is contained in the form factor $F^2(Q)$, which is normalized such that $F(0) = 1$. Therefore using Eq. (4.4) and Eq. (4.5) we can rewrite the differential event rate, given in Eq. (4.1), as

$$dR = \frac{\rho_{\text{DM}} \sigma_0}{2m_{\tilde{\chi}} m_r^2} F^2(Q) \frac{f(\vec{v})}{v} dQ d^3 v. \quad (4.6)$$

In order to find R we have to integrate the last equation over all possible DM velocities and over all deposited energies from E_T to $Q_{\text{max}} = \frac{2m_r^2 v^2}{m_N}$, where E_T is the experimental threshold energy below that no signal can be detected. Integrating over all possible velocities we obtain that

$$\frac{dR}{dQ} = \frac{\rho_{\text{DM}} \sigma_0}{2m_{\tilde{\chi}} m_r^2} F^2(Q) \int_{v \geq v_{\text{min}}} v f(\vec{v}) dv d\Omega \quad (4.7)$$

where

$$v_{\text{min}} = \left(\frac{Q m_N}{2m_r^2} \right)^{1/2}, \quad (4.8)$$

is the smallest velocity which can give a deposit energy equal to Q [53], and v_{max} is the maximal admitted velocity. The DM velocity distribution in the Earth frame, $f(\vec{v})$ is related to the one in the galactic frame $f_G(\vec{v}')$ by

$$f(\vec{v}) = f_G(\vec{v}_G) = f_G(\vec{v} + \vec{v}_E). \quad (4.9)$$

For $f_G(\vec{v}')$, assuming an isotropic galactic halo model, we can use a truncated Maxwellian velocity distribution function, which in term of \vec{v} and \vec{v}_E is defined as [49], [53],

$$f_G(\vec{v}_G) = \frac{e^{-(\vec{v}_G/v_0)^2}}{k} \Theta(v_{\text{esc}} - v_G) = \frac{e^{-(\vec{v} + \vec{v}_E)^2/v_0^2}}{k} \Theta(v_{\text{esc}} - v_G), \quad (4.10)$$

where the quantity k is responsible for the normalization of $f_G(v_G)$, $v_0 \approx 220$ Km/s is the typical velocity of the LSR defined above, and $\Theta(x)$ is the Heaviside function. The quantity v_{esc} is the local escape velocity of DM from the Milky Way², which in the neighbourhood of

¹In the next we will denote all the vector quantities with the usual arrow, while the modulus of these vectors will be denoted simply without the arrow.

²The local escape velocity is the minimum velocity that a body needs in order to escape from the gravitational attraction due to another body and it is equal to $v_{\text{esc}} = \sqrt{2|\Phi(r)|}$, where $\Phi(r)$ is the gravitational potential [23].

the Solar system is about $v_{\text{esc}} = 544 \text{ km/s}$ [27]. Thus substituting the velocity distribution given in Eq. (4.10) into Eq. (4.7) we obtain

$$\frac{dR}{dQ} = \frac{\rho_{\text{DM}} \sigma_0}{2m_{\tilde{\chi}} m_r^2} \frac{F^2(Q)}{k} \int_{v \geq v_{\text{min}}(Q)} v e^{-(\vec{v} + \vec{v}_{\text{E}})^2 / v_0^2} \Theta(v_{\text{esc}} - v_{\text{G}}) dv d\Omega. \quad (4.11)$$

The velocity integral is computed in Appendix D, and substituting that result into the above equation we get that

$$\frac{dR}{dQ} = \frac{\pi \rho_{\text{DM}} \sigma_0 v_0}{m_{\tilde{\chi}} m_r^2} \frac{F^2(Q)}{k} \left\{ \frac{v_0 \sqrt{\pi}}{v_{\text{E}}} \frac{1}{4} \left[\text{erf} \left(\frac{v_{\text{min}} + v_{\text{E}}}{v_0} \right) - \text{erf} \left(\frac{v_{\text{min}} - v_{\text{E}}}{v_0} \right) \right] - e^{v_{\text{esc}}^2 / v_0^2} \right\}, \quad (4.12)$$

where the normalization constant, k , is given in Appendix D, and $\text{erf}(x)$ is the error function which is defined in Appendix D. Note that v_{min} , via Eq. (4.8), is a function of Q . It is worth to note that \vec{v}_{E} is made up by two components, [27]

$$\vec{v}_{\text{E}} = \vec{v}_{\oplus} + \vec{v}_{\odot} \quad (4.13)$$

where with \vec{v}_{\oplus} we denote the Earth's orbital velocity around the Sun while with \vec{v}_{\odot} we denote the sum of the velocity of the LSR and the Sun's proper motion. In particular the Earth motion around the Sun gives rise to a yearly modulation in the event rate [49]. In fact the modulus of \vec{v}_{E} can be expressed as [49]

$$v_{\text{E}} = v_0 \left[1.05 + 0.07 \cos \left(\frac{2\pi(t - t_{\text{p}})}{\text{yr}} \right) \right], \quad (4.14)$$

where $t_{\text{p}} = \text{June 2nd} \pm 1.3 \text{ days}$.

From Eq. (4.12) is evident as the expected interaction rate depends from different quantities, some of which derive from cosmological observations (ρ_{DM}, v_0) others from nuclear physics ($F(Q), m_N$) and others from the particular particle DM model chosen ($\sigma_0, m_{\tilde{\chi}}$). Our interest is mostly on the latter quantities and in particular on σ_0 .

4.1.1 Elastic scattering cross-section in the MSSM

The neutralino-nucleus scattering cross-section, σ_0 , strongly depends on the neutralino-quark interaction. For this reason in order to evaluate σ_0 in the MSSM, we start by evaluating the scattering between neutralinos and quarks. After that we translate the microscopic interaction, among elementary particles, into an interaction between neutralinos and nucleons. As last step we sum the various nucleon contributions in order to find the matrix elements for the neutralinos-nuclei interaction. An important simplification comes from the fact that we can use the effective theory because, as we said above, the scattering processes take place in the non-relativistic limit. In particular from the MSSM Lagrangian given in Appendix D, Eq. (D.13), we recover the following effective four fermion interaction Lagrangian between neutralinos and quarks [34],

$$\mathcal{L}_{\text{eff}} = \alpha_{\tilde{\chi}q_i}^{\text{SD}} \bar{\tilde{\chi}} \gamma^\mu \gamma^5 \tilde{\chi} \bar{q}_i \gamma_\mu \gamma^5 q_i + \alpha_{\tilde{\chi}q_i}^{\text{SI}} \bar{\tilde{\chi}} \chi \bar{q}_i q_i + \beta_{3i} \bar{\tilde{\chi}} \gamma^\mu \gamma^5 \tilde{\chi} \bar{q}_i \gamma_\mu q_i + \beta_{4i} \bar{\tilde{\chi}} \gamma^5 \tilde{\chi} \bar{q}_i \gamma^5 q_i. \quad (4.15)$$

Neglecting all the terms which, in the non-relativistic limit, give rise to a velocity-suppressed contribution into the scattering cross-section, see Appendix D, the above effective Lagrangian becomes

$$\mathcal{L}_{\text{eff}} = \alpha_{\tilde{\chi}q_i}^{\text{SD}} \bar{\tilde{\chi}} \gamma^\mu \gamma^5 \tilde{\chi} \bar{q}_i \gamma_\mu \gamma^5 q_i + \alpha_{\tilde{\chi}q_i}^{\text{SI}} \bar{\tilde{\chi}} \chi \bar{q}_i q_i. \quad (4.16)$$

The index i is $i = 1$ for up-type quarks and $i = 2$ for down-type quarks. Note also that we have suppressed all the flavor and the color indices. The quantity $\alpha_{\tilde{\chi}q_i}^{\text{SD}}$ is equal to, see Appendix D,

$$\alpha_{\tilde{\chi}q_i}^{\text{SD}} = \frac{X_i^2 + Y_i^2}{4(m_{\tilde{q}_{i1}}^2 - m_{\tilde{\chi}}^2)} + \frac{U_i^2 + V_i^2}{4(m_{\tilde{q}_{i2}}^2 - m_{\tilde{\chi}}^2)} - \frac{g^2}{4m_{Z^0}^2 \cos^2 \theta_W} \left[|N_{13}|^2 - |N_{14}|^2 \right] \frac{T_{3i}}{2}, \quad (4.17)$$

while $\alpha_{\tilde{\chi}q_i}^{\text{SI}}$ is

$$\begin{aligned} \alpha_{\tilde{\chi}q_i}^{\text{SI}} = & -\frac{X_i Y_i}{2(m_{\tilde{q}_{1i}}^2 - m_{\tilde{\chi}}^2)} - \frac{U_i V_i}{2(m_{\tilde{q}_{2i}}^2 - m_{\tilde{\chi}}^2)} \\ & - \frac{g m_{q_i}}{4m_W m_h^2} \frac{D_i}{B_i} (N_{13} \sin \alpha + N_{14} \cos \alpha) (g N_{12} - g' N_{11}) \\ & - \frac{g m_{q_i}}{4m_W m_H^2} \frac{C_i}{B_i} (N_{14} \sin \alpha - N_{13} \cos \alpha) (g N_{12} - g' N_{11}). \end{aligned} \quad (4.18)$$

In the above equations $m_{1\tilde{q}_i}, m_{2\tilde{q}_i}$ are the eigenvalues of the squark square mass matrix given in Eq. (3.59) and Eq. (3.57), while η_{ij} are the elements of the matrix which diagonalizes it; Y_{q_i} and e_{q_i} are respectively the hypercharge and the electric charge of the quark q_i . The quantities B_i, C_i and D_i are defined as in [34]

$$B_1 = \sin \beta, \quad B_2 = \cos \beta \quad (4.19)$$

$$C_1 = \sin \alpha, \quad C_2 = \cos \alpha \quad (4.20)$$

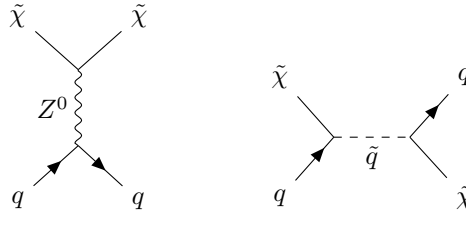
$$D_1 = \cos \alpha, \quad D_2 = -\sin \alpha. \quad (4.21)$$

and X_i, Y_i, U_i, V_i are defined in Appendix B. Note that in the limit where $m_H^2 \gg m_h^2$ we can safely drop out the last term of Eq. (4.18) and using the definition of α given in Eq. (3.37), we get that

$$\sin \alpha \simeq -\cos \beta, \quad \cos \alpha \simeq \sin \beta \quad (4.22)$$

From Eq. (4.16) we see that the scattering processes can be decomposed in a scalar or spin-independent (SI) part and a spin-dependent (SD) one.

We start analyzing the SD interaction. As we can read off from $\alpha_{\tilde{\chi}q_i}^{\text{SD}}$ and from the interaction terms given in Appendix D, the SD interaction, at tree-level, is determined by the following Feynman diagrams



$$(4.23)$$

The matrix elements of the quark axial-vector current into a nucleons are defined by [49]

$$\langle n | \bar{q} \gamma_\mu \gamma^5 q | n \rangle = 2\Delta q^{(n)} s_\mu^{(n)}, \quad (4.24)$$

where $s_\mu^{(n)}$ is the nucleon spin four vector and n denotes a nucleon (generally a proton or a neutron). Therefore the axial-vector interaction term in Eq. (4.16) between neutralinos and quarks is naturally translated into an axial-vector interaction term between neutralinos and nucleons, [27]

$$\alpha_{\tilde{\chi}q_i}^{\text{SD}} \bar{\chi} \gamma^\mu \gamma^5 \tilde{\chi} \bar{q}_i \gamma_\mu \gamma^5 q_i \rightarrow 2c_n \bar{\chi} \gamma^\mu \gamma^5 \tilde{\chi} \bar{n} \gamma_\mu \gamma^5 n \quad (4.25)$$

where and the coefficients c_n are defined as in [27]

$$c_n = \sum_q \alpha_{\tilde{\chi}q_i}^{\text{SD}} \Delta q^{(n)}. \quad (4.26)$$

The $\Delta q^{(n)}$ terms are experimentally determined, and we give a sample of the possible values of $\Delta s^{(p)}$, $\Delta u^{(p)}$ and $\Delta d^{(p)}$ in Table 4.1. The same quantities for neutrons are found using the relations $\Delta s^{(p)} = \Delta s^{(n)}$, $\Delta u^{(p)} = \Delta d^{(n)}$ and $\Delta d^{(p)} = \Delta u^{(n)}$. In order to compute the neutralino-nucleon cross-section, as first, we have to evaluate the scattering average square amplitude

$$\left| \overline{\mathcal{M}}_{\tilde{\chi}n}^{\text{SD}} \right|^2 \equiv \frac{1}{(2s_{\tilde{\chi}} + 1)(2s_n + 1)} \sum_{\text{spins}} |\mathcal{M}_{\tilde{\chi}n}^{\text{SD}}|^2 \quad (4.27)$$

Ref.	$f_{Tu}^{(p)}$	$f_{Tu}^{(n)}$	$f_{Td}^{(p)}$	$f_{Td}^{(n)}$	$f_{Ts}^{(p,n)}$	$\Delta u^{(p)}$	$\Delta d^{(p)}$	$\Delta s^{(p)}$
[35]	0.027	0.022	0.039	0.049	0.36	0.84	-0.43	-0.09
[24]	0.017	0.012	0.023	0.033	0.053	0.84	-0.44	-0.03
[15]	0.015	0.011	0.019	0.027	0.045	0.84	-0.43	-0.085

Table 4.1: In the table are listed the values of the SI coefficients and of the SD ones, from three different references.

where $s_{\tilde{\chi}}$ and s_n denote respectively the spins of the neutralino and the nucleon. The square amplitude $|\mathcal{M}_{\tilde{\chi}n}^{\text{SD}}|^2$ is simply computed sandwiching the interaction term given in Eq. (4.25) between the initial and the final states and then taking the square modulus of the result,

$$\begin{aligned} |\mathcal{M}_{\tilde{\chi}n}^{\text{SD}}|^2 &= 4c_n^2 |\langle \tilde{\chi}, n | \bar{\tilde{\chi}} \gamma^\mu \gamma^5 \tilde{\chi} \bar{n} \gamma_\mu \gamma^5 n | \tilde{\chi}, n \rangle|^2 \\ &= 1024 m_{\tilde{\chi}}^2 m_n^2 |\langle \vec{s}_{\tilde{\chi}} \cdot \vec{s}_n \rangle|^2 c_n^2 \end{aligned} \quad (4.28)$$

where we used the non-relativistic expansions of the neutralino-nucleon scattering amplitudes given in Appendix D. In order to evaluate the average square amplitude we have to sum over all possible initial and final spin states the scalar product $(\vec{s}_{\tilde{\chi}} \cdot \vec{s}_n)^2$. Recalling that both neutralinos and nucleons are spin 1/2 fermions, when they interact they can form one singlet state with total spin $s_{\text{tot}} = 0$, and three triplet states with total spin $s_{\text{tot}} = 1$. Exploiting this and the fact that from the relation $s_{\text{tot}}^2 = (\vec{s}_{\tilde{\chi}} + \vec{s}_n)^2$ we have

$$\vec{s}_{\tilde{\chi}} \cdot \vec{s}_n = \frac{1}{2}(s_{\text{tot}}^2 - s_{\tilde{\chi}}^2 - s_n^2), \quad (4.29)$$

we find that, in natural units,

$$\langle \vec{s}_{\tilde{\chi}} \cdot \vec{s}_n \rangle = -\frac{3}{4} \quad (4.30)$$

for a singlet state, while

$$\langle \vec{s}_{\tilde{\chi}} \cdot \vec{s}_n \rangle = \frac{1}{4} \quad (4.31)$$

for a triplet state. Thus substituting these results into Eq. (4.27) and performing the spins sum, we obtain

$$|\overline{\mathcal{M}_{\tilde{\chi}n}^{\text{SD}}}|^2 = 192 m_{\tilde{\chi}}^2 m_n^2 c_n^2 \quad (4.32)$$

Using the relation $dq^2 = 2\mu_n^2 v^2 d(\cos \theta)$, where μ_n is the neutralino-nucleon reduced mass, and the non-relativistic expansion of the invariant $s \simeq (m_{\tilde{\chi}} + m_n)^2$, we can rewrite the differential scattering cross-section formula, as

$$\frac{d\sigma(q)}{dq^2} = \frac{1}{64\pi m_{\tilde{\chi}}^2 m_n^2 v^2} |\overline{\mathcal{M}_{\tilde{\chi}n}^{\text{SD}}}|^2. \quad (4.33)$$

Substituting in the above formula the result given in Eq. (4.32) we obtain that the differential neutralino-nucleon scattering cross-section at zero momentum transferred is equal to

$$\frac{d\sigma(q)}{dq^2} = \frac{3}{\pi v^2} c_n^2. \quad (4.34)$$

Now, in order to find the total neutralino-nucleon scattering cross-section at zero momentum transferred, we have to integrate Eq. (4.34) over dq^2 obtaining

$$\sigma_{0\text{SD}}^{\tilde{\chi}n} = \int_0^{4\mu_n^2 v^2} \frac{d\sigma(q)}{dq^2} dq^2 = \frac{12m_r^2}{\pi} c_n^2. \quad (4.35)$$

As last step, in order to find the neutralino-nucleus (N) scattering cross-section, we should take into account the effects of the various nucleons inside the nucleus. As first we have to sum the

contribution of the protons separately from that of neutrons. Furthermore we cannot simply sum over all protons and neutrons because two protons(neutrons) which belong to the same orbital must have opposite spins [14] and as a consequence there would be strong compensation between the various spin currents. The interaction between neutralino and nucleus would be proportional to the spin of the neutralino and to the total angular momentum of the nucleus \vec{J}_A , where the subscript A denotes the nuclear mass number. The contribution of the single nucleon to \vec{J}_A can be parametrized as [14]

$$\vec{J}_n^A = \langle s_n \rangle \frac{\vec{J}_A}{J_A} \quad (4.36)$$

where $\langle s_n \rangle \equiv \langle N | s_n | N \rangle$ denotes the expectation value of the spin content of the nucleon n inside the nucleus N [49]. These quantities are obtained using both nuclear experimental calculations and nuclear theory models.

Thus using Eq. (4.28) and replacing m_n with the nucleus mass m_N we find that the square amplitude for the neutralino-nucleus scattering is given by

$$|\mathcal{M}_{\tilde{\chi}N}^{\text{SD}}|^2 = 256m_{\tilde{\chi}}^2 m_N^2 \frac{\langle s_n \rangle^2}{J_A^2} \left| \langle \vec{s}_{\tilde{\chi}} \cdot \vec{J}_A \rangle \right|^2. \quad (4.37)$$

Now in order to find the average square amplitude we should sum over final and average over initial spin states. Labelling the initial polarization states as $s_{\tilde{\chi}}, s_A$ and the final ones as $s'_{\tilde{\chi}}, s'_A$, the spins summation read as [14]

$$\begin{aligned} \sum_{s_{\tilde{\chi}}, s'_A} \sum_{s_A, s'_A} \left| \langle s_{\tilde{\chi}}, s_A | \langle \vec{s}_{\tilde{\chi}} \cdot \vec{J}_A \rangle | s'_{\tilde{\chi}}, s'_A \rangle \right|^2 &= \sum_{s_{\tilde{\chi}}, s'_A} \sum_{s_A, s'_A} \sum_{1 \leq k, l \leq 3} \langle s_{\tilde{\chi}} | s_{\tilde{\chi}}^l | s'_{\tilde{\chi}} \rangle \langle s_{\tilde{\chi}} | s_{\tilde{\chi}}^k | s_{\tilde{\chi}} \rangle \times \\ &\quad \langle s_A | J_A^l | s'_A \rangle \langle s'_A | J_A^k | s_A \rangle \\ &= \sum_{1 \leq k, l \leq 3} \text{Tr}\{s_{\tilde{\chi}}^l s_{\tilde{\chi}}^k\} \text{Tr}\{J_A^l J_A^k\} \\ &= \frac{(2s_{\tilde{\chi}} + 1)s_{\tilde{\chi}}(s_{\tilde{\chi}} + 1)(2J_A + 1)J_A(J_A + 1)}{3} \end{aligned} \quad (4.38)$$

which can be substituted in Eq. (4.27) obtaining

$$\overline{|\mathcal{M}_{\tilde{\chi}N}^{\text{SD}}|^2} = 256m_{\tilde{\chi}}^2 m_N^2 \frac{\langle s_n \rangle^2}{J_A^2} J_A(J_A + 1). \quad (4.39)$$

Note that this result is valid separately for protons and neutrons. Summing their contributions we obtain

$$\begin{aligned} \overline{|\mathcal{M}_{\tilde{\chi}N}^{\text{SD}}|^2} &= 256m_{\tilde{\chi}}^2 m_N^2 \frac{J_A}{J_A^2} (J_A + 1) (\langle s_p \rangle c_p + \langle s_n \rangle c_n)^2 \\ &= 256m_{\tilde{\chi}}^2 m_N^2 J_A (J_A + 1) \Lambda^2 \end{aligned} \quad (4.40)$$

where now the subscript n denotes the neutrons and not a generic nucleon. The quantity Λ is defined as [49]

$$\Lambda \equiv \frac{1}{J_A} (\langle s_p \rangle c_p + \langle s_n \rangle c_n) \quad (4.41)$$

Substituting the result given in Eq. (4.40) into Eq. (4.33), we obtain the differential neutralino-nucleus scattering cross-section at zero momentum transferred

$$\frac{d\sigma(q)}{dq^2} = \frac{4}{\pi v^2} J_A (J_A + 1) \Lambda^2, \quad (4.42)$$

which integrates over dq^2 between 0 and $4\mu_N^2 v^2$ gives the total neutralino-nucleus scattering cross-section at zero momentum transferred

$$\sigma_{0\text{SD}}^{\tilde{\chi}N} = \frac{16\mu_N^2}{\pi} J_A (J_A + 1) \Lambda^2. \quad (4.43)$$

Note that now $\mu_N = m_{\tilde{\chi}} m_N / (m_{\tilde{\chi}} + m_N)$ is the neutralino-nucleus reduced mass. In principle, relaxing the zero momentum transferred condition, in Eq. (4.42) there would be also a $|q|$ dependence which, as we said before, can be parametrized using a nuclear form factor $F_{SD}(q)$ ³

$$\frac{d\sigma(q)}{dq^2} = \frac{4}{\pi v^2} J_A (J_A + 1) \Lambda^2 F_{SD}^2(q). \quad (4.44)$$

In particular in the SD interaction the nuclear form factor is defined as [49]

$$F_{SD}^2(q) \equiv \frac{S(q)}{S(0)}, \quad (4.45)$$

note that when $q \rightarrow 0$ then $F_{SD}^2(q) \rightarrow 1$. The quantity $S(q)$ is equal to [49],[53]

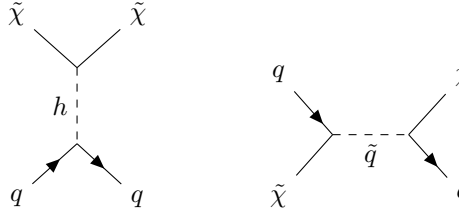
$$S(|q|) = a_0^2 S_{00}(q) + a_1^2 S_{11}(q) + a_0 a_1 S_{10}(q) \quad (4.46)$$

where $a_0 \equiv c_p + c_n$ and $a_1 \equiv c_p - c_n$ are respectively the isoscalar and the isovector coefficients of the scattering amplitude [49], where c_p and c_n are defined in Eq. (4.26). The independent form factors $S_{ij}(q)$ come from detailed nuclear calculations and they can be fitted in terms of the variable $y = 0.25 A^{2/3} q^2$ as [49]

$$S_{ij}(q) = \sum_k c_{ij}^{(k)} y^k, \quad (4.47)$$

where A is the atomic mass number and the coefficients, $c_{ij}^{(k)}$, for various elements are listed in refs. [49].

Now we redo the above analysis for the spin-independent (SI) interaction. This interaction is determined by the second term of the effective Lagrangian given in Eq. (4.16) and as we can read off from $\alpha_{\tilde{\chi}q_i}^{\text{SI}}$, at tree-level, the interaction is determined by the following Feynman diagrams



$$(4.48)$$

The scalar interaction term between neutralinos and quarks is naturally translated into a scalar interaction term between neutralinos and nucleons

$$\alpha_{\tilde{\chi}q_i}^{\text{SI}} \bar{\tilde{\chi}} \tilde{\chi} \bar{q}_i q_i \rightarrow \alpha_{\tilde{\chi}q_i}^{\text{SI}} \langle n | \bar{q}_i q_i | n \rangle \bar{\tilde{\chi}} \tilde{\chi} \bar{n} n. \quad (4.49)$$

where n denotes a nucleon. Thus, as first step, we evaluate the matrix elements of quarks in a nucleon state, $\langle n | \bar{q}_i q_i | n \rangle$. To do this we start by the definition [35]

$$f_{Tq}^{(n)} \equiv \frac{\langle n | m_q \bar{q} q | n \rangle}{m_n} \quad (4.50)$$

which is valid for light quarks, namely, u , d and s . In order to compute the contribution for heavy quarks (c , b and t) we start from the fact that the nucleon matrix element of the trace of the QCD energy momentum tensor is equal to the mass of the nucleon [27], namely

$$m_n \equiv \langle n | \Theta_\mu^\mu | n \rangle = \sum_q \langle n | m_q \bar{q} q | n \rangle + \frac{\beta(\alpha_s)}{4\alpha_s} \langle n | G_{\mu\nu}^a G_a^{\mu\nu} | n \rangle \quad (4.51)$$

where α_s is the strong coupling constant,

$$\beta(\alpha_s) = - \left(11 - \frac{2n_f}{3} \right) \frac{\alpha_s^2}{2\pi} \quad (4.52)$$

³Note that $F_{SD}(Q)$ and $F_{SD}(q)$ are interchangeable.

denotes the beta function and $G_{\mu\nu}^a$ is the gluon field strength tensor. Using the heavy-quark expansion which at the lowest order is equivalent to making the substitution [27]

$$m_q \bar{q}q \rightarrow -\frac{\alpha_s}{12\pi} G_{\mu\nu}^a G_a^{\mu\nu} \quad (4.53)$$

for $q = c, b, t$, it is possible to recast Eq. (4.51) as

$$\begin{aligned} m_n &= \sum_{q=u,d,s} \langle n | m_q \bar{q}q | n \rangle - \frac{9}{8\pi} \alpha_s \langle n | G_{\mu\nu}^a G_a^{\mu\nu} | n \rangle \\ &= \sum_{q=u,d,s} m_n f_{Tq}^{(n)} - \frac{9}{8\pi} \alpha_s \langle n | G_{\mu\nu}^a G_a^{\mu\nu} | n \rangle \end{aligned} \quad (4.54)$$

where we have used the definition given in Eq. (4.50). In this way the gluon contribution can be expressed as

$$-\frac{9}{8\pi} \alpha_s \langle n | G_{\mu\nu}^a G_a^{\mu\nu} | n \rangle = m_n \left(1 - \sum_{q=u,d,s} f_{Tq}^{(n)} \right) \equiv m_n f_{TG}^{(n)}. \quad (4.55)$$

Thus using this result and Eq. (4.53), the matrix element for heavy quarks would be equal to

$$\langle n | m_q \bar{q}q | n \rangle = \frac{2}{27} f_{TG}^{(n)} m_n. \quad (4.56)$$

Now using Eq. (4.50) and Eq. (4.56) we can write the effective coupling between neutralinos and nucleons as

$$f_n = \sum_{q=u,d,s} \frac{m_n}{m_q} f_{Tq}^{(n)} \alpha_{\tilde{\chi}q_i}^{\text{SI}} + \frac{2}{27} f_{TG}^{(n)} \sum_{q=c,b,t} \frac{m_n}{m_q} \alpha_{\tilde{\chi}q_i}^{\text{SI}}. \quad (4.57)$$

A sample of the values of $f_{Tq}^{(n)}$ for proton and neutron are given in Table 4.1. From this formula and with the values given in Table 4.1 we expected that $f_p \simeq f_n$. Sandwiching between the initial and final states the term given in Eq. (4.49) and using the results given in Appendix D, we find that the SI neutralino-nucleon amplitude is

$$\mathcal{M}_{\tilde{\chi}n}^{\text{SI}} = 4m_{\tilde{\chi}} m_n \xi_{\tilde{\chi}}^\dagger \xi'_n \xi_n^\dagger \xi'_n \quad (4.58)$$

where ξ is a numerical two component spinor normalized as $\xi^\dagger \xi = 1$. Using this result we can compute the average square amplitude for the neutralino-nucleon SI interaction in the non-relativistic limit

$$\left| \overline{\mathcal{M}_{\tilde{\chi}n}^{\text{SI}}} \right|^2 = 64m_{\tilde{\chi}}^2 m_n^2 f_n^2. \quad (4.59)$$

Substituting this result into Eq. (4.33) we obtain the differential neutralino-nucleon scattering cross-section in the SI case

$$\frac{d\sigma(q)}{dq^2} = \frac{1}{\pi v^2} f_n^2, \quad (4.60)$$

which integrate over dq^2 from 0 to $4m_{\tilde{\nu}}^2 v^2$ gives

$$\sigma_{0\text{SI}}^{\tilde{\chi}n} = \frac{4\mu_n^2}{\pi} f_n^2, \quad (4.61)$$

that is the total neutralino-nucleon SI scattering cross-section at zero momentum transferred.

The evaluation of the interaction amplitude between the neutralino and the nucleus in the SI case is more simpler than in the SD one. This is because, contrarily to what happens for the SD interaction, the various SI nucleon amplitudes sum up coherently in a constructive way, and so the DM-nucleus amplitude is proportional to the number of the nucleons in the nucleus, i.e. to the atomic mass number A . Thus the average square amplitude for the neutralino-nucleus scattering is simply the sum of the proton and the neutron contributions, namely

$$\left| \overline{\mathcal{M}_{\tilde{\chi}N}^{\text{SI}}} \right|^2 = 64m_{\tilde{\chi}}^2 [Zf_p + (A-Z)f_n]^2 \quad (4.62)$$

where Z is the atomic number. Substituting this equation into Eq. (4.33) and then integrate over dq^2 , we obtain the total neutralino-nucleus scattering cross-section at zero momentum transferred

$$\sigma_{0\text{SI}}^{\tilde{\chi}^N} = \frac{4\mu_N^2}{\pi} [Zf_p + (A - Z)f_n]^2. \quad (4.63)$$

For $f_p \simeq f_n$, $\sigma_{0\text{SI}}^{\tilde{\chi}^N} \propto A^2$ and so it receives a substantial enhancement for heavy nuclei. Thus what we expect, comparing Eq. (4.43) with Eq. (4.63), is that for heavy nuclei the dominant contribution to the scattering between the DM and ordinary matter would be provided by the SI interaction.

As we said for the SD case also here, in principle, there would be a dependence on q in the the SI differential cross-section. As usual this dependence is parametrized using a nuclear form factor $F(Q)$. Thus the SI differential cross-section becomes

$$\frac{d\sigma(q)}{dq^2} = \frac{1}{\pi v^2} [Zf_p + (A - Z)f_n]^2 F_{\text{SI}}^2(q), \quad (4.64)$$

In the case of the scalar interaction the nuclear form factor is related to the Fourier transform of the nucleon density inside the nucleus. For example $F_{\text{SI}}(q)$ can be the Wood-Saxon form factor [53]

$$F_{\text{SI}}^2(q) = \left[\frac{3j_1(qR_1)}{qR_1} \right]^2 e^{-(q\text{fm})^2} \quad (4.65)$$

where j_1 is a spherical Bessel function and $R_1 \equiv (R^2 - 5\text{fm})^{1/2}$ with $R \simeq 1.2\text{fm}A^{1/3}$.

Looking at Eq. (4.1) we observe that the quantity which is relevant for the evaluation of expected rate of events and which can be extracted from the measurements, is the total DM-nuclear differential scattering cross-section, namely $d\sigma_N(q)/dq^2$. This quantity is defined as the coherent sum of the SD and SI DM-nucleus scattering cross-sections given in Eq. (4.44) and Eq. (4.64),

$$\frac{d\sigma_N(q)}{dq^2} = \frac{1}{4\mu_N^2 v^2} \left[\sigma_{0\text{SI}}^{\tilde{\chi}^N} F_{\text{SI}}^2(q) + \sigma_{0\text{SD}}^{\tilde{\chi}^N} F_{\text{SD}}^2(q) \right] \quad (4.66)$$

which in terms of the related DM-protons scattering cross-sections given in Eq. (4.35) and Eq. (4.61) read as

$$\frac{d\sigma_N(q)}{dq^2} = \frac{1}{4\mu_p^2 v^2} \left[\sigma_{0\text{SI}}^{\tilde{\chi}^p} \left(Z + (A - Z) \frac{f_n}{f_p} \right)^2 F_{\text{SI}}^2(Q) + \frac{4}{3} \frac{J_A + 1}{J_A} \left(\langle s_p \rangle + \langle s_n \rangle \frac{c_n}{c_p} \right)^2 \sigma_{0\text{SD}}^{\tilde{\chi}^p} F_{\text{SD}}^2(q) \right]$$

where μ_p is the proton-neutralino reduced mass. From this result we can obtain the total neutralino-nucleus scattering cross-section at zero-momentum transferred which is

$$\begin{aligned} \sigma_0^{\tilde{\chi}^N} &= \frac{\mu_N^2}{\mu_p^2} \left[\sigma_{0\text{SI}}^{\tilde{\chi}^p} \left(Z + (A - Z) \frac{f_n}{f_p} \right)^2 + \frac{4}{3} \frac{J_A + 1}{J_A} \left(\langle s_p \rangle + \langle s_n \rangle \frac{c_n}{c_p} \right)^2 \sigma_{0\text{SD}}^{\tilde{\chi}^p} \right] \\ &\simeq \frac{\mu_N^2}{\mu_p^2} \left[A^2 \sigma_{0\text{SI}}^{\tilde{\chi}^p} + \frac{4}{3} \frac{J_A + 1}{J_A} \left(\langle s_p \rangle + \langle s_n \rangle \frac{c_n}{c_p} \right)^2 \sigma_{0\text{SD}}^{\tilde{\chi}^p} \right] \\ &\simeq \frac{\mu_N^2}{\mu_p^2} \left[A^2 \sigma_{0\text{SI}}^{\tilde{\chi}^p} + \frac{4}{3} \frac{J_A + 1}{J_A} \left(\langle s_p \rangle + \langle s_n \rangle \sqrt{\frac{\sigma_{0\text{SD}}^{\tilde{\chi}^n}}{\sigma_{0\text{SD}}^{\tilde{\chi}^p}}} \right)^2 \sigma_{0\text{SD}}^{\tilde{\chi}^p} \right] \end{aligned} \quad (4.67)$$

where in the last step we assumed that $f_p \simeq f_n$ and $m_p \simeq m_n$, which using Eq. (4.35) implies that $c_n/c_p \simeq \sqrt{\sigma_{0\text{SD}}^{\tilde{\chi}^p}/\sigma_{0\text{SI}}^{\tilde{\chi}^p}}$. In principle the bounds imposed by the direct-detection experiments must be compared with this result which take into account both the SD and the SI interactions. However if the SD or the SI contribute is dominant i.e. $\sigma_{0\text{SI}}^{\tilde{\chi}^N} \gg \sigma_{0\text{SD}}^{\tilde{\chi}^N}$ or $\sigma_{0\text{SI}}^{\tilde{\chi}^N} \ll \sigma_{0\text{SD}}^{\tilde{\chi}^N}$ we can compare the SD and SI bounds separately. In the next we present the

MSSM Parameter	Value-Range
M_1	10 – 250 GeV
$m_{\tilde{t}_R}$	$1.1M_1 - 1.8M_1$
μ	800 GeV
M_2	1.2 TeV
M_3	1.8 TeV
$m_{\tilde{t}_L}$	> 1 TeV
$m_{\tilde{q}_{L,R}}$	> 1.5 TeV
$\tan \beta$	10

Table 4.2: In the table are listed the values of the MSSM parameters that we take into account.

results of direct-detection analysis taking into account the neutralino-nucleon SD and SI cross-section⁴. First we give both contributions separately and then we combine them finding the total neutralino-nucleus scattering cross-section.

4.2 Pure Bino LSP

Now we analyse various neutralino LSP configurations as DM candidates. We start analysing the pure Bino LSP configuration. This is a limiting case, which corresponds to set in the LSP definition given in Eq. (3.44), the following relations [50]

$$\begin{aligned} N_{11} &\rightarrow 1 \\ N_{12}, N_{13}, N_{14} &\rightarrow 0. \end{aligned} \tag{4.68}$$

In many SUSY scenarios the LSP tends naturally to be a Bino-like fermion [36]. In our case the pure Bino configuration is achieved imposing at the electroweak scale that

$$M_1 \ll |\mu| < M_2. \tag{4.69}$$

In particular, imposing this relation into Eqs. (3.48) and Eqs. (3.49), and assuming that $|\mu|, (|\mu| - M_1) \gg m_W$, we have that

$$N_{11} \simeq 1 + \mathcal{O}\left(\frac{m_W^2}{\mu^2}\right) \tag{4.70a}$$

$$N_{12} \simeq -\frac{m_W^2 (M_1 + \mu \sin 2\beta)}{(M_2 - M_1)(\mu^2 - M_1^2)} \simeq \mathcal{O}\left(\frac{m_W^2}{\mu M_2}\right) \tag{4.70b}$$

$$N_{13} \simeq t_W \left[\frac{m_W (M_1 + \mu \sin 2\beta)}{(\mu^2 - M_1^2) \cos \beta} + \frac{m_W \sin \beta}{\mu} \right] \simeq \mathcal{O}\left(\frac{m_W}{\mu}\right) \tag{4.70c}$$

$$N_{14} \simeq t_W \left[\frac{M_1 m_W (M_1 + \mu \sin 2\beta)}{\mu (\mu^2 - M_1^2) \cos \beta} + \frac{m_W \cos \beta}{\mu} \right] \simeq \mathcal{O}\left(\frac{m_W}{\mu}\right) \tag{4.70d}$$

As a consequence the LSP is nearly a pure Bino, $\tilde{\chi}_1^0 = \tilde{B}$, with a mass, at the leading order, equal to $m_{\tilde{\chi}_1^0} \simeq M_1$. The values of the others MSSM parameters that we take into account are defined in Table 4.2.

In order to evaluate the thermal relic density provided by a pure Bino LSP we have to start computing its annihilation rates into SM particles. In the parameter space region provided by Table 4.2, a pair of Binons tend to annihilate mostly into SM fermion anti-fermion pairs [36]. These annihilation processes take place through sfermions exchange in t - u channels [11]. In particular, because we take squarks and left-handed sleptons much heavier than the right-handed sleptons, the favoured final state would be the SM right-handed leptons and anti-leptons.

⁴We give the results for the neutralino-nucleon scattering cross-sections instead of the neutralino-nucleus ones because we want to compare the numerical results with bounds coming from different target nuclei.

The Feynman diagrams for the processes $\tilde{B}\tilde{B} \xrightarrow{\tilde{l}_R} l_R \bar{l}_R$ are given in Appendix E, where we compute the annihilation cross-section times velocity in the limit where the ratio $m_l/M_1 \rightarrow 0$, and with m_l we denote the final lepton masses. Using the results given in Eq. (E.42) we can expand $\sigma_{\tilde{B}\tilde{B}}v$ in the non-relativistic limit which at the first non-zero order read as

$$\sigma_{\tilde{B}\tilde{B}}v = \frac{g^4 \tan^4 \theta_W}{\pi m_{\tilde{l}_R}^2} \frac{r(1+r^2)}{(1+r)^4} \epsilon + \mathcal{O}(\epsilon^2), \quad (4.71)$$

where $r \equiv M_1^2/m_{\tilde{l}_R}^2$, ϵ is the total kinetic energy per unit of mass given in Eq. (2.54), and note that we have summed over the three flavor lepton states. From Table 4.2 we can see that r is varying in the range $0.3 \lesssim r \lesssim 0.9$. Note also that in Eq. (4.71) there is no s-wave contribution (the zero order term in the ϵ expansion), because it is proportional to the vanishing ratio m_l/M_1 .

Substituting the $\sigma_{\tilde{B}\tilde{B}}v$ expansion given in Eq. (4.71), into Eq. (2.57), we recover the thermal average cross-section times velocity for Bino annihilation, which is equal to

$$\langle \sigma_{\tilde{B}\tilde{B}}v \rangle = \frac{3}{2} \frac{g^4 \tan^4 \theta_W}{\pi m_{\tilde{l}_R}^2} \frac{r(1+r^2)}{x(1+r)^4} + \mathcal{O}\left(\frac{1}{x^2}\right), \quad (4.72)$$

where $x \equiv M_1/T$. Substituting this result into the relic density formula, Eq. (2.59), we obtain that the relic abundance for a pure Bino LSP is approximately given by

$$\Omega_{\tilde{B}} h^2 = 1.1 \times 10^{-2} \left(\frac{m_{\tilde{l}_R}}{100 \text{ GeV}} \right)^2 \frac{(1+r)^4}{r(1+r^2)} \left(1 + 0.07 \log \frac{\sqrt{r} 100 \text{ GeV}}{m_{\tilde{l}_R}} \right). \quad (4.73)$$

The values of $\Omega_{\tilde{B}} h^2$ as a function of the LSP mass are given in Fig. 4.1, where we show the result of the micrOmegas 4.2.5 simulation compared with the analytical one given by Eq. (4.73). From numerical simulation we find that the DM constraint provided by Eq. (1.13)

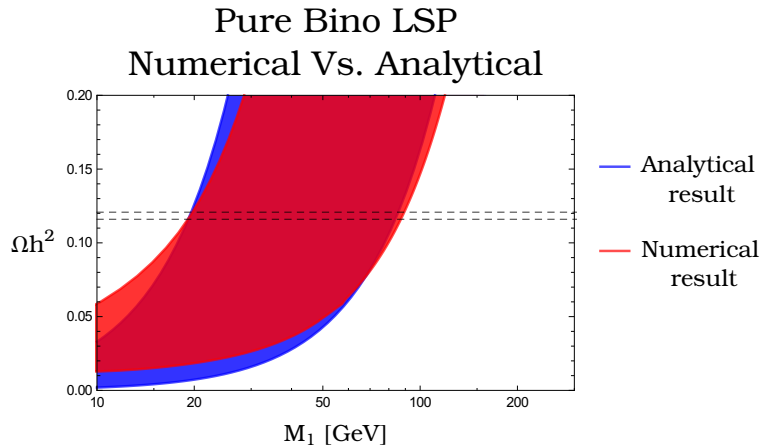


Figure 4.1: In the plot is shown the contribution to Ωh^2 of a pure Bino LSP obtained from the micrOmegas 4.2.5 analysis, compared with the analytical result obtained using Eq. (4.73). The width of the bands is due to a slepton mass parameter which varies in the range $1.1M_1 \leq m_{\tilde{l}_R} \leq 1.8M_1$. The region between the dashed lines denotes the observed DM abundance within 2σ .

within a range of 2σ , is satisfied when the mass M_1 of a pure Bino LSP is in the range $18 \text{ GeV} \lesssim M_1 \lesssim 85 \text{ GeV}$ which, looking at Table 4.2, corresponds to a r.h. slepton mass in the range $33 \text{ GeV} \lesssim m_{\tilde{l}_R} \lesssim 94 \text{ GeV}$.

For what concern direct detection of a pure Bino LSP, we summarize the results of our numerical analysis in Table 4.3. These numerical results and the direct detection exclusion limits provided by the more recent experiments, are depicted in Fig. 4.2. In particular from these plots we can see that all the cross-sections are well below the experimental excluded regions.

Cross-section	Value-Range
$\sigma_{0,SD}^{\tilde{B}p}$	$1.4 \times 10^{-11} - 5.5 \times 10^{-9}$ pb
$\sigma_{0,SD}^{Bn}$	$1.5 \times 10^{-12} - 4.5 \times 10^{-10}$ pb
$\sigma_{0,SI}^{\tilde{B}p,n}$	$3.3 \times 10^{-14} - 5.2 \times 10^{-14}$ pb

Table 4.3: In the table are listed the upper and lower values of the SD and SI neutralino-nucleon cross-sections computed with `micrOmegas 4.2.5`. As usual for the SI interaction we have assumed that $f_p \simeq f_n$.

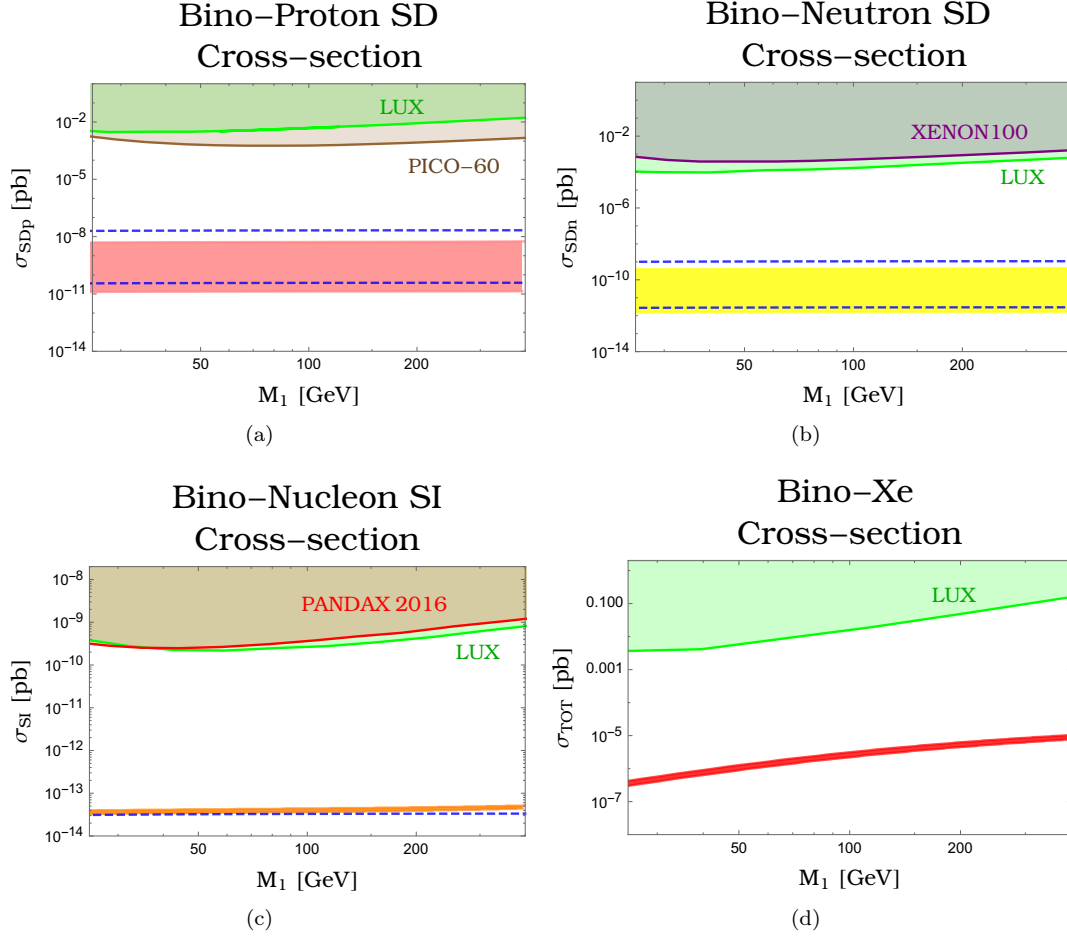


Figure 4.2: In the figure we show the results of the direct detection analysis performed with `micrOmegas 4.2.5`, compared with the analytical results found using the approximate formulae given in Eqs. (4.76). In the panel (a) is shown the SD Bino-proton scattering cross-section (pink band) with the analytical result (the region between the blue-dashed lines), the shaded areas are the excluded regions provided by LUX-2016 (green) and PICO-60 (brown) experiments. In the left panel (b) is shown the SD Bino-neutron scattering cross-section (yellow band) with the analytical result (the region between the blue-dashed lines), the experimental limits come from LUX-2016 (green) and XENON100 (purple) experiments. In the below panel (c) we show the result for the SI Bino-nucleon scattering cross-section (orange band) with the analytical result (blue-dashed line), and where the excluded limits are given by the LUX-2016 (green) and the PANDAX-2016 (red) experiments. In every plot the squark masses are varying in the range $1.5 \text{ TeV} \lesssim m_{\tilde{q}} \lesssim 8 \text{ TeV}$. In plot (d) we show the the combined SI and SD Bino-Xe scattering cross-sections, with the experimental bound from LUX experiment.

These numerical results can be explained using the theoretical ones given in section 4.1. Substituting into Eq. (4.17) and Eq. (4.18) the expressions of N_{1i} given in Eqs. (4.70), and

taking the limit where $\mu, M_{1,2}, (\mu - M_{1,2}) > m_W$, we find that

$$\alpha_{\tilde{B}}^{\text{SD}(q_i)} \simeq g^2 t_W^2 \left[\frac{Y_{q_i \text{L}}^2 (\eta_{11}^i)^2 + 4(\eta_{12})^2 e_{q_i}^2}{16(m_{\tilde{q}_i}^2 - M_1^2)} + \frac{4e_{q_i}^2 (\eta_{11}^i)^2 + Y_{q_i \text{L}}^2 (\eta_{12})^2}{16(m_{\tilde{q}_i}^2 - M_1^2)} \right] + \frac{g^2 t_W^2}{16\mu^2} \cos 2\beta (-1)^i \quad (4.74a)$$

$$\alpha_{\tilde{B}}^{\text{SI}(q_i)} \simeq \frac{e_{q_i} Y_{q_i \text{L}} g^2 t_W^2}{4} \left[\frac{\eta_{11}^i \eta_{12}^i}{(m_{\tilde{q}_i}^2 - M_1^2)} - \frac{\eta_{11}^i \eta_{12}^i}{(m_{\tilde{q}_i}^2 - M_1^2)} \right] + \frac{g^2 t_W^2 m_{q_i} \sin 2\beta}{4\mu m_h^2} \quad (4.74b)$$

where we have assumed that $m_H^2 \gg m_h^2$, which allow us to neglect the contribution of the heavy Higgs field and to make the substitutions given in Eq. (4.22). As usual with $m_{\tilde{q}_{1,2i}}$ we denote the eigenvalues of the squarks mass matrix, while η_{ij} are the elements of the matrix which diagonalizes it. With $Y_{q_i \text{L}}$ and e_{q_i} we denote respectively the l.h. hypercharge and the electric charge of the quarks q_i , where $i = 1$ is for up-type quarks while $i = 2$ is for down-type ones. Substituting Eqs. (4.74) into Eq. (4.35) and Eq. (4.61) we find respectively the Bino-nucleon SD and SI scattering cross-sections at zero momentum transferred,

$$\sigma_{0 \text{SD}}^{\tilde{B}p} = \frac{12}{\pi} \left(\frac{M_1 m_p}{M_1 + m_p} \right)^2 \left[\sum_q \alpha_{\tilde{B}}^{\text{SD}(q_i)} \Delta q^{(p)} \right]^2 \quad (4.75a)$$

$$\sigma_{0 \text{SD}}^{\tilde{B}n} = \frac{12}{\pi} \left(\frac{M_1 m_n}{M_1 + m_n} \right)^2 \left[\sum_q \alpha_{\tilde{B}}^{\text{SD}(q_i)} \Delta q^{(n)} \right]^2 \quad (4.75b)$$

$$\sigma_{0 \text{SI}}^{\tilde{B}p/n} = \frac{4}{\pi} \left(\frac{M_1 m_p}{M_1 + m_p} \right)^2 \left[\sum_{q=u,d,s} \frac{m_{p/n}}{m_q} f_{\text{T}q}^{(p/n)} \alpha_{\tilde{B}}^{\text{SI}(q_i)} + \frac{2}{27} f_{\text{T}G} \sum_{q=c,b,t} \frac{m_{p/n}}{m_q} \alpha_{\tilde{B}}^{\text{SI}(q_i)} \right]^2 \quad (4.75c)$$

where the quantities $\Delta q^{(p/n)}$, $f_{\text{T}q}^{(p/n)}$ are given in Table 4.1 and $f_{\text{T}G}$ is given in Eq. (4.55). First of all from this results and, in particular from Eqs. (4.74), becomes clear that for a pure Bino configuration the SD scattering processes mediated by the Z_0 boson and the SI ones mediated by the neutral Higgs bosons are suppressed respectively by μ^2 and μ . In particular assuming that $m_{\tilde{q}_{1i}} \simeq m_{\tilde{q}_{2i}} = m_{\tilde{q}} \gg M_1$ and the limit of heavy squark masses ($m_{\tilde{q}}^2 \gg a_i, \mu$ where $a_{u,d}$ are the soft-parameters given in Eq. (3.29)), we have that $\eta_{11}^i \rightarrow 1$ and $\eta_{12}^i \rightarrow 0$ and thus Eqs. (4.74) can be approximated as

$$\alpha_{\tilde{B}}^{\text{SD}(q_i)} \simeq \frac{g^2 t_W^2}{16m_{\tilde{q}}^2} \left[Y_{q_i \text{L}}^2 + 4e_{q_i}^2 \right] + \frac{g^2 t_W^2}{16\mu^2} \cos 2\beta (-1)^i + \mathcal{O} \left(\frac{M_1^2}{m_{\tilde{q}_{1,2}}^2}, \eta_{12}^2 \right) \quad (4.76a)$$

$$\begin{aligned} \alpha_{\tilde{B}}^{\text{SI}(q_i)} &\simeq \frac{e_{q_i} Y_{q_i \text{L}} g^2 t_W^2 m_{q_i} \mu (\tan \beta)^{(-1)^i}}{4 m_{\tilde{q}}^4} + \frac{g^2 t_W^2 m_{q_i} \sin 2\beta}{4\mu m_h^2} + \mathcal{O} \left(\frac{M_1^2}{m_{\tilde{q}_{1,2}}^2}, \eta_{12}^2 \right) \\ &\simeq \frac{g^2 t_W^2 m_{q_i} \sin 2\beta}{4\mu m_h^2} + \mathcal{O} \left(\frac{M_1^2}{m_{\tilde{q}_{1,2}}^2}, \frac{m_{q_i} \mu}{m_{\tilde{q}_{1,2}}^2} \right) \end{aligned} \quad (4.76b)$$

where in place of the product $\eta_{11}^i \eta_{12}^i$ we used relation given in Eq. (3.62). These results confirm the numerical ones plotted in Fig. 4.2. In particular assuming that $\mu \gtrsim m_{\tilde{q}}$ the SD interaction is determined principally by the squarks exchange term; in fact the band in plots (a) and (b) is due to a common squark mass which is varying in the range $1.5 \text{ TeV} \leq m_{\tilde{q}} \leq 8 \text{ TeV}$. Note that in the SI case, plot (c), this band is quite absent because, consistently with Eq. (4.76b), the dominant term is the one relative to the Higgs exchange. We take the squark masses greater than 1.5 TeV because light squarks are nearly ruled out by collider searches, which impose a lower limit on the squark masses of $m_{\tilde{q}} \gtrsim 800 \text{ GeV}$ for an LSP mass $M_1 \lesssim 300 \text{ GeV}$ [60].

The combined contributions of SD and SI interactions can be approximately evaluated using Eq. (4.67). Exploiting the numerical results and the fact the the LUX experiment uses ^{131}Xe as nuclear target, we find that Eq. (4.67) becomes

$$\sigma_0^{\tilde{B} \text{Xe}} \simeq \frac{\mu_N^2}{\mu_p^2} A^2 \left[\sigma_{0 \text{SI}}^{\tilde{B}p} + 1.6 \times 10^{-6} \sigma_{0 \text{SD}}^{\tilde{B}p} \right] \quad (4.77)$$

where for $\langle S_p \rangle \simeq -0.041$ and $\langle S_n \rangle \simeq -0.236$ we used the values listed in [49], and to find the ratio $\sqrt{\sigma_{0SD}^{\tilde{B}n}/\sigma_{0SD}^{\tilde{B}p}} \simeq 0.29$ we used the upper limits for $\sigma_{0SD}^{\tilde{B}p}$ and $\sigma_{0SD}^{\tilde{B}n}$ given in Table 4.3. The relative contribution of the the SD Bino-Xe scattering cross-section and the SI one gives that $\sigma_{0SD}^{\tilde{B}Xe}/\sigma_{0SI}^{\tilde{B}Xe} \simeq 0.17$. From this result we can argue that the SD contribution is not totally negligible respect to the SI one. To this end we plot also the combined effect of SD and SI interactions in plot (d) of Fig. 4.2 with the LUX experimental excluded region.

From the micrOmegas 4.2.5 result and also from the analytical one given in Eq. (4.73), we find that if we want to satisfied the relic density constrain, for $r \lesssim 0.9$, we must have that at least $m_{\tilde{l}_R} < 100$ GeV. However the limits set by the LHC searches of the r.h. sleptons decays require that $m_{\tilde{e}_R}, m_{\tilde{\mu}_R} \gtrsim 94$ GeV [60], for degenerate r.h. selectrons and r.h. smuons. The limits for r.h. staus are slightly lower, in fact the LEP2 analysis imposes that the stau mass must be $m_{\tilde{\tau}_R} \gtrsim 87$ GeV [52], [60]. These experimental limits on the slepton masses can be traduced in lower limits on the Bino mass which for $r \simeq 0.3$ implies that $M_1 \gtrsim 23$ GeV while for $r \simeq 0.9$ we have that $M_1 \gtrsim 85$ GeV. Recalling that from the micrOmegas 4.2.5 analysis to fit the right value of the DM relic density (within 2σ) the Bino mass must relies between 18 GeV $\lesssim M_1 \lesssim 21$ GeV for $r \simeq 0.3$ and between 81 GeV $\lesssim M_1 \lesssim 85$ GeV for $r \simeq 0.9$, we find that the experimental constraints from collider searches exclude these mass regions. Thus the natural conclusion is that a pure Bino LSP configuration tends to give a thermal relic density which, compared to the observed one for DM, is too large in a broad range of the parameter space [11].

4.2.1 Pure Bino LSP with co-annihilations

In the context of a pure Bino LSP there is a possibility to reduce its relic abundance, exploiting the mechanism of the co-annihilations. As we saw in Chapter 2 this chance becomes effective when the Bino mass is nearly degenerate with the ones of the next to LSP particles (NLSP's) [33]. In the Bino LSP scenario, perhaps the most studied configuration of this type, is the one where the Bino is nearly degenerate in mass with the r.h. sleptons, and in particular with the r.h. stau [11], [36]. This configuration requires a certain amount of fine tuning between the MSSM parameters, especially between the Bino mass parameter and the r.h. sleptons ones. In fact as we can see from Eq. (2.76), the effect of the co-annihilations is maximal when the exponential factor tends to one. For this reason a good relation that allow us to understand when the co-annihilations are effective is [11]

$$\frac{m_{\tilde{l}_R} - M_1}{M_1} \lesssim \frac{1}{x_{f_0}} \quad (4.78)$$

where, as in Chapter 2, $x_{f_0} \equiv M_1/T_{f_0}$ and T_{f_0} is the freeze-out temperature. Noting that the value of x_{f_0} , from "WIMP miracle" argument, is about $x_{f_0} \sim (20-30)$ [36], and using Eq. (4.78), we find that, the co-annihilations are effective if the square ratio r is at least $r \gtrsim 0.9$. Therefore we will investigate the effects of co-annihilations between Bino and r.h. sleptons assuming that r varies in the range $0.9 \lesssim r \lesssim 1$. Furthermore, following ref. [36], we assume that the three r.h. sleptons are all degenerate in mass, $m_{\tilde{e}_R} = m_{\tilde{\mu}_R} = m_{\tilde{\tau}_R}$, and so, from now on, we refer to them simply as \tilde{l}_R .

Applying the definition of the effective annihilation cross-section given in Eq. (2.78), in this scenario we find that

$$\sigma_{\text{eff}} = \sigma_{\tilde{B}\tilde{B}} r_{\tilde{B}}^2 + 12\sigma_{\tilde{B}\tilde{l}} r_{\tilde{B}} r_{\tilde{l}} + 6(\sigma_{\tilde{l}\tilde{l}} + \sigma_{\tilde{l}\tilde{l}}) r_{\tilde{l}}^2 + 12(\sigma_{\tilde{l}\tilde{l}} + \sigma_{\tilde{l}\tilde{l}}) r_{\tilde{l}}^2 \quad (4.79)$$

where a bar denote an antiparticle while a prime denote a different slepton flavor. The quantities $r_{\tilde{B}}$ and $r_{\tilde{l}}$, using Eq. (2.76), are respectively equal to

$$r_{\tilde{B}} = \frac{r^{3/4}}{r^{3/4} + 3e^{-x(1-\sqrt{r})/\sqrt{r}}} \quad r_{\tilde{l}} = \frac{e^{-x(1-\sqrt{r})/\sqrt{r}}}{r^{3/4} + 3e^{-x(1-\sqrt{r})/\sqrt{r}}. \quad (4.80)$$

Note also that, to obtain Eq. (4.79), we have treated the possible fermion final states as massless. The possible initial and final states are summarized in Table 4.4. The parameters space that

Initial state	Final state	Channels
$\tilde{B}\tilde{B}$	$\bar{l}l$	$u(\tilde{l}_R), t(\tilde{l}_R)$
$\tilde{B}\tilde{l}_R$	$l\gamma, lZ^0, lh$	$s(l), t(\tilde{l}_R)$
$\tilde{l}_R\tilde{l}_R$	ll	$t(\tilde{B}), u(\tilde{B})$
$\tilde{l}_R\tilde{l}'_R$	ll'	$t(\tilde{B})$
$\tilde{l}'_R\tilde{l}_R$	$\bar{l}l'$	$t(\tilde{B})$
$\tilde{l}_R\tilde{l}_R$	$\gamma\gamma, \gamma Z^0$	$t(\tilde{l}_R), u(\tilde{l}_R), p.i.$
	W^+W^-	$s(h), s(\gamma), s(Z^0)$
	hh, Z^0Z^0	$s(h), t(\tilde{l}_R), u(\tilde{l}_R), p.i.$
	Z^0h	$t(\tilde{l}_R), u(\tilde{l}_R), s(Z^0)$
	γh	$t(\tilde{l}_R), u(\tilde{l}_R)$
	$f\bar{f}$	$s(\gamma), s(Z^0), t(\tilde{B})$

Table 4.4: In the table are summarized the possible final state of the co-annihilation processes between Bino and r.h. sleptons. In the third column we list the channels and the exchanged particles which contribute to the process; the abbreviation *p.i.* denotes the point interaction and with *h* we refer to the SM Higgs.

we take into account in our numerical analysis of co-annihilations between Bino LSP and r.h. sleptons is given in Table 4.2 with the difference that $m_{\tilde{l}_R}$ now varies between $M_1 - 1.1M_1$. The results of the `micrOmegas` 4.2.5 simulation show that a Bino mass in the range $127 \text{ GeV} \lesssim M_1 \lesssim 232 \text{ GeV}$ satisfied the DM relic density constraint, within 2σ . The situation is summarized in Fig. 4.3.

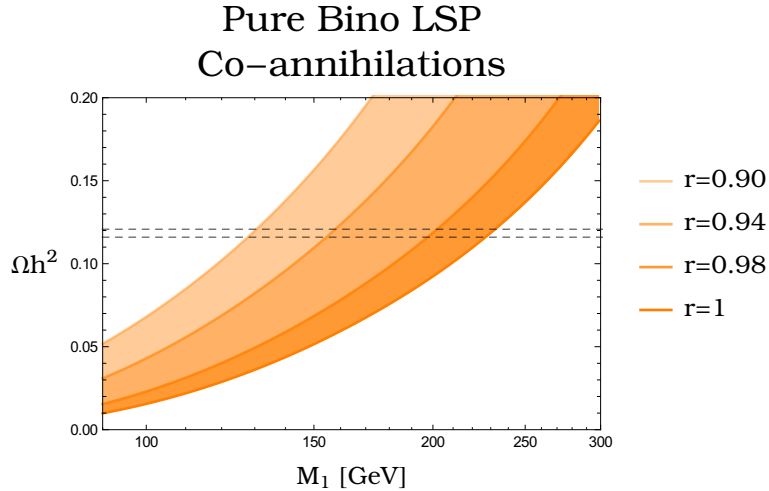


Figure 4.3: The plot shows the `micrOmegas` 4.2.5 result for the relic density provided by a pure Bino LSP taking into account co-annihilations with r.h. sleptons. Every band denote a different value of the ratio $r = M_1^2/m_{\tilde{l}_R}^2$. Comparing this graph with the one given in Fig. 4.1 is possible to observe how co-annihilations have lowered the Bino relic abundance.

To see how the co-annihilations effects can affect the relic abundance of a particular species, in Fig. 4.4 we have plotted the ratio between the relic abundance computed considering co-annihilations and the one computed without considering them, as a function of the Bino mass. From this graph we can see that un-considering co-annihilations, when they are effective, leads

to an overestimation of the relic abundance even 6 times grater.

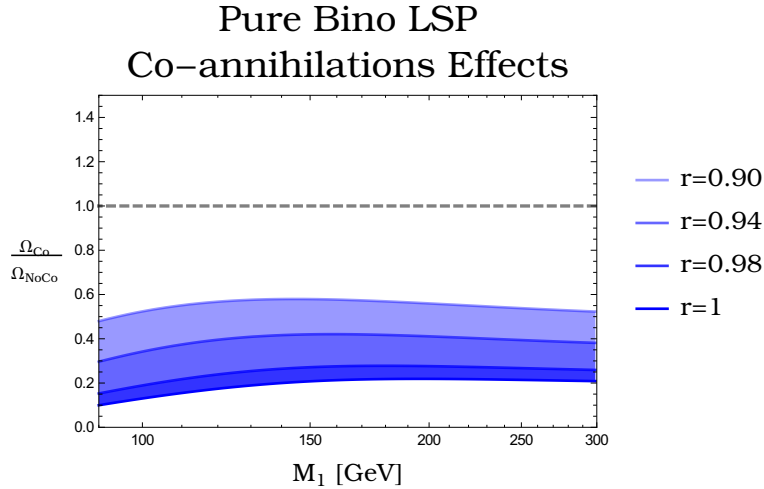


Figure 4.4: In the figure is plotted the ratio $\Omega_{Co}/\Omega_{NoCo}$ as a function of the Bino mass, computed using `micrOmegas 4.2.5`. As in Fig. 4.3 every different colour level denotes a different value of the ratio r .

For what concerns direct detection analysis nothing is changed from the case of a pure Bino without co-annihilations. In fact from Eqs. (4.75), is clear that any possible strong degeneracy between Bino mass and r.h. sleptons ones, cannot affect the previous results. Thus, also in the case of co-annihilations, no exclusion limit on the Bino mass parameter is possible to impose exploiting the results of the direct detection experiments. Furthermore the results of the LHC and LEP searches for slepton decays, show that for a LSP mass $m_{\tilde{\chi}_1} \gtrsim 90$ GeV [60], [52], no limits are imposed on slepton masses. Thus, remembering that with co-annihilations the Bino mass values admitted by the relic density constraint are always greater than 90 GeV, the collider results do not impose any restriction on the slepton masses and so indirectly on the LSP one.

Summarizing, from our analysis and in a good accord with reference [36], we have found that, exploiting co-annihilations, with r.h. sleptons, a pure Bino LSP can be a good DM candidate which satisfies both direct detection and collider constraints, in a fairly broad range of the Bino mass values. The only possible issue comes from the fact that, in order to activate the co-annihilations mechanism, we have to fine tune the value of M_1 and $m_{\tilde{l}_R}$ without any theoretical arguments which justify this.

4.3 Pure Higgsino LSP

Another pure configuration, in the context of neutralino LSP, is provided by the pure Higgsino. This purity state is achieved when, in the LSP composition, the matrix elements N_{13} and N_{14} tend respectively to [56]

$$|N_{13}| \rightarrow 1/\sqrt{2} \quad (4.81)$$

$$|N_{14}| \rightarrow 1/\sqrt{2} \quad (4.82)$$

We note that these relations are well satisfied when⁵

$$|\mu| \ll M_1, M_2. \quad (4.83)$$

⁵Note that we take the absolute value of the parameter μ because, as we said in Chapter 3, we cannot fix its sign.

In fact imposing the above relation into Eqs. (3.49) and Eqs. (3.48), and in the limit where $M_1 - |\mu| \simeq M_2 - |\mu| \gg m_W$, we have that

$$N_{11} \simeq \frac{t_W m_W (\cos \beta - \sin \beta)}{\sqrt{2} (M_1 - |\mu|)} \simeq \mathcal{O} \left(\frac{m_W}{M_1} \right) \quad (4.84a)$$

$$N_{12} \simeq -\frac{m_W (\cos \beta - \sin \beta)}{\sqrt{2} (M_2 - |\mu|)} \simeq \mathcal{O} \left(\frac{m_W}{M_2} \right) \quad (4.84b)$$

$$N_{13} \simeq \frac{1}{\sqrt{2}} + \mathcal{O} \left(\frac{m_W^2}{\mu M_1}, \frac{m_W^2}{\mu M_2} \right) \quad (4.84c)$$

$$N_{14} \simeq \frac{1}{\sqrt{2}} + \mathcal{O} \left(\frac{m_W^2}{\mu M_1}, \frac{m_W^2}{\mu M_2} \right) \quad (4.84d)$$

where, as for the pure Bino, we have taken the limit where $m_H^2 \gg m_h^2$ which implies that $\sin \alpha \simeq -\cos \beta$ and $\cos \alpha \simeq \sin \beta$. Therefore, from these results, we can completely decouple the Bino and the Wino states obtaining a neutralino mass matrix which, in the basis $(\tilde{H}_u^0, \tilde{H}_d^0)$, read as

$$\begin{pmatrix} 0 & \mu \\ \mu & 0 \end{pmatrix} + \mathcal{O} \left(\frac{m_W}{M_1}, \frac{m_W}{M_2} \right). \quad (4.85)$$

Diagonalizing it we obtain two eigenstates, \tilde{H}_1, \tilde{H}_2

$$\tilde{H}_1 = \frac{\tilde{H}_u^0 + \tilde{H}_d^0}{\sqrt{2}} \quad (4.86a)$$

$$\tilde{H}_2 = \frac{\tilde{H}_u^0 - \tilde{H}_d^0}{\sqrt{2}}, \quad (4.86b)$$

with associated eigenvalue respectively equal to μ and $-\mu$; note that, as we said in Chapter 3, the neutralino masses are defined to be the absolute values of the neutralino mass matrix eigenvalues. Therefore in this case the two Higgsino masses are defined to be $|\mu|$ and so, up to corrections of order m_W/M_1 or m_W/M_2 , they are equal for both the Higgsino fields. As a consequence the LSP is completely mass degenerate with the next-to-LSP particle (NLSP). As a reference we will take as LSP \tilde{H}_1 , and as NLSP \tilde{H}_2 , but in the limit of a pure Higgsino LSP their roles are interchangeable. Furthermore, observing at Eqs. (3.56), we can see that Eq. (4.83) implies that the lightest chargino is the charged Higgsino, namely \tilde{H}^\pm , which, up to corrections of order m_W/M_2 , has a mass equal to $|\mu|$. So in the pure Higgsino LSP configuration we have to face with three $(\tilde{H}_1, \tilde{H}_2, \tilde{H}^\pm)$ mass degenerate states with mass $|\mu|$. Hence to go further in the computation of the relic abundance of a Higgsino LSP, we have to estimate if the co-annihilations among the three Higgsino states are relevant or not. As said in the pure Bino section these become important when the relation given in Eq. (4.78) is satisfied, which, in the pure Higgsino case read as

$$\frac{\delta m_{\tilde{H}}}{m_{\tilde{H}_1}} \lesssim \frac{1}{x_{\text{fo}}}. \quad (4.87)$$

Using Eq. (3.48) and Eq. (3.56), the mass splitting, $\delta m_{\tilde{H}}$, between the LSP and the lightest chargino, in the pure Higgsino LSP limit, becomes [39]

$$\delta m_{\tilde{H}} \approx \frac{m_{Z^0}^2}{2M_2} c_W^2 (1 + \sin 2\beta) + \frac{m_{Z^0}^2}{2M_1} s_W^2 (1 - \sin 2\beta) + \mathcal{O} \left(\frac{m_{Z^0}^2}{M_1^2}, \frac{m_{Z^0}^2}{M_2^2} \right), \quad (4.88)$$

note that a similar result can be obtained for the mass splitting among the LSP and NLSP. So taking $\tan \beta \simeq 10$ and $M_1 \simeq M_2 \equiv M_g$, we have that $\delta m_{\tilde{H}}$ turns out to be about⁶

$$\delta m_{\tilde{H}} \approx \frac{800 \text{ GeV}^2}{M_g} \approx 0.8 \text{ GeV} \quad (4.89)$$

⁶We use $M_{Z^0} \simeq 91.188 \text{ GeV}$ and $s_W^2 \simeq 0.233$ from ref. [60].

Initial states	Final states	Channels
$\tilde{H}_{1,2}\tilde{H}_{1,2}$	$W^\pm W^\mp$ $Z^0 Z^0$	$u(\tilde{H}^\pm), t(\tilde{H}^\pm)$ $u(\tilde{H}_{2,1}), t(\tilde{H}_{2,1})$
$\tilde{H}_1\tilde{H}_2$	$W^\pm W^\mp$ $f\bar{f}$	$t(\tilde{H}^\pm), s(Z^0)$ $s(Z^0)$
$\tilde{H}^\pm\tilde{H}_{1,2}$	$W^\pm\gamma$ $W^\pm Z^0$ $f'\bar{f}$	$t(\tilde{H}^\pm), s(W^\pm)$ $t(\tilde{H}^\pm), t(\tilde{H}_{2,1}), s(W^\pm)$ $s(W^\pm)$
$\tilde{H}^\pm\tilde{H}^\mp$	$W^\pm W^\mp$ $Z^0 Z^0, \gamma\gamma$ $f\bar{f}$	$t(\tilde{H}_{1,2}), s(\gamma), s(Z^0)$ $t(\tilde{H}^\pm)$ $s(\gamma), s(Z^0)$
$\tilde{H}^\pm\tilde{H}^\pm$	$W^\pm W^\pm$	$t(\tilde{H}_{1,2}), u(\tilde{H}_{1,2})$

Table 4.5: In the table are summarized the possible final state of the co-annihilation processes between the three Higgsino states. As usual in the last column we give the channels of the tree-level Feynman diagrams with the exchange particle.

where in the last equality we have assumed $M_g \approx 1$ TeV. Therefore substituting this result into Eq. (4.87) and remembering that x_{f_0} lies in the range 20 – 30 is clear that for an LSP mass $m_{\tilde{H}_1} \geq 100$ GeV the co-annihilations effects are of a fundamental importance in the evaluation of the relic abundance of a pure Higgsino LSP [11], [56], [33]. The lower limit in the LSP mass, $m_{\tilde{H}_1} \geq 100$ GeV, is due to the fact that from searches of chargino decays at LEP, the lightest chargino must have a mass which is $m_{\tilde{\chi}^\pm} \gtrsim 103$ GeV. Thus because the mass splitting between the lightest Higgsino and the charged one is at most of few GeV, the lower limit imposed on chargino mass by LEP, forced us to take as lower bound for the LSP mass the value of 100 GeV.

In this scenario the most important annihilation and co-annihilations channels are into gauge bosons and fermion anti-fermion pairs [11]; the possible processes of this types are given in Table 4.5. In Appendix E we give the tree-level Feynman diagrams of the processes listed in Table 4.5, with the corresponding cross-sections at leading order in the non-relativistic expansion. Thus taking into account the results of Eqs. (E.166), and substituting them into Eq. (2.78) and then into Eq. (2.86) we obtain that, the thermal average of the effective cross-section times velocity for a pure Higgsino LSP at the leading order, is given by

$$\langle\sigma_{\text{eff}}v\rangle_{\tilde{H}} = \sum_{i,j}^4 \frac{\sigma_{ij}}{16} = \frac{g^4}{512\mu^2\pi} (21 + 3t_W^2 + 11t_W^4) + \mathcal{O}\left(\frac{1}{x}\right) \quad (4.90)$$

where we have redefined $t_W \equiv \tan\theta_W$. Note that because we have assumed a quite perfect degeneration between LSP, NLSP and the lightest chargino and the fact that they have the same d.o.f., have reduced the formula for the effective cross-section, given in Eq. (2.78), to the average of the various co-annihilation cross-sections. Substituting Eq. (4.90) into the relic density formula, Eq. (2.90), we obtain an approximated expression of the relic abundance of a pure Higgsino LSP

$$\Omega_{\tilde{H}} h^2 = 0.097 \left(\frac{\mu}{1 \text{ TeV}} \right)^2 \quad (4.91)$$

where we have drop out a small logarithmic dependence on μ .

Our simulation with `micrOmegas` 4.2.5 takes into account the MSSM parameters given in Table 4.6, and the result is depicted in Fig. 4.5, where we plot the relic abundance of a Higgsino LSP as a function of its mass compared with the analytical result provided by Eq. (4.91). Note that the analytical result generally give a lower relic density in the region of

MSSM Parameter	Value-Range
μ	100 – 1500 GeV
M_1	2.5 TeV
M_2	3 TeV
M_3	3.8 TeV
$m_{\tilde{l}_{L,R}}$	> 2 TeV
$m_{\tilde{q}_{L,R}}$	> 2 TeV
$\tan \beta$	10

Table 4.6: In the table are summarized the MSSM parameters which we take into account for the pure Higgsino LSP analysis.

interest. This is due to our assumption of a perfect mass degeneration among the LSP, NLSP and the lightest chargino, in the derivation of the Eq. (4.91). In fact, this has the effect of maximizing the co-annihilations mechanism and, as a consequence, the resulting effective cross-section, σ_{eff} , is maximized and so the relic abundance is more lowered. Conversely with the numerical simulation, the three Higgsinos are not perfectly mass degenerate and the remaining small mass differences inhibit the co-annihilation effects resulting in a relic density which is less lowered than the analytical one. On a quantitative ground, from our numerical analysis, a

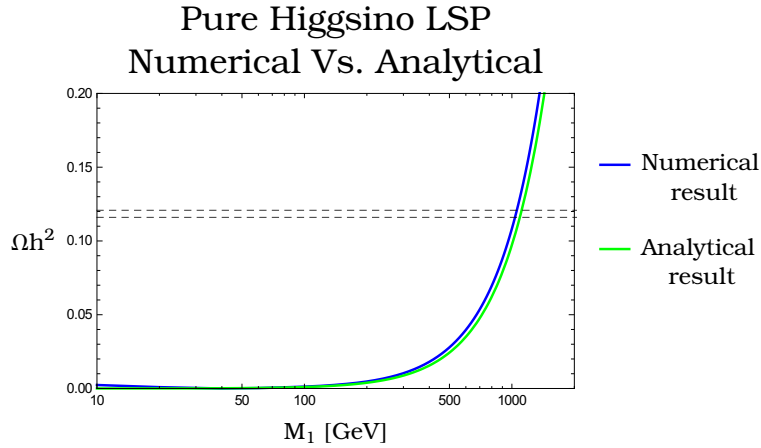


Figure 4.5: In the figure is shown the contribution to Ωh^2 of a pure Higgsino LSP as a function of its mass, obtained from the `micrOmegas` 4.2.5 analysis (blue line) and compared with the analytical result (green line) obtained using Eq. (4.91). As usual the band between the dashed lines denotes the observed DM abundance within 2σ .

pure Higgsino LSP satisfies the DM relic density constraint, within 2σ , if it has a mass which is about $|\mu| \simeq 1$ TeV, or more precisely if its mass is within the range $1.034 \text{ TeV} \lesssim |\mu| \lesssim 1.054 \text{ TeV}$.

For what concerns the direct detection analysis using the results given in Eqs. (4.84), the SD and SI coefficients given in Eq. (4.17) and Eq. (4.18) become

$$\alpha_{\tilde{H}}^{\text{SD}(q_i)} = \frac{g^2 m_{q_i}^2}{16 m_W^2 B_i^2} \left[\frac{(\eta_{11}^i)^2 + (\eta_{12}^i)^2}{(m_{\tilde{q}_{1i}}^2 - \mu^2)} + \frac{(\eta_{11}^i)^2 + (\eta_{12}^i)^2}{(m_{\tilde{q}_{2i}}^2 - \mu^2)} \right] + \frac{g^2}{32 |\mu|} (-1)^i \left(\frac{t_W^2}{M_1} + \frac{1}{M_2} \right) \cos 2\beta \quad (4.92a)$$

$$\alpha_{\tilde{H}}^{\text{SI}(q_i)} = \frac{g^2 m_{q_i}^2}{16 m_W^2 B_i^2} \left[\frac{\eta_{11}^i \eta_{12}^i}{(m_{\tilde{q}_{1i}}^2 - \mu^2)} - \frac{\eta_{11}^i \eta_{12}^i}{(m_{\tilde{q}_{2i}}^2 - \mu^2)} \right] \mp \frac{g^2 m_{q_i}}{8 m_h^2} \left(\frac{t_W^2}{M_1 - |\mu|} + \frac{1}{M_2 - |\mu|} \right) (1 \mp \sin 2\beta) \quad (4.92b)$$

Cross-section	Value-Range
$\sigma_{0\text{SD}}^{\tilde{H}p}$	$7 \times 10^{-10} - 1.1 \times 10^{-7}$ pb
$\sigma_{0\text{SD}}^{\tilde{H}n}$	$5.3 \times 10^{-10} - 8.5 \times 10^{-8}$ pb
$\sigma_{0\text{SI}}^{\tilde{H}p,n}$	$2.1 \times 10^{-12} - 2.5 \times 10^{-12}$ pb

Table 4.7: In the table are listed the upper and lower values of the SD and SI Higgsino-nucleon cross-sections computed with `micrOmegas 4.2.5`.

where the upper signs refers to $\mu > 0$ while the lower ones to $\mu < 0$, B_i is defined as in Eqs. (4.19), and as usual with $i = 1$ we refer to up-type quarks and with $i = 2$ to down-type ones. Substituting these results into Eq. (4.35) and Eq. (4.61) we obtain the Higgsino-nucleon cross-sections at zero momentum transferred

$$\sigma_{0\text{SD}}^{\tilde{H}p} = \frac{12}{\pi} \left(\frac{\mu m_p}{|\mu| + m_p} \right)^2 \left[\sum_{q=u,c,t} \alpha_{\tilde{H}}^{SD(q_1)} \Delta q^{(p)} + \sum_{q=d,s,b} \alpha_{\tilde{H}}^{SD(q_2)} \Delta q^{(p)} \right]^2 \quad (4.93a)$$

$$\sigma_{0\text{SD}}^{\tilde{H}n} = \frac{12}{\pi} \left(\frac{\mu m_n}{|\mu| + m_n} \right)^2 \left[\sum_{q=u,c,t} \alpha_{\tilde{H}}^{SD(q_1)} \Delta q^{(n)} + \sum_{q=d,s,b} \alpha_{\tilde{H}}^{SD(q_2)} \Delta q^{(n)} \right]^2 \quad (4.93b)$$

$$\sigma_{0\text{SI}}^{\tilde{H}p/n} = \frac{4}{\pi} \left(\frac{\mu m_{p/n}}{|\mu| + m_{p/n}} \right)^2 \left[\sum_{q=u,d,s} \frac{m_{p/n}}{m_q} f_{\text{T}q}^{(p/n)} \alpha_{\tilde{H}}^{SI(q_i)} + \frac{2}{27} f_{\text{T}G} \sum_{q=b,c,t} \frac{m_{p/n}}{m_q} \alpha_{\tilde{H}}^{SI(q_i)} \right]^2, \quad (4.93c)$$

where as usual the the quantities $\Delta q^{(p/n)}$, $f_{\text{T}q}^{(p/n)}$ and $f_{\text{T}G}$ are defined in Table 4.1 and in Eq. (4.55). The numerical results of direct detection analysis are summarized in Table 4.7 while in Fig. 4.6 we depict these results compared with the experimental bounds. Here in the limit where $m_{\tilde{q}_{1i}} \simeq m_{\tilde{q}_{2i}} = m_{\tilde{q}} \gg |\mu|$ and of high squark masses which implies $\eta_{11}^i \rightarrow 1$ and $\eta_{12}^i \rightarrow 0$, the results given in Eqs. (4.92) read as

$$\alpha_{\tilde{H}}^{SD(q_i)} \simeq \frac{g^2 m_{q_i}^2}{8m_W^2 B_i^2} \frac{1}{m_{\tilde{q}}^2} + \frac{g^2}{32|\mu|} (-1)^i \left(\frac{t_W^2}{M_1} + \frac{1}{M_2} \right) \cos 2\beta + \mathcal{O} \left(\frac{\mu^2}{m_{\tilde{q}}^2}, \eta_{12}^2 \right) \quad (4.94a)$$

$$\simeq \frac{g^2}{32|\mu|} (-1)^i \left(\frac{t_W^2}{M_1} + \frac{1}{M_2} \right) \cos 2\beta + \mathcal{O} \left(\frac{m_{q_i}^2}{m_{\tilde{q}}^2}, \eta_{12}^2 \right)$$

$$\alpha_{\tilde{H}}^{SI(q_i)} \simeq \frac{g^2 m_{q_i}^3}{16m_W^2 B_i^2} \frac{\mu (\tan \beta)^{(-1)^i}}{m_{\tilde{q}}^4} \quad (4.94b)$$

$$\mp \frac{g^2 m_{q_i}}{8m_h^2} \left(\frac{t_W^2}{M_1} + \frac{1}{M_2} \right) (1 \mp \sin 2\beta) + \mathcal{O} \left(\frac{\mu^2}{m_{\tilde{q}}^2}, \frac{\mu}{M_{1,2}}, \eta_{12}^2 \right)$$

$$\simeq \mp \frac{g^2 m_{q_i}}{8m_h^2} \left(\frac{t_W^2}{M_1} + \frac{1}{M_2} \right) (1 \mp \sin 2\beta) + \mathcal{O} \left(\frac{m_{q_i}^2}{m_{\tilde{q}}^2}, \frac{\mu}{M_{1,2}} \right).$$

where in place of the product $\eta_{11}^i \eta_{12}^i$ we have substituted the relation given in Eq. (3.62). Note that, as in the pure Bino LSP case, the SI interaction is completely determined by the Higgs exchange interaction, because the term relative to the squarks exchange is suppressed by the factor $\mu/m_{\tilde{q}}^4$, see Eq. (4.94b). Furthermore for the SD interaction the term relative to the squarks exchange is completely dominated by the term relative to the Z^0 exchange. In fact as we can see from Eq. (4.94a) the former one is suppressed by $m_{\tilde{q}}^2$ while the latter one by product $\mu M_{1,2}$. Thus assuming that $m_{\tilde{q}} \simeq M_1 \simeq M_2$, we have that the term relative to the Z^0 exchange is $m_{\tilde{q}}/\mu$ times larger than the term due to the squarks exchange. The numerical results plotted in Fig. 4.6 are confirmed by the analytical ones given in Eqs. (4.94). In particular from plots (a) and (b) is evident the μ dependence expected by Eq. (4.94b). Note also that all the numerical results do not depend on the common squarks mass consistently with the approximated formulae given in Eqs. (4.94).

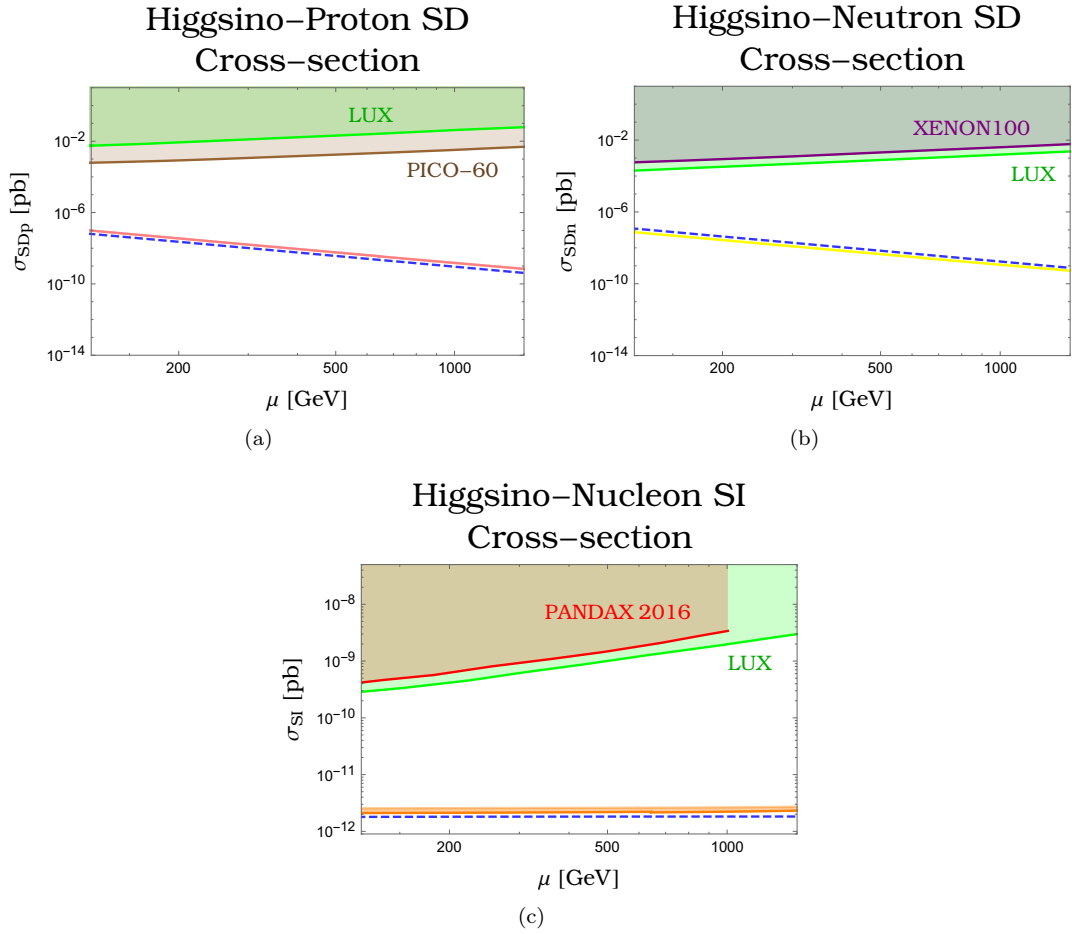


Figure 4.6: In the figure we show the results of the direct detection analysis performed with `micrOmegas` 4.2.5. In the panel (a) is shown the SD Higgsino-proton scattering cross-section (pink) with the analytical result (blue-dashed line), the shaded regions are the excluded regions by LUX-2016 (green) and PICO-60 (brown) experiments. In the left panel (b) is shown the SD Higgsino-neutron scattering cross-section (yellow) and the analytical result (blue-dashed line), with the experimental bounds from LUX-2016 (green) and XENON100 (purple). In the below panel (c) we show the result for the SI Higgsino-nucleon scattering cross-section (orange) and the analytical result (blue-dashed line), with the excluded limits given by the LUX-2016 (green) and PANDAX-2016 (red) experiments. The squark masses run from 2 TeV to 8 TeV and the analytical results are found using Eqs. (4.94).

The combined effect of the SD and SI interactions can be estimated with the help of Eq. (4.67) which, using the values of J_A , A and $\langle S_{p,n} \rangle$ for ^{131}Xe nucleus given in the pure Bino section, reads as

$$\sigma_0^{\tilde{H}\text{Xe}} \simeq \frac{\mu_N^2}{\mu_p^2} A^2 \left[\sigma_{0\text{SI}}^{\tilde{H}p} + 8 \times 10^{-6} \sigma_{0\text{SD}}^{\tilde{H}p} \right] \quad (4.95)$$

where we used the fact that from the values given in Table 4.7 we have that $\sqrt{\sigma_{0\text{SD}}^{\tilde{H}n}/\sigma_{0\text{SD}}^{\tilde{H}p}} \simeq 0.9$. Here the ratio between the SD Higgsino-Xe scattering cross-section and the SI one is about $\sigma_{0\text{SD}}^{\tilde{H}\text{Xe}}/\sigma_{0\text{SI}}^{\tilde{H}\text{Xe}} \simeq 0.03$. Therefore for a pure Higgsino LSP the relative contribution of the SD interaction is negligible respect to the SI one. As a consequence a separate analysis of the SD and SI contribution, as the one performed in Fig. 4.6, is justify.

Anyway from Fig. 4.6 it is appreciable that the expected Higgsino-nucleon scattering cross-sections (SD and SI) are well below the today's direct detection bounds. Thus from direct detection constraints an heavy Higgsino LSP with a mass of about 1 TeV seems to be a good DM candidate.

Nevertheless with this high $|\mu|$ value there would be a potential theoretical issue. This problem is related to the fact that the low energy MSSM model has to reproduce the electroweak symmetry breaking (EWSB). As we know in order to do this we have to minimize the MSSM Higgs potential, given in Eq. (3.33). This operation imposes a relation between the Z^0 boson mass, m_{Z^0} , the Higgs soft-mass parameters, m_{H_u}, m_{H_d} , and the parameter μ [54], [22]. This relation at tree-level and in terms of $\tan\beta$ reads as [22]

$$\frac{m_{Z^0}^2}{2} = \frac{m_{H_d}^2 + |m_{H_u}|^2 \tan^2 \beta}{\tan^2 \beta - 1} - |\mu|^2. \quad (4.96)$$

In the limit of moderate large $\tan\beta$ (condition which is desirable in order to avoid the need for a gigantic stop mass to find the right mass of the lightest Higgs boson [22]) Eq. (4.96) reduces to [22]

$$-\frac{m_{Z^0}^2}{2} \simeq |\mu|^2 - |m_{H_u}|^2. \quad (4.97)$$

From this relation the EWSB fine tuning problem is more clear. In fact if we take values of μ of order of few TeV the required values of m_{H_u} have to be relatively fine tuned in order to obtain the observed value of m_{Z^0} . Therefore a pure Higgsino LSP with a mass of about $|\mu| \simeq 1$ TeV resolves the DM problem, but has also the effect to reintroduce a fine tuning problem in the theory [11]. This is in net contrast with the original motivations at the base of SUSY theory, which was introduced precisely to reproduce the EW scale without too much fine tuning.

Furthermore the possibility of a pure Higgsino DM can be ruled out by future indirect searches. Indirect detection experiments try to observe the radiation produced by DM annihilations in the galaxy [19]. The flux of these gamma radiation depends on the annihilation cross-section of the particular DM candidate. In particular these photons come, indirectly, from the disintegration of the W^\pm bosons produced by the DM annihilation and, directly, from the one-loop annihilation processes such as $\tilde{\chi}\tilde{\chi} \rightarrow \gamma\gamma$ and $\tilde{\chi}\tilde{\chi} \rightarrow \gamma Z^0$, where $\tilde{\chi}$ denotes the DM candidate.⁷ The former processes produce a continuous photon spectrum which falls increasing the energy of the processes, while the latter processes give a distinct signature against the background [17]. In particular, for a Higgsino LSP, the one-loop processes are $\tilde{H}_1\tilde{H}_1 \rightarrow \gamma\gamma$ and $\tilde{H}_1\tilde{H}_1 \rightarrow \gamma Z^0$, a sample of the possible Feynman diagrams for these processes is

$$(4.98)$$

In the limit of a heavy pure Higgsino LSP the thermal average cross-section times velocity of these one-loop annihilation processes are nearly constant i.e. they do not depend on the LSP mass (or the energy of the process) [17], and their values are about $\langle\sigma v\rangle_{\gamma\gamma} \approx 10^{-28}\text{cm}^3/\text{s}$ for two photons emission and $\langle\sigma v\rangle_{\gamma Z^0} \approx 8 \times 10^{-29}\text{cm}^3/\text{s}$ for one photon emission [39]. In particular in this energy regime these one-loop processes dominate over the ones for the W^\pm emission. Furthermore because the annihilation occurs in a non-relativistic regime, the energy of the emitted photons would be $E_\gamma = |\mu|$ for two photons emission, while $E_\gamma = |\mu|(1 - m_{Z^0}^2/(4|\mu|^2))$ for one photon emission [16]. So what we expect is a narrow line in the emitted gamma spectrum that would be peaked at an energy roughly equal to the mass of the Higgsino LSP. Nowadays this typical signal, at $E_\gamma \simeq 1$ TeV is not yet observed [2], probably because the small values of the Higgsino annihilation cross-section into photons. Nevertheless a major sensitivity of the future experiments could exclude pure Higgsino dark matter. However it is worth to note that indirect detection searches suffer of a certain amount of uncertainty due to the fact that the flux of gamma-ray emission depends also on the DM density profile, which is not well known.

⁷Note that these processes are possible when the DM candidate is nearly degenerate with the lightest chargino and so it can couple with the W^\pm SM bosons.

Anyway these arguments suggest that the Higgsino LSP mass has to be strictly less of 1 TeV. This requirement implies that a pure Higgsino LSP has a relic abundance which is too small to agree with the one observed for DM and so it is not acceptable as DM candidate [11]. Note that this situation is diametrically opposed to the one of a pure Bino LSP which, as we said in the previous section, tends to have a relic abundance which is too large compared with the DM one.

4.4 Pure Wino LSP

The last purity configuration which we consider, is the one provided by the pure Wino LSP. This configuration is achieved when in the LSP definition, given in Eq. (3.44), we send [50]

$$\begin{aligned} N_{12} &\rightarrow 1 \\ N_{11}, N_{13}, N_{14} &\rightarrow 0. \end{aligned}$$

The more direct way to satisfied these relations, is to impose at the electroweak scale that

$$M_2 \ll M_1 < |\mu| \quad (4.99)$$

where M_2 is the Wino mass parameter. In fact taking into account Eqs. (3.48) and Eqs. (3.49) we can see that imposing the above relation we obtain that

$$N_{11} \simeq -\frac{t_W m_W^2 (M_2 + \mu \sin 2\beta)}{(M_1 - M_2)(\mu^2 - M_2^2)} \simeq \mathcal{O}\left(\frac{m_W^2}{M_1 \mu}\right) \quad (4.100a)$$

$$N_{12} \simeq 1 + \mathcal{O}\left(\frac{m_W^2}{\mu^2}\right) \quad (4.100b)$$

$$N_{13} \simeq \left(\frac{t_W m_W^2 (M_2 + \mu \sin 2\beta)}{(\mu^2 - M_2^2) \cos \beta} + \frac{m_W \sin \beta}{\mu}\right) \simeq \mathcal{O}\left(\frac{m_W}{\mu}\right) \quad (4.100c)$$

$$N_{14} \simeq \left(\frac{M_2 t_W m_W^2 (M_2 + \mu \sin 2\beta)}{\mu (\mu^2 - M_2^2) \cos \beta} + \frac{m_W \cos \beta}{\mu}\right) \simeq \mathcal{O}\left(\frac{m_W}{\mu}\right), \quad (4.100d)$$

where as above we have assumed that $|\mu|, (|\mu| - M_2) \gg m_W$ and that $m_H^2 \gg m_h^2$. As a consequence the lightest neutralino is nearly a pure Wino, $\tilde{\chi}_1^0 = \tilde{W}^0$, with a mass, at the leading order, equal to $m_{\tilde{\chi}_1^0} \simeq M_2$. Observing at Eqs. (3.56) we note that the above relation among the neutralino mass parameters, imposes also that the lightest chargino is the charged Wino, $\tilde{\chi}_1^\pm = \tilde{W}^\pm$, with a mass equal to $m_{\tilde{\chi}_1^\pm} \simeq M_2$ up to corrections of order m_W/μ , is. So, as in the pure Higgsino case, we have a condition of nearly perfect mass degeneration between the LSP and the lightest chargino. Using Eq. (3.48) and Eq. (3.56) we can evaluate the mass splitting between the Wino LSP and the charged Wino which is about [39]

$$\delta m_{\tilde{W}} = \frac{m_{Z^0}^4}{M_1 \mu^2} s_W^2 c_W^2 \sin^2 2\beta \approx 5 \times 10^{-6} \text{ GeV} \frac{(1 \text{ TeV})^3}{M_1 \mu^2} + \mathcal{O}\left(\frac{m_W^2}{M_1^2}, \frac{m_{Z^0}^4}{\mu^4}\right). \quad (4.101)$$

Comparing this result with the one given in Eq. (4.88) for the pure Higgsino case, we note that, in the pure Wino case, the mass splitting between LSP and lightest chargino is more extreme, because it is suppressed by three powers of the mass parameters; conversely, as is evident from Eq. (4.88), in the pure Higgsino case, the suppression was only of one power of the mass parameters [39]. Taking into account this and assuming that $M_1, |\mu| > 1 \text{ TeV}$ we obtain that the mass splitting is about

$$\delta m_{\tilde{W}} < 5 \times 10^{-6} \text{ GeV}. \quad (4.102)$$

Therefore in the pure Wino case the condition for the effectiveness of the co-annihilations read as

$$\frac{\delta m_{\tilde{W}}}{M_2} < \frac{1}{x_{\text{fo}}} \quad (4.103)$$

Initial states	Final states	Channels
$\tilde{W}^0\tilde{W}^0$	$W^\pm W^\mp$	$u(\tilde{W}^\pm), t(\tilde{W}^\pm)$
$\tilde{W}^\pm\tilde{W}^0$	$W^\pm\gamma, W^\pm Z^0$ $f'\bar{f}$	$t(\tilde{W}^\pm), s(W^\pm)$ $s(W^\pm)$
$\tilde{W}^\pm\tilde{W}^\mp$	$W^\pm W^\mp$ $Z^0 Z^0, \gamma\gamma$ $f\bar{f}$	$t(\tilde{W}^0), s(\gamma), s(Z^0)$ $t(\tilde{W}^\pm)$ $s(\gamma), s(Z^0)$
$\tilde{W}^\pm\tilde{W}^\pm$	$W^\pm W^\pm$	$t(\tilde{W}^0), u(\tilde{W}^0)$

Table 4.8: In the table are summarized the possible final state of the co-annihilation processes between the neutral and charged Winos. Note that in the table we do not show the processes mediated by sfermions, because they are suppressed by the high sfermion masses.

MSSM Parameter	Value-Range
M_2	100 – 2500 GeV
M_1	3 TeV
μ	4 TeV
M_3	5 TeV
$m_{\tilde{l}_{L,R}}$	> 3 TeV
$m_{\tilde{q}_{L,R}}$	> 2.5 TeV
$\tan\beta$	10

Table 4.9: In the table are summarized the MSSM parameters used for the numerical simulation of the pure Wino LSP configuration.

which for $\delta m_{\tilde{W}}$ given above, $M_2 > 100$ GeV and as usual $x_{f_0} \sim 20 - 30$, is certainly satisfied. Thus the co-annihilations between the neutral Winos and the charged ones become of fundamental importance in the computation of the Wino LSP relic abundance.

For a pure Wino LSP the dominant annihilation and co-annihilations channels are into gauge bosons and fermion anti-fermion pairs, in Table 4.8 we summarize these processes with the exchanged particles. In Appendix E we compute the annihilation cross-sections of the processes given in Table 4.8, in the limit of a perfect degeneration between \tilde{W} and \tilde{W}^\pm . Note that in principle, as occurred in the Bino LSP case, there is also a possible contribution from annihilation into final fermion anti-fermion pairs through sfermion exchange. In our analytic analysis we neglect these processes because they are relatively high suppressed by the high sfermions masses.

Substituting into Eq. (2.78) the cross-sections given in the Eqs. (E.116) and then using Eq. (2.86), we obtain that the thermal average of the effective cross-section times velocity for a Wino LSP is

$$\langle\sigma_{\text{eff}}v\rangle_{\tilde{W}} = \sum_{i,j}^3 \frac{\sigma_{ij}}{9} = \frac{3g^4}{16\pi M_2^2} + \mathcal{O}\left(\frac{1}{x}\right). \quad (4.104)$$

Using this result into the relic density formula given in Eq. (2.90), we get that

$$\Omega_{\tilde{W}} h^2 = 0.15 \left(\frac{M_2}{2.5 \text{ TeV}} \right)^2, \quad (4.105)$$

which gives a good approximation of the relic density provided by a pure Wino LSP as a function of its mass. Our numerical analysis of the pure Wino LSP takes into account the values of the MSSM parameters given in Table 4.9. In particular the results of the `micrOmegas`

4.2.5 simulation sets that a Wino LSP fulfill the DM constraint if it has a mass in the range, $2016 \text{ GeV} \lesssim M_2 \lesssim 2140 \text{ GeV}$. In Fig. 4.7 we compare the result of the numerical analysis with the analytical one obtained using Eq. (4.105). As is evident both the analytical and numerical

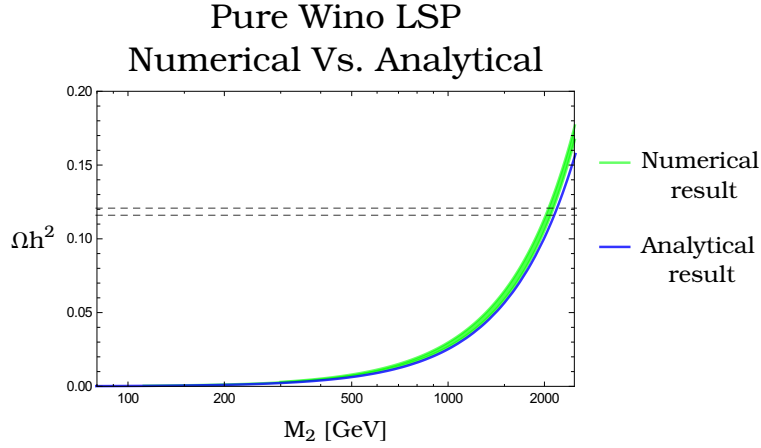


Figure 4.7: In the figure is shown the contribution to Ωh^2 of a pure Wino LSP as a function of its mass, obtained from the `micrOmegas` 4.2.5 simulation (green line), compared with the analytical result (blue line) obtained using Eq. (2.90). The width of band, in the numerical analysis, is obtained varying the parameters $m_{\tilde{t}}$ and $m_{\tilde{q}}$ from 3 TeV to 10 TeV.

analysis show that a value of the Wino mass as larger as $M_2 \sim 2000 \text{ GeV}$ is required in order to reproduce the correct DM relic density. In Fig. 4.7 the band of the numerical result is obtained varying the sploton and the squark mass parameters from 3 TeV to 10 TeV. The smallness of the width of this band, reflects the small contribution of the annihilation processes mediated by sfermions.

For what concern the direct detection analysis, substituting the results given in Eqs. (4.100) into Eq. (4.17) and Eq. (4.18) we get that

$$\alpha_{\tilde{W}}^{\text{SD}(q_i)} = \frac{g^2(\eta_{11}^i)^2}{16} \left[\frac{1}{(m_{\tilde{q}_{1_i}}^2 - M_2^2)} + \frac{1}{(m_{\tilde{q}_{2_i}}^2 - M_2^2)} \right] + \frac{g^2}{16(M_2^2 - \mu^2)} (-1)^i \cos 2\beta \quad (4.106a)$$

$$\alpha_{\tilde{W}}^{\text{SI}(q_i)} = -\frac{g^2 m_{q_i}}{4m_h^2} \left(\frac{M_2 + \mu \sin 2\beta}{M_2^2 - \mu^2} \right) \quad (4.106b)$$

note that in the SI independent interaction is absent the term relative to the squarks exchange, because it is suppressed by a factor $(m_{q_i} m_W)/(\mu m_{\tilde{q}_{1,2_i}}^2)$. Substituting these equations into Eq. (4.35) and Eq. (4.61) we find that the Wino-nucleon cross-sections at zero momentum transferred are equal to

$$\sigma_{0\text{SD}}^{\tilde{W}p} = \frac{12}{\pi} \left(\frac{M_2 m_p}{M_2 + m_p} \right)^2 \left[\sum_{q_i} \alpha_{\tilde{W}}^{\text{SD}(q_i)} \Delta q^{(p)} \right]^2 \quad (4.107a)$$

$$\sigma_{0\text{SD}}^{\tilde{W}n} = \frac{12}{\pi} \left(\frac{M_2 m_n}{M_2 + m_n} \right)^2 \left[\sum_{q_i} \alpha_{\tilde{W}}^{\text{SD}(q_i)} \Delta q^{(n)} \right]^2 \quad (4.107b)$$

$$\sigma_{0\text{SI}}^{\tilde{W}p/n} = \frac{4}{\pi} \left(\frac{M_2 m_p}{M_2 + m_p} \right)^2 \left[\sum_{q=u,d,s} \frac{m_{p/n}}{m_q} f_{\text{T}q}^{(p/n)} \alpha_{\tilde{W}}^{\text{SI}(q_i)} + \frac{2}{27} f_{\text{T}G} \sum_{q=c,b,t} \frac{m_{p/n}}{m_q} \alpha_{\tilde{W}}^{\text{SI}(q_i)} \right]^2. \quad (4.107c)$$

In Fig. 4.8 we plot the `micrOmegas` 4.2.5 results for the SD and SI scattering cross-sections on nucleons for a Wino LSP with the excluded experimental regions and in Table 4.10 we collect these numerical results.

For a pure Wino LSP in the limit where $m_{\tilde{q}_{1_i}} \simeq m_{\tilde{q}_{2_i}} = m_{\tilde{q}} \gg M_2$, and of heavy squark

Cross-section	Value-Range
$\sigma_{0,SD}^{\tilde{W}p}$	$1 \times 10^{-11} - 1.4 \times 10^{-9}$ pb
$\sigma_{0,SD}^{\tilde{W}n}$	$4.5 \times 10^{-11} - 2.3 \times 10^{-9}$ pb
$\sigma_{0,SI}^{\tilde{W}p,n}$	$7.3 \times 10^{-13} - 7.7 \times 10^{-13}$ pb

Table 4.10: In the table are listed the upper and lower values of the SD and SI Wino-nucleon cross-sections computed with `micrOmegas 4.2.5`.

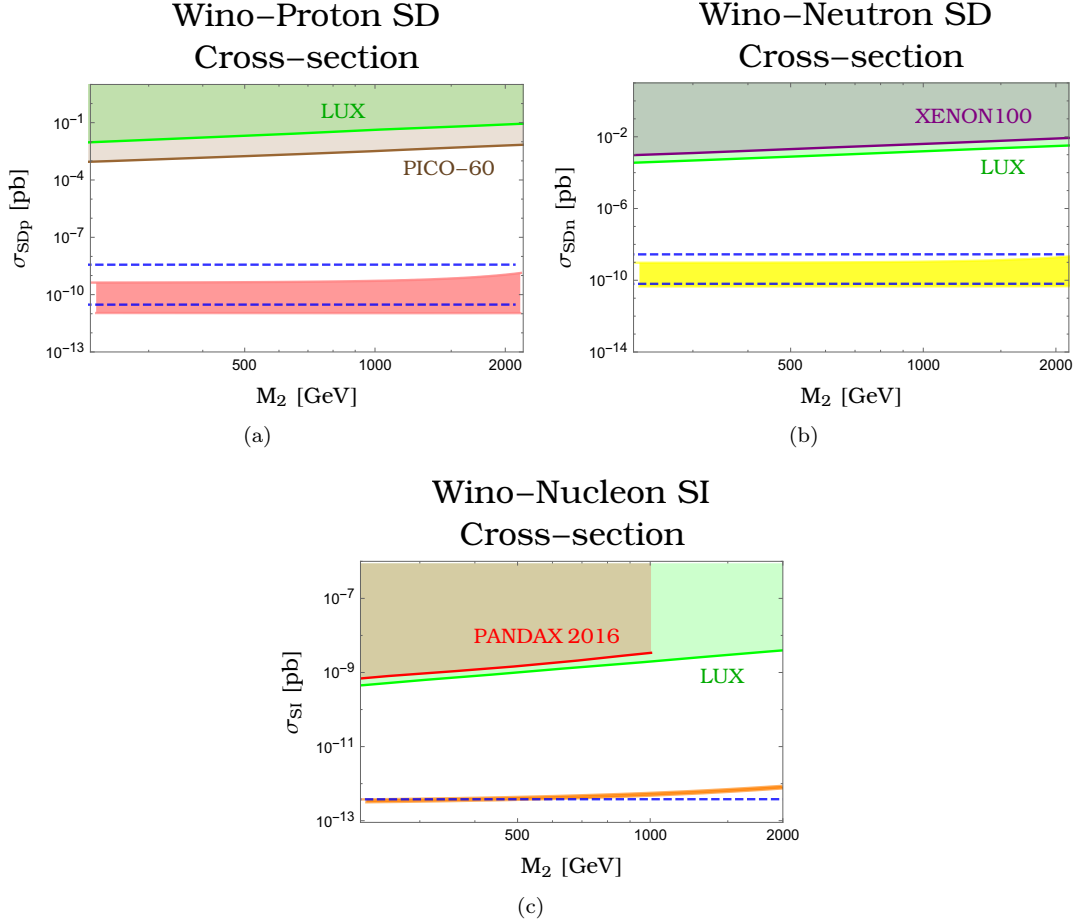


Figure 4.8: In the plot (a) is shown the SD Wino-proton scattering cross-section (pink band) with the experimental excluded regions (shaded regions) provided by LUX-2016 (green) and PICO-60 (brown) experiments. In the left panel (b) is shown the SD Wino-neutron scattering cross-section (yellow band), here the excluded regions are given by the LUX-2016 (green) and XENON100 (purple) experiments. In the below panel (c) we show the result for the SI Wino-nucleon scattering cross-section with the excluded limits given by the LUX-2016 (green) and the PANDAX-2016 (red) analysis. In every graph the squark masses are varying within the range $2.5 \text{ TeV} \lesssim m_{\tilde{q}} \lesssim 8 \text{ TeV}$ and the regions between the blue-dashed lines represent the analytical results which are found using the approximate formulae given in Eqs. (4.108). Note as all the numerical results are well below the forbidden regions.

masses which implies $\eta_{11}^i \rightarrow 1$ and $\eta_{12}^i \rightarrow 0$, Eqs. (4.108) are well approximated by

$$\alpha_{\tilde{W}}^{\text{SD}(q_i)} \simeq \frac{g^2}{8m_{\tilde{q}}^2} - \frac{g^2}{16\mu^2} (-1)^i \cos 2\beta + \mathcal{O}\left(\frac{M_2^2}{m_{\tilde{q}_{1,2}}^2}, \frac{M_2^2}{\mu^2}, \eta_{12}^2\right) \quad (4.108a)$$

$$\alpha_{\tilde{W}}^{\text{SI}(q_i)} \simeq \frac{g^2 m_{q_i} \sin 2\beta}{4m_h^2 |\mu|} + \mathcal{O}\left(\frac{M_2^2}{\mu^2}\right). \quad (4.108b)$$

These results confirm the numerical ones plotted in Fig. 4.8. In particular assuming that $\mu \gtrsim m_{\tilde{q}}$, in the SD interaction the dominant term would be the one relative to squarks exchange. In fact the width of the band in plots (a) and (b) of Fig. 4.8, correspond to a common squark mass which is varying from 2.5 TeV to 8 TeV. In the SI case, plot (c), this dependence disappears, consistently with Eq. (4.108b) where the dominant term is the one relative to the Higgs exchange.

As usual, using Eq. (4.67) and the values of J_A , A and $\langle S_{p,n} \rangle$ for ^{131}Xe nucleus given in the pure Bino section, we can approximately evaluate the total Wino-Xe scattering cross-section, which becomes equal to

$$\sigma_0^{\tilde{H} \text{Xe}} \simeq \frac{\mu_N^2}{\mu_p^2} A^2 \left[\sigma_{0\text{SI}}^{\tilde{W}p/n} + 1.5 \times 10^{-5} \sigma_{0\text{SD}}^{\tilde{W}p} \right]. \quad (4.109)$$

To obtain this result we used the fact that $\sqrt{\sigma_{0\text{SD}}^{\tilde{W}n}/\sigma_{0\text{SD}}^{\tilde{W}p}} \simeq 1.3$, where the values of $\sigma_{0\text{SD}}^{\tilde{W}n}$ and $\sigma_{0\text{SD}}^{\tilde{W}p}$ are given in Table 4.10. For a Wino LSP we have that the ratio between the SD neutralino-nucleus scattering cross-section and the SI one, is about $\sigma_{0\text{SD}}^{\tilde{W} \text{Xe}}/\sigma_{0\text{SI}}^{\tilde{W} \text{Xe}} \simeq 2.7 \times 10^{-2}$. Thus also for a Wino LSP the contribution of the SI interaction is the dominant one.

Although a pure Wino LSP satisfied both direct detection and DM constraints, just as occurred for the pure Higgsino LSP configuration, also here the huge LSP mass value, needed to fit the right DM relic abundance, implies that a significant fine tuning is needed to reproduce the EW scale. Note that in the pure Wino case the situation is even more extreme than in the pure Higgsino one [11]. In fact the requirement that the right LSP mass is $M_2 \sim 2 \text{ TeV}$ imposes that $|\mu| \gg 2 \text{ TeV}$ in order to respect the condition given in Eq. (4.99). As a consequence we need more fine tuning, in Eq. (4.96), to find the observed value of m_{Z^0} .

Furthermore also here there are constraints from indirect searches of gamma-ray emission. For a pure Wino the characteristic one-loop annihilation processes are similar to those for the pure Higgsino, schematically they are $\tilde{W}\tilde{W} \rightarrow \gamma\gamma$ and $\tilde{W}\tilde{W} \rightarrow \gamma Z^0$, and the possible Feynman diagrams are similar to those given in Eq. (4.98) with \tilde{H}_1 and \tilde{H}^\pm respectively replaced by \tilde{W} and \tilde{W}^\pm . The thermal average of their annihilation cross-sections times velocity are respectively equal to $\langle \sigma v \rangle_{\gamma\gamma} \approx 1.6 \times 10^{-27} \text{ cm}^3/\text{s}$ for two photons emission and $\langle \sigma v \rangle_{\gamma Z^0} \approx 1.1 \times 10^{-26} \text{ cm}^3/\text{s}$ for one photon emission [39]; also here it can be demonstrated that, in the limit of high Wino LSP mass, the cross-sections do not depend on LSP mass [17]. Thus we expect a characteristic gamma line at an energy $E_\gamma = M_2$ in the emitted gamma-ray spectrum. Conversely to what occurred in the pure Higgsino case, for a pure Wino LSP the cross-section values are well above the limits reached by the more recent gamma-ray detection experiments such as HESS [2]. So the non observation of typical the gamma line at $E_\gamma \simeq 2 \text{ TeV}$ exclude the possibility that a pure Wino LSP is a good DM candidate [39].

4.5 Well-Tempering

As we saw in the previous sections varying the mass of the proposed DM candidates, we note that we pass from a pure Bino configuration (without co-annihilations), which typically gives a relic abundance which is too large compared to the one of DM, to a pure Higgsino and then to a pure Wino configurations which, conversely, tend to give a relic abundance which is too small to fulfill the DM constraints. This pattern suggests that in the regions where the mixing between Bino and Higgsino or Bino and Wino become important, the resulting neutralino LSP can fulfill the DM constraint for a LSP mass in the range from 100 GeV to 1 TeV. Note that this is possible because Ωh^2 , via $\langle \sigma v \rangle$, is a continuous function of the mass parameters [11]. From our previous analysis is evident that in this mass range the various problems, theoretical and experimental ones, which affect the purities configurations can be alleviated. In particular the problem encountered for the pure Higgsino LSP relative to the excessive fine tuning required to reproduce the Z^0 mass, in this LSP mass range can be partially avoided [11], [9]. Furthermore, the fact that the LSP mass is less than 1 TeV, implies that the one-loop annihilation processes into final photons are strongly inhibited, and so the constraints from indirect detection experiments can be satisfied. Note also that a LSP with a mass greater

than 100 GeV, naturally satisfied the LEP and LHC constraints on the lightest chargino mass, $m_{\tilde{\chi}^\pm} \gtrsim 100$ GeV, which as we will see it would be nearly degenerate with the LSP [60], [11]. In the next we will focus on two mixed configurations of this type; in particular the mixing between Bino, Higgsino and Wino states of these configurations, are adjusted such that the resulting LSP has a thermal relic abundance, which fits the one observed for DM in a wide range of the MSSM parameter space. For this reason these configurations are called "Well-Tempered" neutralino [11] and their realization needs specific relations among neutralino mass parameters, M_1 , M_2 and μ .

4.6 Well-Tempered Bino/Higgsino

The configuration of Well-Tempered Bino/Higgsino (\tilde{B}/\tilde{H}) is realized when [11], [25]

$$M_1 \simeq |\mu|. \quad (4.110)$$

Note that, as we said in Chapter 3, we cannot fix the sign of μ ; as a consequence we can have a Well-Tempered \tilde{B}/\tilde{H} configuration both when μ is positive i.e. when $M_1 \simeq \mu$, and when μ is negative i.e. when $M_1 \simeq -\mu$ ⁸. We assume that all the others superpartners and the Higgs scalars are decoupled, exception made for the SM Higgs ($m_h \simeq 125$ GeV [60]). In particular we are assuming that $M_2 \gg M_1, |\mu|$ and hence the DM candidate composition is fully described by three parameters, namely M_1 , $|\mu|$ and β . The fact that the Wino states is more heavier than the Higgsino and the Bino states, allow us to take into account the effective mass terms obtained decoupling the Wino state [11], which are

$$\mathcal{L}_{\tilde{W}/\tilde{H}}^{\text{eff}} = \frac{g^2 v_u^2}{2M_2} \tilde{H}_u^0 \tilde{H}_d^0 + \frac{g^2 v_d^2}{2M_2} \tilde{H}_d^0 \tilde{H}_d^0 + \frac{g^2 v_u v_d}{M_2} \tilde{H}_u^0 \tilde{H}_d^0. \quad (4.111)$$

Redefining \tilde{H}_u^0 and \tilde{H}_d^0 via Eqs. (4.86) we can recast Eq. (4.111) as

$$\mathcal{L}_{\tilde{W}/\tilde{H}}^{\text{eff}} = -(1 + s_{2\beta}) \frac{M_W^2}{2M_2} \tilde{H}_1^0 \tilde{H}_1^0 - (1 - 2s_{2\beta}) \frac{M_W^2}{2M_2} \tilde{H}_2^0 \tilde{H}_2^0 - \frac{M_W^2}{M_2} c_{2\beta} \tilde{H}_1^0 \tilde{H}_2^0 \quad (4.112)$$

where we have redefined $\sin 2\beta \equiv s_{2\beta}$ and $\cos 2\beta \equiv c_{2\beta}$. Therefore in the basis \tilde{B} , \tilde{H}_1^0 , \tilde{H}_2^0 the effective neutralino mass Lagrangian reads as

$$\mathcal{L}_{\text{Mass}}^{\text{eff}} = \frac{M_1}{2} \tilde{B} \tilde{B} - \frac{s_\beta + c_\beta}{\sqrt{2}} s_W m_{Z^0} \tilde{H}_1^0 \tilde{B} + \frac{s_\beta - c_\beta}{\sqrt{2}} s_W m_{Z^0} \tilde{H}_2^0 \tilde{B} + \frac{\mu}{2} \tilde{H}_1^0 \tilde{H}_1^0 - \frac{\mu}{2} \tilde{H}_2^0 \tilde{H}_2^0 + h.c. + \mathcal{L}_{\tilde{W}/\tilde{H}}^{\text{eff}} \quad (4.113)$$

and so the neutralino mass matrix for a \tilde{B}/\tilde{H} configuration with a decoupled Wino is given by

$$M_{\tilde{B}/\tilde{H}} = \begin{pmatrix} M_1 & -(\mu - M_1)\theta_+ & (\mu + M_1)\theta_- \\ -(\mu - M_1)\theta_+ & \mu - \frac{m_W^2}{2M_2}(1 + s_{2\beta}) & -\frac{m_W^2}{2M_2} c_{2\beta} \\ (\mu + M_1)\theta_- & -\frac{m_W^2}{2M_2} c_{2\beta} & -\mu - \frac{m_W^2}{2M_2}(1 - s_{2\beta}) \end{pmatrix} + \mathcal{O}\left(\frac{m_W^2}{M_2^2}\right), \quad (4.114)$$

where the quantities θ_+ and θ_- are defined as

$$\theta_+ \equiv \frac{(s_\beta + c_\beta) s_W m_{Z^0}}{\sqrt{2}(\mu - M_1)} \quad \theta_- \equiv \frac{(s_\beta - c_\beta) s_W m_{Z^0}}{\sqrt{2}(\mu + M_1)}. \quad (4.115)$$

The details of diagonalization of $M_{\tilde{B}/\tilde{H}}$ are given in Appendix C. In the limit where M_1 , μ , $|M_1 - |\mu|| > m_{Z^0}$, we can assume that the quantities θ_\pm are moderate, and thus the eigenvalues

⁸Conversely M_1 is taken to be a positive quantity, see Chapter 3.

of $M_{\tilde{B}/\tilde{H}}$ are approximately given by

$$m_{\tilde{\chi}_1} = M_1 + \theta_{\pm}^2 (M_1 \mp \mu) + \mathcal{O}\left(\frac{m_W}{M_2}, \theta_{\pm}^3\right) \quad (4.116a)$$

$$m_{\tilde{\chi}_2} = \mp \mu + \mathcal{O}\left(\frac{m_W}{M_2}, \theta_{\pm}^3\right) \quad (4.116b)$$

$$m_{\tilde{\chi}_3} = \mu - \theta_{\pm}^2 (M_1 \mp \mu) + \mathcal{O}\left(\frac{m_W}{M_2}, \theta_{\pm}^3\right) \quad (4.116c)$$

where the upper signs refer to the case $M_1 \simeq \mu$ while the lower ones refer to the case $M_1 \simeq -\mu$. Using the orthogonal matrix N which diagonalized $M_{\tilde{B}/\tilde{H}}$ given in Appendix C we can find that the associated eigenvectors are equal to

$$\tilde{\chi}_1 = \left(1 - \frac{\theta_+^2}{2} - \frac{\theta_-^2}{2}\right) \tilde{B} + \theta_+ \tilde{H}_1^0 + \theta_- \tilde{H}_2^0 \quad (4.117a)$$

$$\tilde{\chi}_2 = -\theta_- \tilde{B} + \theta_+ \theta_- \frac{(M_1 - \mu)}{2\mu} \tilde{H}_1^0 + \left(1 - \frac{\theta_-^2}{2}\right) \tilde{H}_2^0 \quad (4.117b)$$

$$\tilde{\chi}_3 = -\theta_+ \tilde{B} + \left(1 - \frac{\theta_+^2}{2}\right) \tilde{H}_1^0 - \theta_+ \theta_- \frac{(M_1 + \mu)}{2\mu} \tilde{H}_2^0 \quad (4.117c)$$

The fact that the Wino state is completely decoupled has also the effect that the lightest chargino is Higgsino like, namely

$$\tilde{\chi}_1^{\pm} = \tilde{H}^{\pm}. \quad (4.118)$$

Its mass can easily read off from Eqs. (3.56) and at the leading order is equal to

$$m_{\tilde{\chi}_1^{\pm}} = |\mu| + \mathcal{O}\left(\frac{m_W}{M_2}\right). \quad (4.119)$$

Note that, from Eqs. (4.116), the lightest chargino, up to corrections of order m_W/M_2 , is perfectly degenerate with the neutralino $\tilde{\chi}_2^0$ ⁹.

From Eqs. (4.117) and the definitions given in Eqs. (4.115) we can observe that when $M_1 \simeq \mu$ we have that $\theta_- \rightarrow 0$, and so the \tilde{B} and \tilde{H}_1^0 states mix with an angle θ_+ while \tilde{H}_2^0 becomes nearly a pure state with mass $|\mu|$. Conversely when $M_1 \simeq -\mu$ we have that $\theta_+ \rightarrow 0$ and so \tilde{B} and \tilde{H}_2^0 states mix with an angle θ_- while \tilde{H}_1^0 is nearly a pure state with mass $|\mu|$ [11].

Note that the mixing angles, in particular θ_- , have also a dependence on the value of $\tan \beta$. Rewriting Eqs. (4.115) in terms of $\tan \beta$ as

$$\theta_+ \equiv \frac{c_{\beta}(1 + \tan \beta)s_W m_{Z^0}}{\sqrt{2}(\mu - M_1)} \quad \theta_- \equiv \frac{c_{\beta}(1 - \tan \beta)s_W m_{Z^0}}{\sqrt{2}(\mu + M_1)}, \quad (4.120)$$

we can see that when $\tan \beta \rightarrow 1$ implies that $\theta_- \rightarrow 0$. Hence when $M_1 \simeq -\mu$ and $\tan \beta \simeq 1$ the mixing between \tilde{B} and \tilde{H}_2^0 is quite absent. Observing at Eqs. (4.120) we can also note that, for large values of $\tan \beta$, the configurations $M_1 \simeq \mu$ and $M_1 \simeq -\mu$ tend to coincide giving the same results [11].

Relaxing the condition $|M_1 - |\mu|| > m_{Z^0}$ and in particular when $|\mu \pm M_1| \lesssim m_{Z^0}(s_{\beta} \mp c_{\beta})s_w/\sqrt{2}$, the mixing angles θ_+ and θ_- become maximal. As a consequence the eigenvalues given in Eqs. (4.116) are no longer valid. In this limit, in matrix $M_{\tilde{B}/\tilde{H}}$ we can replace μ with M_1 and the diagonalization now gives the following eigenvalues, see Appendix C

$$m_{\tilde{\chi}_1} = M_1 - \frac{(s_{\beta} \pm c_{\beta})s_W m_{Z^0}}{\sqrt{2}} + (1 \mp s_{2\beta}) \frac{s_W^2 m_{Z^0}^2}{8M_1} \quad (4.121a)$$

$$m_{\tilde{\chi}_2} = -M_1 - (1 \mp s_{2\beta}) \frac{s_W^2 m_{Z^0}^2}{4M_1} \quad (4.121b)$$

$$m_{\tilde{\chi}_3} = M_1 + \frac{(s_{\beta} \pm c_{\beta})s_W m_{Z^0}}{\sqrt{2}} + (1 \mp s_{2\beta}) \frac{s_W^2 m_{Z^0}^2}{8M_1} \quad (4.121c)$$

⁹As we said in the pure Higgsino LSP section the masses of the particles have always to be intended as the absolute values of the eigenvalues of the mass matrix, given by Eqs. (4.116).

where the sign convention is the same as above.

Anyway both when $|\mu \pm M_1| > m_{Z^0}$ and when $|\mu \pm M_1| < m_{Z^0}(s_\beta \mp c_\beta)s_w/\sqrt{2}$ the co-annihilations between the three neutralino states and the lightest chargino are important [25]. To test the entity of the co-annihilations mechanism for the \tilde{B}/\tilde{H} configuration we have to estimate the mass splitting, between the various relevant neutralino states and the chargino state. In particular when $|\mu \pm M_1| > m_{Z^0}$ we get that

$$\delta m_1 \equiv |m_{\tilde{\chi}_1} - m_{\tilde{\chi}_2}| \simeq |M_1 \mp \mu|(1 + \theta_\pm^2) + \mathcal{O}\left(\frac{m_W}{M_2}, \theta_\pm^3\right) \quad (4.122a)$$

$$\delta m_2 \equiv |m_{\tilde{\chi}_1} - m_{\tilde{\chi}_3}| = |m_{\tilde{\chi}_1} - m_{\tilde{\chi}_1^\pm}| \simeq |M_1 \mp \mu|(1 + 2\theta_\pm^2) + \mathcal{O}\left(\frac{m_W}{M_2}, \theta_\pm^3\right) \quad (4.122b)$$

$$\delta m_3 \equiv |m_{\tilde{\chi}_2} - m_{\tilde{\chi}_3}| = |m_{\tilde{\chi}_2} - m_{\tilde{\chi}_1^\pm}| \simeq \theta_\pm^2 |M_1 \mp \mu| + \mathcal{O}\left(\frac{m_W}{M_2}, \theta_\pm^3\right) \quad (4.122c)$$

where we have used Eqs. (4.116) and the sign convention is as above. Note that the above mass differences, in the limit of moderate θ_\pm , are related by $\delta m_3 < \delta m_1 \leq \delta m_2$. So the condition to be satisfied, in order to have a significant co-annihilations mechanism among all the three neutralinos and the lightest chargino, is

$$\frac{\delta m_2}{|\mu|} \lesssim \frac{1}{x_{\text{fo}}}, \quad (4.123)$$

which at the leading order and redefining $(|\mu| - M_1)/|\mu| \equiv \Delta$ read as

$$|\Delta| \lesssim \frac{1}{x_{\text{fo}}}. \quad (4.124)$$

Thus, for $x_{\text{fo}} \sim 20$, this relation implies that $-0.05 \lesssim \Delta \lesssim 0.05$. Note that if $\Delta \ll -0.05$ we are moving towards a pure Higgsino LSP configuration, while for $\Delta \gg 0.05$ we are moving towards a pure Bino LSP configuration.

When $|\mu \pm M_1| < m_{Z^0}(s_\beta \mp c_\beta)s_w/\sqrt{2}$ the mass differences are given by

$$\delta m_1 \equiv |m_{\tilde{\chi}_1} - m_{\tilde{\chi}_2}| \simeq \sqrt{2}(s_\beta \pm c_\beta)s_W m_{Z^0} \quad (4.125a)$$

$$\delta m_2 \equiv |m_{\tilde{\chi}_1} - m_{\tilde{\chi}_3}| = |m_{\tilde{\chi}_1} - m_{\tilde{\chi}_1^\pm}| \simeq \frac{(s_\beta \pm c_\beta)s_W m_{Z^0}}{\sqrt{2}} \quad (4.125b)$$

$$\delta m_3 \equiv |m_{\tilde{\chi}_2} - m_{\tilde{\chi}_3}| = |m_{\tilde{\chi}_2} - m_{\tilde{\chi}_1^\pm}| \simeq \frac{-(s_\beta \pm c_\beta)s_W m_{Z^0}}{\sqrt{2}} \quad (4.125c)$$

where we used Eqs. (4.121) with the same signs convention used above. Here the relation among the mass differences is $\delta m_2 = \delta m_3 < \delta m_1$ and so the co-annihilations are effective if

$$\frac{\sqrt{2}(s_\beta \pm c_\beta)s_W m_{Z^0}}{|\mu|} < \frac{1}{x_{\text{fo}}}. \quad (4.126)$$

which is quite well satisfied because we are assuming that $M_1, |\mu| \gg m_{Z^0}$.

In the limit where θ_\pm are moderate ($\theta_\pm \ll 1$) the mixing between the Bino and the Higgsino states is negligible, see Eqs. (4.117), and providing that Eq. (4.124) is quite satisfied, the relic abundance of a \tilde{B}/\tilde{H} is practically determined by the co-annihilations between the Higgsino states [11]. Thus in this limit the thermal average of the effective cross-section times velocity is approximately given by

$$\langle \sigma_{\text{eff}} v \rangle_{\tilde{B}/\tilde{H}} = \frac{\langle \sigma_{\text{eff}} v \rangle_{\tilde{H}}}{\left[1 + \frac{1}{4} \left(\frac{M_1}{\mu} \right)^{3/2} e^{-x \left(\frac{\mu}{M_1} - 1 \right)} \right]^2} \quad (4.127)$$

where we have used Eq. (2.78), Eq. (2.86) and the result for the pure Higgsino LSP given in Eq. (4.90). Using the relic density formula Eq. (2.90) and substituting into it the above result, we obtain that the relic abundance for a \tilde{B}/\tilde{H} is approximately given by

$$\Omega_{\tilde{B}/\tilde{H}} h^2 \simeq 0.097 \left(\frac{\mu}{1 \text{ TeV}} \right)^2 \frac{1}{R_{\tilde{B}/\tilde{H}}} \quad (4.128)$$

MSSM Parameter	Value-Range
M_1	100 – 1200 GeV
μ	$0.95M_1 - 1.05M_1$
M_2	3 TeV
M_3	3.8 TeV
$m_{\tilde{l}_{L,R}}$	> 1.7 TeV
$m_{\tilde{q}_{L,R}}$	> 2 TeV
$\tan\beta$	10

Table 4.11: In the table are listed the values of the MSSM parameters that we take into account for the numerical analysis of the \tilde{B}/\tilde{H} configuration.

where $R_{\tilde{B}/\tilde{H}}$ is defined as

$$\begin{aligned}
R_{\tilde{B}/\tilde{H}} &\equiv \int_{x_{fo}}^{\infty} \frac{dx}{x^2} \left[1 + \frac{1}{4} \left(\frac{M_1}{\mu} \right)^{3/2} e^{-x \left(\frac{\mu}{M_1} - 1 \right)} \right]^{-2} \\
&= \int_{x_{fo}}^{\infty} \frac{dx}{x^2} \left[1 + \frac{1}{4} (1 - \Delta)^{3/2} e^{-x \left(\frac{\Delta}{1-\Delta} \right)} \right]^{-2}.
\end{aligned} \tag{4.129}$$

Note that in Eq. (4.128) we have made use of the relic density result for a pure Higgsino LSP given in Eq. (4.91), because, as we said before, the annihilation rate for a \tilde{B}/\tilde{H} in the limit of moderate θ_{\pm} is mostly determined by the Higgsino co-annihilations. When the mixing angles are not negligible and in particular when they become maximal i.e. when $|\mu \pm M_1| < m_{Z^0} (s_{\beta} \mp c_{\beta}) s_w / \sqrt{2}$ the thermal average of the effective annihilation cross-section is no longer approximate by Eq. (4.127). In fact when the mixing between Bino state and Higgsino state become important there are more co-annihilation processes to take into account. In particular a strong mixing between Bino and Higgsino states enhances the possibility of an annihilation through Higgs exchange into final SM fermions or bosons states.

For our numerical analysis of the \tilde{B}/\tilde{H} configuration we used the MSSM parameters, defined at the EW scale, given in Table 4.11. Our numerical simulations are depicted in Fig. 4.9 and Fig. 4.10. In particular in Fig. 4.9 we compare the numerical result with the analytical one obtained using Eq. (4.128) where the integral $R_{\tilde{B}/\tilde{H}}$ is computed numerically assuming $\Delta \simeq 0.05$. In Fig. 4.10 we analyse the \tilde{B}/\tilde{H} configuration varying the Bino mass parameter M_1 , for different fixed values of the Higgsino mass parameter $|\mu|$. The numerical results show that the DM constraint is satisfied by a \tilde{B}/\tilde{H} configuration with a LSP mass, M_{DM} , within a range $305 \text{ GeV} < M_{DM} < 715 \text{ GeV}$ which correspond to Δ varying in the range $-0.05 < \Delta < 0.05$. As we said before the most sensitive configuration to small values of $\tan\beta$ is for negative values of the Higgsino mass parameter μ . In Fig. 4.11 we show the numerical results for the relic density provided by \tilde{B}/\tilde{H} configuration assuming $\mu < 0$ and $\tan\beta \simeq 1.1$. As is evident the small mixing between Bino fraction and the Higgsino one as the effect to enlarge the right LSP mass region, which is now $261 \text{ GeV} \lesssim M_{DM} \lesssim 994 \text{ GeV}$. Nevertheless it is worth to note that small values of $\tan\beta$ are less favourable. In fact in order to avoid the need of a gigantic stop mass, we have to maximize the Higgs mass at the tree-level, which requires large values of $\tan\beta$ [22].

For what concern the direct detection analysis we encounter a situation which is radically different from the purity cases studied above. For a Well-Tempered \tilde{B}/\tilde{H} , in the limit of moderate θ_{\pm} , using Eq. (4.17) and Eq. (4.18) we get that

$$\alpha_{\tilde{B}/\tilde{H}}^{\text{SD}(q_i)} = (-1)^i \frac{g^2}{16m_{Z^0}^2 \cos^2 \theta_W} [\theta_+^2 - \theta_-^2] + \alpha_{q_i}^{\text{SD}} + \mathcal{O}(\theta_{\pm}^3) \tag{4.130a}$$

$$\alpha_{\tilde{B}/\tilde{H}}^{\text{SI}(q_i)} = -\frac{g^2 m_{q_i} t_W}{4m_W m_h^2} [\theta_+ \cos\beta - \theta_- \sin\beta] + \alpha_{q_i}^{\text{SI}} + \mathcal{O}(\theta_{\pm}^3) \tag{4.130b}$$

where as usual we have assumed that $m_H^2 \gg m_h^2$ and so $\sin\alpha \simeq -\cos\beta$ and $\cos\alpha \simeq \sin\beta$. Substituting Eqs. (4.130) respectively into Eq. (4.35) and into Eq. (4.61) we have that the SD

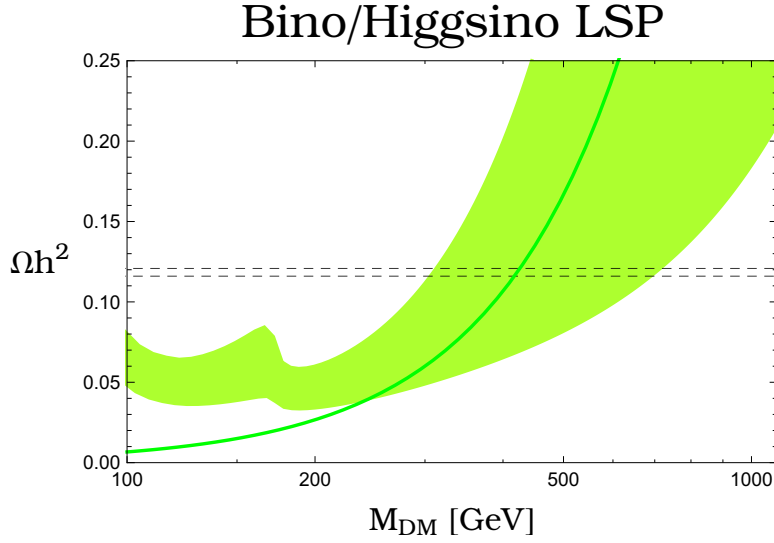


Figure 4.9: In the figure is shown the contribution to Ωh^2 of a Well-Tempered \tilde{B}/\tilde{H} as a function of the LSP mass, obtained from the `micrOmegas` 4.2.5 analysis and compared with the analytical result. The width of the lighter green band correspond to our numerical simulation with Δ varying in the range $-0.05 \lesssim \Delta \lesssim 0.05$ while the darker line is obtained using Eq. (4.128) and assuming $\Delta \simeq 0.05$. As usual the band between the dashed lines denotes the observed DM abundance within 2σ .

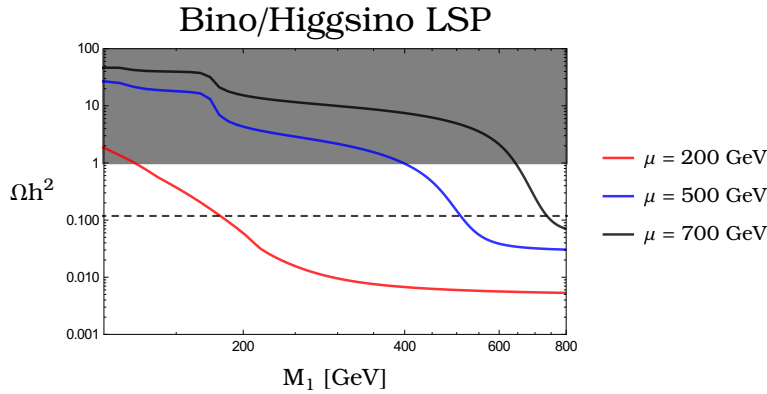


Figure 4.10: In the plot we use an alternative method of analysis of the \tilde{B}/\tilde{H} configuration. We show the contribution to Ωh^2 as a function of the Bino mass parameter M_1 taking fixed the value of $|\mu|$. The dark gray region correspond to an over-abundant relic density $\Omega h^2 > 1$ which has not physical sense, while the dashed line correspond to the observed DM relic density. The zone well above of this line corresponds to a pure Bino LSP configuration while the region well below corresponds to a pure Higgsino LSP configuration.

and SI \tilde{B}/\tilde{H} -nucleon scattering cross-section at zero momentum transferred are equal to

$$\sigma_{0\text{SD}}^{\tilde{B}/\tilde{H} p} = \frac{12}{\pi} \left(\frac{M_{\text{DM}} m_p}{M_{\text{DM}} + m_p} \right)^2 \left[\sum_q \alpha_{\tilde{B}/\tilde{H}}^{\text{SD}(q_i)} \Delta q^{(p)} \right]^2 \quad (4.131a)$$

$$\sigma_{0\text{SD}}^{\tilde{B}/\tilde{H} n} = \frac{12}{\pi} \left(\frac{M_{\text{DM}} m_p}{M_{\text{DM}} + m_p} \right)^2 \left[\sum_q \alpha_{\tilde{B}/\tilde{H}}^{\text{SD}(q_i)} \Delta q^{(n)} \right]^2 \quad (4.131b)$$

$$\sigma_{0\text{SI}}^{\tilde{B}/\tilde{H} p/n} = \frac{4}{\pi} \left(\frac{M_{\text{DM}} m_p}{M_{\text{DM}} + m_p} \right)^2 \left[\sum_{q=u,d,s} \frac{m_{p/n}}{m_q} f_{\text{T}q}^{(p/n)} \alpha_{\tilde{B}/\tilde{H}}^{\text{SI}(q_i)} + \frac{2}{27} f_{\text{T}G} \sum_{q=c,b,t} \frac{m_{p/n}}{m_q} \alpha_{\tilde{B}/\tilde{H}}^{\text{SI}(q_i)} \right]^2. \quad (4.131c)$$

In the above results, with $\alpha_{\tilde{q}_i}^{\text{SD}}$ and $\alpha_{\tilde{q}_i}^{\text{SI}}$, we refer respectively to the coefficients of the processes

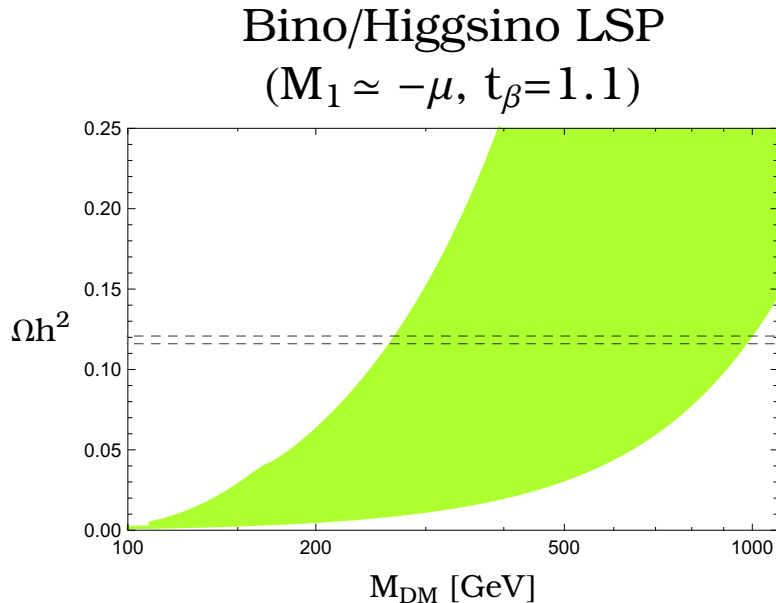


Figure 4.11: In the figure is shown the contribution to Ωh^2 of a Well-Tempered \tilde{B}/\tilde{H} as a function of the LSP mass assuming $\mu < 0$ and imposing $\tan \beta \simeq 1.1$. As above the width of the band correspond to $-0.05 \lesssim \Delta \lesssim 0.05$.

Cross-section	Value-Range
$\sigma_{0\text{SD}}^{\tilde{B}/\tilde{H}p}$	$2.9 \times 10^{-6} - 8.5 \times 10^{-4}$ pb
$\sigma_{0\text{SD}}^{\tilde{B}/\tilde{H}n}$	$2.3 \times 10^{-6} - 6.5 \times 10^{-4}$ pb
$\sigma_{0\text{SI}}^{\tilde{B}/\tilde{H}p,n}$	$5.9 \times 10^{-9} - 1.1 \times 10^{-8}$ pb

Table 4.12: In the table we list the upper and lower values of the SD and SI \tilde{B}/\tilde{H} -nucleon cross-sections for $\Delta \simeq 0.05$.

mediated by squarks in the SD and in the SI cases. From these results we can observe that the presence of a mixing between the Bino and the Higgsino states, implies that the scattering processes which proceed through Higgs boson exchange for the SI interaction, and through the Z^0 boson exchange for the SD one, are highly enhanced. In particular in the SI case, as is evident from Eq. (4.130b), the dominant contribution is the one relative to the Higgs exchange which, being suppressed only by the square of the SM Higgs mass, is less suppressed than the terms relative to the squarks exchange whose are always suppressed by the square of the heavy squark masses ($m_{\tilde{q}} > 2$ TeV). The same thing occur in the SD case where the coefficient of the scattering process mediated by the Z^0 boson is suppressed only by the square of its mass, $m_{Z^0} \simeq 80$ GeV [60]. These facts strongly enhance both the SI and SD LSP-nucleon scattering cross-section. In particular as we can see from Fig. 4.12 this enhancement is so strong that the SI \tilde{B}/\tilde{H} -nucleon cross-section is moved, nearly completely, towards the experimental excluded regions. Note that the enhancement effect is stronger when $M_1 = |\mu|$ i.e. when the mixing angle is maximal, while tends to be alleviated when $\Delta \simeq -0.05$ or $\Delta \simeq 0.05$.

The analytical results in Eqs. (4.131) confirm the numerical behaviours, and in Fig. 4.12 they are plotted using a red dashed line. Note that Eqs. (4.131) have to be compared with the numerical results for and $\Delta \simeq 0.05$ i.e. the blue continuous line in Fig. 4.12.

As we done in the previous sections the total neutralino-nucleus cross-section can be obtained using Eq. (4.67). For \tilde{B}/\tilde{H} we present the approximate result for $\Delta \simeq 0.05$, which is

$$\sigma_0^{\tilde{B}/\tilde{H} \text{Xe}} \simeq \frac{\mu_N^2}{\mu_p^2} A^2 [\sigma_p^{\text{SI}} + 6.8 \times 10^{-6} \sigma_p^{\text{SD}}] \quad (4.132)$$

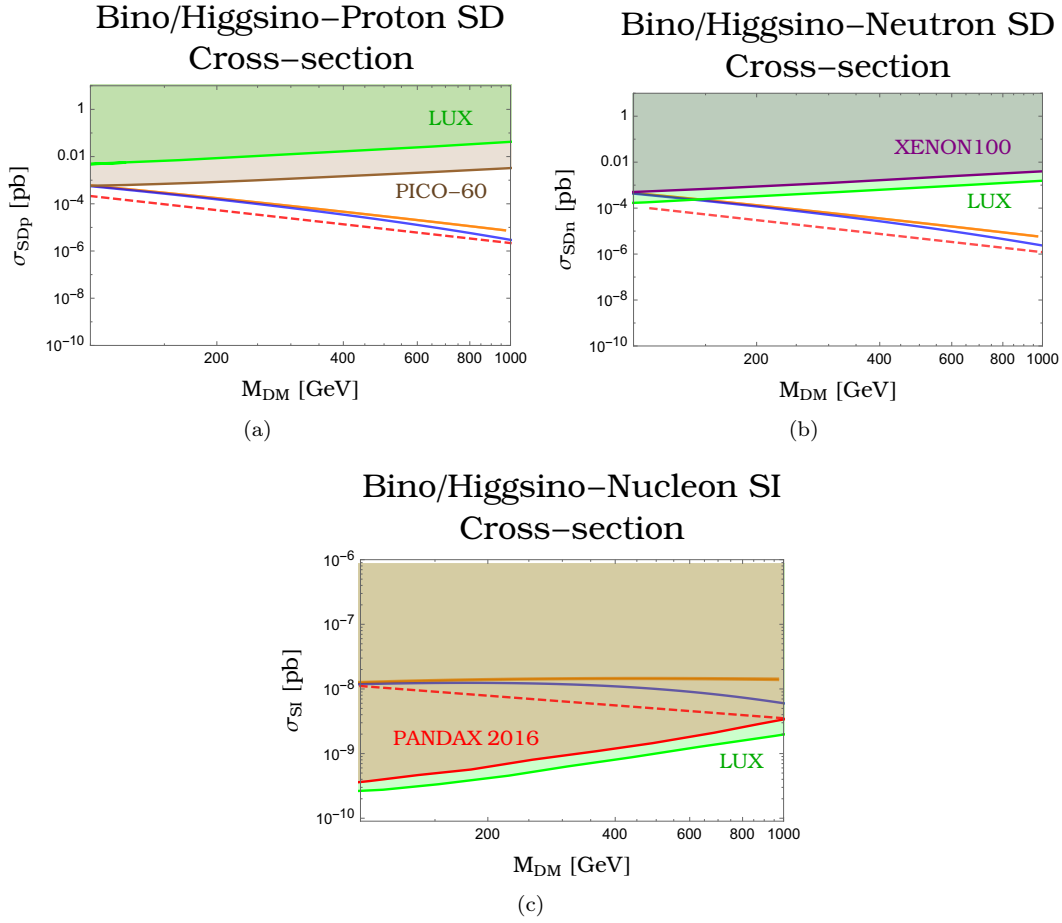


Figure 4.12: In the plot (a) is shown the SD \tilde{B}/\tilde{H} -proton scattering cross-section with the experimental excluded regions (shaded regions) provided by LUX-2016 (green) and PICO (brown) observations. In the left panel (b) is shown the SD \tilde{B}/\tilde{H} -neutron scattering cross-section, with the excluded regions given by the LUX-2016 (green) and XENON100 (purple) experiments. In the below panel (c) we show the result for the SI \tilde{B}/\tilde{H} -nucleon scattering cross-section with the excluded limits given by the LUX-2016 (green) and the PANDAX-2016 (red) analysis. In every plot the two continuous lines correspond respectively to $\Delta \simeq 0.05$ (blue line) and $\Delta \simeq 0$ (orange line) and the red-dashed lines are the analytical results found with formulae given in Eqs. (4.131). Comparing these results with the ones for a pure Higgsino LSP, Fig. 4.6, or a pure Bino LSP, Fig. 4.2, we note the strong enhancement of the LSP-nucleon scattering cross-section, in particular for the SI case.

where we use the values of the \tilde{B}/\tilde{H} -nucleon scattering cross-section given in Table 4.12. For the \tilde{B}/\tilde{H} configuration the comparison between the SD nuclear cross-sections and the SI one gives $\sigma_{0\text{SD}}^{\tilde{B}/\tilde{H}\text{Xe}}/\sigma_{0\text{SI}}^{\tilde{B}/\tilde{H}\text{Xe}} \simeq 0.04$. Therefore, as occurred in the pure Higgsino and in the pure Wino cases, the SI interaction is dominant respectively to the SD one, and so we can study them separately.

For what concern the negative μ values, assuming $\tan\beta \neq 1$, the situation is quite similar to the one for positive values of μ [25]. Nevertheless when μ is negative and $\tan\beta \rightarrow 1$, as we said before, the mixing angle θ_- vanishes. As a consequence the processes mediated by Z^0 and Higgs bosons become more weaker than before. In fact noting that when $\tan\beta \rightarrow 1$ we have that $\sin 2\beta \rightarrow 1$ and $\cos 2\beta \rightarrow 0$, the results given in Eqs. (4.131), with the lower signs, vanish (remember that for $\mu < 0$ we have $\theta_+ \rightarrow 0$). As a consequence the SD and SI \tilde{B}/\tilde{H} -nucleon scattering cross-sections are lowered. In Fig. 4.13 we give the numerical results for $\mu < 0$ and $\tan\beta \simeq 1.1$.

Concluding except in the case when $\mu < 0$ and $\tan\beta = 1$, the Well-Tempered \tilde{B}/\tilde{H} configuration although it greatly satisfies the DM constraint in a wide range of the MSSM parameters

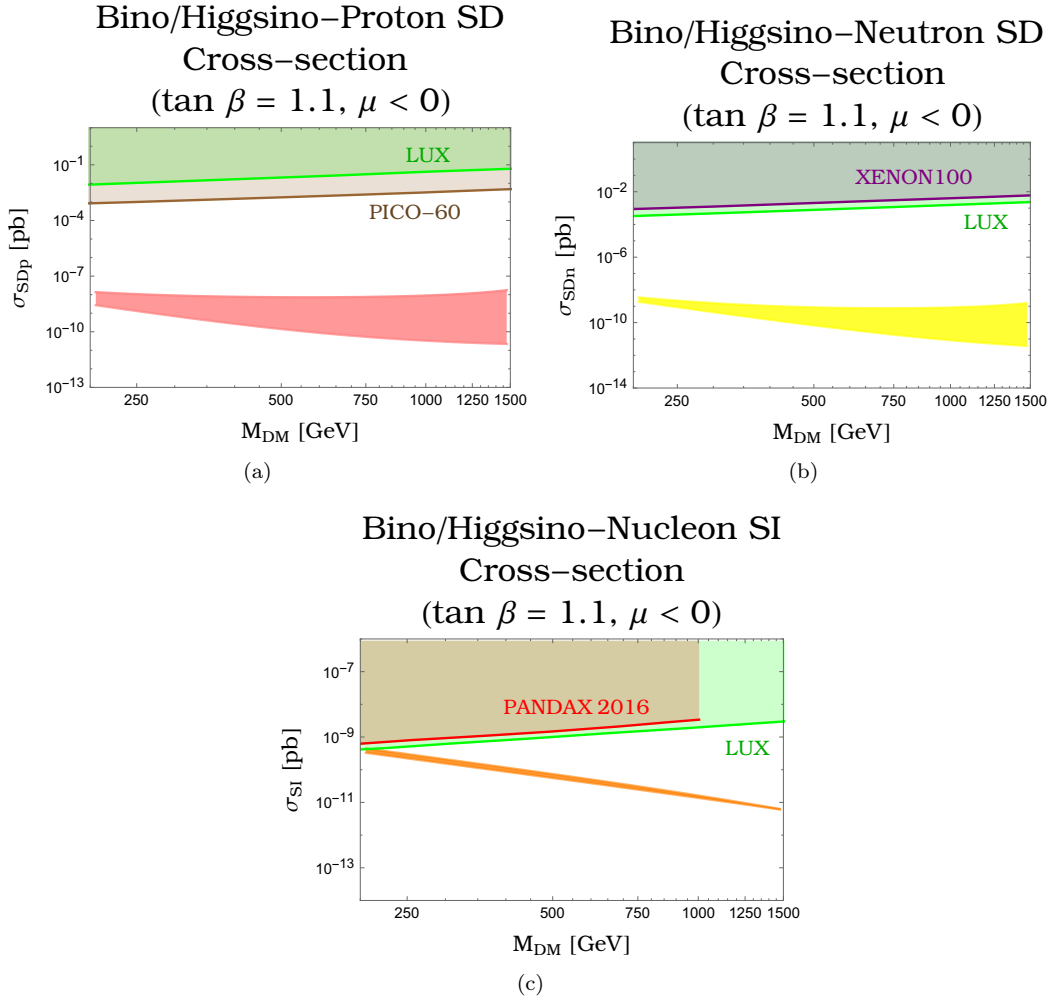


Figure 4.13: In figure are shown the SD \tilde{B}/\tilde{H} -proton (a), SD \tilde{B}/\tilde{H} -neutron (b) and SI \tilde{B}/\tilde{H} -nucleon scattering cross-sections assuming negative μ values, $\tan \beta \simeq 1.1$ and taking $M_1 \simeq -\mu$. Comparing these results with ones given in Fig. 4.12 we note that the small mixing between Bino and Higgsino states has the effect of lower the scattering cross-sections below the experimental limits.

space, it is nearly ruled out by direct detection constraints. Therefore a Well-Tempered \tilde{B}/\tilde{H} cannot provide a viable DM candidate.

4.7 Well-Tempered Bino/Wino

As last we analyse the Well-Tempered Bino/Wino (\tilde{B}/\tilde{W}) configuration. Remembering that we take M_1 and M_2 to be real and positive, the condition to obtain a Well-Tempered \tilde{B}/\tilde{W} configuration is

$$M_1 \simeq M_2. \quad (4.133)$$

Also here we assume that all the others super-particles and the Higgs scalars except the SM Higgs, are more heavier than the Bino and the Wino. In particular here we will assume that $|\mu| \gg M_1, M_2$. This relation between the neutralino mass parameters, allow us to take into account the effective mass terms between Bino and Wino states, obtained decoupling the two Higgsinos, namely

$$\mathcal{L}_{\tilde{B}/\tilde{W}}^{\text{eff}} = -\frac{s_W^2 s_{2\beta} m_{Z^0}^2}{\mu} \tilde{B}\tilde{B} - \frac{c_W^2 s_{2\beta} m_{Z^0}^2}{\mu} \tilde{W}\tilde{W} + \frac{2s_W c_W s_{2\beta} m_{Z^0}^2}{\mu} \tilde{B}\tilde{W}. \quad (4.134)$$

Thus in the \tilde{B}/\tilde{W} configuration the neutralino mass Langrangian is given by

$$\mathcal{L}_{\tilde{B}/\tilde{W}}^{\text{mass}} = \frac{M_1}{2} \tilde{B}\tilde{B} + \frac{M_2}{2} \tilde{W}\tilde{W} + h.c. + \mathcal{L}_{\tilde{B}/\tilde{W}}^{\text{eff}} \quad (4.135)$$

from which we can define the effective \tilde{B}/\tilde{W} mass matrix with decoupled Higgsinos

$$M_{\tilde{B}/\tilde{W}} = \begin{pmatrix} M_1 & 0 \\ 0 & M_2 \end{pmatrix} + M_1 \theta \Delta \begin{pmatrix} -t_W & 1 \\ 1 & -ct_W \end{pmatrix} + \mathcal{O}\left(\frac{1}{\mu^2}\right) \quad (4.136)$$

where we have redefined $\tan\theta_W \equiv t_W$ and $\cotan\theta_W \equiv ct_W$ and the quantities Δ and θ are respectively defined as

$$\Delta \equiv \frac{M_2 - M_1}{M_1} \quad \theta \equiv \frac{s_{2W}s_{2\beta}m_{Z^0}^2}{2|\mu|M_1\Delta}. \quad (4.137)$$

Note that although we have taken the Higgsino states completely decoupled the parameter $|\mu|$ continues to have an important role. In fact from the mass matrix $M_{\tilde{B}/\tilde{W}}$, is evident that the mixing between Bino and Wino is possible only at the first order in an expansion on $m_W/|\mu|$. This situation is different from the one of the \tilde{B}/\tilde{H} case studied in the previous section, where the mixing between Bino and Higgsinos was appreciable also at the leading order in an expansion in m_W/M_2 . In particular the fact that the mixing angle θ is always suppressed by the $|\mu|$ parameter, implies that the mixing between the Bino and the Wino states is less stronger than the mixing between the Bino and Higgsino states in the \tilde{B}/\tilde{H} case.

Diagonalizing the matrix $M_{\tilde{B}/\tilde{W}}$, in the limit where $M_1, M_2 > m_{Z^0}$ and $|M_2 - M_1| > s_{2\beta}m_{Z^0}$, we find that the eigenvalues are equal to

$$m_{\tilde{\chi}_1} = M_1 [1 - \Delta(t_W\theta)] + \mathcal{O}\left(\frac{m_{Z^0}^2}{\mu^2}\right) \quad (4.138a)$$

$$m_{\tilde{\chi}_2} = M_1 [1 + \Delta(1 - ct_W\theta)] + \mathcal{O}\left(\frac{m_{Z^0}^2}{\mu^2}\right) \quad (4.138b)$$

with associated eigenvectors given by

$$\tilde{\chi}_1 \simeq \tilde{B} - \theta\tilde{W} \quad (4.139a)$$

$$\tilde{\chi}_2 \simeq \theta\tilde{B} + \tilde{W} \quad (4.139b)$$

where we used the orthogonal matrix $N_{\tilde{B}/\tilde{W}}$ which diagonalized the mass matrix $M_{\tilde{B}/\tilde{W}}$, given in Appendix C. Note that in the case of a Well-Tempered \tilde{B}/\tilde{W} , the lightest chargino is Wino like

$$\tilde{\chi}_1^\pm = \tilde{W}^\pm. \quad (4.140)$$

Its mass can be read off from Eq. (3.56), and at the first order is

$$m_{\tilde{\chi}_1^\pm} = M_2 - \frac{s_{2\beta}m_W^2}{\mu} + \mathcal{O}\left(\frac{m_W^2}{\mu^2}\right) = m_{\tilde{\chi}_2}. \quad (4.141)$$

Note that from the definition of θ given in Eq. (4.137), when the difference $|M_2 - M_1| \rightarrow 0$, the mixing angle $\theta \rightarrow \infty$ and Eqs. (4.138) and Eqs. (4.139) are no longer valid. So when $|M_2 - M_1| < s_{2W}s_{2\beta}m_{Z^0}^2/(2|\mu|)$, in the mass matrix $M_{\tilde{B}/\tilde{W}}$ we can replace M_2 with M_1 and the eigenvalues are now given by

$$m_{\tilde{\chi}_1} = M_1 + \mathcal{O}\left(\frac{m_{Z^0}^2}{\mu^2}\right) \quad (4.142a)$$

$$m_{\tilde{\chi}_2} = M_1 \left(1 - \frac{m_{Z^0}^2 s_{2\beta}}{|\mu|M_1}\right) + \mathcal{O}\left(\frac{m_{Z^0}^2}{\mu^2}\right) \quad (4.142b)$$

$$m_{\tilde{\chi}_1^\pm} = M_1 \left(1 - \frac{s_{2\beta}m_W^2}{|\mu|M_1}\right) + \mathcal{O}\left(\frac{m_W^2}{\mu^2}\right) \quad (4.142c)$$

where we have also included the lightest chargino mass.

Furthermore the mixing angle depends also on $\tan\beta$, in fact Eq. (4.137) can be recast as

$$\theta = \frac{\tan\beta}{1 + \tan\beta^2} \frac{s_{2W} m_{Z^0}^2}{2|\mu| M_1 \Delta}. \quad (4.143)$$

In particular this equation shows that the mixing angle reaches its maximum value (taking Δ and μ fixed) when $\tan\beta = 1$. Note that for large value of $\tan\beta$ the mixing angle $\theta \rightarrow 0$ and so the mixing effects are more weaker [11].

Also here the co-annihilations between LSP, NLSP and the lightest chargino are effective if the condition

$$\frac{\delta m_{ij}}{M_1} < \frac{1}{x_{fo}} \quad (4.144)$$

is satisfied. In the limit of moderate value of the mixing angle $\theta \lesssim 1$, the mass differences are given by

$$\delta m_{12} \equiv |m_{\tilde{\chi}_2} - m_{\tilde{\chi}_1}| \simeq |M_1 \Delta [1 - 2\theta t_{2W}]| + \mathcal{O}\left(\frac{m_{Z^0}^2}{\mu^2}\right) \quad (4.145a)$$

$$\delta m_{1\pm} \equiv |m_{\tilde{\chi}_1^\pm} - m_{\tilde{\chi}_1}| = \delta m_{12} \quad (4.145b)$$

$$\delta m_{2\pm} \equiv |m_{\tilde{\chi}_2} - m_{\tilde{\chi}_1^\pm}| = \mathcal{O}\left(\frac{m_{Z^0}^2}{\mu^2}\right) \quad (4.145c)$$

where we used Eqs. (4.138) and Eq. (4.141). As is evident from these results the only mass difference which survives, up to corrections of order $m_{Z^0}^2/\mu^2$, is δm_{12} . Thus considering that, as usual, $x_{fo} \simeq 20$ the co-annihilations condition, Eq. (4.144), at the leading order read as

$$|\Delta| \lesssim 0.05. \quad (4.146)$$

When the difference $|M_2 - M_1| \rightarrow 0$, from Eqs. (4.142), the mass differences are equal

$$\delta m_{12} \equiv |m_{\tilde{\chi}_2} - m_{\tilde{\chi}_1}| = \frac{s_{2\beta} m_{Z^0}^2}{|\mu|} + \mathcal{O}\left(\frac{1}{\mu^2}\right) \quad (4.147a)$$

$$\delta m_{1\pm} \equiv |m_{\tilde{\chi}_1^\pm} - m_{\tilde{\chi}_1}| = \frac{s_{2\beta} c_W^2 m_{Z^0}^2}{|\mu|} + \mathcal{O}\left(\frac{1}{\mu^2}\right) \quad (4.147b)$$

$$\delta m_{2\pm} \equiv |m_{\tilde{\chi}_2} - m_{\tilde{\chi}_1^\pm}| = \frac{\tan\beta^2}{1 + \tan\beta^2} \frac{s_{2\beta} m_{Z^0}^2}{|\mu|} + \mathcal{O}\left(\frac{1}{\mu^2}\right) \quad (4.147c)$$

and thus, in this limit, the co-annihilations condition is approximately given by

$$\frac{s_{2\beta} m_{Z^0}^2}{|\mu|} \lesssim 0.05. \quad (4.148)$$

As occurred for the \tilde{B}/\tilde{H} configuration, the relic abundance can be analytically approximate when the mixing angle, θ , is moderate. In particular when $\theta \lesssim 1$ the effective annihilation cross-section is dominated by the Wino co-annihilations [11]. This is due to the fact that all of the co-annihilation processes between Bino and Winos are proportional to θ^2 , while the annihilation among two Binons are mediated by squarks and as a consequence are suppressed by the high squark masses. Therefore in this limit the thermal average of the effective annihilation cross-section times velocity for a Well-Tempered \tilde{B}/\tilde{W} is

$$\langle\sigma_{\tilde{B}/\tilde{W}} v\rangle \simeq \frac{\langle\sigma_{\tilde{W}} v\rangle}{\left[1 + \frac{1}{3} \left(\frac{M_1}{M_2}\right)^{3/2} e^{-x\left(\frac{M_2}{M_1}-1\right)}\right]^2}. \quad (4.149)$$

Putting this result into the relic density formula, Eq. (2.90), we obtain that

$$\Omega_{\tilde{B}/\tilde{W}} h^2 \simeq 0.13 \left(\frac{M_2}{2.5 \text{ TeV}}\right)^2 \frac{1}{R_{\tilde{B}/\tilde{W}}} \quad (4.150)$$

MSSM Parameter	Value-Range
M_1	100 – 1000 GeV
M_2	$0.98M_1 - 1.02M_1$
μ	1000 GeV
M_3	1.8 TeV
$m_{\tilde{l}_{L,R}}$	> 1.2 TeV
$m_{\tilde{q}_{L,R}}$	> 2 TeV
$\tan \beta$	1.5 – 10

Table 4.13: In the table are listed the values of the MSSM parameters that we take into account for the numerical analysis of the \tilde{B}/\tilde{W} configuration.

where $R_{\tilde{B}/\tilde{W}}$ is defined as

$$\begin{aligned}
 R_{\tilde{B}/\tilde{W}} &\equiv \int_{x_{fo}}^{\infty} \frac{dx}{x^2} \left[1 + \frac{1}{3} \left(\frac{M_1}{M_2} \right)^{3/2} e^{-x \left(\frac{M_2}{M_1} - 1 \right)} \right]^{-2} \\
 &= \int_{x_{fo}}^{\infty} \frac{dx}{x^2} \left[1 + \frac{1}{3} \left(\frac{1}{\Delta + 1} \right)^{3/2} e^{-x\Delta} \right]^{-2}.
 \end{aligned} \tag{4.151}$$

Our analysis with `micrOmegas` 4.2.5 is performed taking into account the MSSM parameter space given in Table 4.13. Fixing $\tan \beta = 10$ and varying M_1 and M_2 within the range given in the Table 4.13, the `micrOmegas` 4.2.5 simulation shows that an LSP with a mass, M_{DM} , in the range $260.14 \text{ GeV} \lesssim M_{DM} \lesssim 999.48 \text{ GeV}$ satisfied the DM constraint within 2σ . In Fig. 4.14 we plot the numerical contribution of a Well-Tempered \tilde{B}/\tilde{W} to the relic density as a function of M_{DM} , compared with the analytical result found using Eq. (4.150) where the integral $R_{\tilde{B}/\tilde{W}}$ is computed numerically, and we have assumed that $\Delta \simeq 0.02$; the width of the band correspond to Δ varying in the range $-0.02 \leq \Delta \leq 0.02$. In Fig. 4.15 we plot the contribution to relic density as a function of M_1 fixing the value of M_2 . Lowering the value of

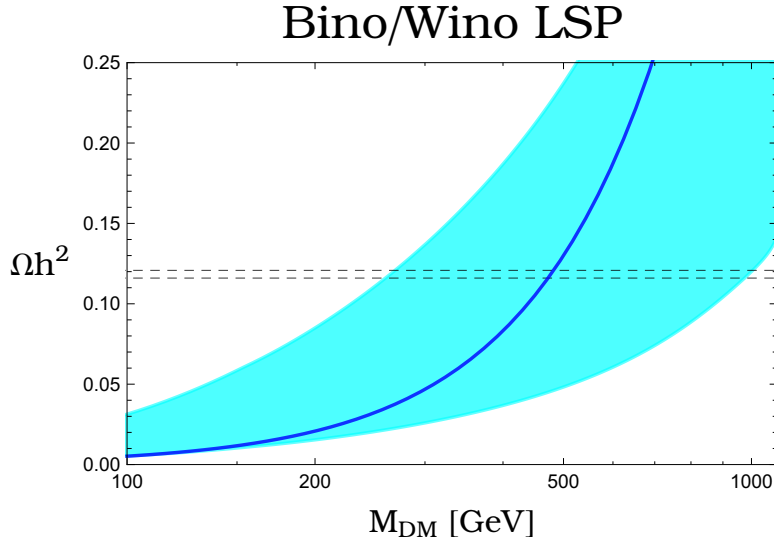


Figure 4.14: In the figure is shown the contribution to Ωh^2 of a Well-Tempered \tilde{B}/\tilde{W} as a function of the LSP mass, obtained from the `micrOmegas` 4.2.5 analysis. The width of the band correspond to $-0.02 \lesssim \Delta \lesssim 0.02$ and the darker blue line is obtained using Eq. (4.150) assuming $\Delta \simeq 0.02$. As usual the band between the dashed lines denotes the observed DM abundance within 2σ .

$\tan \beta$ and fixing it at $\tan \beta = 1.5$, accordingly with Eq. (4.137) the mixing effect is enhanced.

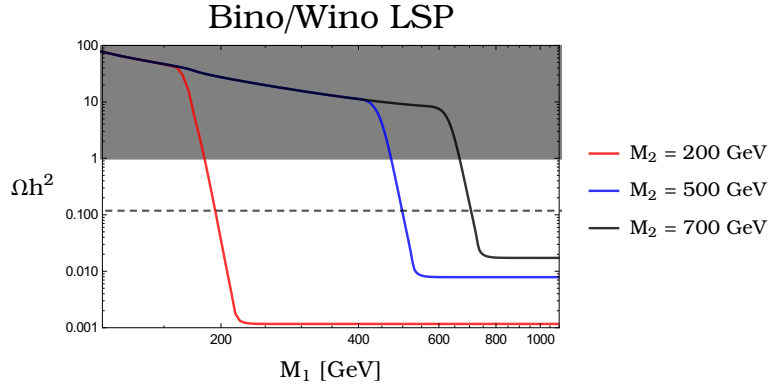


Figure 4.15: In the plot is shown the contribution to Ωh^2 of a Well-Tempered \tilde{B}/\tilde{W} as a function of the Bino mass parameter M_1 taking various fixed values of M_2 . The dark gray region correspond to an over-abundant relic density $\Omega h^2 > 1$ which has not physical sense. The dashed line correspond to the observed DM relic density. Comparing this result with the one for \tilde{B}/\tilde{H} configuration given in Fig. 4.10, we note the effect of the parametrically smaller mixing angle in the \tilde{B}/\tilde{W} case, which leads to a more abrupt transition between the pure Bino configuration (the region above the dashed line) to the pure Wino one (the region below the dashed line).

This leads to a more consistent Wino fraction in the LSP composition. In fact imposing this value of $\tan \beta$, the `micrOmegas 4.2.5` analysis shows that the right LSP mass is now within the range $422 \text{ GeV} \lesssim M_{\text{DM}} \lesssim 1148 \text{ GeV}$, resulting in a \tilde{B}/\tilde{W} configuration which is lifted towards the pure Wino region. The numerical result for $\tan \beta = 1.5$ is depicted in Fig. 4.16.

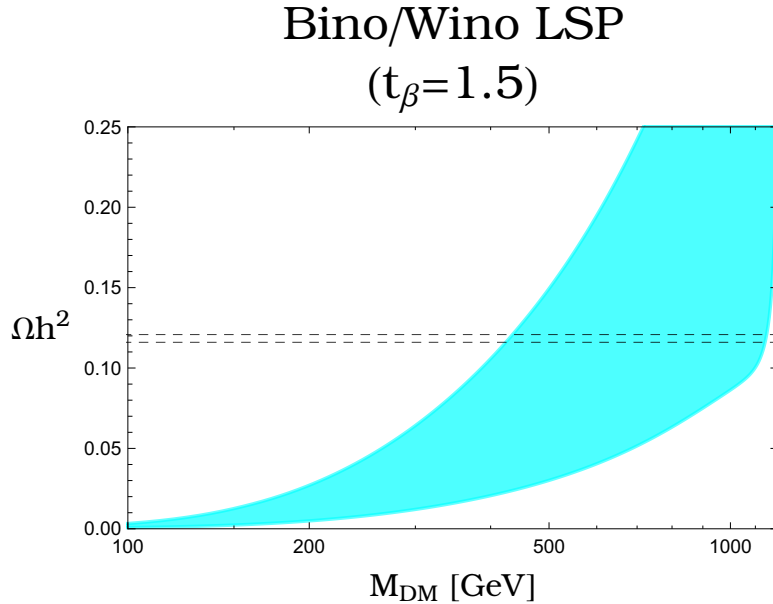


Figure 4.16: In the figure is shown the contribution to Ωh^2 of a Well-Tempered \tilde{B}/\tilde{W} as a function of the LSP mass, obtained from the `micrOmegas 4.2.5` analysis, imposing $\tan \beta = 1.5$. As usual the width of the band correspond to $-0.02 \lesssim \Delta \lesssim 0.02$.

In the case of a \tilde{B}/\tilde{W} the matrix elements N_{13} and N_{14} are respectively given by Eqs. (4.70)

and Eqs. (4.100) which after the substitution $M_1 \simeq M_2 = M_{\text{DM}}$ read as

$$N_{13} \simeq \frac{m_W (M_{\text{DM}} + \mu \sin 2\beta)}{(\mu^2 - M_{\text{DM}}^2) \cos \beta} + \frac{m_W \sin \beta}{\mu} + \mathcal{O}\left(\frac{m_W^2}{\mu^2}\right) \quad (4.152a)$$

$$N_{14} \simeq \frac{m_W \cos \beta}{\mu} + \mathcal{O}\left(\frac{M_{\text{DM}} m_W}{\mu^2}\right). \quad (4.152b)$$

Thus using these results into Eq. (4.17) and Eq. (4.18), we obtain that

$$\begin{aligned} \alpha_{\tilde{B}/\tilde{W}}^{\text{SD}(q_i)} &= \frac{g^2 t_W^2}{4(m_{\tilde{q}_i}^2 - M_{\text{DM}}^2)} \left[(\eta_{11}^i)^2 \frac{Y_{q_i L}^2}{4} + (\eta_{12}^i)^2 e_{q_i}^2 \right] \\ &+ \frac{g^2 t_W^2}{4(m_{\tilde{q}_i}^2 - M_{\text{DM}}^2)} \left[(\eta_{12}^i)^2 \frac{Y_{q_i L}^2}{4} + (\eta_{11}^i)^2 e_{q_i}^2 \right] \\ &+ \frac{g^2}{16\mu^2} (-1)^i \cos 2\beta \end{aligned} \quad (4.153a)$$

$$\begin{aligned} \alpha_{\tilde{B}/\tilde{W}}^{\text{SI}(q_i)} &= \frac{g^2 t_W^2 Y_{q_i L} e_{q_i} \eta_{11}^i \eta_{12}^i}{4} \left[\frac{1}{(m_{\tilde{q}_i}^2 - M_{\text{DM}}^2)} - \frac{1}{(m_{\tilde{q}_i}^2 - M_{\text{DM}}^2)} \right] \\ &- \frac{g^2 t_W m_{q_i} \sin \beta}{2m_h^2 \mu}. \end{aligned} \quad (4.153b)$$

which substituted into Eq. (4.35) and into Eq. (4.61) give respectively the SD and SI scattering cross-sections at zero momentum transferred for a \tilde{B}/\tilde{W} configuration

$$\sigma_{\tilde{B}/\tilde{W} p}^{\text{SD}} = \frac{12}{\pi} \left(\frac{M_{\text{DM}} m_p}{M_{\text{DM}} + m_p} \right)^2 \left[\sum_q \alpha_{\tilde{B}/\tilde{W}}^{\text{SD}(q_i)} \Delta q^{(p)} \right]^2 \quad (4.154a)$$

$$\sigma_{\tilde{B}/\tilde{W} n}^{\text{SD}} = \frac{12}{\pi} \left(\frac{M_{\text{DM}} m_p}{M_{\text{DM}} + m_p} \right)^2 \left[\sum_q \alpha_{\tilde{B}/\tilde{W}}^{\text{SD}(q_i)} \Delta q^{(n)} \right]^2 \quad (4.154b)$$

$$\sigma_{\tilde{B}/\tilde{W} p/n}^{\text{SI}} = \frac{4}{\pi} \left(\frac{M_{\text{DM}} m_p}{M_{\text{DM}} + m_p} \right)^2 \left[\sum_{q=u,d,s} \frac{m_{p/n}}{m_q} f_{\text{T}q}^{(p/n)} \alpha_{\tilde{B}/\tilde{W}}^{\text{SI}(q_i)} + \frac{2}{27} f_{\text{T}G} \sum_{q=c,b,t} \frac{m_{p/n}}{m_q} \alpha_{\tilde{B}/\tilde{W}}^{\text{SI}(q_i)} \right]^2. \quad (4.154c)$$

where to obtain Eqs. (4.153) we have assumed the limit $m_H^2 \gg m_h^2$. Note that in the above results does not appear the mixing angle θ between Bino and Wino states. This is because it gives rise to terms which are suppressed by $1/(\mu m_{\tilde{q}_i}^2)$. In the limit where $m_{\tilde{q}_i} \simeq m_{\tilde{q}_i} \simeq m_{\tilde{q}} \gg M_{\text{DM}}$, and of heavy squark masses, which implies $\eta_{11}^i \rightarrow 1$ and $\eta_{12}^i \rightarrow 0$, we have that Eqs. (4.153) can be approximated as

$$\alpha_{\tilde{B}/\tilde{W}}^{\text{SD}(q_i)} \simeq \frac{g^2 t_W^2}{4m_{\tilde{q}}^2} \left[\frac{Y_{q_i L}^2}{4} + e_{q_i}^2 \right] + \frac{g^2}{16\mu^2} (-1)^i \cos 2\beta + \mathcal{O}\left(\frac{M_{\text{DM}}^2}{m_{\tilde{q}}^2}, \eta_{12}^2\right) \quad (4.155a)$$

$$\begin{aligned} \alpha_{\tilde{B}/\tilde{W}}^{\text{SI}(q_i)} &\simeq \frac{g^2 t_W^2 Y_{q_i L} e_{q_i}}{4} \frac{m_{q_i} \mu (\tan \beta)^{(-1)^i}}{m_{\tilde{q}}^4} + \frac{g^2 m_{q_i} t_W \sin \beta}{2m_h^2 \mu} + \mathcal{O}\left(\frac{M_{\text{DM}}^2}{m_{\tilde{q}}^2}\right) \\ &\simeq \frac{g^2 m_{q_i} t_W \sin \beta}{2m_h^2 \mu} + \mathcal{O}\left(\frac{M_{\text{DM}}^2}{m_{\tilde{q}}^2}, \frac{m_{q_i} \mu}{m_{\tilde{q}}^2}\right). \end{aligned} \quad (4.155b)$$

Thus as occurred to the pure Bino LSP and to the pure Wino LSP, in the SI interaction the squarks term is suppressed by the vanishing factor $(m_{q_i} \mu)/m_{\tilde{q}}^4$, see Eq. (4.155b). Therefore the SI cross-section is nearly completely determined by the term associated to the Higgs exchange. Furthermore, assuming that $\mu \gtrsim m_{\tilde{q}}$, the SD interaction is determined by the term relative

Cross-section	Value-Range
$\sigma_{0SD}^{\tilde{B}/\tilde{W}p}$	$3.4 \times 10^{-11} - 1.5 \times 10^{-8}$ pb
$\sigma_{0SD}^{\tilde{B}/\tilde{W}n}$	$3.7 \times 10^{-12} - 1.1 \times 10^{-9}$ pb
$\sigma_{0SI}^{\tilde{B}/\tilde{W}p,n}$	$8.14 \times 10^{-14} - 1.7 \times 10^{-13}$ pb

Table 4.14: In the table we list the upper and lower values of the SD and SI \tilde{B}/\tilde{W} -nucleon cross-sections from our numerical analysis.

to the squarks exchange, as we can see from Eq. (4.155a). These theoretical behaviours are confirmed by the numerical analysis which is summarized in Fig. 4.17 and in Table 4.14. In particular in plots (a) and (b) we can appreciate the squarks dependence of the SD scattering cross-section, where the width of the band is due to a common squark mass which varies in the range $2 \text{ TeV} \leq m_{\tilde{q}} \leq 8 \text{ TeV}$. On contrary from plot (c) we can observe that the band is nearly completely absent, i.e. the SI scattering cross-section does not depend on the squark masses.

For the Well-Tempered \tilde{B}/\tilde{W} configuration, the analysis of the combined contribution of the SD and SI interactions gives the following neutralino-nucleus scattering cross-section

$$\sigma_0^{\tilde{B}/\tilde{W} \text{Xe}} \simeq \frac{\mu_N^2}{\mu_p^2} A^2 [\sigma_p^{\text{SI}} + 1.4 \times 10^{-6} \sigma_p^{\text{SD}}] \quad (4.156)$$

where we use the values of the \tilde{B}/\tilde{W} -Xe scattering cross-sections given in Table 4.14. In particular for the \tilde{B}/\tilde{W} configuration the ratio between the SD neutralino-nucleus scattering cross-section and the SI one is about $\sigma_{0SD}^{\tilde{B}/\tilde{W} \text{Xe}} / \sigma_{0SI}^{\tilde{B}/\tilde{W} \text{Xe}} \simeq 0.12$. This result shows that the contribution of the SD interaction is not entirely negligible respect to the SI one. For this reason in plot (d) of Fig. 4.17 is shown the total \tilde{B}/\tilde{W} -Xe scattering cross-section with the LUX experimental bound.

Concluding a Well-Tempered \tilde{B}/\tilde{W} satisfies both the DM and the direct detection constraints. Furthermore it is not excluded by indirect detection searches because its one-loop annihilation cross-section into final photons is well below the today's experimental bounds. Therefore a Well-Tempered \tilde{B}/\tilde{W} is still a good DM candidate which satisfied all today experimental constraints from direct, indirect and collider searches.

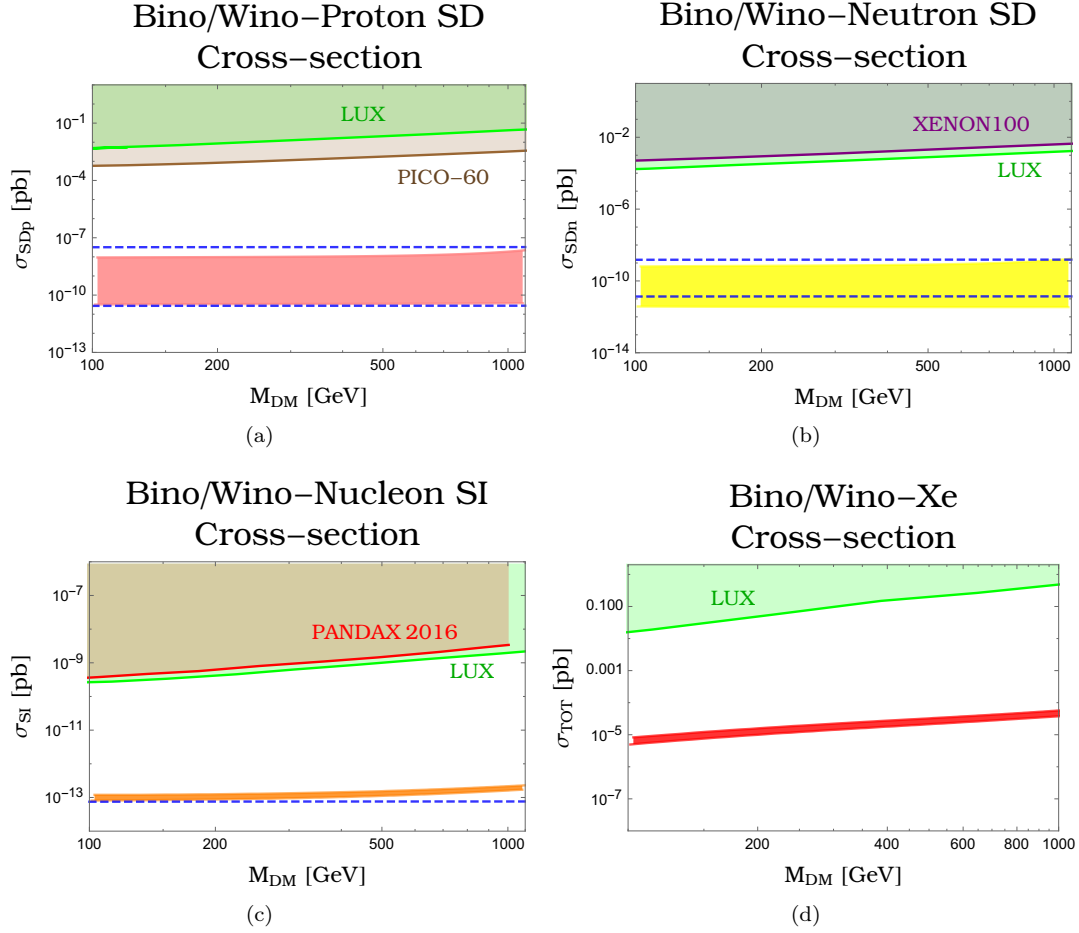


Figure 4.17: In the plot (a) is shown the SD \tilde{B}/\tilde{W} -proton scattering cross-section with the experimental excluded regions (shaded regions) provided by LUX-2016 (green) and PICO (brown) results. In the left panel (b) is shown the SD \tilde{B}/\tilde{W} -neutron scattering cross-section, with the excluded regions given by the LUX-2016 (green) and XENON100 (purple) experiments. In the below panel (c) we show the result for the SI \tilde{B}/\tilde{W} -nucleon scattering cross-section with the excluded limits given by the LUX-2016 (green) and the PANDAX-2016 (red) experiments. In every plot the width of the band corresponds to squark masses in the range $2 \text{ TeV} \lesssim m_{\tilde{q}} \lesssim 8 \text{ TeV}$ and the regions between the blue-dashed lines represent the analytical results which are found using the approximate formulae given in Eqs. (4.155). As last in plot (d) we show the total \tilde{B}/\tilde{W} -Xe scattering cross-section with the experimental bound provided by LUX experiment.

Conclusions

In this thesis we have investigated the nature of the non-visible gravitating matter present in the Universe, the so-called Dark Matter (DM). We focused on the hypothesis of particle DM specializing on the proposal that DM is a thermal relic produced in the early Universe. The theoretical framework chosen to describe particle DM is the one provided by supersymmetric theories, in particular the Minimal Supersymmetric Standard Model (MSSM). In this framework the DM candidate is the lightest supersymmetric neutralino. In this thesis we considered the famous “Well-Tempered” neutralino scenario introduced by N. Arkani-Hamed, A. Delgado and G.F. Giudice [11].

We started taking into account the pure Bino configuration finding that, once the experimental constraints from sleptons searches at LEP are satisfied, its relic density is too large. In order to reduce the relic density, we have studied the possibility that the Bino is nearly degenerate in mass with a right-handed slepton. Exploiting the co-annihilation mechanism, we found the correct relic abundance in a region of the MSSM parameter space which is not ruled out by collider experiments. We have also analysed the possible constraints from direct searches. We found that the Bino-nucleon cross section is well below the current experimental limits both for spin-independent and spin-dependent interactions. This is due to the fact that in the pure Bino configuration the LSP-Higgs and LSP- Z^0 couplings are vanishing and therefore the scattering cross-section is highly suppressed. As a consequence, the Bino is a good DM candidate.

Afterwards we have studied the pure Higgsino and Wino scenarios. The relic density analysis has shown that both of them have a too small relic abundance, unless their masses are heavier than ~ 1 TeV. Such high values of the masses compromise the possibility that the “hierarchy problem” can be solved by supersymmetry. After that, we have performed the direct detection analysis of these two scenarios. We have found that, as in the pure Bino case, also for the pure Higgsino and Wino cases their vanishing couplings with the Higgs and Z^0 bosons reduce the LSP-nucleon scattering cross-section below the direct detection experimental limits.

At last we have analysed the “Well-Tempered” neutralino scenarios. In particular, we have considered the mixing between the Bino and Higgsino and between Bino and Wino. We computed the relic density of these candidates, finding that they can satisfy the DM constraints in wide regions of the parameter space. From the analysis of direct-detection experiments, we found that a Well-Tempered Bino/Higgsino is excluded for masses below the TeV scale. In particular, the spin-independent scattering cross-section with nucleons is well above the bounds imposed by the LUX-2016 and PANDAX-2016 analyses. For what concerns the Well-Tempered Bino/Wino scenario, we have found that its scattering cross-section with nucleons is well below the direct search limits. This is again due to the absence of LSP couplings with Higgs and Z^0 bosons.

Summarizing, from our analysis it follows that the only scenarios which satisfy both relic density and direct detection constraints are those featuring a Well-Tempered Bino/Wino LSP and where a pure Bino LSP co-annihilates with a slepton.

Further investigations beyond our analysis would be welcome. First of all, it would be interesting to implement both the indirect detection and collider experimental results in a more systematic way, in order to further constrain the various models proposed. In particular a deeper study of the current and future indirect detection experimental results could further constrain our scenarios. Finally, it would be interesting to study the impact of future direct detection experiments such as XENON1T, LZ, and DARWIN.

Appendix A

In this appendix we resolve, in an approximate way, the Boltzmann equation demonstrating the solutions for Y_∞ and for x_{fo} respectively given in Eq. (2.32) and in Eq. (2.35). After that we compute the thermal average of the annihilation cross-section times velocity in the non-relativistic limit finding the approximate solution given in Eq. (2.57). At last we summarize the principal steps that we follow to obtain the exact solution of thermal average of $\langle\sigma_{\text{eff}}v\rangle$ in the case of co-annihilations given in Eq. (2.57).

A.1 Approximate solution for the Boltzmann equation

We start from the Boltzmann equation in the form given in Eq. (2.31)

$$\frac{\partial Y}{\partial x} = -\frac{\langle\sigma v_{\text{M}}\rangle s}{Hx} \{Y^2 - (Y^{(0)})^2\}, \quad (\text{A.1})$$

where $x = m/T$ and H is the Hubble constant. Using Eq. (2.24) and Eq. (2.28) we re-express the factor $s/(Hx)$ as

$$\frac{s}{Hx} = \sqrt{\frac{\pi}{45}} \frac{g_{*s}}{g_*^{1/2}} \frac{mM_{\text{Pl}}}{x^2} \equiv \frac{\lambda}{x^2} \quad (\text{A.2})$$

and Eq. (A.1) becomes

$$\frac{\partial Y}{\partial x} = -\lambda \frac{\langle\sigma v_{\text{M}}\rangle}{x^2} \{Y^2 - (Y^{(0)})^2\}. \quad (\text{A.3})$$

Now we consider the above equation in terms of the variable $\Delta \equiv Y - Y^{(0)}$ which expresses the departure from equilibrium, obtaining

$$\frac{\partial \Delta}{\partial x} = -\frac{\partial Y^{(0)}}{\partial x} - \lambda \frac{\langle\sigma v_{\text{M}}\rangle}{x^2} \Delta \{\Delta + 2Y^{(0)}\}. \quad (\text{A.4})$$

At early times, before the “freeze-out” when $x \ll x_{\text{fo}}$, Y tracks very closely $Y^{(0)}$; thus both Δ and $|\frac{\partial \Delta}{\partial x}|$ are small and so an approximate solution is obtained by setting $\frac{\partial \Delta}{\partial x} = 0$,

$$\begin{aligned} \Delta &\simeq -\frac{x^2}{\langle\sigma v_{\text{M}}\rangle \lambda \{\Delta + 2Y^{(0)}\}} \frac{\partial Y^{(0)}}{\partial x} \\ &\simeq \frac{x^2}{2\lambda \langle\sigma v_{\text{M}}\rangle}. \end{aligned} \quad (\text{A.5})$$

Note that the quantity $Y^{(0)}$ in terms of the variable x read as

$$Y^{(0)} \equiv \frac{n^0}{s} = \frac{45}{2\pi^2} \frac{1}{(2\pi)^{3/2}} \frac{g}{g_{*s}} x^{3/2} e^{-x} \equiv wx^{3/2} e^{-x} \quad (\text{A.6})$$

where we used Eq. (2.13) and Eq. (2.24); thus the derivative of $Y^{(0)}$ would be equal to

$$\frac{\partial Y^{(0)}}{\partial x} = Y^{(0)} \left(\frac{3}{2x} - 1 \right) = -Y^{(0)} + \mathcal{O}\left(\frac{1}{x}\right) \quad (\text{A.7})$$

which is a good approximation in the non-relativistic limit i.e. when $x \gg 1$. At later times, after the “freeze-out” when $x \gg x_{\text{fo}}$, Y tracks $Y^{(0)}$ very poorly [51] [19], so $\Delta \simeq Y \gg Y^{(0)}$, and the terms involving $\frac{\partial Y^{(0)}}{\partial x}$ and $Y^{(0)}$ can be safely neglected. Then Eq. (A.4) becomes

$$\frac{1}{\Delta^2} \frac{\partial \Delta}{\partial x} = -\lambda \frac{\langle \sigma v_M \rangle}{x^2}. \quad (\text{A.8})$$

Integrating this equation from x_{fo} to ∞ we get for the left-hand side

$$\begin{aligned} \int_{\Delta(x_{\text{fo}})}^{\Delta(\infty)} \frac{d\Delta}{\Delta^2} &= \left(\frac{1}{\Delta(x_{\text{fo}})} - \frac{1}{\Delta_\infty} \right) \\ &\simeq -\frac{1}{\Delta_\infty} \simeq -\frac{1}{Y_\infty} \end{aligned} \quad (\text{A.9})$$

where we have used the facts that $\Delta(x_{\text{fo}}) \gg \Delta_\infty$ and $Y^{(0)} \rightarrow 0$ as $x \rightarrow \infty$, as we can see from Eq. (A.6). For what concerns the right-hand side remembering the definition given in Eq. (2.33) we have

$$-\lambda \int_{x_{\text{fo}}}^{\infty} \frac{\langle \sigma v_M \rangle}{x^2} dx \equiv -\lambda J(x_{\text{fo}}), \quad (\text{A.10})$$

thus equating Eq. (A.9) and Eq. (2.33) we get a solution for Y_∞

$$Y_\infty = \frac{1}{\lambda J(x_{\text{fo}})} = \sqrt{\frac{45}{\pi}} \frac{g_*^{1/2}}{g_{*s}} \frac{1}{m M_{\text{Pl}} J(x_{\text{fo}})}. \quad (\text{A.11})$$

To determine x_{fo} , we recall that when $x \simeq x_{\text{fo}}$, Y ceases to track $Y^{(0)}$; equivalently we can say that Δ becomes of order $Y^{(0)}$. In fact, schematically, we have

$$\Delta(x_{\text{fo}}) = Y^{(0)} \left(\frac{Y}{Y^{(0)}} - 1 \right) \equiv c Y^{(0)} \quad (\text{A.12})$$

with the numerical constant c of order unity. Taking into account the early time solution, given by Eq. (A.5), and the condition (A.12), we have that

$$c Y^{(0)} \simeq -\frac{x_{\text{fo}}^2}{\langle \sigma v_M \rangle \lambda Y^{(0)} (c+2)} \frac{\partial Y^{(0)}}{\partial x}. \quad (\text{A.13})$$

Using for $Y^{(0)}$ the expression in Eq. (A.6), evaluated at x_{fo} , we rewrite the previous equation as

$$\begin{aligned} e^{-x_{\text{fo}}} &= \frac{x_{\text{fo}}^2}{\langle \sigma v_M \rangle \lambda c (c+2)} \frac{1}{w x_{\text{fo}}^{3/2}} \\ &= \frac{x_{\text{fo}}^{1/2}}{\langle \sigma v_M \rangle \lambda w c (c+2)}. \end{aligned} \quad (\text{A.14})$$

With this result we can find an iterative solution for x_{fo} given in Eq. (2.35)

$$\begin{aligned} x_{\text{fo}} &\simeq \ln \left[\frac{\lambda w c (c+2) \langle \sigma v_M \rangle}{x_{\text{fo}}^{1/2}} \right] = \ln \left[\frac{c(c+2) \sqrt{\frac{45}{2}} g M_{\text{Pl}} m \langle \sigma v_M \rangle}{4\pi^3 g_{*s}^{1/2} x_{\text{fo}}^{1/2}} \right] \\ &\simeq \ln \left[\frac{0.038 c (c+2) g M_{\text{Pl}} m \langle \sigma v_M \rangle}{g_{*s}^{1/2} x_{\text{fo}}^{1/2}} \right]. \end{aligned} \quad (\text{A.15})$$

A.2 Non-relativistic approximate solution for the thermal average of σv

Here we give an approximate solution, in the non-relativistic limit, for $\langle \sigma v \rangle$ in the case of two annihilating particles with equal mass m . Recalling Eq. (2.56) we have that

$$\langle \sigma v_{\text{lab}} \rangle^{\text{lab}} = \frac{\int \sigma v_{\text{lab}} e^{-E_1/T} e^{-E_2/T} d^3 p_1 d^3 p_2}{\int e^{-E_1/T} e^{-E_2/T} d^3 p_1 d^3 p_2} \quad (\text{A.16})$$

where lab means that we are performing the computation in the laboratory frame of particle 1; note that the relation given in Eq. (2.53) assures that the result will be valid in a generic comoving frame.

In the non-relativistic limit we have that

$$E_i = \sqrt{p_i^2 + m^2} = m_i \sqrt{\frac{p_i^2}{m^2} + 1} \simeq m + \frac{p_i^2}{2m} + \mathcal{O}\left(\frac{p_i^4}{m^3}\right) \quad (\text{A.17})$$

and so $\langle \sigma v_{\text{lab}} \rangle^{\text{lab}}$ becomes

$$\langle \sigma v_{\text{lab}} \rangle_{\text{n.r.}}^{\text{lab}} \simeq \frac{\int \sigma v_{\text{lab}} e^{-p_1^2/2mT} e^{-p_2^2/2mT} d^3 p_1 d^3 p_2}{\int e^{-p_1^2/2mT} e^{-p_2^2/2mT} d^3 p_1 d^3 p_2} \quad (\text{A.18})$$

where the subscript n.r. means non-relativistic.

We start by computing the denominator, which we redefined as

$$\int e^{-p_1^2/2mT} e^{-p_2^2/2mT} d^3 p_1 d^3 p_2 = \left(\int e^{-p^2/2mT} d^3 p \right)^2 \equiv \mathcal{D}. \quad (\text{A.19})$$

Performing the integral over the solid angle Ω and changing variable from $|\vec{p}|$ to $y = |\vec{p}|/\sqrt{2mT}$ we have

$$\begin{aligned} \int e^{-p^2/2mT} d^3 p &= 4\pi(2mT)^{3/2} \frac{1}{2} \int_0^\infty e^{-y^2} dy \\ &= (2\pi mT)^{3/2} \end{aligned} \quad (\text{A.20})$$

where we have first performed an integration by parts and then a gaussian integration. Therefore the denominator \mathcal{D} is equal to

$$\mathcal{D} = 8(\pi mT)^3. \quad (\text{A.21})$$

To compute the numerator of Eq. (A.18) we start by changing the integration variables as

$$\vec{p}_1 = \frac{\vec{p}_{\text{tot}} + \vec{p}_r}{2} \quad (\text{A.22a})$$

$$\vec{p}_2 = \frac{\vec{p}_{\text{tot}} - \vec{p}_r}{2} \quad (\text{A.22b})$$

where \vec{p}_{tot} is the total momentum vector defined as $\vec{p}_{\text{tot}} = \vec{p}_1 + \vec{p}_2$ and \vec{p}_r is the relative momentum vector, defined as $\vec{p}_r = \vec{p}_1 - \vec{p}_2$. After this operation the numerator becomes

$$\begin{aligned} \mathcal{N} &\equiv \int \sigma v_{\text{lab}} e^{-p_1^2/2mT} e^{-p_2^2/2mT} d^3 p_1 d^3 p_2 \\ &= \frac{1}{8} \int \sigma v_{\text{lab}} e^{-p_{\text{tot}}^2/4mT} e^{-p_r^2/4mT} d^3 p_{\text{tot}} d^3 p_r \end{aligned} \quad (\text{A.23})$$

where the pre-factor, $1/8$, is the determinant of the Jacobian of the transformation (A.22). Noting that σv_{lab} depends only on p_r , we can integrate over p_{tot} obtaining

$$\begin{aligned} \mathcal{N} &= \frac{1}{8} \int e^{-p_{\text{tot}}^2/4mT} d^3 p_{\text{tot}} \int \sigma v_{\text{lab}} e^{-p_r^2/4mT} d^3 p_r \\ &= \frac{1}{2} (4\pi mT)^{3/2} \pi \int_0^\infty \sigma v_{\text{lab}} e^{-p_r^2/4mT} d|\vec{p}_r|. \end{aligned} \quad (\text{A.24})$$

To go further we have to find the relation between $|\vec{p}_r|$ and the total kinetic energy per unit of mass in the laboratory frame, ϵ , defined in Eq. (2.54) which here we recall

$$\epsilon = \frac{(E_{1\text{lab}} - m) + (E_{2\text{lab}} - m)}{2m} = \frac{E_{2\text{lab}} - m}{2m}. \quad (\text{A.25})$$

In the case of particles of equal masses we have that

$$\vec{v}_{1_{\text{cm}}} = \frac{\vec{v}_1 - \vec{v}_2}{2} \quad (\text{A.26})$$

where $\vec{v}_{1_{\text{cm}}}$ is the velocity of particle 1 in the center-of-mass frame from which we find that $\vec{p}_{1_{\text{cm}}}$ is simply given by

$$\vec{p}_{1_{\text{cm}}} = \vec{v}_{1_{\text{cm}}} m = \frac{\vec{p}_1 - \vec{p}_2}{2} = -\vec{p}_{2_{\text{cm}}} \quad (\text{A.27})$$

Comparing this relation with the definition of \vec{p}_r in Eq. (A.22), we get

$$|\vec{p}_{1_{\text{cm}}}| = |\vec{p}_{2_{\text{cm}}}| \equiv |\vec{p}_{\text{cm}}| = \frac{|\vec{p}_r|}{2}. \quad (\text{A.28})$$

Expressing both $|\vec{p}_{\text{cm}}|$ and ϵ in terms of the invariant s we find

$$|\vec{p}_r|^2 = 4|\vec{p}_{\text{cm}}|^2 = s - 4m^2, \quad \epsilon = \frac{s - 4m^2}{4m^2} \quad (\text{A.29})$$

and so

$$|\vec{p}_r|^2 = 4m^2 \epsilon. \quad (\text{A.30})$$

Thanks to this relation we can change the integration variables in the numerator \mathcal{N} which becomes

$$\begin{aligned} \mathcal{N} &= 16(\pi m T)^{3/2} \pi m^3 \int_0^\infty \sigma v_{\text{lab}} e^{-m\epsilon/T} \sqrt{\epsilon} d\epsilon \\ &= 16(\pi m T)^{3/2} \pi m^3 \sum_{n=0}^\infty \frac{a^{(n)}}{n!} \int_0^\infty e^{-m\epsilon/T} \epsilon^{1/2+n} d\epsilon \end{aligned} \quad (\text{A.31})$$

where in the last equality we have substituted the expansion for σv_{lab} given in Eq. (2.55). Performing another change of variable from ϵ to $t = m\epsilon/T$ we have

$$\begin{aligned} \mathcal{N} &= 16\pi^{5/2} (mT)^3 \sum_{n=0}^\infty \frac{a^{(n)}}{n!} \left(\frac{m}{T}\right)^{-n} \int_0^\infty e^{-t} t^{1/2+n} dt \\ &= 16\pi^{5/2} (mT)^3 \sum_{n=0}^\infty \frac{a^{(n)}}{n!} \left(\frac{m}{T}\right)^{-n} \int_0^\infty e^{-t} t^{(3+2n)/2-1} dt \\ &= 16\pi^{5/2} (mT)^3 \sum_{n=0}^\infty \frac{a^{(n)}}{n!} \frac{1}{x^n} \Gamma\left(\frac{3+2n}{2}\right) \end{aligned} \quad (\text{A.32})$$

where as usual $m/T \equiv x$ and $\Gamma(z)$ denotes the Eulero-Gamma function. Now thanks to the propriety of the Eulero-Gamma function [1]

$$\Gamma\left(\frac{l}{2}\right) = \frac{(l-2)!!}{2^{(l-1)/2}} \sqrt{\pi} \quad (\text{A.33})$$

where l is an integer, the last factor in Eq. (A.32) becomes

$$\Gamma\left(\frac{3+2n}{2}\right) = \frac{(2n+1)!!}{2^n} \frac{\sqrt{\pi}}{2}. \quad (\text{A.34})$$

Replacing this result in Eq. (A.32) we obtain the final form of the numerator \mathcal{N}

$$\mathcal{N} = 8(\pi m T)^3 \sum_{n=0}^\infty \frac{a^{(n)}}{n!} \frac{1}{x^n} \frac{(2n+1)!!}{2^n}. \quad (\text{A.35})$$

Finally, taking the ratio between Eq. (A.35) and Eq. (A.21), we obtain the expansion in powers of $1/x$ of the thermal average, $\langle \sigma v_{\text{lab}} \rangle_{\text{n.r.}}^{\text{lab}}$, in the non-relativistic approximation [43]

$$\begin{aligned} \langle \sigma v_{\text{lab}} \rangle_{\text{n.r.}}^{\text{lab}} &\equiv \frac{\mathcal{N}}{\mathcal{D}} = \sum_{n=0}^\infty \frac{a^{(n)}}{n!} \frac{1}{x^n} \frac{(2n+1)!!}{2^n} \\ &= a^{(0)} + \frac{3}{2} \frac{a^{(1)}}{x} + \frac{15}{8} \frac{a^{(2)}}{x^2} + \mathcal{O}\left(\frac{1}{x^3}\right). \end{aligned} \quad (\text{A.36})$$

A.3 Thermal average of $\sigma_{\text{eff}v}$

Following [33] we start re-expressing the definition of $\langle\sigma_{\text{eff}v}\rangle$, given in Eq. (2.78), into a more convenient form,

$$\langle\sigma_{\text{eff}v}\rangle = \sum_{i,j=1}^N \langle\sigma_{ij}v_{ij}\rangle \frac{n_i^0}{n^0} \frac{n_j^0}{n^{(0)}} \equiv \frac{A}{(n^{(0)})^2}. \quad (\text{A.37})$$

First we simplify the denominator as

$$\begin{aligned} n^{(0)} &= \sum_i g_i \int \frac{d^3p_i}{(2\pi)^3} e^{-\frac{E_i}{T}} \\ &= \sum_i \frac{g_i}{2\pi^2} \int_{m_i}^{\infty} dE_i E_i \sqrt{E_i^2 - m_i^2} e^{-\frac{E_i}{T}} \end{aligned} \quad (\text{A.38})$$

where we have used the relation $p_i = \sqrt{E_i^2 - m_i^2}$. Integrating the last integral by parts we get

$$n^{(0)} = \sum_i \frac{g_i T}{2\pi^2} \int_{m_i}^{\infty} dE_i \frac{2E_i^2 - m_i^2}{\sqrt{E_i^2 - m_i^2}} e^{-\frac{E_i}{T}}. \quad (\text{A.39})$$

Thus making the substitution

$$\frac{E_i}{m_i} = \cosh t \quad (\text{A.40})$$

the above integral becomes

$$\begin{aligned} n^{(0)} &= \sum_i \frac{g_i}{2\pi^2} T m_i^2 \int_0^{\infty} dt \sinh t \left(\frac{2 \cosh^2 t - 1}{\sinh t} \right) e^{-\frac{m_i}{T} \cosh t} \\ &= \sum_i \frac{g_i}{2\pi^2} T m_i^2 \int_0^{\infty} dt \cosh(2t) e^{-\frac{m_i}{T} \cosh t}. \end{aligned} \quad (\text{A.41})$$

Now, remembering that the integral form of the modified Bessel functions of second kind of order ν is [1],

$$K_\nu(x) = \int_0^{\infty} dt \cosh(\nu t) e^{-x \cosh t} \quad (\text{A.42})$$

we can write $n^{(0)}$ as

$$n^{(0)} = \sum_i \frac{g_i}{2\pi^2} T m_i^2 K_2\left(\frac{m_i}{T}\right). \quad (\text{A.43})$$

The numerator of Eq. (A.37), for generic distribution functions f_i, f_j is equal to

$$A = \sum_{i,j} \frac{g_i g_j}{(2\pi)^6} \int d^3p_i d^3p_j f_i f_j \sigma_{ij} v_{ij}. \quad (\text{A.44})$$

It is convenient to recast it in an explicit covariant form, as

$$A = \sum_{i,j} g_i g_j \int W_{ij} f_i f_j \frac{d^3p_i}{(2\pi)^3 2E_i} \frac{d^3p_j}{(2\pi)^3 2E_j} \quad (\text{A.45})$$

where W_{ij} is the un-polarized annihilation rate per unit volume which is equal to

$$W_{ij} = 4E_i E_j \sigma_{ij} v_{ij} = 4\sigma_{ij} \sqrt{(p_i \cdot p_j)^2 - m_i^2 m_j^2} = 4p_{ij} \sqrt{s} \sigma_{ij} \quad (\text{A.46})$$

where we used the definition of the Møller velocity given in Eq. (2.19) and as usual (\cdot) means the Lorentz scalar product. The quantity p_{ij} is the modulus of the 3-momentum of particle

X_i (or X_j) in the center-of-mass frame of the pair of particles $X_i X_j$, which in terms of the invariant s read as

$$p_{ij} = \sqrt{(p_i \cdot p_j)^2 - m_i^2 m_j^2} = \frac{\sqrt{(s - (m_i + m_j)^2)(s - (m_i - m_j)^2)}}{2\sqrt{s}}. \quad (\text{A.47})$$

The general expression of W_{ij} for a n-body final state is

$$W_{ij \rightarrow n} = \frac{1}{g_i g_j S_f} \sum_{\text{internal d.o.f.}} \int |\mathcal{M}|^2 (2\pi)^4 \delta^{(4)}(p_i + p_j - \sum_f p_f) \prod_f \frac{d^3 p_f}{(2\pi)^3 2E_f}$$

where we averaged over initial and summed over final spins and \mathcal{M} is the amplitude of the processes; S_f is a symmetry factor accounting for identical final state particles. In particular for a two-body final state we have

$$W_{ij \rightarrow kl} = \frac{1}{g_i g_j S_f} \sum_{\text{internal d.o.f.}} \int |\mathcal{M}|^2 (2\pi)^4 \delta^{(4)}(p_i + p_j - p_k - p_l) \frac{d^3 p_k}{(2\pi)^3 2E_k} \frac{d^3 p_l}{(2\pi)^3 2E_l} \quad (\text{A.48})$$

where now S_f is equal to 2 if the final particles are identical or 1 if they are different and with i, j we denote the initial particles, while with k, l the final ones. Performing the integral over $d^3 p_k$ and after the integral over $d|p_l|$ we get that [33]

$$W_{ij \rightarrow kl} = \frac{p_{kl}}{16\pi^2 g_i g_j S_f \sqrt{s}} \sum_{\text{internal d.o.f.}} \int d\Omega |\mathcal{M}|^2 \quad (\text{A.49})$$

Now we want to reduce the integral in the definition of A , given in Eq. (A.45), from a 6 dimensional to a 1 dimensional integral. Using the Maxwell-Boltzmann statistics instead of generics statistics f_i, f_j , it reads

$$A = \sum_{i,j} g_i g_j \int W_{ij} e^{-\frac{E_i}{T}} e^{-\frac{E_j}{T}} \frac{d^3 p_i}{(2\pi)^3 2E_i} \frac{d^3 p_j}{(2\pi)^3 2E_j} \quad (\text{A.50})$$

Following ref. [43], we can rewrite the momentum volume element as

$$\begin{aligned} d^3 p_i d^3 p_j &= 4\pi p_i^2 dp_i 2\pi p_j^2 dp_j \sin \theta d\theta \\ &= 4\pi |p_i| E_i dE_i 4\pi |p_j| E_j dE_j \frac{1}{2} d\cos \theta \end{aligned} \quad (\text{A.51})$$

where θ is the angle between \vec{p}_i and \vec{p}_j . Then we perform a change of the integration variables from E_i, E_j and θ to E_+, E_- and s , defined as

$$E_+ = E_i + E_j \quad (\text{A.52})$$

$$E_- = E_i - E_j \quad (\text{A.53})$$

$$s = m_i^2 + m_j^2 + s E_i E_j - 2|p_i||p_j| \cos \theta \quad (\text{A.54})$$

Therefore the volume element becomes equal to

$$\begin{aligned} \frac{d^3 p_i}{(2\pi)^3 2E_i} \frac{d^3 p_j}{(2\pi)^3 2E_j} &= \frac{1}{(2\pi)^4} \frac{|p_i||p_j|}{2} |\det\{J\}|^{-1} dE_+ dE_- ds \\ &= \frac{1}{(2\pi)^4} \frac{dE_+ dE_- ds}{8} \end{aligned} \quad (\text{A.55})$$

where J is the Jacobian of the transformation and

$$\det\{J\} = \begin{vmatrix} 1 & 1 & 2E_j \\ 1 & -1 & 2E_i \\ 0 & 0 & -2|p_i||p_j| \end{vmatrix} = 4|p_i||p_j| \quad (\text{A.56})$$

Note that the new integration region, which in terms of the old variables was $E_i \geq m_i, E_j \geq m_j, |\cos \theta| \leq 1$, now reads as

$$s \geq (m_i + m_j)^2 \quad (\text{A.57})$$

$$E_+ \geq \sqrt{s} \quad (\text{A.58})$$

$$E_+ \frac{m_j^2 - m_i^2}{s} - 2p_{ij} \sqrt{\frac{E_+^2 - s}{s}} \leq E_- \leq E_+ \frac{m_j^2 - m_i^2}{s} + 2p_{ij} \sqrt{\frac{E_+^2 - s}{s}} \quad (\text{A.59})$$

With the substitutions given in Eqs. (A.52) the integral in Eq. (A.45) becomes

$$A = \sum_{i,j} \int \frac{g_i g_j}{8(2\pi)^4} W_{ij}(s) e^{-\frac{E_+}{T}} dE_+ dE_- ds. \quad (\text{A.60})$$

Note that W_{ij} depends only on s , and the equilibrium distribution function depends only on E_+ , and so we can immediately integrate over E_- . Taking into account the region of integration (A.59), we get

$$A = \sum_{i,j} \int 4p_{ij} \sqrt{\frac{E_+^2 - s}{s}} \frac{g_i g_j}{8(2\pi)^4} W_{ij}(s) e^{-\frac{E_+}{T}} dE_+ ds. \quad (\text{A.61})$$

Now we perform the integral over E_+ ; first we integrate by parts obtaining

$$A = \frac{T}{32\pi^4} \sum_{i,j} \int p_{ij} g_i g_j W_{ij}(s) ds \int_{\sqrt{s}}^{\infty} \frac{E_+}{s \sqrt{E_+^2 - s}} e^{-\frac{E_+}{T}} dE_+ \quad (\text{A.62})$$

then changing variable as

$$E_+ = \sqrt{s} \cosh x \Rightarrow dE_+ = \sqrt{s} \sinh x dx \quad (\text{A.63})$$

and remembering the form of modified Bessel functions of second kind, given in Eq. (A.42), the integral becomes

$$\begin{aligned} A &= \frac{T}{32\pi^4} \sum_{i,j} \int g_i g_j p_{ij} W_{ij}(s) ds \int_0^{\infty} \cosh x e^{-\frac{\sqrt{s}}{T} \cosh x} dx \\ &= \frac{T}{32\pi^4} \sum_{i,j} \int_{(m_i + m_j)^2}^{\infty} ds g_i g_j p_{ij} W_{ij} K_1 \left(\frac{\sqrt{s}}{T} \right). \end{aligned} \quad (\text{A.64})$$

Now we define the quantities

$$p_{\text{eff}} \equiv p_{11} = \frac{\sqrt{s - 4m_1^2}}{2} \quad (\text{A.65})$$

and

$$W_{\text{eff}} \equiv \sum_{i,j} \frac{p_{ij}}{p_{\text{eff}}} \frac{g_i g_j}{g_1^2} W_{ij} = \sum_{i,j} \sqrt{\frac{[s - (m_i + m_j)^2][s - (m_i - m_j)^2]}{s(s - 4m_1^2)}} \frac{g_i g_j}{g_1^2} W_{ij}. \quad (\text{A.66})$$

Note that W_{eff} is well defined because $W_{ij}(s) = 0$ iff $s \leq (m_i + m_j)^2$, so the radicand in Eq. (A.66) cannot be negative; with these definitions Eq. (A.64) now reads

$$\begin{aligned} A &= \frac{T g_1^2}{32\pi^4} \int_{4m_1^2}^{\infty} ds p_{\text{eff}} W_{\text{eff}} K_1 \left(\frac{\sqrt{s}}{T} \right) \\ &= \frac{T g_1^2}{4\pi^4} \int_0^{\infty} dp_{\text{eff}} p_{\text{eff}}^2 W_{\text{eff}} K_1 \left(\frac{\sqrt{s}}{T} \right) \end{aligned} \quad (\text{A.67})$$

where in the last equality we have changed variable from s to p_{eff} using the definition (A.65) and the consequent relation $ds = 8p_{\text{eff}} dp_{\text{eff}}$. To conclude using Eq. (A.67) and Eq. (A.43) we can perform the ratio $A/(n^{(0)})^2$, finding that

$$\langle \sigma_{\text{eff}} v \rangle = \frac{\int_0^{\infty} dp_{\text{eff}} p_{\text{eff}}^2 W_{\text{eff}} K_1 \left(\frac{\sqrt{s}}{T} \right)}{m_1^4 T \left[\sum_i \frac{g_i}{g_1} \frac{m_i^2}{m_1^2} K_2 \left(\frac{m_i}{T} \right) \right]^2}. \quad (\text{A.68})$$

Note that the above exact formula for the thermal average of cross-section in the case of co-annihilations can be reduced to an exact formula for the thermal average of the cross-section in the standard case i.e. two equal mass annihilating particles. This can be done observing that the definition for W_{eff} in the standard case becomes

$$W_{\text{eff}} = W_{11}. \tag{A.69}$$

Thus Eq. (A.68) turns out to be

$$\langle \sigma v \rangle = \frac{1}{(m_1^2 K_2 (\frac{m_1}{T}))^2} \int_0^\infty dp_{11} p_{11}^2 W_{11} K_1 (\frac{\sqrt{s}}{T}). \tag{A.70}$$

Appendix B

MSSM Feynman rules

In this appendix we list the MSSM Feynman rules, which will be useful in the evaluation of the neutralino annihilation cross-sections and neutralino-quark scattering cross-sections. We follow ref [63].

We start from the interaction between neutralino/chargino with gauge bosons:

$$\begin{array}{c}
 \tilde{\chi}_i \\
 \swarrow \\
 Z_\mu^0 \text{ wavy line} \\
 \searrow \\
 \tilde{\chi}_j
 \end{array}
 = -\frac{ig}{2c_W} \gamma_\mu (\gamma^5)^{i+j+1} (N_{4i}N_{4j} - N_{3i}N_{3j}) \equiv \alpha_{\tilde{\chi}\tilde{\chi}Z^0}
 \quad (\text{B.1a})$$

$$\begin{array}{c}
 \tilde{\chi}_i \\
 \swarrow \\
 W_\mu^\pm \text{ wavy line} \\
 \searrow \\
 \tilde{\chi}_j^\pm
 \end{array}
 = -ig\gamma_\mu \left[\left(N_{2i}U_{1j} - \frac{1}{\sqrt{2}}N_{4i}U_{2j} \right) P_L + \left(N_{2i}V_{1j} + \frac{1}{\sqrt{2}}N_{3i}V_{2j} \right) P_R \right]
 \quad (\text{B.1b})$$

$$\begin{array}{c}
 \tilde{\chi}_i^\pm \\
 \swarrow \\
 Z_\mu^0 \text{ wavy line} \\
 \searrow \\
 \tilde{\chi}_j^\pm
 \end{array}
 = -\frac{ig}{2c_W} \gamma_\mu (U_{1i}U_{1j}P_L + V_{1i}V_{1j}P_R + \delta^{ij}c_{2W})
 \quad (\text{B.1c})$$

$$\begin{array}{c}
 \tilde{\chi}_i^\pm \\
 \swarrow \\
 \gamma_\mu \text{ wavy line} \\
 \searrow \\
 \tilde{\chi}_j^\pm
 \end{array}
 = -igs_W \gamma_\mu \delta^{ij},
 \quad (\text{B.1d})$$

where with $\tilde{\chi}$ we denote a neutralino, with $\tilde{\chi}^\pm$ a chargino and N_{ij}, U_{ij}, V_{ij} are the matrix elements respectively of the matrices which diagonalize the neutralinos and the charginos mass matrices. Note that the indices i and j run from 1 to 4 for neutralinos, $\tilde{\chi}_i$, and from 1 to 2 for charginos, $\tilde{\chi}_i^\pm$.

For the interaction between the lightest neutralino quark and squark we have:

$$\begin{aligned}
 \begin{array}{c} u \\ \nearrow \\ \tilde{u}_1 \text{---} \\ \searrow \\ \tilde{\chi}_1 \end{array} &= i\sqrt{2} \left\{ - \left[\eta_{11}^u \left(\frac{Y_{u_L}}{2} g' N_{11} + g \frac{N_{12}}{2} \right) + \eta_{12}^u \frac{m_u g}{2m_W \sin \beta} N_{14} \right] P_L + \right. \\
 &\quad \left. \left(\eta_{12}^u e_u g' N_{11} - \eta_{11}^u \frac{m_u g}{2m_W \sin \beta} N_{14} \right) P_R \right\} \equiv i\sqrt{2} \{ -X_1 P_L + Y_1 P_R \} \\
 &\hspace{15em} \text{(B.2a)}
 \end{aligned}$$

$$\begin{aligned}
 \begin{array}{c} u \\ \nearrow \\ \tilde{u}_2 \text{---} \\ \searrow \\ \tilde{\chi}_1 \end{array} &= i\sqrt{2} \left\{ - \left[\eta_{21}^u \left(\frac{Y_{u_L}}{2} g' N_{11} + g \frac{N_{12}}{2} \right) + \eta_{22}^u \frac{m_u g}{2m_W \sin \beta} N_{14} \right] P_L + \right. \\
 &\quad \left. \left(\eta_{22}^u e_u g' N_{11} - \eta_{21}^u \frac{m_u g}{2m_W \sin \beta} N_{14} \right) P_R \right\} \equiv i\sqrt{2} \{ -U_1 P_L + V_1 P_R \} \\
 &\hspace{15em} \text{(B.2b)}
 \end{aligned}$$

$$\begin{aligned}
 \begin{array}{c} d \\ \nearrow \\ \tilde{d}_1 \text{---} \\ \searrow \\ \tilde{\chi}_1 \end{array} &= i\sqrt{2} \left\{ - \left[\eta_{11}^d \left(\frac{Y_{d_L}}{2} g' N_{11} - g \frac{N_{12}}{2} \right) + \eta_{12}^d \frac{m_d g}{2m_W \cos \beta} N_{13} \right] P_L + \right. \\
 &\quad \left. \left(\eta_{12}^d e_d g' N_{11} - \eta_{11}^d \frac{m_d g}{2m_W \cos \beta} N_{13} \right) P_R \right\} \equiv i\sqrt{2} \{ -X_2 P_L + Y_2 P_R \} \\
 &\hspace{15em} \text{(B.2c)}
 \end{aligned}$$

$$\begin{aligned}
 \begin{array}{c} d \\ \nearrow \\ \tilde{u}_2 \text{---} \\ \searrow \\ \tilde{\chi}_1 \end{array} &= i\sqrt{2} \left\{ - \left[\eta_{21}^d \left(\frac{Y_{d_L}}{2} g' N_{11} - g \frac{N_{12}}{2} \right) + \eta_{22}^d \frac{m_d g}{2m_W \cos \beta} N_{13} \right] P_L + \right. \\
 &\quad \left. \left(\eta_{22}^d e_d g' N_{11} - \eta_{21}^d \frac{m_d g}{2m_W \cos \beta} N_{13} \right) P_R \right\} \equiv i\sqrt{2} \{ -U_2 P_L + V_2 P_R \} \\
 &\hspace{15em} \text{(B.2d)}
 \end{aligned}$$

where we have redefined, consistently with ref [34], the quantities X_i, Y_i, U_i, V_i respectively as

$$X_i \equiv \left[\eta_{11}^i \left(\frac{Y_{i_L}}{2} g' N_{11} + (-1)^{i+1} g \frac{N_{12}}{2} \right) + \eta_{12}^i \frac{m_i g}{2m_W B_i} N_{1(5-i)} \right] \quad \text{(B.3)}$$

$$Y_i \equiv \eta_{12}^i e_i g' N_{11} - \eta_{11}^i \frac{m_i g}{2m_W B_i} N_{1(5-i)} \quad \text{(B.4)}$$

$$U_i \equiv \left[\eta_{21}^i \left(\frac{Y_{i_L}}{2} g' N_{11} + (-1)^{i+1} g \frac{N_{12}}{2} \right) + \eta_{22}^i \frac{m_i g}{2m_W B_i} N_{1(5-i)} \right] \quad \text{(B.5)}$$

$$V_i \equiv \eta_{22}^i e_i g' N_{11} - \eta_{21}^i \frac{m_i g}{2m_W B_i} N_{1(5-i)}. \quad \text{(B.6)}$$

The index i is $i = 1$ for up-type quarks or $i = 2$ for down-type quarks. The quantity B_i is $B_1 = \sin \beta$ while $B_2 = \cos \beta$ and η_{kl}^i are the matrix elements of the orthogonal matrices which diagonalize the square mass squark matrix. With Y_{i_L} we refer to the hypercharge of the l.h. quarks while with e_i to the quark electric charge.

For what concern the interaction between the the lightest neutralino and the neutral Higgs bosons we have

$$\begin{aligned}
 h \text{ --- } & \begin{array}{c} \tilde{\chi}_1 \\ \diagup \\ \text{---} \\ \diagdown \\ \tilde{\chi}_1 \end{array} &= -\frac{i}{2} [(N_{13} \sin \alpha + N_{14} \cos \alpha) (N_{11} g' - N_{12} g)] \equiv \alpha_{\tilde{\chi} \tilde{\chi} h} \\
 H \text{ --- } & \begin{array}{c} \tilde{\chi}_1 \\ \diagup \\ \text{---} \\ \diagdown \\ \tilde{\chi}_1 \end{array} &= \frac{i}{2} [(N_{13} \cos \alpha - N_{14} \sin \alpha) (N_{11} g' - N_{12} g)] \equiv \alpha_{\tilde{\chi} \tilde{\chi} H} \\
 A \text{ --- } & \begin{array}{c} \tilde{\chi}_1 \\ \diagup \\ \text{---} \\ \diagdown \\ \tilde{\chi}_1 \end{array} &= \frac{i}{2} \gamma^5 [(N_{13} \sin \beta - N_{14} \cos \beta) (N_{11} g' - N_{12} g)] \equiv \alpha_{\tilde{\chi} \tilde{\chi} A},
 \end{aligned}$$

while for the interaction between quarks and Higgs bosons we have

$$\begin{aligned}
 h \text{ --- } & \begin{array}{c} u \\ \diagup \\ \text{---} \\ \diagdown \\ u \end{array} &= -i \frac{g}{2} \frac{m_u \sin \alpha}{m_W \sin \beta} \equiv \alpha_{qqh}^{(1)}, & H \text{ --- } & \begin{array}{c} u \\ \diagup \\ \text{---} \\ \diagdown \\ u \end{array} &= -i \frac{g}{2} \frac{m_u \cos \alpha}{m_W \sin \beta} \equiv \alpha_{qqH}^{(1)} \\
 A \text{ --- } & \begin{array}{c} u \\ \diagup \\ \text{---} \\ \diagdown \\ u \end{array} &= -i \frac{g}{2} \gamma^5 \frac{m_u}{m_W} \cotan \beta \equiv \alpha_{qqA}^{(1)}, & h \text{ --- } & \begin{array}{c} d \\ \diagup \\ \text{---} \\ \diagdown \\ d \end{array} &= i \frac{g}{2} \frac{m_d \cos \alpha}{m_W \cos \beta} \equiv \alpha_{qqh}^{(2)} \\
 H \text{ --- } & \begin{array}{c} d \\ \diagup \\ \text{---} \\ \diagdown \\ d \end{array} &= -i \frac{g}{2} \frac{m_d \sin \alpha}{m_W \cos \beta} \equiv \alpha_{qqH}^{(2)}, & A \text{ --- } & \begin{array}{c} d \\ \diagup \\ \text{---} \\ \diagdown \\ d \end{array} &= i \frac{g}{2} \frac{m_d}{m_W} \tan \beta \equiv \alpha_{qqA}^{(2)}.
 \end{aligned}$$

As last we recall some useful SM Feynman rules. For the interaction between gauge bosons and

SM fermions

$$\begin{aligned}
 \begin{array}{c} f \\ \nearrow \\ \gamma_\mu \text{ wavy} \\ \searrow \\ f \end{array} &= -ig_e e_f \gamma_\mu, & \begin{array}{c} e \\ \nearrow \\ Z_\mu^0 \text{ wavy} \\ \searrow \\ e \end{array} &= i \frac{g}{2c_W} \gamma_\mu (P_L - 2s_W^2) \\
 \\
 \begin{array}{c} u \\ \nearrow \\ W_\mu^\pm \text{ wavy} \\ \searrow \\ d \end{array} &= -i \frac{g}{\sqrt{2}} \gamma_\mu P_L, & \begin{array}{c} e \\ \nearrow \\ W_\mu^\pm \text{ wavy} \\ \searrow \\ \nu \end{array} &= -i \frac{g}{\sqrt{2}} \gamma_\mu P_L, & \begin{array}{c} \nu \\ \nearrow \\ Z_\mu^0 \text{ wavy} \\ \searrow \\ \nu \end{array} &= -i \frac{g}{2c_W} \gamma_\mu P_L \\
 \\
 \begin{array}{c} d \\ \nearrow \\ Z_\mu^0 \text{ wavy} \\ \searrow \\ d \end{array} &= i \frac{g}{2c_W} \gamma_\mu \left(P_L - \frac{2}{3} s_W^2 \right) \equiv \gamma_\mu \left(v^{(2)} + \gamma^5 a^{(2)} \right) \\
 \\
 \begin{array}{c} u \\ \nearrow \\ Z_\mu^0 \text{ wavy} \\ \searrow \\ u \end{array} &= -i \frac{g}{2c_W} \gamma_\mu \left(P_L - \frac{4}{3} s_W^2 \right) \equiv \gamma_\mu \left(v^{(1)} + \gamma^5 a^{(1)} \right),
 \end{aligned}$$

where $f = u, d, e$ and with e_f we mean the electric charge of the fermion f . The quantities v^i and a^i are respectively defined as

$$v^i \equiv (-1)^i \frac{g}{2c_W} \left(\frac{1}{2} - 2e_i s_W^2 \right) \quad (\text{B.7})$$

$$a^i \equiv (-1)^{i+1} \frac{g}{4c_W} \gamma^5. \quad (\text{B.8})$$

The Feynman rules for the SM triple gauge interactions are

$$\begin{aligned}
 \begin{array}{c} W_\alpha^\pm \\ \nearrow \\ Z_\mu^0 \text{ wavy} \xrightarrow{q} \\ \searrow \\ W_\beta^\mp \\ \nearrow \\ k \end{array} &= ig c_W [g_{\alpha\beta} (k-p)_\mu + g_{\beta\mu} (q-k)_\alpha + g_{\mu\alpha} (p-q)_\beta] \\
 \\
 \begin{array}{c} W_\alpha^\pm \\ \nearrow \\ \gamma_\mu \text{ wavy} \xrightarrow{q} \\ \searrow \\ W_\beta^\mp \\ \nearrow \\ k \end{array} &= -ig s_W [g_{\alpha\beta} (k-p)_\mu + g_{\beta\mu} (q-k)_\alpha + g_{\mu\alpha} (p-q)_\beta]
 \end{aligned}$$

For what concern the propagators we have

$$\begin{aligned} \bullet \overset{p}{\rightsquigarrow} \bullet &= \frac{i}{p^2 - m^2} \left[-g_{\mu\nu} + \frac{p^\mu p^\nu}{m^2} \right] \\ \bullet \overset{p}{\longrightarrow} \bullet &= \frac{i}{p^2 - m^2} (\not{p} + m) \\ \bullet \overset{p}{\dashrightarrow} \bullet &= \frac{i}{p^2 - m^2} \end{aligned}$$

where with m we denote the mass of the exchange particle.

Appendix C

Matrix diagonalization

In this appendix we perform the diagonalization of the mass matrices for the Well-Tempered neutralino configurations. We start from the mass matrix for the \tilde{B}/\tilde{H} , given in Eq. (4.114)

$$M_{\tilde{B}/\tilde{H}} = \begin{pmatrix} M_1 & -(\mu - M_1)\theta_+ & (\mu + M_1)\theta_- \\ -(\mu - M_1)\theta_+ & \mu & 0 \\ (\mu + M_1)\theta_- & 0 & -\mu \end{pmatrix} + \mathcal{O}\left(\frac{m_W}{M_2}\right) \quad (\text{C.1})$$

where θ_{\pm} are defined in Eqs. (4.115). The characteristic polynomial of this matrix is

$$\mathcal{P}(\lambda) = -(M_1 - \lambda)(\mu^2 - \lambda^2) + \theta_+^2(\mu - M_1)^2(\mu + \lambda) - \theta_-^2(\mu + M_1)^2(\mu - \lambda). \quad (\text{C.2})$$

In the case of $\mu > 0$ from Eqs. (4.115) we see that $\theta_- \rightarrow 0$ so we can approximate the above characteristic polynomial as

$$\mathcal{P}(\lambda) = (\mu + \lambda) [(M_1 - \lambda)(\lambda - \mu) + \theta_+^2(\mu - M_1)^2] + \mathcal{O}(\theta_-^2) \quad (\text{C.3})$$

which give the three approximated eigenvalues

$$\lambda_1 = M_1 + \theta_+^2(M_1 - \mu) + \mathcal{O}(\theta_-^2, \theta_+^3) \quad (\text{C.4})$$

$$\lambda_2 = -\mu + \mathcal{O}(\theta_-^2, \theta_+^3) \quad (\text{C.5})$$

$$\lambda_3 = \mu - \theta_+^2(M_1 - \mu) + \mathcal{O}(\theta_-^2, \theta_+^3). \quad (\text{C.6})$$

In the case of $\mu < 0$ the situation is reverse, so from Eqs. (4.115) we have $\theta_+ \rightarrow 0$ and the characteristic polynomial in Eq. (C.2) can be approximated as

$$\mathcal{P}(\lambda) = (\mu - \lambda) [-(M_1 - \lambda)(\mu + \lambda) - \theta_-^2(\mu + M_1)^2] + \mathcal{O}(\theta_+^2) \quad (\text{C.7})$$

with zeros approximated by

$$\lambda_1 = M_1 + \theta_-^2(M_1 + \mu) + \mathcal{O}(\theta_+^2, \theta_-^3) \quad (\text{C.8})$$

$$\lambda_2 = \mu + \mathcal{O}(\theta_+^2, \theta_-^3) \quad (\text{C.9})$$

$$\lambda_3 = -\mu - \theta_-^2(M_1 + \mu) + \mathcal{O}(\theta_+^2, \theta_-^3). \quad (\text{C.10})$$

Resolving the relation $M_{\tilde{B}/\tilde{H}}v_i = \lambda_i v_i$ where v_i denotes an eigenvectors, we have that, up to corrections of order θ_{\pm}^3 , they are respectively given by

$$v_1 = \begin{pmatrix} \alpha_1 \\ \theta_+ \\ \theta_- \end{pmatrix}, \quad v_2 = \begin{pmatrix} -\theta_+ \\ \alpha_2 \\ -\frac{\mu+M_1}{2\mu}\theta_-\theta_+ \end{pmatrix}, \quad v_3 = \begin{pmatrix} -\theta_- \\ \frac{M_1-\mu}{2\mu}\theta_-\theta_+ \\ \alpha_3 \end{pmatrix}. \quad (\text{C.11})$$

The parameters $\alpha_1, \alpha_2, \alpha_3$ can be fixed requiring that the above vectors are normalized to one, obtaining that

$$v_1 = \begin{pmatrix} 1 - \frac{\theta_+^2}{2} - \frac{\theta_-^2}{2} \\ \theta_+ \\ \theta_- \end{pmatrix}, \quad v_2 = \begin{pmatrix} -\theta_+ \\ 1 - \frac{\theta_+^2}{2} \\ -\frac{\mu+M_1}{2\mu}\theta_-\theta_+ \end{pmatrix}, \quad v_3 = \begin{pmatrix} -\theta_- \\ \frac{M_1-\mu}{2\mu}\theta_-\theta_+ \\ 1 - \frac{\theta_-^2}{2} \end{pmatrix} \quad (\text{C.12})$$

Note that the above eigenvectors are equal both in the case $\mu > 0$ that $\mu < 0$. Using this eigenvectors we can find that the orthogonal matrix N which diagonalizes $M_{\tilde{B}/\tilde{H}}$, is

$$N = \begin{pmatrix} 1 - \frac{\theta_+^2}{2} - \frac{\theta_-^2}{2} & -\theta_+ & -\theta_- \\ \theta_+ & 1 - \frac{\theta_+^2}{2} & -\frac{\mu+M_1}{2\mu}\theta_-\theta_+ \\ \theta_- & \frac{M_1-\mu}{2\mu}\theta_-\theta_+ & 1 - \frac{\theta_-^2}{2} \end{pmatrix}. \quad (\text{C.13})$$

When θ_{\pm} are not moderate and in particular when is verified the relation $|\mu \pm M_1| \lesssim m_{Z^0}(s_{\beta} \mp c_{\beta})s_w/\sqrt{2}$, we cannot expand the characteristic polynomial and its zeros for $\theta_{\pm} \rightarrow 0$. In this situation the above results are not longer valid. However in this limit we can assume that M_1 is nearly equal to μ ($-\mu$), and so we can rewrite the matrix $M_{\tilde{B}/\tilde{H}}$ as

$$M_{\tilde{B}/\tilde{H}} = \begin{pmatrix} M_1 & -\frac{s_{\beta}+c_{\beta}}{\sqrt{2}}s_w m_{Z^0} & \frac{s_{\beta}-c_{\beta}}{\sqrt{2}}s_w m_{Z^0} \\ -\frac{s_{\beta}+c_{\beta}}{\sqrt{2}}s_w m_{Z^0} & \pm M_1 & 0 \\ \frac{s_{\beta}-c_{\beta}}{\sqrt{2}}s_w m_{Z^0} & 0 & \mp M_1 \end{pmatrix} \quad (\text{C.14})$$

where the upper signs are for $M_1 = \mu$ configuration, while the lower ones for the $M_1 = -\mu$ configuration. The associated characteristic polynomial is given by

$$\mathcal{P}(\lambda) = -(M_1 - \lambda)(M_1^2 - \lambda^2) + \left[\frac{s_{\beta} + c_{\beta}}{\sqrt{2}}s_w m_{Z^0} \right]^2 (M_1 + \lambda) - \left[\frac{s_{\beta} - c_{\beta}}{\sqrt{2}}s_w m_{Z^0} \right]^2 (M_1 - \lambda) \quad (\text{C.15})$$

Using the NewtonRaphson method we can find that the three eigenvalues are given by

$$\lambda_1 = M_1 - \frac{(s_{\beta} \pm c_{\beta})s_w m_{Z^0}}{\sqrt{2}} + (1 \mp s_{2\beta}) \frac{s_W^2 m_{Z^0}^2}{8M_1} + \mathcal{O}\left(\frac{m_{Z^0}^2}{M_1^2}\right) \quad (\text{C.16})$$

$$\lambda_2 = -M_1 - (1 \mp s_{2\beta}) \frac{s_W^2 m_{Z^0}^2}{4M_1} + \mathcal{O}\left(\frac{m_{Z^0}^2}{M_1^2}\right) \quad (\text{C.17})$$

$$\lambda_3 = M_1 + \frac{(s_{\beta} \pm c_{\beta})s_w m_{Z^0}}{\sqrt{2}} + (1 \mp s_{2\beta}) \frac{s_W^2 m_{Z^0}^2}{8M_1} + \mathcal{O}\left(\frac{m_{Z^0}^2}{M_1^2}\right). \quad (\text{C.18})$$

For what concern the \tilde{B}/\tilde{W} configuration the mass matrix is give in Eq. (4.136)

$$M_{\tilde{B}/\tilde{W}} = \begin{pmatrix} M_1 - M_1\theta\Delta t_W & M_1\theta\Delta \\ M_1\theta\Delta & M_2 - M_1\theta\Delta ct_W \end{pmatrix} + \mathcal{O}\left(\frac{m_{Z^0}^2}{\mu^2}\right) \quad (\text{C.19})$$

where Δ and θ are given in Eqs. (4.137). The associated characteristic polynomial is given by

$$\mathcal{P}(\lambda) = (M_1 - M_1\theta\Delta t_W - \lambda)(M_2 - M_1\theta\Delta ct_W - \lambda) - M_1^2\theta^2\Delta^2 \quad (\text{C.20})$$

which, at the second order in θ , gives the following eigenvalues

$$\lambda_1 = M_1 - (M_2 - M_1) [t_W\theta + \theta^2] + \mathcal{O}(\theta^3) \quad (\text{C.21})$$

$$= M_1 [1 - \Delta (t_W\theta + \theta^2)] + \mathcal{O}(\theta^3) \quad (\text{C.22})$$

$$\lambda_2 = M_2 - (M_2 - M_1) [ct_W\theta - \theta^2] + \mathcal{O}(\theta^3) \quad (\text{C.23})$$

$$= M_1 [1 + \Delta (1 - ct_W\theta + \theta^2)] + \mathcal{O}(\theta^3). \quad (\text{C.24})$$

The associated eigenvectors are equal to

$$v_1 = \begin{pmatrix} 1 - \frac{\theta^2}{2} \\ \theta + (t_W - ct_W)\theta^2 \end{pmatrix}, \quad v_2 = \begin{pmatrix} -\theta - (t_W - ct_W)\theta^2 \\ 1 - \frac{\theta^2}{2} \end{pmatrix}, \quad (\text{C.25})$$

thus the orthogonal matrix N which diagonalized the \tilde{B}/\tilde{W} mass matrix is

$$N = \begin{pmatrix} 1 - \frac{\theta^2}{2} & \theta + (t_W - ct_W)\theta^2 \\ -\theta - (t_W - ct_W)\theta^2 & 1 - \frac{\theta^2}{2} \end{pmatrix}. \quad (\text{C.26})$$

As occurred in the \tilde{B}/\tilde{H} case when the difference between M_1 and M_2 approaches zero the value of θ diverges and the above results, which are all obtained expanding in terms of $\theta \rightarrow 0$, are non longer valid. Thus when θ is not moderate the \tilde{B}/\tilde{W} mass matrix can be rewrite as

$$M_{\tilde{B}/\tilde{W}} = \begin{pmatrix} M_1 - s_W^2 s_{2\beta} \frac{m_{Z^0}^2}{\mu} & s_W c_W s_{2\beta} \frac{m_{Z^0}^2}{\mu} \\ s_W c_W s_{2\beta} \frac{m_{Z^0}^2}{\mu} & M_1 - c_W^2 s_{2\beta} \frac{m_{Z^0}^2}{\mu} \end{pmatrix} + \mathcal{O}\left(\frac{m_{Z^0}^2}{\mu^2}\right) \quad (\text{C.27})$$

where we have approximate M_2 with M_1 . Its characteristic polynomial is given by

$$\mathcal{P}(\lambda) = \lambda^2 + \lambda \left(s_{2\beta} \frac{m_{Z^0}^2}{\mu} - 2M_1 \right) + M_1 \left(M_1 - s_{2\beta} \frac{m_{Z^0}^2}{\mu} \right) \quad (\text{C.28})$$

which has the following zeros

$$\lambda_1 = M_1 + \mathcal{O}\left(\frac{m_{Z^0}^2}{\mu^2}\right) \quad (\text{C.29})$$

$$\lambda_2 = M_1 - \frac{m_{Z^0}^2 s_{2\beta}}{\mu} + \mathcal{O}\left(\frac{m_{Z^0}^2}{\mu^2}\right). \quad (\text{C.30})$$

Appendix D

In this appendix we evaluate the normalization constant k and the velocity integral given in Eq. (4.11). Then we review the principal steps that lead us to find the effective four-fermions Lagrangian, which suitably describes the neutralino-quark elastic scattering. After that we give the non-relativistic expansion of the scattering of the neutralino-nucleon amplitudes, which are useful in computing the associated scattering cross-sections. We always assume CP conservation neglecting terms which are not CP -invariant. We principally follow refs. [34], [27].

D.1 Velocity integral

The normalization condition of the velocity distribution function $f_G(\vec{v}_G)$ is

$$\int f_G(\vec{v}_G) d^3v = \frac{1}{k} \int e^{-(\vec{v}+\vec{v}_E)^2/v_0^2} \Theta(v_{\text{esc}} - v_G) d^3v = 1 \quad (\text{D.1})$$

where we have used the definition given in Eq. (4.10). Therefore the normalization constant would be equal to

$$\begin{aligned} k &= \frac{1}{k} \int v^2 e^{-(\vec{v}+\vec{v}_E)^2/v_0^2} \Theta(v_{\text{esc}} - v_G) dv d\Omega \\ &= 2\pi \int_0^{v_{\text{max}}} v^2 e^{-(v^2+v_E^2)/v_0^2} \int_{-1}^{c_{\text{max}}} e^{-2vv_E \cos \theta/v_0^2} d(\cos \theta) dv. \end{aligned} \quad (\text{D.2})$$

In order to find v_{max} and c_{max} we use the condition imposed by the $\Theta(x)$ which is that $v_G \leq v_{\text{esc}}$ where v_{esc} is the local escape velocity. In terms of \vec{v} and \vec{v}_E this condition reads as

$$(\vec{v} + \vec{v}_E)^2 \leq v_{\text{esc}}^2. \quad (\text{D.3})$$

Thus to find v_{max} we have to resolve the system

$$\begin{cases} v^2 + v_E^2 + 2vv_E \cos \theta \leq v_{\text{esc}}^2 \\ -1 \leq \cos \theta \leq 1 \end{cases} \quad (\text{D.4})$$

which can be recast as

$$\begin{cases} v_{\text{esc}}^2 - v^2 - v_E^2 \geq -2vv_E \\ v_{\text{esc}}^2 - v^2 - v_E^2 \leq 2vv_E \end{cases} \quad (\text{D.5})$$

Imposing that $v > 0$ the solutions of the above equations are

$$\begin{cases} v \leq v_{\text{esc}} + v_E \\ v \leq v_{\text{esc}} - v_E \end{cases} \quad (\text{D.6})$$

which imply that $v_{\text{max}} = v_{\text{esc}} + v_E$. In particular when $v \leq v_{\text{esc}} - v_E$ we have that $-1 \leq \cos \theta \leq 1$ always, and so $c_{\text{max}} = 1$. When $v_{\text{esc}} - v_E < v \leq v_{\text{esc}} + v_E$ we have that $-1 \leq \cos \theta \leq$

$(v_{\text{esc}}^2 - v^2 - v_{\text{E}}^2)/2vv_{\text{E}}$ and so $c_{\text{max}} = (v_{\text{esc}}^2 - v^2 - v_{\text{E}}^2)/2vv_{\text{E}}$. Therefore the integral in Eq. (D.2) becomes

$$\begin{aligned}
k &= 2\pi \left\{ \int_0^{v_{\text{esc}} - v_{\text{E}}} v^2 e^{-(v^2 + v_{\text{E}}^2)/v_0^2} \int_{-1}^1 e^{-2vv_{\text{E}} \cos \theta / v_0^2} d(\cos \theta) dv \right. \\
&\quad \left. + \int_{v_{\text{esc}} - v_{\text{E}}}^{v_{\text{esc}} + v_{\text{E}}} v^2 e^{-(v^2 + v_{\text{E}}^2)/v_0^2} \int_{-1}^{(v_{\text{esc}}^2 - v^2 - v_{\text{E}}^2)/2vv_{\text{E}}} e^{-2vv_{\text{E}} \cos \theta / v_0^2} d(\cos \theta) dv \right\} \\
&= \frac{\pi v_0^2}{v_{\text{E}}} \left\{ \int_0^{v_{\text{esc}} - v_{\text{E}}} v e^{-(v^2 + v_{\text{E}}^2)/v_0^2} \left[e^{2vv_{\text{E}}/v_0^2} - e^{-2vv_{\text{E}}/v_0^2} \right] dv \right. \\
&\quad \left. + \int_{v_{\text{esc}} - v_{\text{E}}}^{v_{\text{esc}} + v_{\text{E}}} v e^{-(v^2 + v_{\text{E}}^2)/v_0^2} \left[e^{2vv_{\text{E}}/v_0^2} - e^{-(v_{\text{esc}}^2 - v^2 - v_{\text{E}}^2)/v_0^2} \right] dv \right\}
\end{aligned} \tag{D.7}$$

where in the second equality we have performed the integral over $d(\cos \theta)$. After some manipulations the above result can be recast as

$$k = \frac{\pi v_0^2}{v_{\text{E}}} \left\{ \int_0^{v_{\text{esc}} + v_{\text{E}}} v e^{-(v - v_{\text{E}})^2 / v_0^2} dv - \int_0^{v_{\text{esc}} - v_{\text{E}}} v e^{-(v + v_{\text{E}})^2 / v_0^2} dv - e^{-v_{\text{esc}}^2 / v_0^2} \int_{v - v_{\text{E}}}^{v + v_{\text{E}}} v dv \right\}.$$

Now making the substitutions $(v - v_{\text{E}})/v_0 = y$ and $(v + v_{\text{E}})/v_0 = y$ respectively in the first and in the second integral, and computing the last integral we obtain

$$\begin{aligned}
k &= \frac{\pi v_0^2}{v_{\text{E}}} \left\{ v_0 \left[\int_{-v_{\text{E}}/v_0}^{v_{\text{esc}}/v_0} (v_0 y + v_{\text{E}}) e^{-y^2} dy - \int_{v_{\text{E}}/v_0}^{v_{\text{esc}}/v_0} (v_0 y + v_{\text{E}}) e^{-y^2} dy \right] - 2v_{\text{esc}} v_{\text{E}} e^{-v_{\text{esc}}^2 / v_0^2} \right\} \\
&= \frac{\pi v_0^2}{v_{\text{E}}} \left\{ v_0^2 \int_{-v_{\text{E}}/v_0}^{v_{\text{E}}/v_0} y e^{-y^2} dy + \int_0^{v_{\text{esc}}/v_0} e^{-y^2} dy - 2v_{\text{esc}} v_{\text{E}} e^{-v_{\text{esc}}^2 / v_0^2} \right\} \\
&= \frac{\pi v_0^2}{v_{\text{E}}} \left\{ \int_0^{v_{\text{esc}}/v_0} e^{-y^2} dy - 2v_{\text{esc}} v_{\text{E}} e^{-v_{\text{esc}}^2 / v_0^2} \right\}.
\end{aligned}$$

Recalling the definition of the error function [1]

$$\text{erf}(x) \equiv \frac{2}{\sqrt{\pi}} \int_0^x e^{-x^2} dx \tag{D.8}$$

we can rewrite k as

$$k = 2\pi v_0^2 \left[\frac{\sqrt{\pi}}{2} \text{erf}\left(\frac{v_{\text{esc}}}{v_0}\right) - \frac{v_{\text{esc}}}{v_0} e^{-v_{\text{esc}}^2 / v_0^2} \right]. \tag{D.9}$$

For what concern the velocity integral what we have to compute is

$$A(v_{\text{min}}, v_{\text{E}}, v_{\text{esc}}) = \int_{v \leq v_{\text{max}}} v e^{-(\vec{v} + \vec{v}_{\text{E}})^2 / v_0^2} dv d\Omega. \tag{D.10}$$

This integral is similar to the one given in Eq. (D.2), thus following the same steps made above we obtain that

$$\begin{aligned}
A(v_{\text{min}}, v_{\text{E}}, v_{\text{esc}}) &= 2\pi \left\{ \int_{v_{\text{min}}}^{v_{\text{esc}} - v_{\text{E}}} v e^{-(v^2 + v_{\text{E}}^2)/v_0^2} \int_{-1}^1 e^{-2vv_{\text{E}} \cos \theta / v_0^2} d(\cos \theta) dv \right. \\
&\quad \left. + \int_{v_{\text{esc}} - v_{\text{E}}}^{v_{\text{esc}} + v_{\text{E}}} v e^{-(v^2 + v_{\text{E}}^2)/v_0^2} \int_{-1}^{(v_{\text{esc}}^2 - v^2 - v_{\text{E}}^2)/2vv_{\text{E}}} e^{-2vv_{\text{E}} \cos \theta / v_0^2} d(\cos \theta) dv \right\} \\
&= \frac{\pi v_0^2}{v_{\text{E}}} \left\{ \int_{v_{\text{min}}}^{v_{\text{esc}} + v_{\text{E}}} e^{-(v - v_{\text{E}})^2 / v_0^2} dv - \int_{v_{\text{min}}}^{v_{\text{esc}} - v_{\text{E}}} e^{-(v + v_{\text{E}})^2 / v_0^2} dv \right. \\
&\quad \left. - e^{-v_{\text{esc}}^2 / v_0^2} \int_{v - v_{\text{E}}}^{v + v_{\text{E}}} v dv \right\}
\end{aligned} \tag{D.11}$$

where we have assumed that $v_{\min} < (v_{\text{esc}} - v_E)$. Now, as before, making the substitutions $(v - v_E)/v_0 = y$ and $(v + v_E)/v_0 = y$ in the first and in the second integral and performing the last one, we obtain

$$\begin{aligned} A(v_{\min}, v_E, v_{\text{esc}}) &= \frac{\pi v_0^2}{v_E} \left\{ v_0 \left[\int_{(v_{\min}-v_E)/v_0}^{v_{\text{esc}}/v_0} e^{-y^2} dy - \int_{(v_{\min}+v_E)/v_0}^{v_{\text{esc}}/v_0} e^{-y^2} dy \right] - 2v_E e^{-v_{\text{esc}}^2/v_0^2} \right\} \\ &= \frac{\pi v_0^2}{v_E} \left\{ v_0 \int_{(v_{\min}-v_E)/v_0}^{(v_{\min}+v_E)/v_0} e^{-y^2} dy - 2v_E e^{-v_{\text{esc}}^2/v_0^2} \right\} \\ &= \frac{\pi v_0^2}{v_E} \left\{ v_0 \left[\int_0^{(v_{\min}+v_E)/v_0} e^{-y^2} dy - \int_0^{(v_{\min}-v_E)/v_0} e^{-y^2} dy \right] - 2v_E e^{-v_{\text{esc}}^2/v_0^2} \right\}. \end{aligned}$$

Using the definition of the error function given in Eq. (D.8) the last result can be rewritten as

$$(D.12) \quad A(v_{\min}, v_E, v_{\text{esc}}) = \frac{\pi v_0^2}{v_E} \left[\frac{v_0 \sqrt{\pi}}{2} \left[\text{erf} \left(\frac{v_{\min} + v_E}{v_0} \right) - \text{erf} \left(\frac{v_{\min} - v_E}{v_0} \right) \right] - 2v_E e^{-v_{\text{esc}}^2/v_0^2} \right].$$

D.2 Effective Lagrangian for neutralino-quark interaction

As we said in Chapter 4 the tree-level scattering processes between neutralinos and quarks can be mediated by the Z^0 boson, the squarks \tilde{q} and the Higgs bosons h, H, A , where with h we refer to the SM Higgs, with H to the heavier neutral Higgs scalar and with A to the neutral pseudo-scalar Higgs boson. Therefore the relevant interaction terms from the MSSM Lagrangian are

$$\begin{aligned} \mathcal{L}_{\tilde{\chi}q} &= i\sqrt{2}\tilde{q}_{1i}\tilde{\chi}(-X_i P_L + Y_i P_R)q_i + i\sqrt{2}\tilde{q}_{2i}\tilde{\chi}(-U_i P_L + V_i P_R)q_i + \alpha_{\tilde{\chi}\tilde{Z}}\tilde{\chi}\gamma^\mu\gamma^5\tilde{\chi}Z_\mu^0 \\ &\quad + \tilde{q}_i\gamma^\mu(v^i + a^i\gamma^5)q_i Z_\mu^0 + \alpha_{qqh}^i\tilde{q}_i q_i h + \alpha_{qqH}^i\tilde{q}_i q_i H + \alpha_{\tilde{\chi}\tilde{h}}\tilde{\chi}\tilde{\chi}h \\ &\quad + \alpha_{\tilde{\chi}\tilde{H}}\tilde{\chi}\tilde{\chi}H + \alpha_{\tilde{\chi}\tilde{A}}\tilde{\chi}\gamma^5\tilde{\chi}A + \alpha_{qqA}^i\tilde{q}_i\gamma^5 q_i A + h.c. \end{aligned} \quad (D.13)$$

where the coefficients X_i, Y_i, a, v and the α 's are given in Appendix A and $i = 1$ denotes up-type quarks while $i = 2$ denotes down-type quarks. Note that we are considering the eigenvectors of the squark mass matrices given in Chapter 3 which are denoted respectively with the subscripts 1 and 2. With P_L and P_R we refer respectively to the left-handed (l.h.) and to the right-handed (r.h.) chirality projectors which are defined as [61]

$$P_L \equiv \frac{1 - \gamma^5}{2}, \quad P_R \equiv \frac{1 + \gamma^5}{2}. \quad (D.14)$$

This interaction terms lead to the following effective neutralino-quark interaction Lagrangian

$$\begin{aligned} \mathcal{L}_{\tilde{\chi}q}^{\text{eff}} &= -\frac{2}{m_{\tilde{q}_{1i}}^2 - m_{\tilde{\chi}}^2}\tilde{\chi}(-X_i P_L + Y_i P_R)q_i\tilde{q}_i(-X_i P_R + Y_i P_L)\chi \\ &\quad -\frac{2}{m_{\tilde{q}_{2i}}^2 - m_{\tilde{\chi}}^2}\tilde{\chi}(-U_i P_L + V_i P_R)q_i\tilde{q}_i(-U_i P_R + V_i P_L)\chi \\ &\quad + \frac{\alpha_{\tilde{\chi}\tilde{Z}}}{m_{Z^0}^2}\tilde{\chi}\gamma^\mu\gamma^5\tilde{\chi}\tilde{q}_i\gamma_\mu(v^i + a^i\gamma^5)q_i + \frac{\alpha_{qqh}^i\alpha_{\tilde{\chi}\tilde{h}}}{m_h^2}\tilde{\chi}\tilde{\chi}\tilde{q}_i q_i \\ &\quad + \frac{\alpha_{qqH}^i\alpha_{\tilde{\chi}\tilde{H}}}{m_H^2}\tilde{\chi}\tilde{\chi}\tilde{q}_i q_i + \frac{\alpha_{qqA}^i\alpha_{\tilde{\chi}\tilde{A}}}{m_A^2}\tilde{\chi}\gamma^5\tilde{\chi}\tilde{q}_i\gamma^5 q_i. \end{aligned} \quad (D.15)$$

Now we want to rewrite the first two terms in the form $\tilde{\chi}\Gamma\tilde{\chi}\tilde{q}_i\Gamma q_i$ where Γ denotes a generic combination of gamma matrices. To do this we start expliciting the l.h. and r.h. projectors, so

the first term read as

$$\begin{aligned}
& - \frac{X_i^2}{4(m_{\tilde{q}_i}^2 - m_{\tilde{\chi}}^2)} (\bar{\chi} q_i \bar{q}_i \chi - \bar{\chi} \gamma^5 q_i \bar{q}_i \gamma^5 \chi - \bar{\chi} \gamma^5 q_i \bar{q}_i \chi + \bar{\chi} q_i \bar{q}_i \gamma^5 \chi) + \\
& - \frac{Y_i^2}{4(m_{\tilde{q}_i}^2 - m_{\tilde{\chi}}^2)} (\bar{\chi} q_i \bar{q}_i \chi - \bar{\chi} \gamma^5 q_i \bar{q}_i \gamma^5 \chi - \bar{\chi} \gamma^5 q_i \bar{q}_i \chi + \bar{\chi} q_i \bar{q}_i \gamma^5 \chi) + \\
& + \frac{X_i Y_i}{(m_{\tilde{q}_i}^2 - m_{\tilde{\chi}}^2)} (\bar{\chi} q_i \bar{q}_i \chi + \bar{\chi} \gamma^5 q_i \bar{q}_i \gamma^5 \chi).
\end{aligned} \tag{D.16}$$

note that the same result holds for the second term in Eq. (D.15) with \tilde{q}_{2i}, U_i, V_i respectively in place of \tilde{q}_{1i}, X_i, Y_i . Using the Fierz transformations [59] the above result can be rewritten as

$$\begin{aligned}
& + \frac{X_i^2}{2(m_{\tilde{q}_i}^2 - m_{\tilde{\chi}}^2)} \left[\frac{1}{2} (\bar{\chi} \gamma^\mu \gamma^5 \tilde{\chi} \bar{q}_i \gamma_\mu \gamma^5 q_i + \bar{\chi} \gamma^\mu \tilde{\chi} \bar{q}_i \gamma_\mu q_i) + \right. \\
& \quad \left. + \frac{1}{4} (\bar{\chi} \sigma^{\mu\nu} \tilde{\chi} \bar{q}_i \sigma_{\mu\nu} \gamma^5 q_i - \bar{\chi} \sigma^{\mu\nu} \gamma^5 \tilde{\chi} \bar{q}_i \sigma_{\mu\nu} q_i) \right] + \\
& + \frac{Y_i^2}{2(m_{\tilde{q}_i}^2 - m_{\tilde{\chi}}^2)} \left[\frac{1}{2} (\bar{\chi} \gamma^\mu \gamma^5 \tilde{\chi} \bar{q}_i \gamma_\mu \gamma^5 q_i + \bar{\chi} \gamma^\mu \tilde{\chi} \bar{q}_i \gamma_\mu q_i) + \right. \\
& \quad \left. + \frac{1}{4} (-\bar{\chi} \sigma^{\mu\nu} \tilde{\chi} \bar{q}_i \sigma_{\mu\nu} \gamma^5 q_i + \bar{\chi} \sigma^{\mu\nu} \gamma^5 \tilde{\chi} \bar{q}_i \sigma_{\mu\nu} q_i) \right] + \\
& - \frac{X_i Y_i}{2(m_{\tilde{q}_i}^2 - m_{\tilde{\chi}}^2)} (\bar{\chi} \chi \bar{q}_i q_i + \bar{\chi} \sigma^{\mu\nu} \tilde{\chi} \bar{q}_i \sigma_{\mu\nu} q_i + \bar{\chi} \gamma^5 \tilde{\chi} \bar{q}_i \gamma^5 q_i).
\end{aligned} \tag{D.17}$$

Knowing that a Majorana fermion must satisfied

$$\tilde{\chi}_i = C \bar{\chi}_i^T \tag{D.18}$$

the following equalities hold

$$\bar{\chi}_i \gamma^\mu \tilde{\chi}_j = -\bar{\chi}_j \gamma^\mu \tilde{\chi}_i \tag{D.19}$$

$$\bar{\chi}_i \sigma^{\mu\nu} \tilde{\chi}_j = -\bar{\chi}_j \sigma^{\mu\nu} \tilde{\chi}_i \tag{D.20}$$

$$\bar{\chi}_i \sigma^{\mu\nu} \gamma^5 \tilde{\chi}_j = -\bar{\chi}_j \sigma^{\mu\nu} \gamma^5 \tilde{\chi}_i \tag{D.21}$$

$$\bar{\chi}_i \gamma^\mu \gamma^5 \tilde{\chi}_j = \bar{\chi}_j \gamma^\mu \gamma^5 \tilde{\chi}_i \tag{D.22}$$

$$\bar{\chi}_i \gamma^5 \tilde{\chi}_j = \bar{\chi}_j \gamma^5 \tilde{\chi}_i \tag{D.23}$$

$$\bar{\chi}_i \tilde{\chi}_j = \bar{\chi}_j \tilde{\chi}_i, \tag{D.24}$$

and in particular when $i = j$ we have

$$\bar{\chi} \gamma^\mu \tilde{\chi} = \bar{\chi} \sigma^{\mu\nu} \tilde{\chi} = \bar{\chi} \sigma^{\mu\nu} \gamma^5 \tilde{\chi} = 0. \tag{D.25}$$

Taking into account this some of the terms in Eq. (D.17) cancel leaving us with

$$+ \frac{X_i^2 + Y_i^2}{4(m_{\tilde{q}_i}^2 - m_{\tilde{\chi}}^2)} \bar{\chi} \gamma^\mu \gamma^5 \tilde{\chi} \bar{q}_i \gamma_\mu \gamma^5 q_i - \frac{X_i Y_i}{2(m_{\tilde{q}_i}^2 - m_{\tilde{\chi}}^2)} (\bar{\chi} \chi \bar{q}_i q_i + \bar{\chi} \gamma^5 \tilde{\chi} \bar{q}_i \gamma^5 q_i). \tag{D.26}$$

Using this result we can rewrite the effective Lagrangian given in Eq. (D.15) as

$$\mathcal{L}_{\tilde{\chi}q}^{\text{eff}} = \beta_{1i} \bar{\chi} \gamma^\mu \gamma^5 \tilde{\chi} \bar{q}_i \gamma_\mu \gamma^5 q_i + \beta_{2i} \bar{\chi} \chi \bar{q}_i q_i + \beta_{3i} \bar{\chi} \gamma^\mu \gamma^5 \tilde{\chi} \bar{q}_i \gamma_\mu q_i + \beta_{4i} \bar{\chi} \gamma^5 \tilde{\chi} \bar{q}_i \gamma^5 q_i \tag{D.27}$$

where the β 's are defined as

$$\begin{aligned}\beta_{1i} &\equiv +\frac{X_i^2 + Y_i^2}{4(m_{\tilde{q}_{1i}}^2 - m_{\tilde{\chi}}^2)} + \frac{U_i^2 + V_i^2}{4(m_{\tilde{q}_{2i}}^2 - m_{\tilde{\chi}}^2)} + \frac{\alpha_{\tilde{\chi}\tilde{\chi}Z} a^i}{m_{Z^0}^2} \\ \beta_{2i} &\equiv -\frac{X_i Y_i}{2(m_{\tilde{q}_{1i}}^2 - m_{\tilde{\chi}}^2)} - \frac{U_i V_i}{2(m_{\tilde{q}_{2i}}^2 - m_{\tilde{\chi}}^2)} + \frac{\alpha_{qqh}^i \alpha_{\tilde{\chi}\tilde{\chi}h}}{m_h^2} + \frac{\alpha_{qqH}^i \alpha_{\tilde{\chi}\tilde{\chi}H}}{m_H^2} \\ \beta_{3i} &\equiv \frac{\alpha_{\tilde{\chi}\tilde{\chi}Z} v^i}{m_{Z^0}^2} \\ \beta_{4i} &\equiv -\frac{X_i Y_i}{2(m_{\tilde{q}_{1i}}^2 - m_{\tilde{\chi}}^2)} - \frac{U_i V_i}{2(m_{\tilde{q}_{2i}}^2 - m_{\tilde{\chi}}^2)} + \frac{\alpha_{qQA}^i \alpha_{\tilde{\chi}\tilde{\chi}A}}{m_A^2}\end{aligned}$$

D.3 Non-relativistic expansion of scattering amplitudes

From the effective Lagrangian given in Eq. (D.27) we can read off four effective operators which describe the interaction between neutralinos and quarks. This effective operators induce an effective Lagrangian which describes the interaction between neutralinos and nucleons, in particular

$$\mathcal{L}_{\tilde{\chi}n}^{\text{eff}} = f_n \bar{\chi} \tilde{\chi} \bar{n} n + c_n \bar{\chi} \gamma^\mu \gamma^5 \tilde{\chi} \bar{n} \gamma_\mu \gamma^5 n + a_n \bar{\chi} \gamma^\mu \gamma^5 \tilde{\chi} \bar{n} \gamma_\mu n + b_n \bar{\chi} \gamma^5 \tilde{\chi} \bar{n} \gamma^5 n \quad (\text{D.28})$$

where the quantities c_n and f_n are given in Chapter 4. Because the scattering processes between DM and ordinary matter occur at low energies, we want to express the amplitudes of the various processes in the non-relativistic limit. To do this we start from the Dirac equation expressed in the momentum space

$$(\gamma^\mu p_\mu - m)u(p)^s = 0 \quad (\text{D.29})$$

where m is the mass of the particle (nucleon or neutralino) and $p_\mu \equiv (E, \vec{p})$ is its four momentum. The solution $u(p)^s$ can be expressed as [61]

$$u(p)^s = \begin{pmatrix} \sqrt{p^\mu \sigma_\mu} \xi^s \\ \sqrt{p^\mu \bar{\sigma}_\mu} \xi^s \end{pmatrix} \quad (\text{D.30})$$

where $\sigma_\mu \equiv (\mathbb{1}, \sigma_i)$, $\bar{\sigma}_\mu \equiv (\mathbb{1}, -\sigma_i)$ and with σ_i we denote the Pauli matrices. Taking into account that

$$(p^\mu \sigma_\mu)(p^\nu \bar{\sigma}_\nu) = m^2 \quad (\text{D.31})$$

we have that the quantity

$$(\sqrt{p^\mu \sigma_\mu} + \sqrt{p^\mu \bar{\sigma}_\mu})^2 = p^\mu \sigma_\mu + p^\mu \bar{\sigma}_\mu + 2m = 2(E + m) \quad (\text{D.32})$$

where we used the definitions of σ_μ and $\bar{\sigma}_\mu$. Using this result we can usefully re-express the spinor expression in Eq. (D.30) as

$$u(p)^s = \frac{\sqrt{p^\mu \sigma_\mu} + \sqrt{p^\mu \bar{\sigma}_\mu}}{\sqrt{p^\mu \sigma_\mu} + \sqrt{p^\mu \bar{\sigma}_\mu}} \begin{pmatrix} \sqrt{p^\mu \sigma_\mu} \xi^s \\ \sqrt{p^\mu \bar{\sigma}_\mu} \xi^s \end{pmatrix} = \frac{1}{\sqrt{2(E+m)}} \begin{pmatrix} (p^\mu \sigma_\mu + m) \xi^s \\ (p^\mu \bar{\sigma}_\mu + m) \xi^s \end{pmatrix}. \quad (\text{D.33})$$

Using this result and taking the non-relativistic limit, ($E \rightarrow m$) we obtain that

$$u(p)^s = \frac{1}{2\sqrt{m}} \begin{pmatrix} (2m - p^i \sigma_i) \xi^s \\ (2m + p^i \sigma_i) \xi^s \end{pmatrix} + \mathcal{O}\left(\frac{p^2}{m^2}\right) \quad (\text{D.34})$$

With this expression we can express the relevant spinor bilinears at the first order in the 3-momentum expansion, as

$$\begin{aligned}\bar{u}^s(p)u^s(p') &\simeq 2m\xi^{\dagger s}\xi^s \\ \bar{u}^s(p)\gamma^\mu\gamma^5u^s(p') &\simeq \begin{pmatrix} P^i\xi^{\dagger s}\sigma_i\xi^s \\ 2m\xi^{\dagger s}\sigma_i\xi^s \end{pmatrix} \simeq \begin{pmatrix} 2P^i s_i \\ 4m\vec{s} \end{pmatrix} \\ \bar{u}^s(p)\gamma^\mu u^s(p') &\simeq \begin{pmatrix} 2m \\ \vec{P} + \epsilon_{ijk}q^i\xi^{\dagger s}\sigma_j\xi^s \end{pmatrix} \simeq \begin{pmatrix} 2m \\ \vec{P} + 2\epsilon_{ijk}q^i s_j \end{pmatrix} \\ \bar{u}^s(p)\gamma^5u^s(p') &\simeq q^i\xi^{\dagger s}\sigma_i\xi^s \simeq 2q^i s_i\end{aligned}$$

where $P_i \equiv p'_i + p_i$, $q_i \equiv p'_i - p_i$ and we have redefined $s_i \equiv \xi^{\dagger s} \frac{\sigma_i}{2} \xi^s$.

Using the above non-relativistic expressions for Dirac bilinears we can see that the terms of the effective Langrangian in Eq. (D.28) give rise to amplitudes respectively equal to

$$\langle \tilde{\chi}, n | \bar{\tilde{\chi}} \tilde{\chi} \bar{n} n | \tilde{\chi}, n \rangle \simeq 4m_{\tilde{\chi}} m_n \quad (\text{D.35})$$

$$\langle \tilde{\chi}, n | \bar{\tilde{\chi}} \gamma^\mu \gamma^5 \tilde{\chi} \bar{n} \gamma_\mu \gamma^5 n | \tilde{\chi}, n \rangle \simeq -16m_{\tilde{\chi}} m_n \vec{s}_{\tilde{\chi}} \cdot \vec{s}_n \quad (\text{D.36})$$

$$\begin{aligned} \langle \tilde{\chi}, n | \bar{\tilde{\chi}} \gamma^\mu \gamma^5 \tilde{\chi} \bar{n} \gamma_\mu n | \tilde{\chi}, n \rangle &\simeq 8m_{\tilde{\chi}} \left[m_n \left(\frac{\vec{P}_{\tilde{\chi}}}{m_{\tilde{\chi}}} - \frac{\vec{P}_n}{m_n} \right) \cdot \vec{s}_{\tilde{\chi}} + i (\vec{s}_n \times \vec{q}) \cdot \vec{s}_{\tilde{\chi}} \right] \\ &\simeq 8m_{\tilde{\chi}} \left[m_n \left(2\vec{v} - \frac{\vec{q}}{\mu_n} \right) \cdot \vec{s}_{\tilde{\chi}} + i (\vec{s}_n \times \vec{q}) \cdot \vec{s}_{\tilde{\chi}} \right] \end{aligned} \quad (\text{D.37})$$

$$\langle \tilde{\chi}, n | \bar{\tilde{\chi}} \gamma^5 \tilde{\chi} \bar{n} \gamma^5 n | \tilde{\chi}, n \rangle \simeq 4 (\vec{q} \cdot \vec{s}_{\tilde{\chi}}) (\vec{q} \cdot \vec{s}_n). \quad (\text{D.38})$$

In the third line we have used the fact that

$$\vec{P}_{\tilde{\chi}} = 2\vec{p}_{\tilde{\chi}} - \vec{q} \quad (\text{D.39})$$

$$\vec{P}_n = 2\vec{p}_n - \vec{q} \quad (\text{D.40})$$

which implies that

$$\frac{\vec{P}_{\tilde{\chi}}}{m_{\tilde{\chi}}} - \frac{\vec{P}_n}{m_n} = 2\vec{v} - \frac{\vec{q}}{\mu_n} \quad (\text{D.41})$$

where $\vec{v} \equiv \vec{v}_{\tilde{\chi}} - \vec{v}_n$ is the relative velocity between the incoming particles, and $\mu_n = m_{\tilde{\chi}} m_n / (m_{\tilde{\chi}} + m_n)$ is the reduced mass. Note that the quantities \vec{v} , \vec{q} and the spins $\vec{s}_{\tilde{\chi}}$ and \vec{s}_n are all invariant under Galilean velocity transformations [27].

Because we are interested in processes at zero momentum transferred and which occur at small relative velocities we can neglect the last two amplitudes of the above list, because they depend on \vec{v} and on \vec{q} . Note that this is equivalent to neglect the last two terms in the Langrangians given in Eq. (D.28) and in Eq. (D.27). As a consequence the relevant effective four fermion Langrangian which we take into account when we analyse neutralino-quarks scattering processes will be

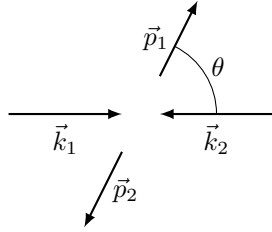
$$\mathcal{L}_{\tilde{\chi}q}^{\text{eff}} = \beta_{1i} \bar{\tilde{\chi}} \gamma^\mu \gamma^5 \tilde{\chi} \bar{q}_i \gamma_\mu \gamma^5 q_i + \beta_{2i} \bar{\tilde{\chi}} \tilde{\chi} \bar{q}_i q_i. \quad (\text{D.42})$$

Appendix E

In this appendix we perform the calculation of the neutralinos annihilation/co-annihilation cross-sections. We start summarizing the kinematical invariants and their expansion in terms of the total kinetic energy per unit of mass ϵ , which will be useful in the non relativistic expansion of the cross-sections. After that we explain our convention and Feynman rules for Majorana fermions. In the last part of this appendix we compute the neutralino annihilation/co-annihilation cross-sections.

E.1 Kinematical quantities

In the next we will refer to $2 \rightarrow 2$ annihilation processes calculated in the center of mass frame,



where k_1, k_2 are the four-momentum vectors of the initial particles and p_1, p_2 are the four-momentum vectors for final particles.

Choosing the z axes in the direction of the outgoing particles and the x axes perpendicular to it the various four-momentum vectors are defined as

$$k_1^\mu \equiv \begin{pmatrix} E_1 \\ |\vec{k}_1| \sin \theta \\ 0 \\ |\vec{k}_1| \cos \theta \end{pmatrix}, \quad k_2^\mu \equiv \begin{pmatrix} E_2 \\ -|\vec{k}_1| \sin \theta \\ 0 \\ -|\vec{k}_1| \cos \theta \end{pmatrix}, \quad p_1^\mu \equiv \begin{pmatrix} E'_1 \\ 0 \\ 0 \\ |\vec{p}_1| \end{pmatrix}, \quad p_2^\mu \equiv \begin{pmatrix} E'_2 \\ 0 \\ 0 \\ -|\vec{p}_1| \end{pmatrix} \quad (\text{E.1})$$

remember that in the center-of-mass (CoM) frame we have that $\vec{p}_1 = -\vec{p}_2$ and $\vec{k}_1 = -\vec{k}_2$, and θ is the angle between \vec{k}_1 and \vec{p}_1 in the CoM frame.

Because the processes in which we are interested involve also massive vector bosons we give the expressions of the polarization vectors. The two transverse polarizations, in the chosen frame, can be expressed as [61]

$$\epsilon_\mu^+ \equiv \frac{1}{\sqrt{2}} \begin{pmatrix} 0 \\ 1 \\ i \\ 0 \end{pmatrix}, \quad \epsilon_\mu^- \equiv \frac{1}{\sqrt{2}} \begin{pmatrix} 0 \\ 1 \\ -i \\ 0 \end{pmatrix}, \quad (\text{E.2})$$

where the upper-scripts $+$ and $-$ means respectively right-handed and left-handed. For massive

vector bosons there is also the longitudinal polarization, which can be defined as [61]

$$\epsilon_\mu^L \equiv \frac{1}{m_V} \begin{pmatrix} |\vec{p}| \\ 0 \\ 0 \\ E \end{pmatrix}, \quad (\text{E.3})$$

where \vec{p} , E and m_V are respectively the three-momentum vector the energy and the mass of the vector boson. In the limit where $E \gg m_V$ we have that the longitudinal polarization vector can be approximated as [61]

$$\epsilon_\mu^L \simeq \frac{p_\mu}{m_V} + \mathcal{O}\left(\frac{m_V^2}{E}\right) \quad (\text{E.4})$$

Note that for the transverse polarization vectors given in Eqs. (E.2) the following relations hold

$$\epsilon^+ \cdot \epsilon^+ = \epsilon^- \cdot \epsilon^- = \epsilon^+ \cdot (\epsilon^-)^* = 0 \quad (\text{E.5a})$$

$$\epsilon^+ \cdot \epsilon^- = \epsilon^+ \cdot (\epsilon^+)^* = \epsilon^- \cdot (\epsilon^-)^* = -1, \quad (\text{E.5b})$$

where as usual the (\cdot) means the Lorentz scalar product.

Now we go further recalling the Mandelstam variables [61]

$$s \equiv (k_1 + k_2)^2 = (p_1 + p_2)^2 \quad (\text{E.6a})$$

$$t \equiv (k_1 - p_1)^2 = (k_2 - p_2)^2 \quad (\text{E.6b})$$

$$u \equiv (k_2 - p_1)^2 = (k_1 - p_2)^2. \quad (\text{E.6c})$$

Considering the identity

$$s + t + u = \sum_i (m_i^2 + M_i^2), \quad (\text{E.7})$$

where m_i is the mass of the final i -particle and M_i is the mass of the initial i -particle, we can rewrite Eq. (E.6b) and Eq. (E.6c) as

$$t = \frac{1}{2} \left(\sum_i (m_i^2 + M_i^2) - s + (t - u) \right) \quad (\text{E.8a})$$

$$u = \frac{1}{2} \left(\sum_i (m_i^2 + M_i^2) - s - (t - u) \right). \quad (\text{E.8b})$$

The quantity $(t - u)$ is equal to

$$t - u = -\frac{(M_1^2 - M_2^2)(m_1^2 - m_2^2)}{s} + |\vec{k}_1| |\vec{p}_1| \cos \theta \quad (\text{E.9})$$

where $|\vec{k}_1|$ and $|\vec{p}_1|$ are the magnitude of the three-momentum in the CoM frame, which are given by

$$|\vec{k}_1| = \frac{\sqrt{(s - (M_1 + M_2)^2)(s - (M_1 - M_2)^2)}}{2\sqrt{s}} \quad (\text{E.10a})$$

$$|\vec{p}_1| = \frac{\sqrt{(s - (m_1 + m_2)^2)(s - (m_1 - m_2)^2)}}{2\sqrt{s}}. \quad (\text{E.10b})$$

Now thanks to the relations given in Eqs. (E.9), Eq. (E.10a) and Eq. (E.10b) we can rewrite the Mandelstam variables t and u as functions of s and θ .

Now, since our computation of the annihilation cross-sections will be performed in the non-relativistic limit, we are more interested in the non-relativistic expansion of s , t , and u variables in terms of the total kinetic energy per unit of mass, ϵ , given in Eq. (A.25), or, equivalently, in terms of the relative velocity of incoming particles, v . Assuming equal masses for the colliding

particles ($M_1 = M_2 \equiv M$) and the limit of massless final particles ($m_1 = m_2 = 0$), the expansions in terms of ϵ of the Mandelstam variables [E.6a](#), [E.6b](#) and [E.6c](#) are

$$s \simeq 4M^2(1 + \epsilon) + \mathcal{O}(\epsilon^2) \quad (\text{E.11a})$$

$$t \simeq -M^2(1 + 2\epsilon - 2\sqrt{\epsilon} \cos \theta_{\text{CM}}) + \mathcal{O}(\epsilon^2) \quad (\text{E.11b})$$

$$u \simeq -M^2(1 + 2\epsilon + 2\sqrt{\epsilon} \cos \theta_{\text{CM}}) + \mathcal{O}(\epsilon^2). \quad (\text{E.11c})$$

To finish this section we recall the cross-section formula [\[61\]](#)

$$\sigma = \frac{1}{64\pi^2} \frac{|\vec{p}_1|}{s|\vec{k}_1|} \int |\overline{\mathcal{M}}|^2 d\Omega \quad (\text{E.12})$$

with $|\vec{p}_1|$ and $|\vec{k}_1|$ given by [Eqs. \(E.10\)](#).

Since in the relic density formula enters $\langle \sigma v \rangle$, namely the thermal average of the cross-section times velocity, another important formula is

$$\sigma v = \frac{|\vec{k}_1| \sqrt{s}}{E_1 E_2} \sigma = \frac{|\vec{p}_1|}{(E_1 E_2) 64\pi^2 \sqrt{s}} \int |\overline{\mathcal{M}}|^2 d\Omega \quad (\text{E.13})$$

where E_1 and E_2 are the energies of the colliding particles; In the laboratory frame of particle 1 and in the limit ($M_1 = M_2 \equiv M$) and ($m_1 = m_2 = 0$) [Eq. \(E.13\)](#) becomes

$$\sigma v = \frac{1}{128M^2(2\epsilon + 1)\pi^2} \int |\overline{\mathcal{M}}|^2 d\Omega \quad (\text{E.14})$$

where we have used the explicit expression of ϵ in the laboratory frame given in [Eq. \(A.25\)](#).

As last we give some useful formulae for the computation of the trace of gamma matrices [\[61\]](#)

$$\text{Tr} \{ \gamma^\mu \gamma^\nu \} = 4g^{\mu\nu} \quad (\text{E.15a})$$

$$\text{Tr} \{ \gamma^\mu \gamma^\nu \gamma^\alpha \gamma^\beta \} = 4(g^{\mu\nu} g^{\alpha\beta} - g^{\mu\alpha} g^{\nu\beta} + g^{\mu\beta} g^{\nu\alpha}) \quad (\text{E.15b})$$

$$\text{Tr} \{ \gamma^\mu \gamma^\nu \gamma^\alpha \gamma^\beta \gamma^5 \} = -4i\epsilon^{\mu\nu\alpha\beta} \quad (\text{E.15c})$$

where $\epsilon^{\mu\nu\alpha\beta}$ is the total anti-symmetric tensor.

E.2 Majorana fermions and Feynman rules

When we compute annihilation cross-sections in supersymmetry we have often to deal with neutralinos, which are Majorana particles. For this reason we dedicate this paragraph to list a useful set of Feynman rules involving Majorana fermions. We start recalling some proprieties of the charge conjugation matrix

(i) $C^\dagger = C^{-1}$,

(ii) $C^T = -C$,

(iii) With $\Gamma_i = \mathbb{1}, i\gamma^5, \gamma^\mu \gamma^5, \sigma^{\mu\nu}$ we have $C^\dagger \Gamma_i C = \eta_i \Gamma_i^T$,

where $\eta_i = +1$ for the first six $\Gamma_i = \mathbb{1}, i\gamma^5, \gamma^\mu \gamma^5$ and $\eta_i = -1$ for the last ten $\Gamma_i = \gamma^\mu, \sigma^{\mu\nu}$. The operation of charge conjugation of a generic fermion field is defined as

$$\psi^c = C\overline{\psi}^T, \quad \overline{\psi^c} = -\psi^T C^\dagger \quad (\text{E.16})$$

where ψ^c means charge conjugated field and $\overline{\psi} \equiv \psi^\dagger \gamma^0$. In particular a Majorana field satisfied

$$\psi_M^c = C\overline{\psi}_M^T = \psi_M, \quad \overline{\psi^c}_M = -\psi_M^T C^\dagger = \overline{\psi}_M. \quad (\text{E.17})$$

The most important consequence of the Eq. (E.17) is the fact that a Majorana field cannot be invariant under any $U(1)$, global or local, symmetry. In particular this implies that a Majorana fermion cannot carry any conserved additive quantum number, such as the electric charge or the fermion number. Thus any interaction that involves both Majorana and Dirac fermions violates the conservation of the fermion quantum number, and so we cannot use the ordinary Feynman rules. What we need is a more extended set of rules that takes into account the fact that a Majorana fermion cannot be associated with any fermion number flow. We will denote a Majorana fermion with a solid line without any arrow and a Dirac fermion with a solid line with an arrow, which indicates the flow of the conserved fermionic number. For the Feynman rules involving Majorana fermion we follow reference [30], which gives the following rules for the vertices,

$$\begin{aligned}
 i\Gamma_{ab} &= \text{wavy line} \begin{cases} \nearrow \psi_a^M \\ \searrow \psi_b^M \end{cases} &
 i\Gamma_{ab} &= \text{wavy line} \begin{cases} \nearrow \psi_a^M \\ \searrow \psi_b^M \end{cases} &
 i\Gamma_{ab} &= \text{wavy line} \begin{cases} \nearrow \psi_a \\ \searrow \psi_b \end{cases} &
 i\Gamma'_{ab} &= \text{wavy line} \begin{cases} \nearrow \psi_a \\ \searrow \psi_b \end{cases} \\
 i\Gamma_{ab} &= \text{wavy line} \begin{cases} \nearrow \psi_a \\ \searrow \psi_b^M \end{cases} &
 i\Gamma_{ab} &= \text{wavy line} \begin{cases} \nearrow \psi_a^M \\ \searrow \psi_b \end{cases} &
 i\Gamma'_{ab} &= \text{wavy line} \begin{cases} \nearrow \psi_a \\ \searrow \psi_b^M \end{cases} &
 i\Gamma'_{ab} &= \text{wavy line} \begin{cases} \nearrow \psi_a^M \\ \searrow \psi_b \end{cases}
 \end{aligned} \tag{E.18}$$

where $\Gamma' = C\Gamma^T C^\dagger$ and the thin arrows indicate the verse of the fermionic flow. The Feynman rules for propagators are

$$\begin{aligned}
 \text{---} \xrightarrow{\text{thin arrow}} \text{---} &= iS(q) \\
 \text{---} \xleftarrow{\text{thin arrow}} \text{---} &= iS(-q) \\
 \text{---} \xrightarrow{\text{thin arrow}} \text{---} &= iS(q)
 \end{aligned} \tag{E.19}$$

with $S(q) = \frac{1}{q-m}$, m the fermion mass, and we take the momentum flow from left to right. The Feynman rules for external fermion legs are

$$\begin{aligned}
 \text{---} \xrightarrow{\text{thin arrow}} \bullet & \quad \text{---} \xrightarrow{\text{thin arrow}} \bullet & \quad \text{---} \xrightarrow{\text{thin arrow}} \bullet & \quad \bar{u}(p, s) \\
 \text{---} \xleftarrow{\text{thin arrow}} \bullet & \quad \text{---} \xleftarrow{\text{thin arrow}} \bullet & \quad \text{---} \xleftarrow{\text{thin arrow}} \bullet & \quad v(p, s) \\
 \text{---} \xrightarrow{\text{thin arrow}} \bullet & \quad \text{---} \xrightarrow{\text{thin arrow}} \bullet & \quad \text{---} \xrightarrow{\text{thin arrow}} \bullet & \quad u(p, s) \\
 \text{---} \xleftarrow{\text{thin arrow}} \bullet & \quad \text{---} \xleftarrow{\text{thin arrow}} \bullet & \quad \text{---} \xleftarrow{\text{thin arrow}} \bullet & \quad \bar{v}(p, s)
 \end{aligned} \tag{E.20}$$

where like before the momentum flow is from left to right.

The idea is to follow a fermionic flow (the thin arrow), which corresponds to an orientation of the complete fermions chain, formed by Dirac and/or Majorana fermions, instead to follow the fermionic number flow (the arrows over Dirac fermions). The choice of the orientation, of the fermionic flow, is totally arbitrary and a matter of convenience.

Following [30] we can summarize the Feynman rules as:

- Draw all independent Feynman diagrams that contribute to a given process.
- Fix a fermion flow for each fermionic chain (the choice of the direction of the flow is arbitrary).

- Write down Dirac matrices and the appropriate spinors following in the opposite direction the chosen fermion flow.
- For each fermion line, propagator and vertices use the analytic expressions given in E.18, E.19 and E.20.
- To find any relative signs between different Feynman diagrams, multiply by (-1) every odd permutation of the spinors with respect to an already fixed reference order.

As last when we have to compute cross-sections or decay rates we usually average and sum over initial and final spin state of the fermions involved in the interaction. To do this we use the familiar spins sum formulas [61]

$$\sum_s u(p, s)\bar{u}(p, s) = (\not{p} + m) \quad (\text{E.21a})$$

$$\sum_s v(p, s)\bar{v}(p, s) = (\not{p} - m) \quad (\text{E.21b})$$

where m is the fermion mass. However when we have to deal with Majorana fermions Eqs. (E.21) are not enough. Using the relations

$$u(p, s) = C\bar{v}(p, s)^T \quad (\text{E.22a})$$

$$v(p, s) = C\bar{u}(p, s)^T \quad (\text{E.22b})$$

which are valid for every spinor that satisfied the Dirac equations, $(\not{p} - m)u(p, s) = 0$ and $(\not{p} + m)v(p, s) = 0$, we can obtain other spins sum formulas that will be useful in processes which involve Majorana fermions

$$\sum_s u(p, s)v^T(p, s) = (\not{p} + m)(-C) \quad (\text{E.23a})$$

$$\sum_s \bar{u}^T(p, s)\bar{v}(p, s) = C^\dagger(\not{p} - m) \quad (\text{E.23b})$$

$$\sum_s \bar{v}^T(p, s)\bar{u}(p, s) = C^\dagger(\not{p} + m) \quad (\text{E.23c})$$

$$\sum_s v(p, s)u^T(p, s) = (\not{p} - m)(-C). \quad (\text{E.23d})$$

E.3 Pure Bino LSP annihilation cross-section

Here we compute the tree-level annihilation cross-section times velocity which is important in the evaluation of the relic abundance provided by a pure Bino LSP, without co-annihilations.

As we said in Chapter 3 the Bino, \tilde{B} , is the fermionic superpartner of the B SM gauge boson. It is a gauge singlet whose annihilation into a pair of fermion and anti-fermion occurs through sfermion exchange, in u/t -channel, $\tilde{B}\tilde{B} \xrightarrow{\tilde{f}} \bar{f}f$, where \tilde{f} denotes a sfermion. The associated interaction terms in the supersymmetric lagrangian are given by

$$\mathcal{L}_{\tilde{B}\tilde{f}f} = -g'\tilde{f}_R\bar{f}_R\tilde{B}\frac{Y_{f_R}}{\sqrt{2}} - g'\tilde{f}_L\bar{f}_L\tilde{B}\frac{Y_{f_L}}{\sqrt{2}} + h.c. \quad (\text{E.24})$$

where g' is the $U(1)_Y$ coupling constant and Y_{f_R} and Y_{f_L} are respectively the right-handed and left-handed fermion hypercharges, defined by

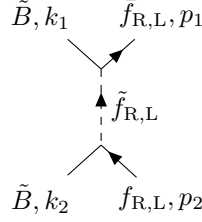
$$\frac{Y_{f_{R,L}}}{2} \equiv \tau_{f_L}^3 - Q_{f_{R,L}}, \quad (\text{E.25})$$

where $\tau_{f_L}^3$ denote the component of the $SU(2)_L$ diagonal generator associated to the fermion f_L , and $Q_{f_{R,L}}$ denote the electric charge of the fermion $f_{L,R}$. The associated Feynman rule for

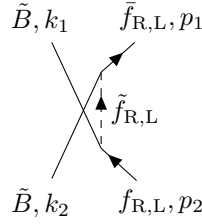
the vertex in Eq. (E.24) is

$$\begin{array}{c} \tilde{f}_{R,L} \\ \nearrow \\ \tilde{B} \text{---} \\ \searrow \\ f_{R,L} \end{array} = ig' \frac{Y_{f_{R,L}}}{\sqrt{2}} = ig \tan \theta_W \frac{Y_{f_{R,L}}}{\sqrt{2}}. \quad (\text{E.26})$$

The relevant Feynman diagrams for the annihilation process $\tilde{B}\tilde{B} \xrightarrow{\tilde{f}} \bar{f}f$ are the t -channel diagram



and, because the two annihilating particles are equals, there is also the u -channel diagram obtained exchanging the two initial particles



Following the rules given in Eqs. (E.18), Eqs. (E.19) and Eqs. (E.20), the amplitude of the t -channel diagram is equal to

$$i\mathcal{M}_t = \frac{g^2 \tan^2 \theta_W Y_{\tilde{f}_{L,R}}^2}{2(t - m_{\tilde{f}_{L,R}}^2)} \bar{u}_f(p_1, r_1) P_{L,R} u_{\tilde{B}}(k_1, s_1) \bar{v}_{\tilde{B}}(k_2, s_2) P_{R,L} v_f(p_2, r_2) \quad (\text{E.27})$$

where the k_i and s_i denotes respectively the four momentum and the spin of the incoming Bino particles while the p_i and r_i denotes the four momentum and the spin of the outgoing fermion and anti-fermion particles; with $m_{\tilde{f}_{L,R}}$ we denote the mass of the exchange sfermion. The u -channel has an amplitude given by

$$i\mathcal{M}_u = -\frac{g^2 \tan^2 \theta_W Y_{\tilde{f}_{L,R}}^2}{2(u - m_{\tilde{f}_{L,R}}^2)} \bar{u}_f(p_1, r_1) P_{L,R} u_{\tilde{B}}(k_2, s_2) \bar{v}_{\tilde{B}}(k_1, s_1) P_{R,L} v_f(p_2, r_2) \quad (\text{E.28})$$

note the appearance of the minus sign in front of the amplitude for the u -channel diagram due to the fact that we have exchange the two initial fermions. The total amplitude is given by

$$i\mathcal{M}_{\tilde{B}\tilde{B}} = i\mathcal{M}_t + i\mathcal{M}_u. \quad (\text{E.29})$$

Now in order to find the cross-section of the process, we have to square the total amplitude and then to average over initial spins, s_i , and sum over final ones, namely ones, r_i

$$\overline{|\mathcal{M}_{\tilde{B}\tilde{B}}|^2} \equiv \frac{1}{4} \sum_{s_i, r_i} |\mathcal{M}_{\tilde{B}\tilde{B}}|^2 = \frac{1}{4} \sum_{s_i, r_i} |\mathcal{M}_t|^2 + |\mathcal{M}_u|^2 - 2 \text{Re} [\mathcal{M}_u \mathcal{M}_t^\dagger] \quad (\text{E.30})$$

where we have explicitated the relative minus sign in front of the interference term.

We perform the computation assuming massless final state, $m_f = 0$. In this limit the first term of the sum Eq. (E.30) is

$$\begin{aligned}
\sum_{s_i, r_i} |\mathcal{M}_t|^2 &= \frac{g^4 \tan^4 \theta_W Y_{f_{L,R}}^4}{4(t - m_{\tilde{f}_{L,R}}^2)^2} \text{Tr}\{\not{p}_1 P_{L,R}(k_1 + M_{\tilde{B}}) P_{R,L}\} \times \\
&\quad \text{Tr}\{\not{p}_2 P_{L,R}(k_2 - M_{\tilde{B}}) P_{R,L}\} \\
&= \frac{g^4 \tan^4 \theta_W Y_{f_{L,R}}^4}{4(t - m_{\tilde{f}_{L,R}}^2)^2} [4(p_1 k_1)(p_2 k_2)] \\
&= g^4 \tan^4 \theta_W Y_{f_{L,R}}^4 \frac{(t - M_{\tilde{B}}^2)^2}{4(t - m_{\tilde{f}_{L,R}}^2)^2}
\end{aligned} \tag{E.31}$$

where $M_{\tilde{B}}$ is the Bino mass parameter. The second term of the sum in Eq. (E.30) is equal to the t -channel result given in Eq. (E.31), with the variable t replaced by the variable u , thus we have

$$\sum_{s_i, r_i} |\mathcal{M}_u|^2 = g^4 \tan^4 \theta_W Y_{f_{L,R}}^4 \frac{(u - M_{\tilde{B}}^2)^2}{4(u - m_{\tilde{f}_{L,R}}^2)^2} \tag{E.32}$$

For what concern the interference term, $\mathcal{M}_u \mathcal{M}_t^\dagger$, we have that

$$\begin{aligned}
\sum_{s_i, r_i} \mathcal{M}_u \mathcal{M}_t^\dagger &= \sum_{s_i, r_i} \frac{g^4 \tan^4 \theta_W Y_{f_{L,R}}^4}{4(t - m_{\tilde{f}_{L,R}}^2)(u - m_{\tilde{f}_{L,R}}^2)} \times \\
&\quad \bar{u}_f(p_1, r_1) P_{L,R} u_{\tilde{B}}(k_2, s_2) \bar{v}_{\tilde{B}}(k_1, s_1) P_{R,L} v_f(p_2, r_2) \times \\
&\quad \bar{v}_f(p_2, r_2) P_{L,R} v_{\tilde{B}}(k_2, s_2) \bar{u}_{\tilde{B}}(k_1, s_1) P_{R,L} u_f(p_1, r_1) \\
&= \sum_{s_i} \frac{g^4 \tan^4 \theta_W Y_{f_{L,R}}^4}{4(t - m_{\tilde{f}_{L,R}}^2)(u - m_{\tilde{f}_{L,R}}^2)} \times \\
&\quad [\bar{u}_{\tilde{B}}(k_1, s_1) P_{R,L} \not{p}_1 P_{L,R} u_{\tilde{B}}(k_2, s_2)] \times \\
&\quad \bar{v}_{\tilde{B}}(k_1, s_1) P_{R,L} \not{p}_2 P_{L,R} v_{\tilde{B}}(k_2, s_2).
\end{aligned} \tag{E.33}$$

As it stands there is no obvious way to perform the sum over initial spins using standard trace technologies. However taking the transpose of the term in the square brackets and using the spins sum formulae given in Eq. (E.23) we obtain

$$\begin{aligned}
\sum_{s_i, r_i} \mathcal{M}_u \mathcal{M}_t^\dagger &= \sum_{s_i} \frac{g^4 \tan^4 \theta_W Y_{f_{L,R}}^4}{4(t - m_{\tilde{f}_{L,R}}^2)(u - m_{\tilde{f}_{L,R}}^2)} \times \\
&\quad [u_{\tilde{B}}^T(k_2, s_2) P_{L,R}^T \not{p}_1^T P_{R,L}^T \bar{u}_{\tilde{B}}^T(k_1, s_1)] \times \\
&\quad \bar{v}_{\tilde{B}}(k_1, s_1) P_{R,L} \not{p}_2 P_{L,R} v_{\tilde{B}}(k_2, s_2) \\
&= \frac{g^4 \tan^4 \theta_W Y_{f_{L,R}}^4}{4(t - m_{\tilde{f}_{L,R}}^2)(u - m_{\tilde{f}_{L,R}}^2)} \times \\
&\quad \text{Tr}\{(k_2 - M_{\tilde{B}})(-C) P_{L,R}^T \not{p}_1^T P_{R,L}^T C^\dagger (k_1 - M_{\tilde{B}}) P_{R,L} \not{p}_2 P_{L,R}\} \\
&= \frac{g^4 \tan^4 \theta_W Y_{f_{L,R}}^4}{4(t - m_{\tilde{f}_{L,R}}^2)(u - m_{\tilde{f}_{L,R}}^2)} \times \\
&\quad \text{Tr}\{(k_2 - M_{\tilde{B}}) P_{L,R} \not{p}_1 P_{R,L} (k_1 - M_{\tilde{B}}) P_{R,L} \not{p}_2 P_{L,R}\}
\end{aligned} \tag{E.34}$$

where C is the charge conjugation operator, and we made explicit use of the proprieties of charge conjugation matrix given in the previous section. Performing the trace we have

$$\begin{aligned}
\sum_{s_i, r_i} \mathcal{M}_u \mathcal{M}_t^\dagger &= \frac{g^4 \tan^4 \theta_W Y_{f_{L,R}}^4}{4(t - m_{\tilde{f}_{L,R}}^2)(u - m_{\tilde{f}_{L,R}}^2)} [2(p_1 p_2) M_{\tilde{B}}^2] \\
&= g^4 \tan^4 \theta_W Y_{f_{L,R}}^4 \frac{s M_{\tilde{B}}^2}{4(t - m_{\tilde{f}_{L,R}}^2)(u - m_{\tilde{f}_{L,R}}^2)}.
\end{aligned} \tag{E.35}$$

Finally, summing up all these results, we obtain that the total average square amplitude for the process $\tilde{B}\tilde{B} \xrightarrow{\tilde{f}} \tilde{f}f$, is

$$|\overline{\mathcal{M}}_{\tilde{B}\tilde{B}}|^2 = \frac{g^4 \tan^4 \theta_W Y_{f_{L,R}}^4}{16} \left[\frac{(t - M_{\tilde{B}}^2)^2}{(t - m_{\tilde{f}_{L,R}}^2)^2} + \frac{(u - M_{\tilde{B}}^2)^2}{(u - m_{\tilde{f}_{L,R}}^2)^2} - \frac{2sM_{\tilde{B}}^2}{(t - m_{\tilde{f}_{L,R}}^2)(u - m_{\tilde{f}_{L,R}}^2)} \right]. \quad (\text{E.36})$$

Now to compute the relic density what we need is the expansion of $\sigma_{\tilde{B}\tilde{B} \rightarrow \tilde{f}f} v$ in terms of the kinetic energy per unit of mass, ϵ . Thus what we have to do now is to expand the total average square amplitude, Eq. (E.36), in terms of ϵ . Using the expansions of the Mandelstam variables given in Eqs. (E.11) we can expand Eq. (E.36) at the first order in ϵ . Thus, defining $\Delta \equiv (M_{\tilde{B}}^2 + m_{\tilde{f}_{L,R}}^2)$, for the first term of Eq. (E.36) we have

$$\frac{(t - M_{\tilde{B}}^2)^2}{(t - m_{\tilde{f}_{L,R}}^2)^2} \simeq \frac{4M_{\tilde{B}}^4}{\Delta^2} \left\{ 1 + \left[2 - \frac{4M_{\tilde{B}}^2}{\Delta} + \left(1 + \frac{12M_{\tilde{B}}^4}{\Delta^2} - \frac{8M_{\tilde{B}}^2}{\Delta} \right) \cos^2 \theta_{\text{CM}} \right] \epsilon \right\} + \mathcal{O}(\epsilon^2), \quad (\text{E.37})$$

while the second term of Eq. (E.36) becomes

$$\frac{(u - M_{\tilde{B}}^2)^2}{(u - m_{\tilde{f}_{L,R}}^2)^2} \simeq \frac{4M_{\tilde{B}}^4}{\Delta^2} \left\{ 1 + \left[2 - \frac{4M_{\tilde{B}}^2}{\Delta} + \left(1 + \frac{12M_{\tilde{B}}^4}{\Delta^2} - \frac{8M_{\tilde{B}}^2}{\Delta} \right) \cos^2 \theta_{\text{CM}} \right] \epsilon \right\} + \mathcal{O}(\epsilon^2), \quad (\text{E.38})$$

and as last the interference term is equal to

$$\frac{2sM_{\tilde{B}}^2}{(t - m_{\tilde{f}_{L,R}}^2)(u - m_{\tilde{f}_{L,R}}^2)} \simeq \frac{8M_{\tilde{B}}^4}{\Delta^2} \left[1 + \left(1 - \frac{4M_{\tilde{B}}^2}{\Delta} + \frac{4M_{\tilde{B}}^4}{\Delta^2} \cos^2 \theta_{\text{CM}} \right) \epsilon \right] + \mathcal{O}(\epsilon^2). \quad (\text{E.39})$$

Note that we have neglected terms proportional to $\sqrt{\epsilon}$ or to $\epsilon\sqrt{\epsilon}$ because they are always multiply by odd powers of $\cos \theta_{\text{CM}}$ and they will vanish, upon an integration over $d\Omega$. Summing up the above equations we obtain the expansion, at first order of the total amplitude $|\overline{\mathcal{M}}|^2$, which is

$$|\overline{\mathcal{M}}|^2 \simeq \frac{g^4 \tan^4 \theta_W Y_{f_{L,R}}^4}{8\Delta^2} \left[1 + \left(1 - \frac{8M_{\tilde{B}}^2}{\Delta} + \frac{8M_{\tilde{B}}^4}{\Delta^2} \right) \cos^2 \theta_{\text{CM}} \right] \epsilon + \mathcal{O}(\epsilon^2). \quad (\text{E.40})$$

Note the absence of the leading order term in this expansion. This is due to fact that we have considered massless final states. Substituting Eq. (E.40) in the formula for σv given in Eq. (E.14) and then integrate over $d\Omega$, at the first order in ϵ we obtain that

$$\sigma_{\tilde{B}\tilde{B} \rightarrow \tilde{f}f} v \simeq \frac{g^4 \tan^4 \theta_W Y_{f_{L,R}}^4}{48\pi m_{\tilde{f}_{L,R}}^2} \frac{r(1+r^2)}{(1+r)^4} \epsilon + \mathcal{O}(\epsilon^2) \quad (\text{E.41})$$

where r is defined as $r \equiv M_{\tilde{B}}^2/m_{\tilde{f}_{L,R}}^2$. In order to obtain the total cross-section times velocity, this result must be summed over all possible final states, so

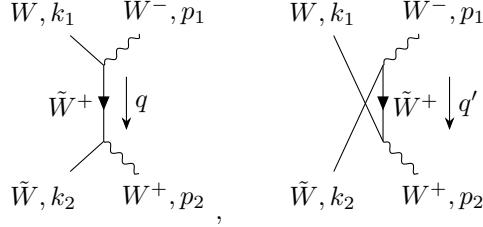
$$\sigma_{\tilde{B}\tilde{B}} v \simeq \sum_{f_{L,R}} \frac{g^4 \tan^4 \theta_W Y_{f_{L,R}}^4}{48\pi m_{\tilde{f}_{L,R}}^2} \frac{r(1+r^2)}{(1+r)^4} \epsilon + \mathcal{O}(\epsilon^2). \quad (\text{E.42})$$

E.4 Pure Wino LSP annihilation and co-annihilation cross-sections

Here we compute the relevant annihilation and co-annihilation cross-sections times velocity, at tree-level, which are relevant in the evaluation of the pure Wino LSP relic abundance. We take into account three annihilating states (\tilde{W}, \tilde{W}^\pm) with equal mass M_2 , and we assume the limit $M_2 \gg m_W$, where m_W is the mass of the W^\pm SM gauge bosons. We also assume that all the supersymmetric scalars, such as squarks and sleptons, and the Higgs scalars (except the

SM Higgs, h), are more heavier than the LSP. All the relevant processes are summarized in Table 4.8. The fundamental Feynman rules which we need can be obtained from the general ones listed in Appendix B with the substitutions $N_{11}, N_{13}, N_{14} \rightarrow 0$, $N_{12} \rightarrow 1$ and $U_{11}, V_{11} \rightarrow 1$, $U_{12}, V_{12} \rightarrow 0$.

The annihilation process between two neutral Winos into final gauge bosons occur via the exchange, in t/u -channel, of a charged Wino, schematically $\tilde{W}\tilde{W} \xrightarrow{\tilde{W}^\pm} W^+W^-$. The associated Feynman diagrams are



which are respectively the t -channel and u -channel process. The associated amplitudes are

$$i\mathcal{M}_t = \frac{g^2}{t - M_2^2} \bar{v}(k_2, s_2) \gamma^\nu (\not{q} + M_2) \gamma^\mu u(k_1, s_1) \epsilon_\nu(p_2) \epsilon_\mu(p_1), \quad (\text{E.43})$$

for the t -channel process and

$$i\mathcal{M}_u = -\frac{g^2}{u - M_2^2} \bar{v}(k_1, s_1) \gamma^\nu (\not{q}' + M_2) \gamma^\mu u(k_2, s_2) \epsilon_\nu(p_2) \epsilon_\mu(p_1), \quad (\text{E.44})$$

for the u -channel one. In the above expressions the exchange four-momenta are $q^\mu = k_1^\mu - p_1^\mu$ and $q'^\mu = k_2^\mu - p_1^\mu$. Note that in order to write down the amplitudes for both processes we have chosen the verse of the fermionic flow from up to down. Using the Dirac equations

$$(\not{p} - M_2)u(p) = 0, \quad (\not{p} + M_2)v(p) = 0 \quad (\text{E.45})$$

the amplitudes given in Eq. (E.43) and Eq. (E.44) can be rewritten as

$$i\mathcal{M}_t = \frac{g^2}{t - M_2^2} [2\bar{v}(k_2, s_2) \gamma^\nu u(k_1, s_1) \epsilon_\nu(p_2) (q \cdot \epsilon_\mu(p_1)) + \bar{v}(k_2, s_2) \gamma^\nu \gamma^\mu \not{p}_1 u(k_1, s_1) \epsilon_\nu(p_2) \epsilon_\mu(p_1)], \quad (\text{E.46a})$$

$$i\mathcal{M}_u = -\frac{g^2}{u - M_2^2} [2\bar{v}(k_1, s_1) \gamma^\nu u(k_2, s_2) \epsilon_\nu(p_2) (q' \cdot \epsilon_\mu(p_1)) + \bar{v}(k_1, s_1) \gamma^\nu \gamma^\mu \not{p}_1 u(k_2, s_2) \epsilon_\nu(p_2) \epsilon_\mu(p_1)]. \quad (\text{E.46b})$$

Now in order to find the total average square amplitude of the process we first compute the average square amplitudes for definite final polarization states and then we sum up the various results. We start by considering the transverse polarizations. Considering the expressions given in Eqs. (E.2) and in Eqs. (E.1) we have that

$$\epsilon^\pm \cdot p_{1,2} = 0 \quad (\text{E.47})$$

and

$$\epsilon^\pm \cdot k_{1,2} = \pm \frac{|\vec{k}_1|}{\sqrt{2}} \sin \theta \simeq \mathcal{O}(\sqrt{\epsilon}) \quad (\text{E.48})$$

where with ϵ_μ^\pm we refer to one of the transverse polarization vectors given in Eqs. (E.2) and ϵ is the total kinetic energy for unit of mass given in Eq. (A.25). In particular we ignore terms of

order $\sqrt{\epsilon}$ because we are interested to find the leading order of the expansion of the cross-section times velocity in ϵ . Using these results the amplitudes given in Eqs. (E.46) become

$$i\mathcal{M}_t = \frac{g^2}{t - M_2^2} \bar{v}(k_2, s_2) \gamma^\nu \gamma^\mu \not{p}_1 u(k_1, s_1) \epsilon_\nu^\pm \epsilon_\mu^\pm + \mathcal{O}(\sqrt{\epsilon}), \quad (\text{E.49a})$$

$$i\mathcal{M}_u = -\frac{g^2}{u - M_2^2} \bar{v}(k_1, s_1) \gamma^\nu \gamma^\mu \not{p}_1 u(k_2, s_2) \epsilon_\nu^\pm \epsilon_\mu^\pm + \mathcal{O}(\sqrt{\epsilon}). \quad (\text{E.49b})$$

where with $\epsilon_{1\mu}^\pm$ we refer to the polarization vector associated to the vector boson with momentum p_1 while with $\epsilon_{2\mu}^\pm$ to the one associated to the vector boson with momentum p_2 . Squaring and averaging over initial states the t -channel amplitude, we obtain

$$\begin{aligned} |\overline{\mathcal{M}_t}|^2 &= \frac{1}{4} \sum_{s_1, s_2} \frac{g^4}{(t - M_2^2)^2} \bar{v}(k_2, s_2) \gamma^\nu \gamma^\mu \not{p}_1 u(k_1, s_1) \bar{u}(k_1, s_1) \not{p}_1 \gamma^\alpha \gamma^\beta v(k_2, s_2) \epsilon_{1\nu}^\pm \epsilon_{2\mu}^\pm \left(\epsilon_{1\alpha}^\pm \epsilon_{2\beta}^\pm \right)^* \\ &= \frac{g^4}{4(t - M_2^2)^2} \text{Tr} \left\{ (\not{k}_2 - M_2) \not{\epsilon}_2^\pm \not{\epsilon}_1^\pm \not{p}_1 (\not{k}_1 + M_2) \not{p}_1 \not{\epsilon}_1^{\pm*} \not{\epsilon}_2^{\pm*} \right\} \\ &= \frac{g^4}{4(t - M_2^2)^2} \text{Tr} \left\{ \not{k}_2 \not{\epsilon}_2^\pm \not{\epsilon}_1^\pm \not{p}_1 \not{k}_1 \not{p}_1 \not{\epsilon}_1^{\pm*} \not{\epsilon}_2^{\pm*} \right\} - \frac{g^4 m_W^2 M_2^2}{4(t - M_2^2)^2} \text{Tr} \left\{ \not{\epsilon}_2^\pm \not{\epsilon}_1^\pm \not{\epsilon}_1^{\pm*} \not{\epsilon}_2^{\pm*} \right\} \\ &= \frac{g^4}{4(t - M_2^2)^2} \text{Tr} \left\{ \not{k}_2 \not{\epsilon}_2^\pm \not{\epsilon}_1^\pm \not{p}_1 \not{k}_1 \not{p}_1 \not{\epsilon}_1^{\pm*} \not{\epsilon}_2^{\pm*} \right\} + \mathcal{O} \left(\frac{m_W^2}{M_2^2}, \epsilon \right) \end{aligned} \quad (\text{E.50})$$

where in the last equality we dropped out terms which would be suppressed by the ratio m_W^2/M_2^2 . Using the Clifford algebra

$$\{\gamma^\mu, \gamma^\nu\} = 2g^{\mu\nu} \quad (\text{E.51})$$

the above trace, of eight gamma matrices, is equal to

$$\begin{aligned} \text{Tr} \left\{ \not{k}_2 \not{\epsilon}_2^\pm \not{\epsilon}_1^\pm \not{p}_1 \not{k}_1 \not{p}_1 \not{\epsilon}_1^{\pm*} \not{\epsilon}_2^{\pm*} \right\} &= 2(p_1 \cdot k_1) \text{Tr} \left\{ \not{k}_2 \not{\epsilon}_2^\pm \not{\epsilon}_1^\pm \not{p}_1 \not{\epsilon}_1^{\pm*} \not{\epsilon}_2^{\pm*} \right\} \\ &\quad + m_W^2 \text{Tr} \left\{ \not{k}_2 \not{\epsilon}_2^\pm \not{\epsilon}_1^\pm \not{k}_1 \not{\epsilon}_1^{\pm*} \not{\epsilon}_2^{\pm*} \right\} \\ &= 2(p_1 \cdot k_1)(p_1 \cdot k_2) \text{Tr} \left\{ \not{\epsilon}_2^\pm \not{\epsilon}_1^\pm \not{\epsilon}_1^{\pm*} \not{\epsilon}_2^{\pm*} \right\} \\ &= 8(p_1 \cdot k_1)(p_1 \cdot k_2) \left[(\epsilon_2^\pm \cdot \epsilon_1^\pm) (\epsilon_1^{\pm*} \cdot \epsilon_2^{\pm*})^* \right. \\ &\quad \left. - (\epsilon_2^\pm \cdot \epsilon_1^{\pm*}) (\epsilon_1^\pm \cdot \epsilon_2^{\pm*}) + (\epsilon_2^\pm \cdot \epsilon_2^{\pm*}) (\epsilon_1^\pm \cdot \epsilon_1^{\pm*}) \right] \end{aligned} \quad (\text{E.52})$$

where in the second passage we have neglect term proportional to m_W^2 and in the last step we made use of the formula for the trace of four gamma matrices given in Eq. (E.15). Substituting this result into Eq. (E.50) we find that

$$\begin{aligned} |\overline{\mathcal{M}_t}|^2 &= \frac{2g^4}{(t - M_2^2)^2} (p_1 \cdot k_1)(p_1 \cdot k_2) \left[(\epsilon_2^\pm \cdot \epsilon_1^\pm) (\epsilon_1^{\pm*} \cdot \epsilon_2^{\pm*})^* \right. \\ &\quad \left. - (\epsilon_2^\pm \cdot \epsilon_1^{\pm*}) (\epsilon_1^\pm \cdot \epsilon_2^{\pm*}) + (\epsilon_2^\pm \cdot \epsilon_2^{\pm*}) (\epsilon_1^\pm \cdot \epsilon_1^{\pm*}) \right] + \mathcal{O} \left(\frac{m_W^2}{M_2^2}, \epsilon \right) \\ &= \frac{g^4}{2} \frac{u - M_2^2}{t - M_2^2} \mathcal{P}(\pm, \pm) + \mathcal{O} \left(\frac{m_W^2}{M_2^2}, \epsilon \right) \end{aligned} \quad (\text{E.53})$$

where in the last step we used the relations

$$2(p_1 \cdot k_1) = 2(p_2 \cdot k_2) = M_2^2 + m_W^2 - t \quad (\text{E.54a})$$

$$2(p_1 \cdot k_2) = 2(p_2 \cdot k_1) = M_2^2 + m_W^2 - u, \quad (\text{E.54b})$$

and we have redefined

$$\left[(\epsilon_2^\pm \cdot \epsilon_1^\pm) (\epsilon_1^{\pm*} \cdot \epsilon_2^{\pm*})^* - (\epsilon_2^\pm \cdot \epsilon_1^{\pm*}) (\epsilon_1^\pm \cdot \epsilon_2^{\pm*}) + (\epsilon_2^\pm \cdot \epsilon_2^{\pm*}) (\epsilon_1^\pm \cdot \epsilon_1^{\pm*}) \right] \equiv \mathcal{P}(\pm, \pm). \quad (\text{E.55})$$

The average over initial states of the square of the u -channel amplitude can be calculated following the same steps used for the t -channel one, obtaining that

$$\overline{|\mathcal{M}_u|^2} = \frac{g^4}{2} \frac{t - M_2^2}{u - M_2^2} \mathcal{P}(\pm, \pm) + \mathcal{O}\left(\frac{m_W^2}{M_2^2}, \epsilon\right). \quad (\text{E.56})$$

The average over initial states of the interference term $\text{Re} [\mathcal{M}_t \mathcal{M}_u^\dagger]$ read as

$$\begin{aligned} \text{Re} [\overline{\mathcal{M}_t \mathcal{M}_u^\dagger}] &= \frac{1}{4} \sum_{s_1, s_2} - \frac{g^4}{(t - M_2^2)(u - M_2^2)} \bar{v}(k_2, s_2) \gamma^\nu \gamma^\mu \not{k}_1 u(k_1, s_1) \bar{u}(k_2, s_2) \not{k}_1 \gamma^\alpha \gamma^\beta v(k_1, s_1) \times \\ &\quad \epsilon_{1\nu}^\pm \epsilon_{2\mu}^\pm \left(\epsilon_{1\alpha}^\pm \epsilon_{2\beta}^\pm \right)^*. \end{aligned} \quad (\text{E.57})$$

Following the same procedure applied for the computation of the interference for the Bino annihilation process we obtain that

$$\begin{aligned} \text{Re} [\overline{\mathcal{M}_t \mathcal{M}_u^\dagger}] &= - \frac{g^4}{4(t - M_2^2)(u - M_2^2)} \text{Tr} \{ (k_2 - M_2) \not{\epsilon}_2^\pm \not{\epsilon}_1^\pm \not{k}_1 (k_1 + M_2) \not{\epsilon}_2^{\pm*} \not{\epsilon}_1^{\pm*} \not{k}_1 \} \\ &= - \frac{g^4}{4(t - M_2^2)(u - M_2^2)} \text{Tr} \{ k_2 \not{\epsilon}_2^\pm \not{\epsilon}_1^\pm \not{k}_1 \not{k}_1 \not{k}_1 \not{\epsilon}_2^{\pm*} \not{\epsilon}_1^{\pm*} \} \end{aligned} \quad (\text{E.58})$$

where in the last step we used the Clifford algebra and we neglected term proportional to m_W^2 . The above trace can be performed following the same method used above obtaining

$$\begin{aligned} \text{Re} [\overline{\mathcal{M}_t \mathcal{M}_u^\dagger}] &= -2g^4 \frac{(p_1 \cdot k_1)(p_1 \cdot k_2)}{(t - M_2^2)(u - M_2^2)} \left[(\epsilon_2^\pm \cdot \epsilon_1^\pm) (\epsilon_1^\pm \cdot \epsilon_2^\pm)^* - (\epsilon_2^\pm \cdot \epsilon_2^{\pm*}) (\epsilon_1^\pm \cdot \epsilon_1^{\pm*}) \right. \\ &\quad \left. + (\epsilon_2^\pm \cdot \epsilon_1^{\pm*}) (\epsilon_1^\pm \cdot \epsilon_2^{\pm*}) \right] + \mathcal{O}(\epsilon) \\ &= - \frac{g^4}{2} \mathcal{P}'(\pm, \pm) + \mathcal{O}(\epsilon) \end{aligned} \quad (\text{E.59})$$

where we used Eqs. (E.54) and the redefinition

$$\left[(\epsilon_2^\pm \cdot \epsilon_1^\pm) (\epsilon_1^\pm \cdot \epsilon_2^\pm)^* - (\epsilon_2^\pm \cdot \epsilon_2^{\pm*}) (\epsilon_1^\pm \cdot \epsilon_1^{\pm*}) + (\epsilon_2^\pm \cdot \epsilon_1^{\pm*}) (\epsilon_1^\pm \cdot \epsilon_2^{\pm*}) \right] \equiv \mathcal{P}'(\pm, \pm) \quad (\text{E.60})$$

The possible transverse polarizations are the four configurations $(+, -)$, $(-, +)$, $(+, +)$, $(-, -)$ and using the definitions of $\mathcal{P}(\pm, \pm)$ and of $\mathcal{P}'(\pm, \pm)$, respectively given in Eq. (E.55) and Eq. (E.60), we can observe that

$$\mathcal{P}(+, -) = \mathcal{P}(-, +) = 2, \quad \mathcal{P}(+, +) = \mathcal{P}(-, -) = 0 \quad (\text{E.61a})$$

$$\mathcal{P}'(+, -) = \mathcal{P}'(-, +) = \mathcal{P}'(+, +) = \mathcal{P}'(-, -) = 0. \quad (\text{E.61b})$$

For what concern longitudinal polarizations, taking into account the approximation for the longitudinal polarization vector given in Eq. (E.4) and substituting it into the t -channel amplitude given in Eqs. (E.46a) we obtain that

$$\begin{aligned} i\mathcal{M}_t^{LL} &= \frac{g^2}{t - M_2^2} [2\bar{v}(k_2, s_2) \gamma^\nu u(k_1, s_1) \frac{p_{2\nu}}{m_W^2} (q \cdot p_1) \\ &\quad + \bar{v}(k_2, s_2) \gamma^\nu \gamma^\mu \not{k}_1 u(k_1, s_1) \frac{p_{1\mu} p_{2\nu}}{m_W^2}] + \mathcal{O}\left(\frac{m_W^2}{M_2^2}\right) \\ &= \frac{g^2}{t - M_2^2} [2\bar{v}(k_2, s_2) \not{k}_2 u(k_1, s_1) \frac{(q \cdot p_1)}{m_W^2} \\ &\quad + \bar{v}(k_2, s_2) \not{k}_2 \gamma^\mu \not{k}_1 u(k_1, s_1)] + \mathcal{O}\left(\frac{m_W^2}{M_2^2}\right) \\ &= \frac{g^2}{t - M_2^2} \left[2 \frac{(k_1 \cdot p_1)}{m_W^2} - 1 \right] \bar{v}(k_2, s_2) \not{k}_2 u(k_1, s_1) + \mathcal{O}\left(\frac{m_W^2}{M_2^2}\right) \\ &= - \frac{g^2}{m_W^2} \bar{v}(k_2, s_2) \not{k}_2 u(k_1, s_1) + \mathcal{O}\left(\frac{m_W^2}{M_2^2}\right) \end{aligned} \quad (\text{E.62})$$

where in the last passage we used the relations given in Eqs. (E.54). Following the same steps the u -channel amplitude given in Eq. (E.46b) becomes

$$i\mathcal{M}_u^{LL} = \frac{g^2}{m_W^2} \bar{v}(k_1, s_1) \gamma^\nu \gamma^\mu \not{p}_1 u(k_2, s_2) + \mathcal{O}\left(\frac{m_W^2}{M_2^2}\right) \quad (\text{E.63})$$

which using the relations given in Eqs. (E.22) can be recast as

$$\begin{aligned} i\mathcal{M}_u^{LL} &= \frac{g^2}{m_W^2} \bar{v}(k_1, s_1) \not{p}_2 u(k_2, s_2) + \mathcal{O}\left(\frac{m_W^2}{M_2^2}\right) \\ &= \frac{g^2}{m_W^2} [\bar{v}(k_1, s_1) \not{p}_2 u(k_2, s_2)]^T + \mathcal{O}\left(\frac{m_W^2}{M_2^2}\right) \\ &= \frac{g^2}{m_W^2} [\bar{v}(k_2, s_2) \mathbf{C}^T \not{p}_2^T \mathbf{C} u(k_1, s_1)]^T + \mathcal{O}\left(\frac{m_W^2}{M_2^2}\right) \\ &= \frac{g^2}{m_W^2} \bar{v}(k_2, s_2) \not{p}_2 u(k_1, s_1) + \mathcal{O}\left(\frac{m_W^2}{M_2^2}\right) \end{aligned} \quad (\text{E.64})$$

where in the last line we used the proprieties of the charge conjugation operator. Thus summing up the two amplitudes we get that

$$i\mathcal{M}^{LL} = i\mathcal{M}_t^{LL} + i\mathcal{M}_u^{LL} \simeq \mathcal{O}\left(\frac{m_W^2}{M_2^2}\right) \quad (\text{E.65})$$

So in the limit where $M_2^2 \gg m_W^2$ and at the leading order the non-relativistic expansion, we have that the longitudinal polarizations do not contribute to the total amplitude of the annihilation process $\tilde{W}\tilde{W} \xrightarrow{\tilde{W}^\pm} W^+W^-$. Note that the amplitudes for the emission of one longitudinal and one transverse vector boson give rise to an identical result. In fact taking, for example, $\epsilon^L(p_1)$ and $\epsilon^\pm(p_2)$ we would obtain the same result as above with the vector $\epsilon^\pm(p_2)$ in place of p_2 .

In light of this the total average square amplitudes for the process $\tilde{W}\tilde{W} \xrightarrow{\tilde{W}^\pm} W^+W^-$ is

$$\overline{|\mathcal{M}_{\tilde{W}\tilde{W}}|^2} = \sum_{(\pm\pm)} \overline{|\mathcal{M}_t|^2} + \overline{|\mathcal{M}_u|^2} + 2 \text{Re} \left[\overline{\mathcal{M}_t \mathcal{M}_u^\dagger} \right] \quad (\text{E.66})$$

where the sum runs over all possible transverse polarization configurations because the longitudinal ones are of order m_W^2/M_2^2 . Thus using the expressions found for $\overline{|\mathcal{M}_t|^2}$, $\overline{|\mathcal{M}_u|^2}$ and $\text{Re} \left[\overline{\mathcal{M}_t \mathcal{M}_u^\dagger} \right]$, and exploiting the results found in Eqs. (E.61), we obtain that

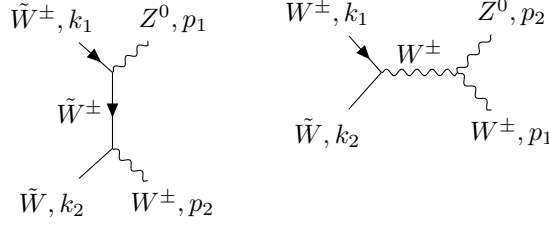
$$\begin{aligned} \overline{|\mathcal{M}_{\tilde{W}\tilde{W}}|^2} &= \sum_{(\pm\pm)} \frac{g^4}{2} \frac{u - M_2^2}{t - M_2^2} \mathcal{P}(\pm, \pm) + \frac{g^4}{2} \frac{u - M_2^2}{t - M_2^2} \mathcal{P}(\pm, \pm) - g^4 \mathcal{P}'(\pm, \pm) + \mathcal{O}\left(\frac{m_W^2}{M_2^2}, \epsilon\right) \\ &= 2g^4 \frac{u - M_2^2}{t - M_2^2} + 2g^4 \frac{t - M_2^2}{u - M_2^2} + \mathcal{O}\left(\frac{m_W^2}{M_2^2}, \epsilon\right) \\ &= 4g^4 + \mathcal{O}\left(\frac{m_W^2}{M_2^2}, \epsilon\right) \end{aligned} \quad (\text{E.67})$$

where in the last step we used the expansions of the Mandelstam variables given in Eqs. (E.6). Substituting this result into the cross-section times velocity formula given in Eq. (E.14) and integrating over $d\Omega$ we find that

$$\sigma_{\tilde{W}\tilde{W}v} = \frac{g^4}{8\pi M_2^2} + \mathcal{O}\left(\frac{m_W^2}{M_2^2}, \epsilon\right). \quad (\text{E.68})$$

Now we go further computing the cross-section times velocity, at the leading order in the non-relativistic expansion, for the co-annihilation process between a Wino LSP, \tilde{W} , and a

charged Wino, \tilde{W}^\pm . The possible final states of this annihilation are summarized in Table 4.8. We start from the process $\tilde{W}\tilde{W}^\pm \rightarrow Z^0 W^\pm$. The tree-level Feynman diagrams are



The t -channel process has an amplitude equal to

$$i\mathcal{M}_t = \frac{g^2 c_W}{t - M_2^2} [2\bar{v}(k_2, s_2)\gamma^\nu u(k_1, s_1)\epsilon_\nu(p_2)(q \cdot \epsilon_\mu(p_1)) + \bar{v}(k_2, s_2)\gamma^\nu \not{p}_1 u(k_1, s_1)\epsilon_\nu(p_2)\epsilon_\mu(p_1)]$$

while the s -channel process has an amplitude given by

$$i\mathcal{M}_s = \frac{g^2 c_W}{s - m_W^2} \bar{v}(k_2, s_2)\gamma^\mu u(k_1, s_1) \left[-g_{\mu\nu} + \frac{(k_1 + k_2)_\mu (k_1 + k_2)_\nu}{m_W^2} \right] \Gamma^{\nu\alpha\beta} \epsilon_\alpha(p_1)\epsilon_\beta(p_2) \quad (\text{E.69})$$

where for the massive vector boson propagator we used the Feynman rules given in Appendix B. Note that both the t -channel and s -channel amplitudes are obtained choosing the verse of the fermionic flow from up to down. The tensor $\Gamma^{\nu\alpha\beta}$ is defined as

$$\Gamma^{\nu\alpha\beta} = [g^{\alpha\beta}(p_2 - p_1)^\nu - g^{\beta\nu}(2p_2 - p_1)^\alpha + g^{\alpha\nu}(2p_1 + p_2)^\beta]. \quad (\text{E.70})$$

Using the Dirac equation and the fact that the masses of \tilde{W} and \tilde{W}^\pm are equal, the s -channel amplitude reduce to

$$i\mathcal{M}_s = -\frac{g^2 c_W}{s - m_W^2} \bar{v}(k_2, s_2)\gamma^\mu u(k_1, s_1) g_{\mu\nu} \Gamma^{\nu\alpha\beta} \epsilon_\alpha(p_1)\epsilon_\beta(p_2). \quad (\text{E.71})$$

As first we compute the average square amplitudes for specific final polarization configurations and then we sum up, the various results. We start by considering the transverse polarizations. Using the relation in Eq. (E.47) and the explicit form of the tensor $\Gamma^{\nu\alpha\beta}$ the s -channel amplitude on transverse polarization read as

$$\begin{aligned} i\mathcal{M}_s &= -\frac{g^2 c_W}{s - m_W^2} \bar{v}(k_2, s_2)\gamma^\mu u(k_1, s_1) \left[(\epsilon_2^\pm \cdot \epsilon_1^\pm) (p_2 - p_1)_\mu - 2\epsilon_{2\mu}^\pm (p_2 \cdot \epsilon_1^\pm) + 2\epsilon_{1\mu}^\pm (p_1 \cdot \epsilon_2^\pm) \right] \\ &= -\frac{g^2 c_W}{s} \bar{v}(k_2, s_2)\gamma^\mu u(k_1, s_1) (\epsilon_2^\pm \cdot \epsilon_1^\pm) (p_2 - p_1)_\mu + \mathcal{O}\left(\frac{m_W^2}{M_2^2}\right). \end{aligned} \quad (\text{E.72})$$

This expression can be further simplify using the Dirac equation and the four momentum conservation, obtaining

$$i\mathcal{M}_s = -2\frac{g^2 c_W}{s} \bar{v}(k_2, s_2) \not{p}_2 u(k_1, s_1) (\epsilon_2^\pm \cdot \epsilon_1^\pm) + \mathcal{O}\left(\frac{m_W^2}{M_2^2}\right). \quad (\text{E.73})$$

The average over initial states of the square of this amplitude is equal to

$$\begin{aligned} |\overline{\mathcal{M}_s}|^2 &= \frac{g^4 c_W^2}{s^2} \text{Tr} \{ (\not{k}_2 - M_2^2) \not{p}_2 (\not{k}_1 + M_2^2) \not{p}_2 \} |(\epsilon_2^\pm \cdot \epsilon_1^\pm)|^2 + \mathcal{O}\left(\frac{m_W^2}{M_2^2}\right) \\ &= 4\frac{g^4 c_W^2}{s^2} [2(k_2 \cdot p_2)(k_1 \cdot p_2)] |(\epsilon_2^\pm \cdot \epsilon_1^\pm)|^2 + \mathcal{O}\left(\frac{m_W^2}{M_2^2}\right) \\ &= 2\frac{g^4 c_W^2}{s^2} (t - M_2^2)(u - M_2^2) |(\epsilon_2^\pm \cdot \epsilon_1^\pm)|^2 + \mathcal{O}\left(\frac{m_W^2}{M_2^2}\right) \end{aligned} \quad (\text{E.74})$$

where as usual we with $\epsilon_{1,2}$ we refer to the polarization vectors associated respectively to the outgoing gauge bosons with momentums $p_{1,2}$. The t -channel amplitude given in Eq. (E.69) on transverse polarization read as

$$i\mathcal{M}_t = \frac{g^2 c_W}{t - M_2^2} \bar{v}(k_2, s_2) \gamma^\nu \gamma^\mu \not{p}_1 u(k_1, s_1) \epsilon_\nu^\pm \epsilon_\mu^\pm + \mathcal{O}(\sqrt{\epsilon}) \quad (\text{E.75})$$

where we dropped out terms which are of order $\sqrt{\epsilon}$. In order to calculate the average over initial states of the square of the t -channel amplitude given in Eq. (E.69) we can exploit the result of Eq. (E.53), so using the right coefficients we get that

$$|\overline{\mathcal{M}_t}|^2 = \frac{g^4 c_W^2}{2} \frac{u - M_2^2}{t - M_2^2} \mathcal{P}(\pm, \pm) + \mathcal{O}\left(\frac{m_W^2}{M_2^2}, \epsilon\right). \quad (\text{E.76})$$

As last the average over initial states of the interference term $\text{Re}[\mathcal{M}_t \mathcal{M}_s^\dagger]$ is equal to

$$\begin{aligned} \text{Re}[\mathcal{M}_t \mathcal{M}_s^\dagger] &= \frac{1}{4} \sum_{s_1, s_2} -2 \frac{g^4 c_W^2}{(t - M_2^2)s} \bar{v}(k_2, s_2) \gamma^\nu \gamma^\mu \not{p}_1 u(k_1, s_1) \bar{u}(k_1, s_1) \not{p}_2 v(k_2, s_2) \epsilon_\nu^\pm \epsilon_\mu^\pm \times \\ &\quad (\epsilon_2^\pm \cdot \epsilon_1^\pm)^* + \mathcal{O}\left(\frac{m_W^2}{M_2^2}, \epsilon\right) \\ &= \frac{1}{4} \sum_{s_1, s_2} 2 \frac{g^4 c_W^2}{(t - M_2^2)s} \bar{v}(k_2, s_2) \gamma^\nu \gamma^\mu \not{p}_1 u(k_1, s_1) \bar{u}(k_1, s_1) \not{p}_1 v(k_2, s_2) \epsilon_\nu^\pm \epsilon_\mu^\pm \times \\ &\quad (\epsilon_2^\pm \cdot \epsilon_1^\pm)^* + \mathcal{O}\left(\frac{m_W^2}{M_2^2}, \epsilon\right) \\ &= \frac{g^4 c_W^2}{2(t - M_2^2)s} \text{Tr}\left\{(\not{k}_2 - M_2^2) \not{\epsilon}_2 \not{\epsilon}_1 \not{p}_1 (\not{k}_1 + M_2^2) \not{p}_1\right\} (\epsilon_2^\pm \cdot \epsilon_1^\pm)^* + \mathcal{O}\left(\frac{m_W^2}{M_2^2}, \epsilon\right) \end{aligned} \quad (\text{E.77})$$

where in the second passage we used the conservation of the four momentum and the Dirac equation. Computing the trace with the help of the Clifford algebra, we obtain that

$$\begin{aligned} \text{Re}[\mathcal{M}_t \mathcal{M}_s^\dagger] &= 4 \frac{g^4 c_W^2}{(t - M_2^2)s} [(k_2 \cdot p_2)(k_1 \cdot p_2)] |(\epsilon_2^\pm \cdot \epsilon_1^\pm)|^2 + \mathcal{O}\left(\frac{m_W^2}{M_2^2}, \epsilon\right) \\ &= \frac{g^4 c_W^2}{s} (u - M_2^2) |(\epsilon_2^\pm \cdot \epsilon_1^\pm)|^2 + \mathcal{O}\left(\frac{m_W^2}{M_2^2}, \epsilon\right) \end{aligned} \quad (\text{E.78})$$

where we made use of the relations given in Eqs. (E.54). Now we consider the amplitude for the emission of two longitudinal boson in the limit $E \gg m_W^2$. The t -channel amplitude for longitudinal polarizations is similar, apart for the vertex coefficients, to the one given in Eq. (E.62) for the two neutral Winos annihilation. So we have that

$$i\mathcal{M}_t^{LL} = -\frac{g^2 c_W}{m_W^2} \bar{v}(k_2, s_2) \not{p}_2 u(k_1, s_1) + \mathcal{O}\left(\frac{m_W^2}{M_2^2}\right). \quad (\text{E.79})$$

Substituting the approximation given in Eq. (E.4) into the expression of the s -channel amplitude given in Eq. (E.71) we obtain

$$\begin{aligned} i\mathcal{M}_s^{LL} &= -\frac{g^2 c_W}{s - m_W^2} \bar{v}(k_2, s_2) \gamma^\mu u(k_1, s_1) g_{\mu\nu} \Gamma^{\nu\alpha\beta} \frac{p_{1\alpha} p_{2\beta}}{m_W^2} + \mathcal{O}\left(\frac{m_W^2}{M_2^2}\right) \\ &= -\frac{g^2 c_W}{s} \bar{v}(k_2, s_2) \gamma^\mu u(k_1, s_1) \left[\frac{(p_1 \cdot p_2)}{m_W^2} + 1 \right] (p_1 - p_2)_\mu + \mathcal{O}\left(\frac{m_W^2}{M_2^2}\right) \\ &= 2 \frac{g^2 c_W}{s} \bar{v}(k_2, s_2) \not{p}_2 u(k_1, s_1) \left[\frac{(p_1 \cdot p_2)}{m_W^2} + 1 \right] + \mathcal{O}\left(\frac{m_W^2}{M_2^2}\right) \end{aligned} \quad (\text{E.80})$$

where we used the explicit expression of $\Gamma^{\nu\alpha\beta}$, the conservation of the four momentum and the Dirac equation. Remembering that $2(p_1 \cdot p_2) = s + 2m_W^2$ the above result becomes

$$i\mathcal{M}_s^{LL} = \frac{g^2 c_W}{m_W^2} \bar{v}(k_2, s_2) \not{p}_2 u(k_1, s_1) + \mathcal{O}\left(\frac{m_W^2}{M_2^2}\right). \quad (\text{E.81})$$

Summing the t -channel contribution, given Eq. (E.79), with s -channel the one, we have that

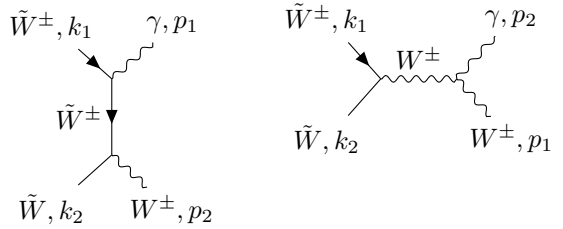
$$i\mathcal{M}^{LL} = i\mathcal{M}_t^{LL} + i\mathcal{M}_s^{LL} \simeq \mathcal{O}\left(\frac{m_W^2}{M_2^2}\right) \quad (\text{E.82})$$

and as a consequence up to correction of order m_W^2/M_2^2 the longitudinal polarizations do not contribute to the total amplitude of the process $\tilde{W}\tilde{W}^\pm \rightarrow Z^0 W^\pm$. Note that we have a similar result for the emission of one longitudinal and one transverse vector bosons. Thus the total average square amplitude, $|\overline{\mathcal{M}_{Z^0 W^\pm}}|^2$, for the annihilation process $\tilde{W}\tilde{W}^\pm \rightarrow Z^0 W^\pm$, at the leading order in ϵ and m_W^2/M_2^2 is determined only by the transverse polarization configurations. So we get

$$\begin{aligned} |\overline{\mathcal{M}_{Z^0 W^\pm}}|^2 &= \sum_{(\pm\pm)} |\overline{\mathcal{M}_t}|^2 + |\overline{\mathcal{M}_s}|^2 + 2 \text{Re} [\overline{\mathcal{M}_t \mathcal{M}_s^\dagger}] \\ &= \sum_{(\pm\pm)} \frac{g^4 c_W^2}{2} \frac{u - M_2^2}{t - M_2^2} \mathcal{P}(\pm, \pm) + 2 \frac{g^4 c_W^2}{s^2} (t - M_2^2)(u - M_2^2) |(\epsilon_2^\pm \cdot \epsilon_1^\pm)|^2 \\ &\quad + 2 \frac{g^4 c_W^2}{s} (u - M_2^2) |(\epsilon_2^\pm \cdot \epsilon_1^\pm)|^2 + \mathcal{O}\left(\frac{m_W^2}{M_2^2}, \epsilon\right) \\ &= 2g^4 c_W^2 \frac{u - M_2^2}{t - M_2^2} + 4 \frac{g^4 c_W^2}{s^2} (t - M_2^2)(u - M_2^2) + 4 \frac{g^4 c_W^2}{s} (u - M_2^2) + \mathcal{O}\left(\frac{m_W^2}{M_2^2}, \epsilon\right) \\ &= g^4 c_W^2 + \mathcal{O}\left(\frac{m_W^2}{M_2^2}, \epsilon\right) \end{aligned} \quad (\text{E.83})$$

where we used the results for $|\overline{\mathcal{M}_t}|^2$, $|\overline{\mathcal{M}_s}|^2$ and $\text{Re} [\overline{\mathcal{M}_t \mathcal{M}_s^\dagger}]$. Note that in the last two steps we used the relations given in Eqs. (E.61) and Eqs. (E.5), and the expansions of the Mandelstam variables given in Eqs. (E.6).

From Table 4.8 the other process which contribute to the co-annihilation between \tilde{W} and \tilde{W}^\pm is $\tilde{W}\tilde{W}^\pm \rightarrow \gamma W^\pm$, where γ denotes a photon, which has associated Feynman diagrams



Choosing the verse of the fermionic flow from up to down and using the Feynman rules given in Appendix B the associated amplitudes are

$$\begin{aligned} i\mathcal{M}_t &= \frac{g^2 s_W}{t - M_2^2} [2\bar{v}(k_2, s_2) \gamma^\nu u(k_1, s_1) \epsilon_\nu(p_2) (q \cdot \epsilon_\mu(p_1)) \\ &\quad + \bar{v}(k_2, s_2) \gamma^\nu \gamma^\mu \not{p}_1 u(k_1, s_1) \epsilon_\nu(p_2) \epsilon_\mu(p_1)] \end{aligned}$$

for the t -channel process and

$$i\mathcal{M}_s = -\frac{g^2 s_W}{s - m_W^2} \bar{v}(k_2, s_2) \gamma^\mu u(k_1, s_1) g_{\mu\nu} \Gamma^{\nu\alpha\beta} \epsilon_\alpha(p_1) \epsilon_\beta(p_2) \quad (\text{E.84})$$

for the s -channel one. Note that apart for the vertex coefficients these amplitudes are identical to the one given in Eq. (E.69) and in Eq. (E.71). Therefore following the same procedures used above we obtain that on transverse polarizations the average of the square amplitudes and of the interference term are respectively equal to

$$|\overline{\mathcal{M}_t}|^2 = \frac{g^4 c_W^2}{2} \frac{u - M_2^2}{t - M_2^2} \mathcal{P}(\pm, \pm) + \mathcal{O}\left(\frac{m_W^2}{M_2^2}, \epsilon\right) \quad (\text{E.85a})$$

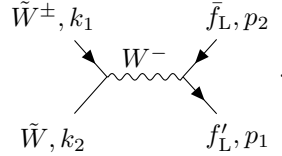
$$|\overline{\mathcal{M}_s}|^2 = 2 \frac{g^4 c_W^2}{s^2} (t - M_2^2)(u - M_2^2) |\epsilon_2^\pm \cdot \epsilon_1^\pm|^2 + \mathcal{O}\left(\frac{m_W^2}{M_2^2}\right) \quad (\text{E.85b})$$

$$\text{Re} \left[\overline{\mathcal{M}_t \mathcal{M}_s^\dagger} \right] = \frac{g^4 c_W^2}{s} (u - M_2^2) |\epsilon_2^\pm \cdot \epsilon_1^\pm|^2 + \mathcal{O}\left(\frac{m_W^2}{M_2^2}, \epsilon\right). \quad (\text{E.85c})$$

Furthermore also here the total amplitude for the emission of one transverse and one longitudinal bosons¹ is of order (m_W^2/M_2^2) and so don not contribute to the total amplitude of the process. Therefore as above the total average square amplitude for the process $\tilde{W}\tilde{W}^\pm \rightarrow \gamma W^\pm$ is equal to

$$\begin{aligned} |\overline{\mathcal{M}_{\gamma W^\pm}}|^2 &= \sum_{(\pm\pm)} |\overline{\mathcal{M}_t}|^2 + |\overline{\mathcal{M}_s}|^2 + 2 \text{Re} \left[\overline{\mathcal{M}_t \mathcal{M}_s^\dagger} \right] \\ &= 2g^4 s_W^2 \frac{u - M_2^2}{t - M_2^2} + 4 \frac{g^4 s_W^2}{s^2} (t - M_2^2)(u - M_2^2) + 4 \frac{g^4 s_W^2}{s} (u - M_2^2) + \mathcal{O}\left(\frac{m_W^2}{M_2^2}, \epsilon\right) \\ &= g^4 s_W^2 + \mathcal{O}\left(\frac{m_W^2}{M_2^2}, \epsilon\right) \end{aligned} \quad (\text{E.86})$$

The last process which contributes to the co-annihilation between \tilde{W} and \tilde{W}^\pm is $\tilde{W}\tilde{W}^\pm \rightarrow \bar{f}_L f_L'$ where with f_L and f_L' we denote two SM left-handed fermions². The Feynman diagram for this process is



with associated amplitude given by

$$\begin{aligned} i\mathcal{M}_{ff'} &= \frac{g^2}{\sqrt{2}(s - m_W^2)} \bar{v}(k_2, s_2) \gamma^\mu u(k_1, s_1) \left[-g_{\mu\nu} + \frac{(k_1 + k_2)_\mu (k_1 + k_2)_\nu}{m_W^2} \right] \bar{u}(p_1, r_1) \gamma_\nu P_L v(p_2, r_2) \\ &= -\frac{g^2}{\sqrt{2}(s - m_W^2)} \bar{v}(k_2, s_2) \gamma^\mu u(k_1, s_1) \bar{u}(p_1, r_1) \gamma_\mu P_L v(p_2, r_2) \end{aligned} \quad (\text{E.87})$$

where we have chosen the verse of the fermionic flow from up to down for both the fermion chains and we used the Feynman rules given in Appendix B. Note that the second term in the square bracket can be removed using the Dirac equation. In the limit $M_2 \gg m_W, m_f$ where with m_f we denote the mass of an outgoing fermion, the average of the square amplitude given

¹Note that, here, this is the only possible configuration which involve longitudinal polarizations; in fact the photon, being a massless gauge boson, has only two transverse polarizations.

²Note that from charge and flavor conservation the possible couples of SM fermions are $(e, \nu_e), (\mu, \nu_\mu), (\tau, \nu_\tau), (q, d), (c, s), (t, b)$.

in Eq. (E.87) is equal to

$$\begin{aligned}
|\overline{\mathcal{M}}_{ff'}|^2 &= \frac{g^4}{8s^2} \text{Tr}\{(k_2 - M_2)\gamma^\mu(k_1 + M_2)\gamma^\nu\} \text{Tr}\{\not{p}_1\gamma_\mu\not{p}_2\gamma_\nu P_L\} + \mathcal{O}\left(\frac{m_W^2}{M_2^2}\right) \\
&= 2\frac{g^4}{s^2} \left\{ (k_1 \cdot p_2)(k_2 \cdot p_1) + (k_1 \cdot p_1)(k_2 \cdot p_2) + (p_1 \cdot p_2)M_2^2 \right. \\
&\quad \left. - i\epsilon_{\alpha\beta\mu\nu} [k_2^\mu k_1^\nu + k_2^\nu k_1^\mu - g^{\mu\nu}((k_1 \cdot k_2) + M_2^2)] p_1^\alpha p_2^\beta \right\} + \mathcal{O}\left(\frac{m_W^2}{M_2^2}\right) \\
&= \frac{g^4}{s^2} \left[\frac{(u - M_2^2)^2}{2} + \frac{(t - M_2^2)^2}{2} + M_2^2 s \right] + \mathcal{O}\left(\frac{m_W^2}{M_2^2}\right)
\end{aligned} \tag{E.88}$$

where we used the trace formulae given in Eqs. (E.15). Note that the term proportional to the antisymmetric tensor $\epsilon_{\alpha\beta\mu\nu}$ vanishes because of the symmetry, under the exchange of $\mu \leftrightarrow \nu$ indices, of the tensor $[k_2^\mu k_1^\nu + k_2^\nu k_1^\mu - g^{\mu\nu}((k_1 \cdot k_2) + M_2^2)]$. Substituting into the above result the expansions of the Mandelstam variables given in Eqs. (E.6) we find that

$$|\overline{\mathcal{M}}_{ff'}|^2 = \frac{g^4}{2} + \mathcal{O}\left(\frac{m_W^2}{M_2^2}, \epsilon\right). \tag{E.89}$$

To find the total cross-section for the co-annihilation among \tilde{W} and \tilde{W}^\pm we have to sum the total average square amplitudes associated to the various contributing processes. Note that this is possible, at this level, because in the assumed limit ($M_2 \gg m_W, m_{Z^0}, m_f$) the final states can be considered all massless and so the phase spaces associated to them would be identical. Thus the total average square amplitude for the co-annihilation between \tilde{W} and \tilde{W}^\pm is

$$\begin{aligned}
|\overline{\mathcal{M}}_{\tilde{W}\tilde{W}^\pm}|^2 &= \sum_{f,f'} N_c |\overline{\mathcal{M}}_{ff'}|^2 + |\overline{\mathcal{M}}_{\gamma W^\pm}|^2 + |\overline{\mathcal{M}}_{Z^0 W^\pm}|^2 \\
&= 6g^4 + g^4 c_W^2 + g^4 s_W^2 + \mathcal{O}\left(\frac{m_W^2}{M_2^2}, \epsilon\right) \\
&= 7g^4 + \mathcal{O}\left(\frac{m_W^2}{M_2^2}, \epsilon\right)
\end{aligned} \tag{E.90}$$

where we used the results given in Eq. (E.83), Eq. (E.86) and Eq. (E.89). Note that in the above expression the sum run over the admitted final SM fermion states and N_c is a colour factor, which is $N_c = 3$ for quarks and $N_c = 1$ for leptons. Inserting this expression into the cross-section times velocity formula, Eq. (E.14), we obtain that

$$\sigma_{\tilde{W}\tilde{W}^\pm} v = \frac{7g^4}{32\pi M_2^2} + \mathcal{O}\left(\frac{m_W^2}{M_2^2}, \epsilon\right). \tag{E.91}$$

Now we go on computing the co-annihilation between two charge Winos with opposite charge. The processes which contribute to this co-annihilation are listed in Table 4.8. We start by considering the process $\tilde{W}^\pm \tilde{W}^\mp \rightarrow W^\pm W^\mp$, which is described by the following Feynman diagrams

$$\begin{aligned}
&\begin{array}{c} \tilde{W}^\pm, k_1 \quad W^\pm, p_1 \\ \diagdown \quad \diagup \\ \tilde{W} \\ \diagup \quad \diagdown \\ \tilde{W}^\mp, k_2 \quad W^\mp, p_2 \end{array} \quad \begin{array}{c} \tilde{W}^\pm, k_1 \quad W^\pm, p_2 \\ \diagdown \quad \diagup \\ Z^0 \\ \diagup \quad \diagdown \\ \tilde{W}, k_2 \quad W^\mp, p_1 \end{array} \quad \begin{array}{c} \tilde{W}^\pm, k_1 \quad W^\pm, p_2 \\ \diagdown \quad \diagup \\ \gamma \\ \diagup \quad \diagdown \\ \tilde{W}^\mp, k_2 \quad W^\mp, p_1 \end{array}
\end{aligned} \tag{E.92}$$

The related amplitudes are equal to

$$\begin{aligned}
i\mathcal{M}_t &= \frac{g^2}{t - M_2^2} [2\bar{v}(k_2, s_2)\gamma^\nu u(k_1, s_1)\epsilon_\nu(p_2)(q \cdot \epsilon_\mu(p_1)) \\
&\quad + \bar{v}(k_2, s_2)\gamma^\nu\gamma^\mu\not{p}_1 u(k_1, s_1)\epsilon_\nu(p_2)\epsilon_\mu(p_1)]
\end{aligned}$$

for the t -channel process,

$$\begin{aligned} i\mathcal{M}_{sZ^0} &= \frac{g^2 c_W^2}{s - m_W^2} \bar{v}(k_2, s_2) \gamma^\mu u(k_1, s_1) \left[-g_{\mu\nu} + \frac{(k_1 + k_2)_\mu (k_1 + k_2)_\nu}{m_W^2} \right] \Gamma^{\nu\alpha\beta} \epsilon_\alpha(p_1) \epsilon_\beta(p_2) \\ &= -\frac{g^2 s_W}{s - m_W^2} \bar{v}(k_2, s_2) \gamma^\mu u(k_1, s_1) g_{\mu\nu} \Gamma^{\nu\alpha\beta} \epsilon_\alpha(p_1) \epsilon_\beta(p_2) \end{aligned} \quad (\text{E.93})$$

for the s -channel process mediated by the Z^0 boson and

$$i\mathcal{M}_{s\gamma} = -\frac{g^2 s_W^2}{s - m_W^2} \bar{v}(k_2, s_2) \gamma^\mu u(k_1, s_1) g_{\mu\nu} \Gamma^{\nu\alpha\beta} \epsilon_\alpha(p_1) \epsilon_\beta(p_2). \quad (\text{E.94})$$

for the s -channel process mediated by the photon. Note that in the expression for the amplitude mediated by the Z^0 boson we used the Dirac equation. As usual we compute the average over initial states of the square amplitudes and of the interference terms for definite final polarization states. As first we consider the transverse polarizations. Exploiting the results found for the previous processes it is possible to argue that the average of the square amplitudes and of the interference terms on transverse polarizations read as

$$|\overline{\mathcal{M}_t}|^2 = \frac{g^4 c_W^2}{2} \frac{u - M_2^2}{t - M_2^2} \mathcal{P}(\pm, \pm) + \mathcal{O}\left(\frac{m_W^2}{M_2^2}, \epsilon\right) \quad (\text{E.95a})$$

$$|\overline{\mathcal{M}_{sZ^0}}|^2 = 2 \frac{g^4 c_W^4}{s^2} (t - M_2^2)(u - M_2^2) |(\epsilon_2^\pm \cdot \epsilon_1^\pm)|^2 + \mathcal{O}\left(\frac{m_W^2}{M_2^2}\right) \quad (\text{E.95b})$$

$$|\overline{\mathcal{M}_{s\gamma}}|^2 = 2 \frac{g^4 s_W^4}{s^2} (t - M_2^2)(u - M_2^2) |(\epsilon_2^\pm \cdot \epsilon_1^\pm)|^2 + \mathcal{O}\left(\frac{m_W^2}{M_2^2}\right) \quad (\text{E.95c})$$

$$\text{Re} \left[\overline{\mathcal{M}_t \mathcal{M}_{sZ^0}^\dagger} \right] = \frac{g^4 c_W^2}{s} (u - M_2^2) |(\epsilon_2^\pm \cdot \epsilon_1^\pm)|^2 + \mathcal{O}\left(\frac{m_W^2}{M_2^2}, \epsilon\right) \quad (\text{E.95d})$$

$$\text{Re} \left[\overline{\mathcal{M}_t \mathcal{M}_{s\gamma}^\dagger} \right] = \frac{g^4 s_W^2}{s} (u - M_2^2) |(\epsilon_2^\pm \cdot \epsilon_1^\pm)|^2 + \mathcal{O}\left(\frac{m_W^2}{M_2^2}, \epsilon\right) \quad (\text{E.95e})$$

$$\text{Re} \left[\overline{\mathcal{M}_{sZ^0} \mathcal{M}_{s\gamma}^\dagger} \right] = 2 \frac{g^4 c_W^2 s_W^2}{s^2} (t - M_2^2)(u - M_2^2) |(\epsilon_2^\pm \cdot \epsilon_1^\pm)|^2 + \mathcal{O}\left(\frac{m_W^2}{M_2^2}\right). \quad (\text{E.95f})$$

For what concern the longitudinal polarizations, replacing the polarization vectors with the approximation given Eq. (E.4) into the three amplitudes given in Eq. (E.93), Eq. (E.93) and Eq. (E.94), and applying the same methods used in the previous cases we find that

$$i\mathcal{M}_t^{LL} = -\frac{g^2}{m_W^2} \bar{v}(k_2, s_2) \not{p}_2 u(k_1, s_1) + \mathcal{O}\left(\frac{m_W^2}{M_2^2}\right) \quad (\text{E.96a})$$

$$i\mathcal{M}_{sZ^0}^{LL} = \frac{g^2 c_W^2}{m_W^2} \bar{v}(k_2, s_2) \not{p}_2 u(k_1, s_1) + \mathcal{O}\left(\frac{m_W^2}{M_2^2}\right) \quad (\text{E.96b})$$

$$i\mathcal{M}_{s\gamma}^{LL} = \frac{g^2 s_W^2}{m_W^2} \bar{v}(k_2, s_2) \not{p}_2 u(k_1, s_1) + \mathcal{O}\left(\frac{m_W^2}{M_2^2}\right). \quad (\text{E.96c})$$

Thus summing up together these contributes we have that

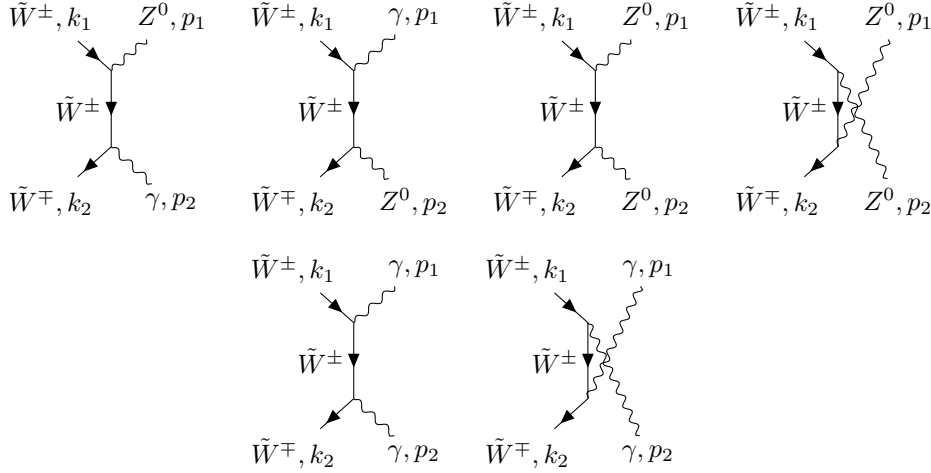
$$i\mathcal{M}^{LL} = i\mathcal{M}_t^{LL} + i\mathcal{M}_{sZ^0}^{LL} + i\mathcal{M}_{s\gamma}^{LL} = \mathcal{O}\left(\frac{m_W^2}{M_2^2}\right) \quad (\text{E.97})$$

and so as occurred for the previous processes the longitudinal bosons, in the assumed limit, give a contribution which is of order (m_W^2/M_2^2) . Therefore the total average square amplitude

for the annihilation process $\tilde{W}^\pm \tilde{W}^\mp \rightarrow W^\pm W^\mp$ becomes

$$\begin{aligned}
|\overline{\mathcal{M}_{W^\pm W^\mp}}|^2 &= \sum_{(\pm\pm)} |\overline{\mathcal{M}_t}|^2 + |\overline{\mathcal{M}_{s Z^0}}|^2 + |\overline{\mathcal{M}_{s \gamma}}|^2 + 2 \operatorname{Re} \left[\overline{\mathcal{M}_t \mathcal{M}_{s Z^0}^\dagger} \right] + 2 \operatorname{Re} \left[\overline{\mathcal{M}_t \mathcal{M}_{s \gamma}^\dagger} \right] \\
&\quad + 2 \operatorname{Re} \left[\overline{\mathcal{M}_{s Z^0} \mathcal{M}_{s \gamma}^\dagger} \right] \\
&= 2g^4 c_W^2 \frac{u - M_2^2}{t - M_2^2} + 4 \frac{g^4 c_W^4}{s^2} (t - M_2^2)(u - M_2^2) + 4 \frac{g^4 s_W^4}{s^2} (t - M_2^2)(u - M_2^2) \\
&\quad + 4 \frac{g^4 c_W^2}{s} (u - M_2^2) + 4 \frac{g^4 s_W^2}{s} (u - M_2^2) + 8 \frac{g^4 c_W^2 s_W^2}{s^2} (t - M_2^2)(u - M_2^2) + \mathcal{O} \left(\frac{m_W^2}{M_2^2}, \epsilon \right) \\
&= g^4 + \mathcal{O} \left(\frac{m_W^2}{M_2^2}, \epsilon \right)
\end{aligned} \tag{E.98}$$

where in the last step we used the expansion of the Mandelstam variables given in Eqs. (E.6). The other processes which contributes to the co-annihilation among \tilde{W}^\pm and \tilde{W}^\mp are $\tilde{W}^\pm \tilde{W}^\mp \rightarrow Z^0 \gamma$, $\tilde{W}^\pm \tilde{W}^\mp \rightarrow Z^0 Z^0$ and $\tilde{W}^\pm \tilde{W}^\mp \rightarrow \gamma \gamma$ with associated Feynman diagrams given by



Choosing the verse of the fermionic flow from up to down, we have that the related amplitudes are equal to

$$\begin{aligned}
i\mathcal{M}_{t Z^0 \gamma} &= \frac{g^2 c_W s_W}{t - M_2^2} [2\bar{v}(k_2, s_2) \gamma^\nu u(k_1, s_1) \epsilon_\nu(p_2) (q \cdot \epsilon_\mu(p_1)) \\
&\quad + \bar{v}(k_2, s_2) \gamma^\nu \gamma^\mu \not{p}_1 u(k_1, s_1) \epsilon_\nu(p_2) \epsilon_\mu(p_1)]
\end{aligned} \tag{E.99a}$$

$$\begin{aligned}
i\mathcal{M}_{u Z^0 \gamma} &= \frac{g^2 c_W s_W}{u - M_2^2} [2\bar{v}(k_2, s_2) \gamma^\nu u(k_1, s_1) \epsilon_\nu(p_1) (q' \cdot \epsilon_\mu(p_2)) \\
&\quad + \bar{v}(k_2, s_2) \gamma^\nu \gamma^\mu \not{p}_2 u(k_1, s_1) \epsilon_\nu(p_1) \epsilon_\mu(p_2)]
\end{aligned} \tag{E.99b}$$

for the process $\tilde{W}^\pm \tilde{W}^\mp \rightarrow Z^0 \gamma$,

$$\begin{aligned}
i\mathcal{M}_{t Z^0 Z^0} &= \frac{g^2 c_W^2}{t - M_2^2} [2\bar{v}(k_2, s_2) \gamma^\nu u(k_1, s_1) \epsilon_\nu(p_2) (q \cdot \epsilon_\mu(p_1)) \\
&\quad + \bar{v}(k_2, s_2) \gamma^\nu \gamma^\mu \not{p}_1 u(k_1, s_1) \epsilon_\nu(p_2) \epsilon_\mu(p_1)]
\end{aligned} \tag{E.100a}$$

$$\begin{aligned}
i\mathcal{M}_{u Z^0 Z^0} &= \frac{g^2 c_W^2}{u - M_2^2} [2\bar{v}(k_2, s_2) \gamma^\nu u(k_1, s_1) \epsilon_\nu(p_1) (q' \cdot \epsilon_\mu(p_2)) \\
&\quad + \bar{v}(k_2, s_2) \gamma^\nu \gamma^\mu \not{p}_2 u(k_1, s_1) \epsilon_\nu(p_1) \epsilon_\mu(p_2)]
\end{aligned} \tag{E.100b}$$

for the process $\tilde{W}^\pm \tilde{W}^\mp \rightarrow Z^0 Z^0$ and

$$i\mathcal{M}_{t\ \gamma\gamma} = \frac{g^2 s_W^2}{t - M_2^2} [2\bar{v}(k_2, s_2) \gamma^\nu u(k_1, s_1) \epsilon_\nu(p_2) (q \cdot \epsilon_\mu(p_1)) \\ + \bar{v}(k_2, s_2) \gamma^\nu \gamma^\mu \not{p}_1 u(k_1, s_1) \epsilon_\nu(p_2) \epsilon_\mu(p_1)] \quad (\text{E.101a})$$

$$i\mathcal{M}_{u\ \gamma\gamma} = \frac{g^2 s_W^2}{u - M_2^2} [2\bar{v}(k_2, s_2) \gamma^\nu u(k_1, s_1) \epsilon_\nu(p_1) (q' \cdot \epsilon_\mu(p_2)) \\ + \bar{v}(k_2, s_2) \gamma^\nu \gamma^\mu \not{p}_2 u(k_1, s_1) \epsilon_\nu(p_1) \epsilon_\mu(p_2)] \quad (\text{E.101b})$$

for the process $\tilde{W}^\pm \tilde{W}^\mp \rightarrow \gamma\gamma$. In the above expressions the transferred momentum q' is $q'_\mu = k_{1\mu} - p_{2\mu}$. Noting that the amplitudes just given, apart some vertex coefficients, are identical to the ones given for the Wino annihilation process, see Eqs. (E.46), we can use the results found above to write down the average over initial states of the square amplitudes for transverse polarizations. In particular note that for the u -channel processes the first term of the amplitudes is unimportant for transverse polarizations. Thus on transverse polarizations we have

$$|\overline{\mathcal{M}_{t\ Z^0\gamma}}|^2 = \frac{g^4 s_W^2 c_W^2}{2} \frac{u - M_2^2}{t - M_2^2} \mathcal{P}(\pm, \pm) + \mathcal{O}\left(\frac{m_W^2}{M_2^2}, \epsilon\right) \quad (\text{E.102a})$$

$$|\overline{\mathcal{M}_{u\ Z^0\gamma}}|^2 = \frac{g^4 s_W^2 c_W^2}{2} \frac{t - M_2^2}{u - M_2^2} \mathcal{P}(\pm, \pm) + \mathcal{O}\left(\frac{m_W^2}{M_2^2}, \epsilon\right) \quad (\text{E.102b})$$

$$\text{Re} \left[\overline{\mathcal{M}_{t\ Z^0\gamma} \mathcal{M}_{u\ Z^0\gamma}^\dagger} \right] = -\frac{g^4 s_W^2 c_W^2}{2} \mathcal{P}'(\pm, \pm) + \mathcal{O}\left(\frac{m_W^2}{M_2^2}, \epsilon\right) \quad (\text{E.102c})$$

for the process $\tilde{W}^\pm \tilde{W}^\mp \rightarrow Z^0 \gamma$,

$$|\overline{\mathcal{M}_{t\ Z^0 Z^0}}|^2 = \frac{g^4 c_W^4}{2} \frac{u - M_2^2}{t - M_2^2} \mathcal{P}(\pm, \pm) + \mathcal{O}\left(\frac{m_W^2}{M_2^2}, \epsilon\right) \quad (\text{E.103a})$$

$$|\overline{\mathcal{M}_{u\ Z^0 Z^0}}|^2 = \frac{g^4 c_W^4}{2} \frac{t - M_2^2}{u - M_2^2} \mathcal{P}(\pm, \pm) + \mathcal{O}\left(\frac{m_W^2}{M_2^2}, \epsilon\right) \quad (\text{E.103b})$$

$$\text{Re} \left[\overline{\mathcal{M}_{t\ Z^0 Z^0} \mathcal{M}_{u\ Z^0 Z^0}^\dagger} \right] = -\frac{g^4 c_W^4}{2} \mathcal{P}'(\pm, \pm) + \mathcal{O}\left(\frac{m_W^2}{M_2^2}, \epsilon\right) \quad (\text{E.103c})$$

for what concern the process $\tilde{W}^\pm \tilde{W}^\mp \rightarrow Z^0 Z^0$ and

$$|\overline{\mathcal{M}_{t\ \gamma\gamma}}|^2 = \frac{g^4 s_W^4}{2} \frac{u - M_2^2}{t - M_2^2} \mathcal{P}(\pm, \pm) + \mathcal{O}\left(\frac{m_W^2}{M_2^2}, \epsilon\right) \quad (\text{E.104a})$$

$$|\overline{\mathcal{M}_{u\ \gamma\gamma}}|^2 = \frac{g^4 s_W^4}{2} \frac{t - M_2^2}{u - M_2^2} \mathcal{P}(\pm, \pm) + \mathcal{O}\left(\frac{m_W^2}{M_2^2}, \epsilon\right) \quad (\text{E.104b})$$

$$\text{Re} \left[\overline{\mathcal{M}_{t\ \gamma\gamma} \mathcal{M}_{u\ \gamma\gamma}^\dagger} \right] = -\frac{g^4 s_W^4}{2} \mathcal{P}'(\pm, \pm) + \mathcal{O}\left(\frac{m_W^2}{M_2^2}, \epsilon\right) \quad (\text{E.104c})$$

for the process $\tilde{W}^\pm \tilde{W}^\mp \rightarrow \gamma\gamma$. The longitudinal polarizations as in the previous cases, in the limit where $M_2 \gg m_W$ do not contribute. To see this we can substitute the approximation for longitudinal polarization vectors given in Eq. (E.4) into the various amplitudes given in Eqs. (E.99) and Eqs. (E.100)³. Thus for example the amplitudes in Eqs. (E.100) on longitudinal bosons read as

$$i\mathcal{M}_{t\ Z^0 Z^0}^{LL} = -\frac{g^2 c_W^2}{m_W^2} \bar{v}(k_2, s_2) \not{p}_2 u(k_1, s_1) + \mathcal{O}\left(\frac{m_W^2}{M_2^2}\right) \quad (\text{E.105a})$$

$$i\mathcal{M}_{u\ Z^0 Z^0}^{LL} = -\frac{g^2 c_W^2}{m_W^2} \bar{v}(k_2, s_2) \not{p}_1 u(k_1, s_1) + \mathcal{O}\left(\frac{m_W^2}{M_2^2}\right) \\ = +\frac{g^2 c_W^2}{m_W^2} \bar{v}(k_2, s_2) \not{p}_2 u(k_1, s_1) + \mathcal{O}\left(\frac{m_W^2}{M_2^2}\right) \quad (\text{E.105b})$$

³Note that these arguments do not apply to the process $\tilde{W}^\pm \tilde{W}^\mp \rightarrow \gamma\gamma$ because the two final photons can have only transverse polarizations.

where in the last step we used the conservation of the four momentum and the Dirac equation. The sum of the two contributes is

$$i\mathcal{M}_{Z^0 Z^0}^{LL} = i\mathcal{M}_{t Z^0 Z^0}^{LL} + i\mathcal{M}_{u Z^0 Z^0}^{LL} = \mathcal{O}\left(\frac{m_W^2}{M_2^2}\right) \quad (\text{E.106})$$

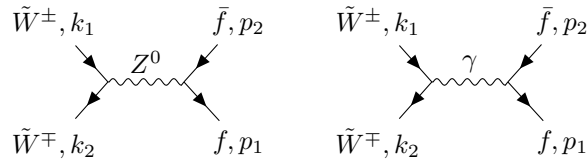
which shows that, at the leading order, the longitudinal polarizations do not contribute to the total amplitude. Note that a similar result can be found for the emission of one longitudinal and one transverse boson final states. As a consequence the total average square amplitudes for the processes $\tilde{W}^\pm \tilde{W}^\mp \rightarrow Z^0 \gamma$, $\tilde{W}^\pm \tilde{W}^\mp \rightarrow Z^0 Z^0$ and $\tilde{W}^\pm \tilde{W}^\mp \rightarrow \gamma \gamma$ are respectively equal to

$$\begin{aligned} |\overline{\mathcal{M}_{Z^0 \gamma}}|^2 &= \sum_{(\pm \pm)} |\overline{\mathcal{M}_{t Z^0 \gamma}}|^2 + |\overline{\mathcal{M}_{u Z^0 \gamma}}|^2 + 2 \operatorname{Re} \left[\overline{\mathcal{M}_{t Z^0 \gamma} \mathcal{M}_{u Z^0 \gamma}^\dagger} \right] \\ &= 2g^4 s_W^2 c_W^2 \left[\frac{u - M_2^2}{t - M_2^2} + \frac{t - M_2^2}{u - M_2^2} \right] + \mathcal{O}\left(\frac{m_W^2}{M_2^2}, \epsilon\right) \\ &= 4g^4 s_W^2 c_W^2 + \mathcal{O}\left(\frac{m_W^2}{M_2^2}, \epsilon\right) \end{aligned} \quad (\text{E.107a})$$

$$\begin{aligned} |\overline{\mathcal{M}_{Z^0 Z^0}}|^2 &= \sum_{(\pm \pm)} |\overline{\mathcal{M}_{t Z^0 Z^0}}|^2 + |\overline{\mathcal{M}_{u Z^0 Z^0}}|^2 + 2 \operatorname{Re} \left[\overline{\mathcal{M}_{t Z^0 Z^0} \mathcal{M}_{u Z^0 Z^0}^\dagger} \right] \\ &= 2g^4 c_W^4 \left[\frac{u - M_2^2}{t - M_2^2} + \frac{t - M_2^2}{u - M_2^2} \right] + \mathcal{O}\left(\frac{m_W^2}{M_2^2}, \epsilon\right) \\ &= 4g^4 c_W^4 + \mathcal{O}\left(\frac{m_W^2}{M_2^2}, \epsilon\right) \end{aligned} \quad (\text{E.107b})$$

$$\begin{aligned} |\overline{\mathcal{M}_{\gamma \gamma}}|^2 &= \sum_{(\pm \pm)} |\overline{\mathcal{M}_{t \gamma \gamma}}|^2 + |\overline{\mathcal{M}_{u \gamma \gamma}}|^2 + 2 \operatorname{Re} \left[\overline{\mathcal{M}_{t \gamma \gamma} \mathcal{M}_{u \gamma \gamma}^\dagger} \right] \\ &= 2g^4 s_W^4 \left[\frac{u - M_2^2}{t - M_2^2} + \frac{t - M_2^2}{u - M_2^2} \right] + \mathcal{O}\left(\frac{m_W^2}{M_2^2}, \epsilon\right) \\ &= 4g^4 s_W^4 + \mathcal{O}\left(\frac{m_W^2}{M_2^2}, \epsilon\right) \end{aligned} \quad (\text{E.107c})$$

From Table 4.8 the last process which contributes to the $\tilde{W}^\pm \tilde{W}^\mp$ co-annihilation is $\tilde{W}^\pm \tilde{W}^\mp \rightarrow \bar{f} f$ where as usual f denote a SM fermion. Note that now the final states are fermion anti-fermion pairs. The Feynman diagrams which describe this process are



which have amplitudes equal to

$$\begin{aligned} i\mathcal{M}_{Z^0 ff} &= \frac{g^2}{2(s - m_W^2)} \bar{v}(k_2, s_2) \gamma^\mu u(k_1, s_1) \left[-g_{\mu\nu} + \frac{(k_1 + k_2)_\mu (k_1 + k_2)_\nu}{m_{Z^0}^2} \right] \times \\ &\quad \bar{u}(p_1, r_1) \gamma_\nu (P_L - 2e_q s_W^2) v(p_2, r_2) \\ &= -\frac{g^2}{2s} \bar{v}(k_2, s_2) \gamma^\mu u(k_1, s_1) \bar{u}(p_1, r_1) \gamma_\mu (P_L - 2e_q s_W^2) v(p_2, r_2) + \mathcal{O}\left(\frac{m_W^2}{M_2^2}\right) \end{aligned} \quad (\text{E.108a})$$

$$i\mathcal{M}_{\gamma ff} = -\frac{g^2 s_W^2}{s} \bar{v}(k_2, s_2) \gamma^\mu u(k_1, s_1) \bar{u}(p_1, r_1) \gamma_\mu v(p_2, r_2). \quad (\text{E.108b})$$

where with e_q we refer to the electric charge of the outgoing fermions in unit of e . Summing

these contributions we have that the total amplitude for the process $\tilde{W}^\pm \tilde{W}^\mp \rightarrow \bar{f} f$ is

$$\begin{aligned} i\mathcal{M}_{ff} &= i\mathcal{M}_{Z^0 ff} + i\mathcal{M}_{\gamma ff} \\ &= \frac{g^2}{2s} \bar{v}(k_2, s_2) \gamma^\mu u(k_1, s_1) \bar{u}(p_1, r_1) \gamma_\mu P_L v(p_2, r_2) + \mathcal{O}\left(\frac{m_W^2}{M_2^2}\right). \end{aligned} \quad (\text{E.109})$$

Thus using the result found for the process $\tilde{W} \tilde{W}^\pm \rightarrow \bar{f}_L f'_L$ given in Eq. (E.89) we have that the total square amplitude for the annihilation between $\tilde{W}^\pm \tilde{W}^\mp$ into final fermion anti fermion pairs is equal to

$$\begin{aligned} |\overline{\mathcal{M}_{ff}}|^2 &= \frac{g^4}{2s^2} \left[\frac{(u - M_2^2)^2}{2} + \frac{(t - M_2^2)^2}{2} + M_2^2 s \right] + \mathcal{O}\left(\frac{m_W^2}{M_2^2}\right) \\ &= \frac{g^4}{4} + \mathcal{O}\left(\frac{m_W^2}{M_2^2}, \epsilon\right). \end{aligned} \quad (\text{E.110})$$

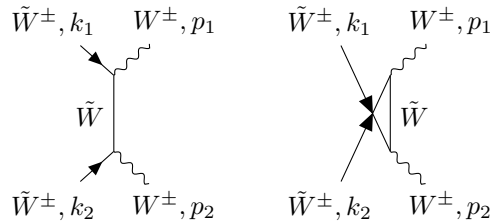
Remembering that in the limit where $M_2 \gg m_W, m_{Z^0}, m_f$ all the final states can be considered massless, to find the total cross-section times velocity for the co-annihilation between $\tilde{W}^\pm \tilde{W}^\mp$, we sum all the total average square amplitudes of the various contributing processes and then we substitute the result into Eq. (E.14). So using the results given in Eq. (E.98), Eqs. (E.107) and Eq. (E.110) the total average square amplitude for the $\tilde{W}^\pm \tilde{W}^\mp$ co-annihilation is

$$\begin{aligned} |\overline{\mathcal{M}_{\tilde{W}^\pm \tilde{W}^\mp}}|^2 &= \sum_f N_c |\overline{\mathcal{M}_{ff}}|^2 + |\overline{\mathcal{M}_{W^\pm W^\mp}}|^2 + |\overline{\mathcal{M}_{Z^0 \gamma}}|^2 + \frac{1}{2} |\overline{\mathcal{M}_{Z^0 Z^0}}|^2 + \frac{1}{2} |\overline{\mathcal{M}_{\gamma \gamma}}|^2 \\ &= 6g^4 + g^4 + 2g^4 (2c_W^2 s_W^2 + c_W^4 + s_W^4) \mathcal{O}\left(\frac{m_W^2}{M_2^2}, \epsilon\right) \\ &= 9g^4 + \mathcal{O}\left(\frac{m_W^2}{M_2^2}, \epsilon\right). \end{aligned} \quad (\text{E.111})$$

where N_c is the colour factor defined above. Note the appearance of the pre-factor 1/2 in front of $|\overline{\mathcal{M}_{Z^0 Z^0}}|^2$ and $|\overline{\mathcal{M}_{\gamma \gamma}}|^2$. This is a symmetry factor which is due to the fact that the final particles are equals. Substituting this result into Eq. (E.14) we find that

$$\sigma_{\tilde{W}^\pm \tilde{W}^\mp} v = \frac{9g^4}{32\pi M_2^2} + \mathcal{O}\left(\frac{m_W^2}{M_2^2}, \epsilon\right). \quad (\text{E.112})$$

The last co-annihilation process which is important for the computation of the relic density associated to a pure Wino LSP, is the one between two charge Winos with identical charge, schematically $\tilde{W}^\pm \tilde{W}^\pm \rightarrow W^\pm W^\pm$. This process can occur only via t/u -channel exchange of a neutral Wino. The related Feynman diagrams are



with associated amplitudes given by

$$\begin{aligned} i\mathcal{M}_t &= \frac{g^2}{t - M_2^2} [2\bar{v}(k_2, s_2) \gamma^\nu u(k_1, s_1) \epsilon_\nu(p_2) (q \cdot \epsilon_\mu(p_1)) \\ &\quad + \bar{v}(k_2, s_2) \gamma^\nu \gamma^\mu \not{p}_1 u(k_1, s_1) \epsilon_\nu(p_2) \epsilon_\mu(p_1)], \end{aligned} \quad (\text{E.113a})$$

$$\begin{aligned} i\mathcal{M}_u &= -\frac{g^2}{u - M_2^2} [2\bar{v}(k_1, s_1) \gamma^\nu u(k_2, s_2) \epsilon_\nu(p_2) (q' \cdot \epsilon_\mu(p_1)) \\ &\quad + \bar{v}(k_1, s_1) \gamma^\nu \gamma^\mu \not{p}_1 u(k_2, s_2) \epsilon_\nu(p_2) \epsilon_\mu(p_1)]. \end{aligned} \quad (\text{E.113b})$$

Note that, because we have assumed that \tilde{W} and \tilde{W}^\pm have the same mass, these amplitudes are exactly identical to the one given in Eqs. (E.46) for the annihilation between two neutral Winos. Therefore performing the same steps as above the total average square amplitude associated to the process $\tilde{W}^\pm \tilde{W}^\pm \rightarrow W^\pm W^\pm$ is

$$|\overline{\mathcal{M}}_{\tilde{W}^\pm \tilde{W}^\pm}|^2 = 4g^4 + \mathcal{O}\left(\frac{m_W^2}{M_2^2}, \epsilon\right) \quad (\text{E.114})$$

and so substituting this result into Eq. (E.14), the cross-section times velocity is equal to

$$\sigma_{\tilde{W}^\pm \tilde{W}^\pm v} = \frac{1}{2} \left(\frac{g^4}{8\pi M_2^2} \right) + \mathcal{O}\left(\frac{m_W^2}{M_2^2}, \epsilon\right) = \frac{g^4}{16\pi M_2^2} + \mathcal{O}\left(\frac{m_W^2}{M_2^2}, \epsilon\right). \quad (\text{E.115})$$

where appears the symmetry factor $1/2$ because the final particles are identical.

Summarizing we have that the total annihilation/co-annihilation cross-sections times velocity at the leading order in ϵ and m_W^2/M_2^2 expansions, for a Wino LSP are

$$\sigma_{\tilde{W}\tilde{W}v} = \frac{g^4}{8\pi M_2^2} + \mathcal{O}\left(\frac{m_W^2}{M_2^2}, \epsilon\right) \quad (\text{E.116a})$$

$$\sigma_{\tilde{W}\tilde{W}^\pm v} = \frac{7g^4}{32\pi M_2^2} + \mathcal{O}\left(\frac{m_W^2}{M_2^2}, \epsilon\right) \quad (\text{E.116b})$$

$$\sigma_{\tilde{W}^\pm \tilde{W}^\mp v} = \frac{9g^4}{32\pi M_2^2} + \mathcal{O}\left(\frac{m_W^2}{M_2^2}, \epsilon\right) \quad (\text{E.116c})$$

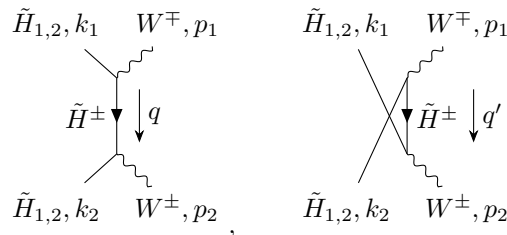
$$\sigma_{\tilde{W}^\pm \tilde{W}^\pm v} = \frac{g^4}{16\pi M_2^2} + \mathcal{O}\left(\frac{m_W^2}{M_2^2}, \epsilon\right). \quad (\text{E.116d})$$

E.5 Pure Higgsino LSP annihilation and co-annihilation cross-sections

In this section we compute the relevant cross-section times velocity for the evaluation of the relic abundance associated to a pure Higgsino LSP. We consider annihilations and co-annihilations among four Higgsino states with equal mass $|\mu|$, namely $\tilde{H}_1, \tilde{H}_2, \tilde{H}^\pm$ where \tilde{H}_1 and \tilde{H}_2 are defined in Eqs. (4.86). In the computation we assume the limit where $|\mu| \gg m_W$ and we take heavy supersymmetric scalars. The various processes are listed in Table 4.5.

The relevant Feynman rules which involve the four Higgsino states can be deduced from the general ones given in Appendix B with the substitutions $N_{14}, N_{13}, N_{23} \rightarrow 1/\sqrt{2}$, $N_{24} \rightarrow -1/\sqrt{2}$, $N_{11}, N_{12} \rightarrow 0$ and $U_{22}, V_{22} \rightarrow 1$, $U_{12}, V_{12} \rightarrow 0$. As we will see many processes will have amplitudes which, apart some vertex coefficients, will be similar to those encountered in the previous section, and so, in the next, we will often refer them.

Looking at Table 4.5 the first process which we take into account is the annihilation between two Higgsino LSP⁴. This annihilation can occur via t/u -channel exchange of a charged Higgsino, \tilde{H}^\pm , into charged SM vector bosons, W^\pm , schematically $\tilde{H}_{1,2} \tilde{H}_{1,2} \rightarrow W^\pm, W^\mp$. The associated Feynman diagrams are



⁴Note that because we assumed that \tilde{H}_1 and \tilde{H}_2 are mass degenerate the annihilation process among two Higgsino LSPs is identical to the one between two Higgsino NLSPs.

Thus we have that the associated amplitudes are

$$i\mathcal{M}_{t W^\pm W^\mp} = \frac{g^2}{4(t - \mu^2)} [2\bar{v}(k_2, s_2)\gamma^\nu u(k_1, s_1)\epsilon_\nu(p_2) (q \cdot \epsilon_\mu(p_1)) + \bar{v}(k_2, s_2)\gamma^\nu \gamma^\mu \not{p}_1 u(k_1, s_1)\epsilon_\nu(p_2)\epsilon_\mu(p_1)], \quad (\text{E.117a})$$

$$i\mathcal{M}_{u W^\pm W^\mp} = -\frac{g^2}{4(u - \mu^2)} [2\bar{v}(k_1, s_1)\gamma^\nu u(k_2, s_2)\epsilon_\nu(p_2) (q' \cdot \epsilon_\mu(p_1)) + \bar{v}(k_1, s_1)\gamma^\nu \gamma^\mu \not{p}_1 u(k_2, s_2)\epsilon_\nu(p_2)\epsilon_\mu(p_1)]. \quad (\text{E.117b})$$

Using the results given in the above section for the annihilation process $\tilde{W}\tilde{W} \rightarrow W^\pm W^\mp$, we have that the average over initial states of the square amplitudes and of the interference term for final transverse polarizations, are equal to

$$|\overline{\mathcal{M}_{t W^\pm W^\mp}}|^2 = \frac{g^4}{32} \frac{u - \mu^2}{t - \mu^2} \mathcal{P}(\pm, \pm) + \mathcal{O}\left(\frac{m_W^2}{\mu^2}, \epsilon\right) \quad (\text{E.118a})$$

$$|\overline{\mathcal{M}_{u W^\pm W^\mp}}|^2 = \frac{g^4}{32} \frac{t - \mu^2}{u - \mu^2} \mathcal{P}(\pm, \pm) + \mathcal{O}\left(\frac{m_W^2}{\mu^2}, \epsilon\right) \quad (\text{E.118b})$$

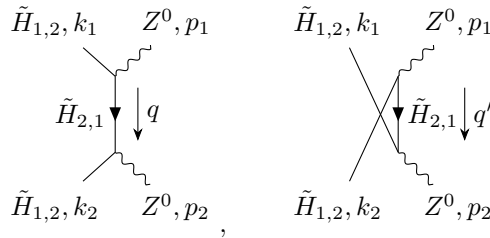
$$\text{Re} \left[\overline{\mathcal{M}_{t W^\pm W^\mp} \mathcal{M}_{u W^\pm W^\mp}^\dagger} \right] = -\frac{g^4}{32} \mathcal{P}'(\pm, \pm) + \mathcal{O}\left(\frac{m_W^2}{\mu^2}, \epsilon\right). \quad (\text{E.118c})$$

The longitudinal polarizations, as occurred in the Wino annihilation case, also here give a contribution which is of order m_W^2/μ^2 . Thus the total average square amplitude associated to the process $\tilde{H}_{1,2}\tilde{H}_{1,2} \rightarrow W^\pm, W^\mp$ is equal to

$$\begin{aligned} |\overline{\mathcal{M}_{W^\pm W^\mp}}|^2 &= \sum_{(\pm\pm)} |\overline{\mathcal{M}_{t W^\pm W^\mp}}|^2 + |\overline{\mathcal{M}_{u W^\pm W^\mp}}|^2 + 2 \text{Re} \left[\overline{\mathcal{M}_{t W^\pm W^\mp} \mathcal{M}_{u W^\pm W^\mp}^\dagger} \right] \\ &= \frac{g^4}{8} \left[\frac{u - \mu^2}{t - \mu^2} + \frac{t - \mu^2}{u - \mu^2} \right] + \mathcal{O}\left(\frac{m_W^2}{\mu^2}, \epsilon\right) \\ &= \frac{g^4}{4} + \mathcal{O}\left(\frac{m_W^2}{\mu^2}, \epsilon\right) \end{aligned} \quad (\text{E.119})$$

where we used the relations given in Eqs. (E.61) and the expansions of the Mandelstam variables given in Eqs. (E.6).

The annihilation between two $\tilde{H}_{1,2}$ can also occur via t/u -channel exchange of a neutral Higgsino, $\tilde{H}_{2,1}$, into two Z^0 bosons, schematically $\tilde{H}_{1,2}\tilde{H}_{1,2} \rightarrow Z^0 Z^0$. The associated Feynman diagrams are



note that the exchange Higgsino must be different from the annihilating ones i.e. if the annihilation occurs between two \tilde{H}_1 the exchange Higgsino would be \tilde{H}_2 and vice versa. The amplitudes for the t and u channels are

$$i\mathcal{M}_{t Z^0 Z^0} = \frac{g^2}{4c_W^2(t - \mu^2)} [2\bar{v}(k_2, s_2)\gamma^\nu u(k_1, s_1)\epsilon_\nu(p_2) (q \cdot \epsilon_\mu(p_1)) + \bar{v}(k_2, s_2)\gamma^\nu \gamma^\mu \not{p}_1 u(k_1, s_1)\epsilon_\nu(p_2)\epsilon_\mu(p_1)], \quad (\text{E.120a})$$

$$i\mathcal{M}_{u Z^0 Z^0} = -\frac{g^2}{4c_W^2(u - \mu^2)} [2\bar{v}(k_1, s_1)\gamma^\nu u(k_2, s_2)\epsilon_\nu(p_2) (q' \cdot \epsilon_\mu(p_1)) + \bar{v}(k_1, s_1)\gamma^\nu \gamma^\mu \not{p}_1 u(k_2, s_2)\epsilon_\nu(p_2)\epsilon_\mu(p_1)]. \quad (\text{E.120b})$$

Exploiting the results for the process $\tilde{H}_{1,2}\tilde{H}_{1,2} \rightarrow W^\pm W^\mp$ we have that, for transverse outgoing bosons, the average over initial states of the squares of the amplitudes just given are

$$|\overline{\mathcal{M}_{t Z^0 Z^0}}|^2 = \frac{g^4}{c_W^4 32} \frac{u - \mu^2}{t - \mu^2} \mathcal{P}(\pm, \pm) + \mathcal{O}\left(\frac{m_W^2}{\mu^2}, \epsilon\right) \quad (\text{E.121a})$$

$$|\overline{\mathcal{M}_{u Z^0 Z^0}}|^2 = \frac{g^4}{c_W^4 32} \frac{t - \mu^2}{u - \mu^2} \mathcal{P}(\pm, \pm) + \mathcal{O}\left(\frac{m_W^2}{\mu^2}, \epsilon\right) \quad (\text{E.121b})$$

$$\text{Re} \left[\overline{\mathcal{M}_{t Z^0 Z^0} \mathcal{M}_{u Z^0 Z^0}^\dagger} \right] = -\frac{g^4}{c_W^4 32} \mathcal{P}'(\pm, \pm) + \mathcal{O}\left(\frac{m_W^2}{\mu^2}, \epsilon\right). \quad (\text{E.121c})$$

As before the contribution of the longitudinal polarizations to the total amplitude is of order m_W^2/μ^2 , this can be seen applying the same procedure used for the annihilation between two Winos, see Eq. (E.62). Thus the total average square amplitude for the process $\tilde{H}_{1,2}\tilde{H}_{1,2} \rightarrow Z^0 Z^0$ is

$$\begin{aligned} |\overline{\mathcal{M}_{Z^0 Z^0}}|^2 &= \sum_{(\pm\pm)} |\overline{\mathcal{M}_{t Z^0 Z^0}}|^2 + |\overline{\mathcal{M}_{u Z^0 Z^0}}|^2 + 2 \text{Re} \left[\overline{\mathcal{M}_{t Z^0 Z^0} \mathcal{M}_{u Z^0 Z^0}^\dagger} \right] \\ &= \frac{g^4}{c_W^4 8} \left[\frac{u - \mu^2}{t - \mu^2} + \frac{t - \mu^2}{u - \mu^2} \right] + \mathcal{O}\left(\frac{m_W^2}{\mu^2}, \epsilon\right) \\ &= \frac{g^4}{c_W^4 4} + \mathcal{O}\left(\frac{m_W^2}{\mu^2}, \epsilon\right) = \frac{g^4}{4} (1 + t_W^2)^2 + \mathcal{O}\left(\frac{m_W^2}{\mu^2}, \epsilon\right) \end{aligned} \quad (\text{E.122})$$

where in the last step we have used the identity $1/c_W^2 \equiv (1 + t_W^2)$.

Therefore the total average square amplitude associated to the annihilation process between two identical neutral Higgsinos $\tilde{H}_{1,2}$ and $\tilde{H}_{1,2}$ is

$$\begin{aligned} |\overline{\mathcal{M}_{\tilde{H}_{1,2}\tilde{H}_{1,2}}}|^2 &= |\overline{\mathcal{M}_{W^\pm W^\mp}}|^2 + \frac{1}{2} |\overline{\mathcal{M}_{Z^0 Z^0}}|^2 \\ &= \frac{g^4}{4} + \frac{g^4}{8} (1 + t_W^2)^2 + \mathcal{O}\left(\frac{m_W^2}{\mu^2}, \epsilon\right) \\ &= \frac{g^4}{4} \left[\frac{3}{2} + t_W^2 + \frac{t_W^4}{2} \right] + \mathcal{O}\left(\frac{m_W^2}{\mu^2}, \epsilon\right). \end{aligned} \quad (\text{E.123})$$

where as usual the term associated to the process with identical final particles is multiply by the symmetry factor 1/2. Substituting this result into Eq. (E.14), we find that the cross-section times velocity for the annihilation among two identical Higgsinos at the leading order in ϵ and m_W^2/μ^2 is equal to

$$\sigma_{\tilde{H}_{1,2}\tilde{H}_{1,2}} v = \frac{g^4}{128\pi\mu^2} \left[\frac{3}{2} + t_W^2 + \frac{t_W^4}{2} \right] + \mathcal{O}\left(\frac{m_W^2}{\mu^2}, \epsilon\right). \quad (\text{E.124})$$

Now we move on considering the co-annihilation between $\tilde{H}_{1,2}$ and $\tilde{H}_{2,1}$. From Table 4.5 we can see that the final states can be two charged vector bosons of opposite charge, or fermion anti-fermion pairs, schematically $\tilde{H}_{1,2}\tilde{H}_{2,1} \rightarrow W^\pm W^\mp$ and $\tilde{H}_{1,2}\tilde{H}_{2,1} \rightarrow \bar{f}f$. The Feynman diagram associated to the former process are

$$(\text{E.125})$$

with associated amplitudes

$$i\mathcal{M}_t = \frac{g^2}{2(t-\mu^2)} [2\bar{v}(k_2, s_2)\gamma^\nu u(k_1, s_1)\epsilon_\nu(p_2) (q \cdot \epsilon_\mu(p_1)) + \bar{v}(k_2, s_2)\gamma^\nu \gamma^\mu \not{p}_1 u(k_1, s_1)\epsilon_\nu(p_2)\epsilon_\mu(p_1)], \quad (\text{E.126a})$$

$$i\mathcal{M}_s = -\frac{g^2}{2(s-m_{Z^0}^2)} \bar{v}(k_2, s_2)\gamma^\mu u(k_1, s_1)g_{\mu\nu}\Gamma^{\nu\alpha\beta}\epsilon_\alpha(p_1)\epsilon_\beta(p_2) \quad (\text{E.126b})$$

where $\Gamma^{\nu\alpha\beta}$ is defined in Eq. (E.70) and in the last amplitude we used the Dirac equation. The associate square amplitudes and interference terms averaged over initial states and considering final transverse polarizations, are

$$|\overline{\mathcal{M}_t}|^2 = \frac{g^4}{8} \frac{u-\mu^2}{t-\mu^2} \mathcal{P}(\pm, \pm) + \mathcal{O}\left(\frac{m_W^2}{\mu^2}, \epsilon\right) \quad (\text{E.127a})$$

$$|\overline{\mathcal{M}_s}|^2 = \frac{g^4}{8} (t-\mu^2)(u-\mu^2) |(\epsilon_2^\pm \cdot \epsilon_1^\pm)|^2 + \mathcal{O}\left(\frac{m_W^2}{\mu^2}\right) \quad (\text{E.127b})$$

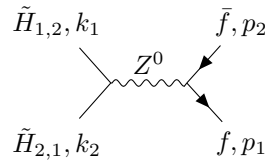
$$\text{Re}[\overline{\mathcal{M}_t\mathcal{M}_s^\dagger}] = \frac{g^4}{4s} (u-\mu^2) |(\epsilon_2^\pm \cdot \epsilon_1^\pm)|^2 + \mathcal{O}\left(\frac{m_W^2}{\mu^2}, \epsilon\right) \quad (\text{E.127c})$$

$$(\text{E.127d})$$

Summing up these contributions we have that the total average square amplitude for the the process $\tilde{H}_{1,2}\tilde{H}_{2,1} \rightarrow W^\pm W^\mp$ is

$$\begin{aligned} |\overline{\mathcal{M}_{W^\pm W^\mp}}|^2 &= \sum_{(\pm\pm)} |\overline{\mathcal{M}_t}|^2 + |\overline{\mathcal{M}_s}|^2 + 2\text{Re}[\overline{\mathcal{M}_t\mathcal{M}_s^\dagger}] \\ &= \frac{g^4}{2} + \frac{g^4}{4} - \frac{g^4}{2} + \mathcal{O}\left(\frac{m_W^2}{\mu^2}, \epsilon\right) \\ &= \frac{g^4}{4} + \mathcal{O}\left(\frac{m_W^2}{\mu^2}, \epsilon\right) \end{aligned} \quad (\text{E.128})$$

The other process which contributes to the co-annihilation between $\tilde{H}_{1,2}$ and $\tilde{H}_{2,1}$ is $\tilde{H}_{1,2}\tilde{H}_{2,1} \rightarrow \bar{f}f$, with associated Feynmna diagram



and amplitude

$$i\mathcal{M}_{ff} = -\frac{g^2}{4c_W^2 s} \bar{v}(k_2, s_2)\gamma^\mu u(k_1, s_1)\bar{u}(p_1, r_1)\gamma_\mu (P_L - 2e_q s_W^2) v(p_2, r_2) + \mathcal{O}\left(\frac{m_W^2}{\mu^2}\right). \quad (\text{E.129})$$

The total average square amplitude associated to the above result is

$$\begin{aligned} |\overline{\mathcal{M}_{ff}}|^2 &= \frac{g^4}{16c_W^4 s^2} [1 - 2e_q s_W^2 + 4e_q^2 s_W^4] \left[\frac{(u-\mu^2)^2}{2} + \frac{(t-\mu^2)^2}{2} + \mu^2 s \right] + \mathcal{O}\left(\frac{m_W^2}{\mu^2}\right) \\ &= \frac{g^4}{16c_W^4} [1 - 4e_q s_W^2 + 16e_q^2 s_W^4] + \mathcal{O}\left(\frac{m_W^2}{\mu^2}, \epsilon\right). \end{aligned} \quad (\text{E.130})$$

Thus summing up the contributions of the processes $\tilde{H}_{1,2}\tilde{H}_{2,1} \rightarrow W^\pm W^\mp$ and $\tilde{H}_{1,2}\tilde{H}_{2,1} \rightarrow \bar{f}f$ we obtain that the total average square amplitude for the co-annihilation between \tilde{H}_1 and \tilde{H}_2

is

$$\begin{aligned} |\overline{\mathcal{M}_{\tilde{H}_{1,2}\tilde{H}_{2,1}}}|^2 &= \sum_f N_c |\overline{\mathcal{M}_{ff}}|^2 + |\overline{\mathcal{M}_{W^\pm W^\mp}}|^2 \\ &= \frac{g^4}{4} \left[\frac{29}{4} + \frac{21}{2} t_W^4 \right] + \mathcal{O} \left(\frac{m_W^2}{\mu^2}, \epsilon \right). \end{aligned} \quad (\text{E.131})$$

where the sum runs over all admitted SM fermions. Substituting this result into Eq. (E.14) we obtain the total cross-section times velocity for the $\tilde{H}_{1,2}\tilde{H}_{2,1}$ co-annihilation, which is

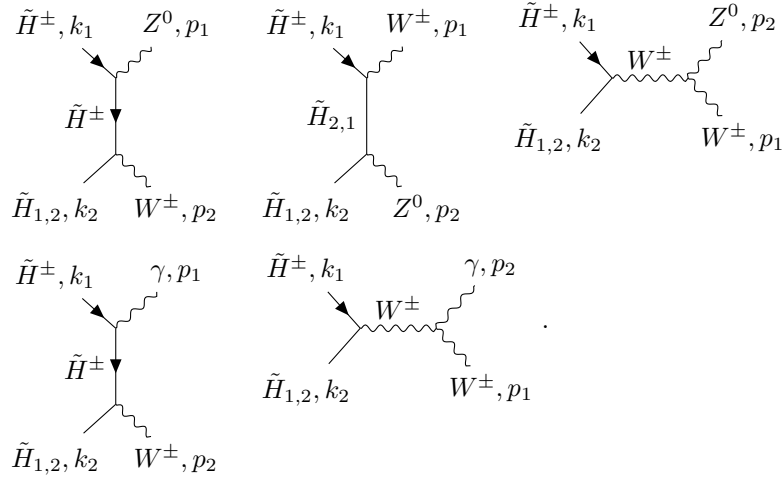
$$\sigma_{\tilde{H}_{1,2}\tilde{H}_{2,1}} v = \frac{g^4}{128\pi\mu^2} \left[\frac{29}{4} + \frac{21}{2} t_W^4 \right] + \mathcal{O} \left(\frac{m_W^2}{\mu^2}, \epsilon \right). \quad (\text{E.132})$$

The other co-annihilation process which we take into account is the one between one charged and one neutral Higgsinos $\tilde{H}_{1,2}, \tilde{H}^\mp$. All the processes which contributes to this co-annihilation are summarized in Table 4.5. In particular those with vector bosons as final states are

$$\tilde{H}_{1,2}\tilde{H}^\pm \xrightarrow{\tilde{H}^\pm} Z^0 W^\mp, \quad \tilde{H}_{1,2}\tilde{H}^\pm \xrightarrow{\tilde{H}_{2,1}} Z^0 W^\mp, \quad \tilde{H}_{1,2}\tilde{H}^\pm \xrightarrow{W^\pm} Z^0 W^\mp \quad (\text{E.133a})$$

$$\tilde{H}_{1,2}\tilde{H}^\pm \xrightarrow{\tilde{H}^\pm} \gamma W^\mp, \quad \tilde{H}_{1,2}\tilde{H}^\pm \xrightarrow{W^\pm} \gamma W^\mp \quad (\text{E.133b})$$

with associated Feynman diagrams given by



The amplitudes related to the processes given in Eq. (E.133a) are

$$\begin{aligned} i\mathcal{M}_{t Z^0 W^\pm} &= \frac{g^2(c_W^2 - s_W^2)}{4c_W(t - \mu^2)} [2\bar{v}(k_2, s_2)\gamma^\nu u(k_1, s_1)\epsilon_\nu(p_2)(q \cdot \epsilon_\mu(p_1)) \\ &\quad + \bar{v}(k_2, s_2)\gamma^\nu \gamma^\mu \not{p}_1 u(k_1, s_1)\epsilon_\nu(p_2)\epsilon_\mu(p_1)], \end{aligned} \quad (\text{E.134a})$$

$$\begin{aligned} i\mathcal{M}_{u Z^0 W^\pm} &= \frac{g^2}{4c_W(u - \mu^2)} [2\bar{v}(k_1, s_1)\gamma^\nu u(k_2, s_2)\epsilon_\nu(p_2)(q' \cdot \epsilon_\mu(p_1)) \\ &\quad + \bar{v}(k_1, s_1)\gamma^\nu \gamma^\mu \not{p}_1 u(k_2, s_2)\epsilon_\nu(p_2)\epsilon_\mu(p_1)] \end{aligned} \quad (\text{E.134b})$$

$$i\mathcal{M}_{s Z^0 W^\pm} = -\frac{g^2 c_W}{2(s - m_W^2)} \bar{v}(k_2, s_2)\gamma^\mu u(k_1, s_1)g_{\mu\nu} \Gamma^{\nu\alpha\beta} \epsilon_\alpha(p_1)\epsilon_\beta(p_2). \quad (\text{E.134c})$$

The ones associated to the processes given in Eq. (E.133b) are

$$\begin{aligned} i\mathcal{M}_{t \gamma W^\pm} &= \frac{g^2 s_W}{2(t - \mu^2)} [2\bar{v}(k_2, s_2)\gamma^\nu u(k_1, s_1)\epsilon_\nu(p_2)(q \cdot \epsilon_\mu(p_1)) \\ &\quad + \bar{v}(k_2, s_2)\gamma^\nu \gamma^\mu \not{p}_1 u(k_1, s_1)\epsilon_\nu(p_2)\epsilon_\mu(p_1)], \end{aligned} \quad (\text{E.135a})$$

$$i\mathcal{M}_{s \gamma W^\pm} = -\frac{g^2 s_W}{2(s - m_W^2)} \bar{v}(k_2, s_2)\gamma^\mu u(k_1, s_1)g_{\mu\nu} \Gamma^{\nu\alpha\beta} \epsilon_\alpha(p_1)\epsilon_\beta(p_2). \quad (\text{E.135b})$$

Using the results found in the previous section for the process $\tilde{W}\tilde{W}^\pm \rightarrow Z^0W^\pm$ we can argue that, on transverse polarizations, the average over initial states of the square amplitudes just given and the interference terms, are equal to

$$|\overline{\mathcal{M}_{t Z^0 W^\pm}}|^2 = \frac{g^4 (c_W^2 - s_W^2)^2}{32 c_W^2} \frac{u - \mu^2}{t - \mu^2} \mathcal{P}(\pm, \pm) + \mathcal{O}\left(\frac{m_W^2}{\mu^2}, \epsilon\right) \quad (\text{E.136a})$$

$$|\overline{\mathcal{M}_{u Z^0 W^\pm}}|^2 = \frac{g^4}{c_W^2 32} \frac{t - \mu^2}{u - \mu^2} \mathcal{P}(\pm, \pm) + \mathcal{O}\left(\frac{m_W^2}{\mu^2}, \epsilon\right) \quad (\text{E.136b})$$

$$|\overline{\mathcal{M}_{s Z^0 W^\pm}}|^2 = \frac{g^4 c_W^2}{2s^2} (t - \mu^2)(u - \mu^2) |(\epsilon_2^\pm \cdot \epsilon_1^\pm)|^2 + \mathcal{O}\left(\frac{m_W^2}{\mu^2}\right) \quad (\text{E.136c})$$

$$\text{Re} \left[\overline{\mathcal{M}_{t Z^0 W^\pm} \mathcal{M}_{u Z^0 W^\pm}^\dagger} \right] = -\frac{g^4 (c_W^2 - s_W^2)}{32 c_W^2} \mathcal{P}'(\pm, \pm) + \mathcal{O}\left(\frac{m_W^2}{\mu^2}, \epsilon\right) \quad (\text{E.136d})$$

$$\text{Re} \left[\overline{\mathcal{M}_{t Z^0 W^\pm} \mathcal{M}_{s Z^0 W^\pm}^\dagger} \right] = (c_W^2 - s_W^2) \frac{g^4}{8s} (u - \mu^2) |(\epsilon_2^\pm \cdot \epsilon_1^\pm)|^2 + \mathcal{O}\left(\frac{m_W^2}{\mu^2}, \epsilon\right) \quad (\text{E.136e})$$

$$\text{Re} \left[\overline{\mathcal{M}_{u Z^0 W^\pm} \mathcal{M}_{s Z^0 W^\pm}^\dagger} \right] = \frac{g^4}{8s} (t - \mu^2) |(\epsilon_2^\pm \cdot \epsilon_1^\pm)|^2 + \mathcal{O}\left(\frac{m_W^2}{\mu^2}, \epsilon\right) \quad (\text{E.136f})$$

for the process $\tilde{H}_{1,2}\tilde{H}^\pm \rightarrow Z^0W^\mp$, while for the process $\tilde{H}_{1,2}\tilde{H}^\pm \rightarrow \gamma W^\mp$ they are given by

$$|\overline{\mathcal{M}_{t \gamma W^\pm}}|^2 = \frac{g^4 s_W^2}{8} \frac{u - \mu^2}{t - \mu^2} \mathcal{P}(\pm, \pm) + \mathcal{O}\left(\frac{m_W^2}{\mu^2}, \epsilon\right) \quad (\text{E.137a})$$

$$|\overline{\mathcal{M}_{s \gamma W^\pm}}|^2 = \frac{g^4 s_W^2}{8} (t - \mu^2)(u - \mu^2) |(\epsilon_2^\pm \cdot \epsilon_1^\pm)|^2 + \mathcal{O}\left(\frac{m_W^2}{\mu^2}\right) \quad (\text{E.137b})$$

$$\text{Re} \left[\overline{\mathcal{M}_{t \gamma W^\pm} \mathcal{M}_{s \gamma W^\pm}^\dagger} \right] = \frac{g^4 s_W^2}{4s} (u - \mu^2) |(\epsilon_2^\pm \cdot \epsilon_1^\pm)|^2 + \mathcal{O}\left(\frac{m_W^2}{\mu^2}, \epsilon\right) \quad (\text{E.137c})$$

$$(\text{E.137d})$$

Also here the longitudinal polarization, up to correction of order m_W^2/μ^2 , do not contribute to the total amplitude of the processes in Eqs. (E.133). This is possible to see substituting the approximation given in Eq. (E.4) into the amplitudes given in Eqs. (E.134) and Eqs. (E.135) and then sum up the results. Thus the total average square amplitudes for the processes given in Eqs. (E.133) are

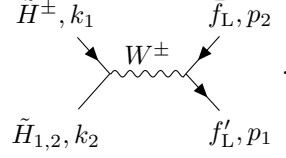
$$\begin{aligned} |\overline{\mathcal{M}_{Z^0 W^\pm}}|^2 &= \sum_{(\pm\pm)} |\overline{\mathcal{M}_{t Z^0 W^\pm}}|^2 + |\overline{\mathcal{M}_{u Z^0 W^\pm}}|^2 + |\overline{\mathcal{M}_{s Z^0 W^\pm}}|^2 + 2 \text{Re} \left[\overline{\mathcal{M}_{t Z^0 W^\pm} \mathcal{M}_{u Z^0 W^\pm}^\dagger} \right] \\ &\quad + 2 \text{Re} \left[\overline{\mathcal{M}_{t Z^0 W^\pm} \mathcal{M}_{s Z^0 W^\pm}^\dagger} \right] + 2 \text{Re} \left[\overline{\mathcal{M}_{u Z^0 W^\pm} \mathcal{M}_{s Z^0 W^\pm}^\dagger} \right] \\ &= \frac{g^4 (c_W^2 - s_W^2)^2}{8 c_W^2} + \frac{g^4}{8c_W^2} + \frac{g^4 c_W^2}{4} - (c_W^2 - s_W^2) \frac{g^4}{4} - \frac{g^4}{4} + \mathcal{O}\left(\frac{m_W^2}{\mu^2}, \epsilon\right) \\ &= \frac{g^4 t_W^2}{4} - \frac{g^4 s_W^2}{4} + \mathcal{O}\left(\frac{m_W^2}{\mu^2}, \epsilon\right) \end{aligned} \quad (\text{E.138})$$

for the process $\tilde{H}_{1,2}\tilde{H}^\pm \rightarrow Z^0W^\mp$, and

$$\begin{aligned} |\overline{\mathcal{M}_{\gamma W^\pm}}|^2 &= \sum_{(\pm\pm)} |\overline{\mathcal{M}_{t \gamma W^\pm}}|^2 + |\overline{\mathcal{M}_{s \gamma W^\pm}}|^2 + 2 \text{Re} \left[\overline{\mathcal{M}_{t \gamma W^\pm} \mathcal{M}_{s \gamma W^\pm}^\dagger} \right] \\ &= \frac{g^4 s_W^2}{2} + \frac{g^4 s_W^2}{4} - \frac{g^4 s_W^2}{2} + \mathcal{O}\left(\frac{m_W^2}{\mu^2}, \epsilon\right) \\ &= \frac{g^4 s_W^2}{4} + \mathcal{O}\left(\frac{m_W^2}{\mu^2}, \epsilon\right) \end{aligned} \quad (\text{E.139})$$

for the process $\tilde{H}_{1,2}\tilde{H}^\pm \rightarrow \gamma W^\mp$.

From Table 4.5 we can observe that the other process which contribute to the co-annihilation among $\tilde{H}_{1,2}$ and \tilde{H}^\pm proceeds exchanging a W^\pm vector boson in s -channel, with two SM fermions as final states, f and f' , schematically $\tilde{H}_{1,2}\tilde{H}^\pm \rightarrow \bar{f}_L f'_L$. The Feynman diagram is



with associated amplitude given by

$$\begin{aligned} i\mathcal{M}_{ff'} &= \frac{g^2}{2\sqrt{2}(s - m_W^2)} \bar{v}(k_2, s_2) \gamma^\mu u(k_1, s_1) \left[-g_{\mu\nu} + \frac{(k_1 + k_2)_\mu (k_1 + k_2)_\nu}{m_W^2} \right] \bar{u}(p_1, r_1) \gamma_\nu P_L v(p_2, r_2) \\ &= -\frac{g^2}{\sqrt{2}(s - m_W^2)} \bar{v}(k_2, s_2) \gamma^\mu u(k_1, s_1) \bar{u}(p_1, r_1) \gamma_\mu P_L v(p_2, r_2). \end{aligned} \quad (\text{E.140})$$

Noting that this amplitude, apart an extra 1/2 factor, is identical to the one for the process $\tilde{W}\tilde{W}^\pm \rightarrow \bar{f}_L f'_L$, given in Eq. (E.87), we have that the average square amplitude for the annihilation between $\tilde{H}_{1,2}$ and \tilde{H}^\pm into final fermions is

$$|\overline{\mathcal{M}_{ff'}}|^2 = \frac{g^4}{8} + \mathcal{O}\left(\frac{m_W^2}{\mu^2}, \epsilon\right). \quad (\text{E.141})$$

Therefore the total average square amplitude for the co-annihilation among $\tilde{H}_{1,2}$ and \tilde{H}^\pm is given by the sum of the contributions in Eq. (E.138), Eq. (E.139), and Eq. (E.141), namely

$$\begin{aligned} |\overline{\mathcal{M}_{\tilde{H}_{1,2}\tilde{H}^\pm}}|^2 &= \sum_{f,f'} N_c |\overline{\mathcal{M}_{ff'}}|^2 + |\overline{\mathcal{M}_{\gamma W^\pm}}|^2 + |\overline{\mathcal{M}_{Z^0 W^\pm}}|^2 \\ &= \frac{3}{2}g^4 + \frac{g^4 s_W^2}{2} + \frac{g^4 t_W^2}{4} - \frac{g^4 s_W^2}{2} + \mathcal{O}\left(\frac{m_W^2}{\mu^2}, \epsilon\right) \\ &= \frac{g^4}{4} [6 + t_W^2] + \mathcal{O}\left(\frac{m_W^2}{\mu^2}, \epsilon\right) \end{aligned} \quad (\text{E.142})$$

where N_c is the colour factor defined above. Thus substituting this result into Eq. (E.14) we have that the associated cross-section times velocity is

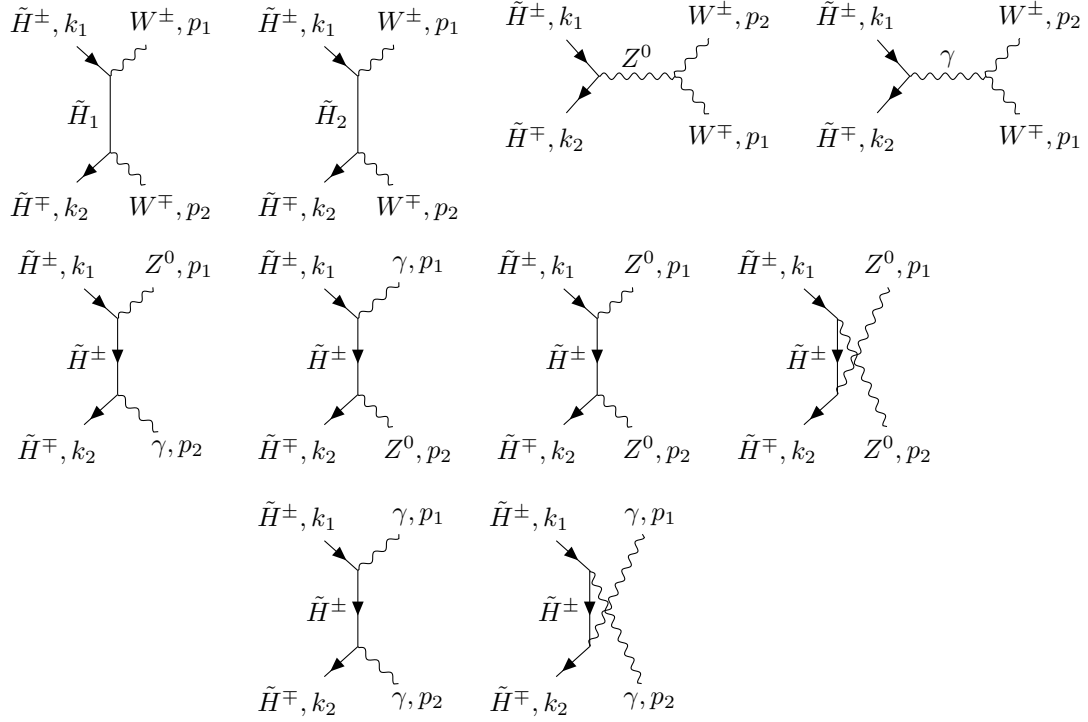
$$\sigma_{\tilde{H}_{1,2}\tilde{H}^\pm} v = \frac{g^4}{128\pi\mu^2} [6 + t_W^2] + \mathcal{O}\left(\frac{m_W^2}{\mu^2}, \epsilon\right). \quad (\text{E.143})$$

Another co-annihilation process which is important in the evaluation of the relic density of a pure Higgsino LSP, is the one between two charged Higgsinos with opposite electric charge, namely \tilde{H}^\pm and \tilde{H}^\mp . The relevant processes which contribute to this co-annihilation are summarized in Table 4.5. We start by those processes in which the final states are gauge vector bosons. The various processes can be schematically summarized as

$$\tilde{H}^\pm \tilde{H}^\mp \xrightarrow{\tilde{H}_{1,2}} W^\pm W^\mp, \quad \tilde{H}^\pm \tilde{H}^\mp \xrightarrow{Z^0} W^\pm W^\mp, \quad \tilde{H}^\pm \tilde{H}^\mp \xrightarrow{\gamma} W^\pm W^\mp \quad (\text{E.144a})$$

$$\tilde{H}^\pm \tilde{H}^\mp \xrightarrow{\tilde{H}^\pm} Z^0 Z^0, \quad \tilde{H}^\pm \tilde{H}^\mp \xrightarrow{\tilde{H}^\pm} \gamma\gamma, \quad \tilde{H}^\pm \tilde{H}^\mp \xrightarrow{\tilde{H}^\pm} Z^0\gamma \quad (\text{E.144b})$$

with associated Feynman diagrams given by



Using the Feynman rules given in Appendix B we have that the various amplitudes are equal to

$$i\mathcal{M}_{t_1} = \frac{g^2}{4(t - \mu^2)} [2\bar{v}(k_2, s_2)\gamma^\nu u(k_1, s_1)\epsilon_\nu(p_2)(q \cdot \epsilon_\mu(p_1)) + \bar{v}(k_2, s_2)\gamma^\nu \gamma^\mu \not{p}_1 u(k_1, s_1)\epsilon_\nu(p_2)\epsilon_\mu(p_1)] \quad (\text{E.145a})$$

$$i\mathcal{M}_{t_2} = \frac{g^2}{4(t - \mu^2)} [2\bar{v}(k_2, s_2)\gamma^\nu u(k_1, s_1)\epsilon_\nu(p_2)(q \cdot \epsilon_\mu(p_1)) + \bar{v}(k_2, s_2)\gamma^\nu \gamma^\mu \not{p}_1 u(k_1, s_1)\epsilon_\nu(p_2)\epsilon_\mu(p_1)] \quad (\text{E.145b})$$

$$i\mathcal{M}_{s Z^0} = -\frac{g^2(c_W^2 - s_W^2)}{2(s - m_W^2)} \bar{v}(k_2, s_2)\gamma^\mu u(k_1, s_1)g_{\mu\nu}\Gamma^{\nu\alpha\beta}\epsilon_\alpha(p_1)\epsilon_\beta(p_2) \quad (\text{E.145c})$$

$$i\mathcal{M}_{s \gamma} = -\frac{g^2 s_W^2}{s} \bar{v}(k_2, s_2)\gamma^\mu u(k_1, s_1)g_{\mu\nu}\Gamma^{\nu\alpha\beta}\epsilon_\alpha(p_1)\epsilon_\beta(p_2). \quad (\text{E.145d})$$

for the processes given in Eq. (E.144a). Exploiting the facts that up to corrections of order m_W^2/μ^2 the amplitudes for $\mathcal{M}_{s Z^0}$ and $\mathcal{M}_{s \gamma}$ are equal, and that the Higgsinos \tilde{H}_1 and \tilde{H}_2 have the same mass, we can sum up these amplitudes as

$$i\mathcal{M}_t = i\mathcal{M}_{t_1} + i\mathcal{M}_{t_2} = \frac{g^2}{2(t - \mu^2)} [2\bar{v}(k_2, s_2)\gamma^\nu u(k_1, s_1)\epsilon_\nu(p_2)(q \cdot \epsilon_\mu(p_1)) + \bar{v}(k_2, s_2)\gamma^\nu \gamma^\mu \not{p}_1 u(k_1, s_1)\epsilon_\nu(p_2)\epsilon_\mu(p_1)] \quad (\text{E.146a})$$

$$i\mathcal{M}_s = i\mathcal{M}_{s Z^0} + i\mathcal{M}_{s \gamma} = -\frac{g^2}{2s} \bar{v}(k_2, s_2)\gamma^\mu u(k_1, s_1)g_{\mu\nu}\Gamma^{\nu\alpha\beta}\epsilon_\alpha(p_1)\epsilon_\beta(p_2) + \mathcal{O}\left(\frac{m_W^2}{\mu^2}\right). \quad (\text{E.146b})$$

The other amplitudes related to the processes given in Eqs. (E.144), are

$$i\mathcal{M}_{t Z^0 \gamma} = \frac{g^2}{t - \mu^2} \frac{(c_W^2 - s_W^2) s_W}{2c_W} [2\bar{v}(k_2, s_2) \gamma^\nu u(k_1, s_1) \epsilon_\nu(p_2) (q \cdot \epsilon_\mu(p_1)) \\ + \bar{v}(k_2, s_2) \gamma^\nu \gamma^\mu \not{p}_1 u(k_1, s_1) \epsilon_\nu(p_2) \epsilon_\mu(p_1)] \quad (\text{E.147a})$$

$$i\mathcal{M}_{u Z^0 \gamma} = \frac{g^2}{u - \mu^2} \frac{(c_W^2 - s_W^2) s_W}{2c_W} [2\bar{v}(k_2, s_2) \gamma^\nu u(k_1, s_1) \epsilon_\nu(p_1) (q' \cdot \epsilon_\mu(p_2)) \\ + \bar{v}(k_2, s_2) \gamma^\nu \gamma^\mu \not{p}_2 u(k_1, s_1) \epsilon_\nu(p_1) \epsilon_\mu(p_2)] \quad (\text{E.147b})$$

for the process $\tilde{H}^\pm \tilde{H}^\mp \rightarrow Z^0 \gamma$,

$$i\mathcal{M}_{t Z^0 Z^0} = \frac{g^2}{t - \mu^2} \frac{(c_W^2 - s_W^2)^2}{4c_W^2} [2\bar{v}(k_2, s_2) \gamma^\nu u(k_1, s_1) \epsilon_\nu(p_2) (q \cdot \epsilon_\mu(p_1)) \\ + \bar{v}(k_2, s_2) \gamma^\nu \gamma^\mu \not{p}_1 u(k_1, s_1) \epsilon_\nu(p_2) \epsilon_\mu(p_1)] \quad (\text{E.148a})$$

$$i\mathcal{M}_{u Z^0 Z^0} = \frac{g^2}{u - \mu^2} \frac{(c_W^2 - s_W^2)^2}{4c_W^2} [2\bar{v}(k_2, s_2) \gamma^\nu u(k_1, s_1) \epsilon_\nu(p_1) (q' \cdot \epsilon_\mu(p_2)) \\ + \bar{v}(k_2, s_2) \gamma^\nu \gamma^\mu \not{p}_2 u(k_1, s_1) \epsilon_\nu(p_1) \epsilon_\mu(p_2)] \quad (\text{E.148b})$$

for the process $\tilde{H}^\pm \tilde{H}^\mp \rightarrow Z^0 Z^0$ and

$$i\mathcal{M}_{t \gamma \gamma} = \frac{g^2 s_W^2}{t - \mu^2} [2\bar{v}(k_2, s_2) \gamma^\nu u(k_1, s_1) \epsilon_\nu(p_2) (q \cdot \epsilon_\mu(p_1)) \\ + \bar{v}(k_2, s_2) \gamma^\nu \gamma^\mu \not{p}_1 u(k_1, s_1) \epsilon_\nu(p_2) \epsilon_\mu(p_1)] \quad (\text{E.149a})$$

$$i\mathcal{M}_{u \gamma \gamma} = \frac{g^2 s_W^2}{u - \mu^2} [2\bar{v}(k_2, s_2) \gamma^\nu u(k_1, s_1) \epsilon_\nu(p_1) (q' \cdot \epsilon_\mu(p_2)) \\ + \bar{v}(k_2, s_2) \gamma^\nu \gamma^\mu \not{p}_2 u(k_1, s_1) \epsilon_\nu(p_1) \epsilon_\mu(p_2)] \quad (\text{E.149b})$$

for the remaining one, namely $\tilde{H}^\pm \tilde{H}^\mp \rightarrow \gamma \gamma$. As discussed in the previous section also here the longitudinal polarizations do not contribute in the assumed limit i.e. up to corrections of order m_W^2/μ^2 . Thus the total square amplitudes of the various processes are determined by the transverse polarizations. Therefore using the results of the previous section we have that on transverse polarizations the average of the squares of the amplitudes just given are

$$|\overline{\mathcal{M}_t}|^2 = \frac{g^4}{8} \frac{u - \mu^2}{t - \mu^2} \mathcal{P}(\pm, \pm) + \mathcal{O}\left(\frac{m_W^2}{\mu^2}, \epsilon\right) \quad (\text{E.150a})$$

$$|\overline{\mathcal{M}_s}|^2 = \frac{g^4}{8s^2} (t - \mu^2)(u - \mu^2) |(\epsilon_2^\pm \cdot \epsilon_1^\pm)|^2 + \mathcal{O}\left(\frac{m_W^2}{\mu^2}\right) \quad (\text{E.150b})$$

$$\text{Re} \left[\overline{\mathcal{M}_t \mathcal{M}_s^\dagger} \right] = \frac{g^4}{4s} (u - \mu^2) |(\epsilon_2^\pm \cdot \epsilon_1^\pm)|^2 + \mathcal{O}\left(\frac{m_W^2}{\mu^2}, \epsilon\right) \quad (\text{E.150c})$$

for the process $\tilde{H}^\pm \tilde{H}^\mp \rightarrow W^\pm W^\mp$ which sum up to give a total square amplitude equal to

$$|\overline{\mathcal{M}_{W^\pm W^\mp}}|^2 = \sum_{(\pm \pm)} |\overline{\mathcal{M}_t}|^2 + |\overline{\mathcal{M}_s}|^2 + 2 \text{Re} \left[\overline{\mathcal{M}_t \mathcal{M}_s^\dagger} \right] \\ = \frac{g^4}{16} + \mathcal{O}\left(\frac{m_W^2}{\mu^2}, \epsilon\right). \quad (\text{E.151})$$

The average square amplitudes related to $\tilde{H}^\pm \tilde{H}^\mp \rightarrow Z^0 \gamma$ are

$$|\overline{\mathcal{M}_{t Z^0 \gamma}}|^2 = \frac{g^4 (c_W^2 - s_W^2)^2 t_W^2}{8} \frac{u - \mu^2}{t - \mu^2} \mathcal{P}(\pm, \pm) + \mathcal{O}\left(\frac{m_W^2}{\mu^2}, \epsilon\right) \quad (\text{E.152a})$$

$$|\overline{\mathcal{M}_{u Z^0 \gamma}}|^2 = \frac{g^4 (c_W^2 - s_W^2)^2 t_W^2}{8} \frac{t - \mu^2}{u - \mu^2} \mathcal{P}(\pm, \pm) + \mathcal{O}\left(\frac{m_W^2}{\mu^2}, \epsilon\right) \quad (\text{E.152b})$$

$$\text{Re} \left[\overline{\mathcal{M}_{t Z^0 \gamma} \mathcal{M}_{u Z^0 \gamma}^\dagger} \right] = -\frac{g^4 (c_W^2 - s_W^2)^2 t_W^2}{8} \mathcal{P}'(\pm, \pm) + \mathcal{O}\left(\frac{m_W^2}{\mu^2}, \epsilon\right) \quad (\text{E.152c})$$

which sum up giving

$$\begin{aligned} |\overline{\mathcal{M}_{Z^0\gamma}}|^2 &= \sum_{(\pm\pm)} |\overline{\mathcal{M}_{tZ^0\gamma}}|^2 + |\overline{\mathcal{M}_{uZ^0\gamma}}|^2 + 2 \operatorname{Re} \left[\overline{\mathcal{M}_{tZ^0\gamma}\mathcal{M}_{uZ^0\gamma}^\dagger} \right] \\ &= g^4 (c_W^2 - s_W^2)^2 t_W^2 + \mathcal{O} \left(\frac{m_W^2}{\mu^2}, \epsilon \right). \end{aligned} \quad (\text{E.153})$$

The square amplitudes average over initial states for what concern the process $\tilde{H}^\pm \tilde{H}^\mp \rightarrow Z^0 Z^0$ are

$$|\overline{\mathcal{M}_{tZ^0Z^0}}|^2 = \frac{g^4 (c_W^2 - s_W^2)^4}{32 c_W^4} \frac{u - \mu^2}{t - \mu^2} \mathcal{P}(\pm, \pm) + \mathcal{O} \left(\frac{m_W^2}{\mu^2}, \epsilon \right) \quad (\text{E.154a})$$

$$|\overline{\mathcal{M}_{uZ^0Z^0}}|^2 = \frac{g^4 (c_W^2 - s_W^2)^4}{32 c_W^4} \frac{t - \mu^2}{u - \mu^2} \mathcal{P}(\pm, \pm) + \mathcal{O} \left(\frac{m_W^2}{\mu^2}, \epsilon \right) \quad (\text{E.154b})$$

$$\operatorname{Re} \left[\overline{\mathcal{M}_{tZ^0Z^0}\mathcal{M}_{uZ^0Z^0}^\dagger} \right] = -\frac{g^4 (c_W^2 - s_W^2)^4}{32 c_W^4} \mathcal{P}'(\pm, \pm) + \mathcal{O} \left(\frac{m_W^2}{\mu^2}, \epsilon \right) \quad (\text{E.154c})$$

and summing up together we obtain

$$\begin{aligned} |\overline{\mathcal{M}_{Z^0Z^0}}|^2 &= \sum_{(\pm\pm)} |\overline{\mathcal{M}_{tZ^0Z^0}}|^2 + |\overline{\mathcal{M}_{uZ^0Z^0}}|^2 + 2 \operatorname{Re} \left[\overline{\mathcal{M}_{tZ^0Z^0}\mathcal{M}_{uZ^0Z^0}^\dagger} \right] \\ &= \frac{g^4 (c_W^2 - s_W^2)^4}{4 c_W^4} + \mathcal{O} \left(\frac{m_W^2}{\mu^2}, \epsilon \right). \end{aligned} \quad (\text{E.155})$$

As last the square amplitudes for the process $\tilde{H}^\pm \tilde{H}^\mp \rightarrow \gamma\gamma$ are

$$|\overline{\mathcal{M}_{t\gamma\gamma}}|^2 = \frac{g^4 s_W^4}{2} \frac{u - \mu^2}{t - \mu^2} \mathcal{P}(\pm, \pm) + \mathcal{O} \left(\frac{m_W^2}{\mu^2}, \epsilon \right) \quad (\text{E.156a})$$

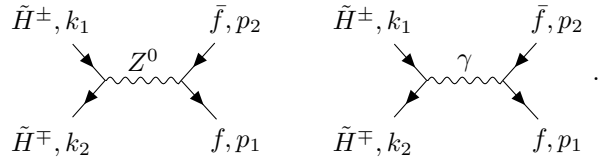
$$|\overline{\mathcal{M}_{u\gamma\gamma}}|^2 = \frac{g^4 s_W^4}{2} \frac{t - \mu^2}{u - \mu^2} \mathcal{P}(\pm, \pm) + \mathcal{O} \left(\frac{m_W^2}{\mu^2}, \epsilon \right) \quad (\text{E.156b})$$

$$\operatorname{Re} \left[\overline{\mathcal{M}_{t\gamma\gamma}\mathcal{M}_{u\gamma\gamma}^\dagger} \right] = -\frac{g^4 s_W^4}{2} \mathcal{P}'(\pm, \pm) + \mathcal{O} \left(\frac{m_W^2}{\mu^2}, \epsilon \right) \quad (\text{E.156c})$$

which give a total average square amplitude equal to

$$\begin{aligned} |\overline{\mathcal{M}_{\gamma\gamma}}|^2 &= \sum_{(\pm\pm)} |\overline{\mathcal{M}_{t\gamma\gamma}}|^2 + |\overline{\mathcal{M}_{u\gamma\gamma}}|^2 + 2 \operatorname{Re} \left[\overline{\mathcal{M}_{t\gamma\gamma}\mathcal{M}_{u\gamma\gamma}^\dagger} \right] \\ &= 4g^4 s_W^4 + \mathcal{O} \left(\frac{m_W^2}{\mu^2}, \epsilon \right). \end{aligned} \quad (\text{E.157})$$

The other process which contribute to the co-annihilation among \tilde{H}^\pm and \tilde{H}^\mp is the one where the final states are fermion anti-fermion pairs. The associated Feynman diagrams are



with associated amplitudes given by

$$i\mathcal{M}_{Z^0 ff} = -\frac{g^2 (c_W^2 - s_W^2)}{4s c_W^2} \bar{v}(k_2, s_2) \gamma^\mu u(k_1, s_1) \bar{u}(p_1, r_1) \gamma_\mu (P_L - 2e_q s_W^2) v(p_2, r_2) + \mathcal{O} \left(\frac{m_W^2}{\mu^2} \right) \quad (\text{E.158a})$$

$$i\mathcal{M}_{\gamma ff} = -\frac{g^2 e_q s_W^2}{s} \bar{v}(k_2, s_2) \gamma^\mu u(k_1, s_1) \bar{u}(p_1, r_1) \gamma_\mu v(p_2, r_2). \quad (\text{E.158b})$$

which can be sum up giving

$$\begin{aligned} i\mathcal{M}_{ff} &= i\mathcal{M}_{Z^0 ff} + i\mathcal{M}_{\gamma ff} \\ &= \frac{g^2}{2s} \bar{v}(k_2, s_2) \gamma^\mu u(k_1, s_1) \bar{u}(p_1, r_1) \gamma_\mu \left(P_L \frac{(1-t_W^2)}{2} - e_q t_W^2 \right) v(p_2, r_2) + \mathcal{O}\left(\frac{m_W^2}{\mu^2}\right). \end{aligned} \quad (\text{E.159})$$

So using the results of the previous section we arrive to the following average square amplitudes

$$\begin{aligned} |\overline{\mathcal{M}_{ff}}|^2 &= \frac{g^4}{4s^2} \left[\frac{(1-t_W^2)^2}{4} + e_q (1-t_W^2) t_W^2 + 2e_q^2 t_W^4 \right] \left[\frac{(u-\mu^2)^2}{2} + \frac{(t-\mu^2)^2}{2} + \mu^2 s \right] + \mathcal{O}\left(\frac{m_W^2}{\mu^2}\right) \\ &= \frac{g^4}{8} \left[\frac{(1-t_W^2)^2}{4} + e_q (1-t_W^2) t_W^2 + 2e_q^2 t_W^4 \right] + \mathcal{O}\left(\frac{m_W^2}{\mu^2}, \epsilon\right). \end{aligned} \quad (\text{E.160})$$

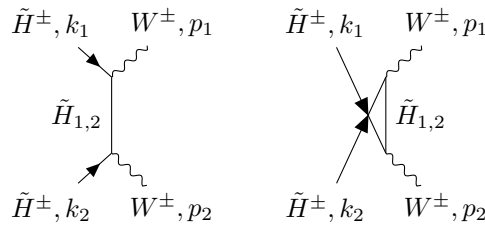
Therefore the total average square amplitude associated with the co-annihilation between two charged Higgsino with opposite charge is equal to

$$\begin{aligned} |\overline{\mathcal{M}_{\tilde{H}^\pm \tilde{H}^\mp}}|^2 &= \sum_f N_c |\overline{\mathcal{M}_{ff}}|^2 + |\overline{\mathcal{M}_{W^\pm W^\mp}}|^2 + |\overline{\mathcal{M}_{Z^0 \gamma}}|^2 + \frac{1}{2} |\overline{\mathcal{M}_{Z^0 Z^0}}|^2 + \frac{1}{2} |\overline{\mathcal{M}_{\gamma \gamma}}|^2 \\ &= \frac{g^4}{4} \left[\frac{29}{4} + t_W^2 + 11t_W^4 \right] + \mathcal{O}\left(\frac{m_W^2}{\mu^2}, \epsilon\right), \end{aligned} \quad (\text{E.161})$$

which substituted into Eq. (E.14) gives the total cross-section times velocity, that is

$$\sigma_{\tilde{H}^\pm \tilde{H}^\mp} v = \frac{g^4}{128\pi\mu^2} \left[\frac{29}{4} + t_W^2 + 11t_W^4 \right] + \mathcal{O}\left(\frac{m_W^2}{\mu^2}, \epsilon\right). \quad (\text{E.162})$$

The last co-annihilation process which we take into account is the annihilation between two charged Higgsinos with the same charge, namely \tilde{H}^\pm and \tilde{H}^\pm . This process can occur only exchanging a neutral Higgsino, in t/u -channel, into two charged vector bosons, W^\pm . The Feynman diagrams are



with associated amplitudes given by

$$\begin{aligned} i\mathcal{M}_t &= \frac{g^2}{2(t-\mu^2)} [2\bar{v}(k_2, s_2) \gamma^\nu u(k_1, s_1) \epsilon_\nu(p_2) (q \cdot \epsilon_\mu(p_1)) \\ &\quad + \bar{v}(k_2, s_2) \gamma^\nu \gamma^\mu \not{p}_1 u(k_1, s_1) \epsilon_\nu(p_2) \epsilon_\mu(p_1)], \end{aligned} \quad (\text{E.163a})$$

$$\begin{aligned} i\mathcal{M}_u &= -\frac{g^2}{2(u-\mu^2)} [2\bar{v}(k_1, s_1) \gamma^\nu u(k_2, s_2) \epsilon_\nu(p_2) (q' \cdot \epsilon_\mu(p_1)) \\ &\quad + \bar{v}(k_1, s_1) \gamma^\nu \gamma^\mu \not{p}_1 u(k_2, s_2) \epsilon_\nu(p_2) \epsilon_\mu(p_1)]. \end{aligned} \quad (\text{E.163b})$$

where we used the fact that \tilde{H}_1 and \tilde{H}_2 have the same mass, which allow us to sum the amplitude for the process mediated by \tilde{H}_1 with the one mediated by \tilde{H}_2 . Now using the result given in

Eqs. (E.118) we have that on transverse polarizations the total square amplitude is

$$\begin{aligned}
|\overline{\mathcal{M}_{W^\pm W^\mp}}|^2 &= \sum_{(\pm\pm)} |\overline{\mathcal{M}_t}|^2 + |\overline{\mathcal{M}_u}|^2 + 2 \operatorname{Re} [\overline{\mathcal{M}_t \mathcal{M}_u^\dagger}] \\
&= \frac{g^4}{2} \left[\frac{u - \mu^2}{t - \mu^2} + \frac{t - \mu^2}{u - \mu^2} \right] + \mathcal{O} \left(\frac{m_W^2}{\mu^2}, \epsilon \right) \\
&= g^4 + \mathcal{O} \left(\frac{m_W^2}{\mu^2}, \epsilon \right)
\end{aligned} \tag{E.164}$$

Note that also here the longitudinal polarization do not contribute in the limit $\mu \gg m_W$. Thus substituting the result just found into Eq. (E.14), and remembering to take into account the symmetry factor of 1/2 because the final particles are identical, we have that the total cross-section times velocity is

$$\sigma_{\tilde{H}^\pm \tilde{H}^\pm v} = \frac{g^4}{64\pi\mu^2} + \mathcal{O} \left(\frac{m_W^2}{\mu^2}, \epsilon \right). \tag{E.165}$$

Summarizing we have that the total cross-sections times velocity at the leading order, relevant for the computation of the relic density of a Higgsino LSP are

$$\sigma_{\tilde{H}_{1,2} \tilde{H}_{1,2} v} = \frac{g^4}{128\pi\mu^2} \left[\frac{3}{2} + t_W^2 + \frac{t_W^4}{2} \right] + \mathcal{O} \left(\frac{m_W^2}{\mu^2}, \epsilon \right) \tag{E.166a}$$

$$\sigma_{\tilde{H}_1 \tilde{H}_2 v} = \frac{g^4}{128\pi\mu^2} \left[\frac{29}{4} + \frac{21}{2} t_W^4 \right] + \mathcal{O} \left(\frac{m_W^2}{\mu^2}, \epsilon \right) \tag{E.166b}$$

$$\sigma_{\tilde{H}_{1,2} \tilde{H}^\pm v} = \frac{g^4}{128\pi\mu^2} (6 + t_W^2) + \mathcal{O} \left(\frac{m_W^2}{\mu^2}, \epsilon \right) \tag{E.166c}$$

$$\sigma_{\tilde{H}^\pm \tilde{H}^\mp v} = \frac{g^4}{128\pi\mu^2} \left[\frac{29}{4} + t_W^2 + 11t_W^4 \right] + \mathcal{O} \left(\frac{m_W^2}{\mu^2}, \epsilon \right) \tag{E.166d}$$

$$\sigma_{\tilde{H}^\pm \tilde{H}^\pm v} = \frac{g^4}{64\pi\mu^2} + \mathcal{O} \left(\frac{m_W^2}{\mu^2}, \epsilon \right). \tag{E.166e}$$

Bibliography

- [1] Milton Abramowitz, Irene A Stegun, et al. *Handbook of mathematical functions*. Vol. 1046. Dover New York, 1965.
- [2] A. Abramowski et al. “Search for Photon-Linelike Signatures from Dark Matter Anihilations with H.E.S.S.” In: *Phys. Rev. Lett.* 110 (2013), p. 041301. DOI: [10.1103/PhysRevLett.110.041301](https://doi.org/10.1103/PhysRevLett.110.041301). arXiv: [1301.1173](https://arxiv.org/abs/1301.1173) [[astro-ph.HE](#)].
- [3] P. A. R. Ade et al. “Planck 2015 results. XIII. Cosmological parameters”. In: *Astron. Astrophys.* 594 (2016), A13. DOI: [10.1051/0004-6361/201525830](https://doi.org/10.1051/0004-6361/201525830). arXiv: [1502.01589](https://arxiv.org/abs/1502.01589) [[astro-ph.CO](#)].
- [4] N. Aghanim et al. “Planck 2015 results. XI. CMB power spectra, likelihoods, and robustness of parameters”. In: *Astron. Astrophys.* 594 (2016), A11. DOI: [10.1051/0004-6361/201526926](https://doi.org/10.1051/0004-6361/201526926). arXiv: [1507.02704](https://arxiv.org/abs/1507.02704) [[astro-ph.CO](#)].
- [5] I. J. R. Aitchison. *Supersymmetry in Particle Physics. An Elementary Introduction*. 2007. URL: <http://www-public.slac.stanford.edu/sciDoc/docMeta.aspx?slacPubNumber=slac-r-865>.
- [6] D. S. Akerib et al. “Results from a search for dark matter in the complete LUX exposure”. In: (2016). arXiv: [1608.07648](https://arxiv.org/abs/1608.07648) [[astro-ph.CO](#)].
- [7] D. S. Akerib et al. “Results on the Spin-Dependent Scattering of Weakly Interacting Massive Particles on Nucleons from the Run 3 Data of the LUX Experiment”. In: *Phys. Rev. Lett.* 116.16 (2016), p. 161302. DOI: [10.1103/PhysRevLett.116.161302](https://doi.org/10.1103/PhysRevLett.116.161302). arXiv: [1602.03489](https://arxiv.org/abs/1602.03489) [[hep-ex](#)].
- [8] C. Amole et al. “Dark matter search results from the PICO-60 CF₃I bubble chamber”. In: *Phys. Rev.* D93.5 (2016), p. 052014. DOI: [10.1103/PhysRevD.93.052014](https://doi.org/10.1103/PhysRevD.93.052014). arXiv: [1510.07754](https://arxiv.org/abs/1510.07754) [[hep-ex](#)].
- [9] Archana Anandakrishnan and Kuver Sinha. “Viability of thermal well-tempered dark matter in SUSY GUTs”. In: *Phys. Rev.* D89.5 (2014), p. 055015. DOI: [10.1103/PhysRevD.89.055015](https://doi.org/10.1103/PhysRevD.89.055015). arXiv: [1310.7579](https://arxiv.org/abs/1310.7579) [[hep-ph](#)].
- [10] E. Aprile et al. “Limits on spin-dependent WIMP-nucleon cross sections from 225 live days of XENON100 data”. In: *Phys. Rev. Lett.* 111.2 (2013), p. 021301. DOI: [10.1103/PhysRevLett.111.021301](https://doi.org/10.1103/PhysRevLett.111.021301). arXiv: [1301.6620](https://arxiv.org/abs/1301.6620) [[astro-ph.CO](#)].
- [11] N. Arkani-Hamed, A. Delgado, and G. F. Giudice. “The Well-tempered neutralino”. In: *Nucl. Phys.* B741 (2006), pp. 108–130. DOI: [10.1016/j.nuclphysb.2006.02.010](https://doi.org/10.1016/j.nuclphysb.2006.02.010). arXiv: [hep-ph/0601041](https://arxiv.org/abs/hep-ph/0601041) [[hep-ph](#)].
- [12] Vernon D. Barger, M. S. Berger, and P. Ohmann. “The Supersymmetric particle spectrum”. In: *Phys. Rev.* D49 (1994), pp. 4908–4930. DOI: [10.1103/PhysRevD.49.4908](https://doi.org/10.1103/PhysRevD.49.4908). arXiv: [hep-ph/9311269](https://arxiv.org/abs/hep-ph/9311269) [[hep-ph](#)].
- [13] Jacob D. Bekenstein. “Relativistic gravitation theory for the MOND paradigm”. In: *Phys. Rev.* D70 (2004). [Erratum: *Phys. Rev.*D71,069901(2005)], p. 083509. DOI: [10.1103/PhysRevD.70.083509](https://doi.org/10.1103/PhysRevD.70.083509), [10.1103/PhysRevD.71.069901](https://doi.org/10.1103/PhysRevD.71.069901). arXiv: [astro-ph/0403694](https://arxiv.org/abs/astro-ph/0403694) [[astro-ph](#)].

- [14] G. Belanger et al. “Dark matter direct detection rate in a generic model with micrOMEGAs 2.2”. In: *Comput. Phys. Commun.* 180 (2009), pp. 747–767. DOI: [10.1016/j.cpc.2008.11.019](https://doi.org/10.1016/j.cpc.2008.11.019). arXiv: [0803.2360](https://arxiv.org/abs/0803.2360) [hep-ph].
- [15] G. Belanger et al. “micrOMEGAs 3.1: A program for calculating dark matter observables”. In: *Comput. Phys. Commun.* 185 (2014), pp. 960–985. DOI: [10.1016/j.cpc.2013.10.016](https://doi.org/10.1016/j.cpc.2013.10.016). arXiv: [1305.0237](https://arxiv.org/abs/1305.0237) [hep-ph].
- [16] Lars Bergstrom, Piero Ullio, and James H. Buckley. “Observability of gamma-rays from dark matter neutralino annihilations in the Milky Way halo”. In: *Astropart. Phys.* 9 (1998), pp. 137–162. DOI: [10.1016/S0927-6505\(98\)00015-2](https://doi.org/10.1016/S0927-6505(98)00015-2). arXiv: [astro-ph/9712318](https://arxiv.org/abs/astro-ph/9712318) [astro-ph].
- [17] Zvi Bern, Paolo Gondolo, and Maxim Perelstein. “Neutralino annihilation into two photons”. In: *Phys. Lett.* B411 (1997), pp. 86–96. DOI: [10.1016/S0370-2693\(97\)00990-8](https://doi.org/10.1016/S0370-2693(97)00990-8). arXiv: [hep-ph/9706538](https://arxiv.org/abs/hep-ph/9706538) [hep-ph].
- [18] Gianfranco Bertone and Dan Hooper. “A History of Dark Matter”. In: *Submitted to: Rev. Mod. Phys.* (2016). arXiv: [1605.04909](https://arxiv.org/abs/1605.04909) [astro-ph.CO].
- [19] Gianfranco Bertone, Dan Hooper, and Joseph Silk. “Particle dark matter: Evidence, candidates and constraints”. In: *Phys. Rept.* 405 (2005), pp. 279–390. DOI: [10.1016/j.physrep.2004.08.031](https://doi.org/10.1016/j.physrep.2004.08.031). arXiv: [hep-ph/0404175](https://arxiv.org/abs/hep-ph/0404175) [hep-ph].
- [20] W. J. G. de Blok et al. “Mass density profiles of LSB galaxies”. In: *Astrophys. J.* 552 (2001), pp. L23–L26. DOI: [10.1086/320262](https://doi.org/10.1086/320262). arXiv: [astro-ph/0103102](https://arxiv.org/abs/astro-ph/0103102) [astro-ph].
- [21] G. Bélanger et al. “micrOMEGAs4.1: two dark matter candidates”. In: *Comput. Phys. Commun.* 192 (2015), pp. 322–329. DOI: [10.1016/j.cpc.2015.03.003](https://doi.org/10.1016/j.cpc.2015.03.003). arXiv: [1407.6129](https://arxiv.org/abs/1407.6129) [hep-ph].
- [22] J. Alberto Casas et al. “What is a Natural SUSY scenario?” In: *JHEP* 06 (2015), p. 070. DOI: [10.1007/JHEP06\(2015\)070](https://doi.org/10.1007/JHEP06(2015)070). arXiv: [1407.6966](https://arxiv.org/abs/1407.6966) [hep-ph].
- [23] David G. Cerdeno and Anne M. Green. “Direct detection of WIMPs”. In: (2010). arXiv: [1002.1912](https://arxiv.org/abs/1002.1912) [astro-ph.CO].
- [24] Hai-Yang Cheng and Cheng-Wei Chiang. “Revisiting Scalar and Pseudoscalar Couplings with Nucleons”. In: *JHEP* 07 (2012), p. 009. DOI: [10.1007/JHEP07\(2012\)009](https://doi.org/10.1007/JHEP07(2012)009). arXiv: [1202.1292](https://arxiv.org/abs/1202.1292) [hep-ph].
- [25] Clifford Cheung et al. “Prospects and Blind Spots for Neutralino Dark Matter”. In: *JHEP* 05 (2013), p. 100. DOI: [10.1007/JHEP05\(2013\)100](https://doi.org/10.1007/JHEP05(2013)100). arXiv: [1211.4873](https://arxiv.org/abs/1211.4873) [hep-ph].
- [26] D. J. H. Chung et al. “The Soft supersymmetry breaking Lagrangian: Theory and applications”. In: *Phys. Rept.* 407 (2005), pp. 1–203. DOI: [10.1016/j.physrep.2004.08.032](https://doi.org/10.1016/j.physrep.2004.08.032). arXiv: [hep-ph/0312378](https://arxiv.org/abs/hep-ph/0312378) [hep-ph].
- [27] Marco Cirelli, Eugenio Del Nobile, and Paolo Panci. “Tools for model-independent bounds in direct dark matter searches”. In: *JCAP* 1310 (2013), p. 019. DOI: [10.1088/1475-7516/2013/10/019](https://doi.org/10.1088/1475-7516/2013/10/019). arXiv: [1307.5955](https://arxiv.org/abs/1307.5955) [hep-ph].
- [28] Sidney R. Coleman and J. Mandula. “All Possible Symmetries of the S Matrix”. In: *Phys. Rev.* 159 (1967), pp. 1251–1256. DOI: [10.1103/PhysRev.159.1251](https://doi.org/10.1103/PhysRev.159.1251).
- [29] P. Coles and F. Lucchin. *Cosmology: The Origin and evolution of cosmic structure*. 1995.
- [30] Ansgar Denner et al. “Feynman rules for fermion number violating interactions”. In: *Nucl. Phys.* B387 (1992), pp. 467–481. DOI: [10.1016/0550-3213\(92\)90169-C](https://doi.org/10.1016/0550-3213(92)90169-C).
- [31] Scott Dodelson. *Modern Cosmology*. Amsterdam: Academic Press, 2003. ISBN: 9780122191411. URL: <http://www.slac.stanford.edu/spires/find/books/www?cl=QB981:D62:2003>.
- [32] Manuel Drees and Mihoko Nojiri. “Neutralino - nucleon scattering revisited”. In: *Phys. Rev.* D48 (1993), pp. 3483–3501. DOI: [10.1103/PhysRevD.48.3483](https://doi.org/10.1103/PhysRevD.48.3483). arXiv: [hep-ph/9307208](https://arxiv.org/abs/hep-ph/9307208) [hep-ph].

- [33] Joakim Edsjo and Paolo Gondolo. “Neutralino relic density including coannihilations”. In: *Phys. Rev. D* 56 (1997), pp. 1879–1894. DOI: [10.1103/PhysRevD.56.1879](https://doi.org/10.1103/PhysRevD.56.1879). arXiv: [hep-ph/9704361](https://arxiv.org/abs/hep-ph/9704361) [hep-ph].
- [34] John R. Ellis, Andrew Ferstl, and Keith A. Olive. “Reevaluation of the elastic scattering of supersymmetric dark matter”. In: *Phys. Lett. B* 481 (2000), pp. 304–314. DOI: [10.1016/S0370-2693\(00\)00459-7](https://doi.org/10.1016/S0370-2693(00)00459-7). arXiv: [hep-ph/0001005](https://arxiv.org/abs/hep-ph/0001005) [hep-ph].
- [35] John R. Ellis, Keith A. Olive, and Christopher Savage. “Hadronic Uncertainties in the Elastic Scattering of Supersymmetric Dark Matter”. In: *Phys. Rev. D* 77 (2008), p. 065026. DOI: [10.1103/PhysRevD.77.065026](https://doi.org/10.1103/PhysRevD.77.065026). arXiv: [0801.3656](https://arxiv.org/abs/0801.3656) [hep-ph].
- [36] John R. Ellis et al. “Calculations of neutralino-stau coannihilation channels and the cosmologically relevant region of MSSM parameter space”. In: *Astropart. Phys.* 13 (2000). [Erratum: *Astropart. Phys.* 15,413(2001)], pp. 181–213. DOI: [10.1016/S0927-6505\(99\)00104-8](https://doi.org/10.1016/S0927-6505(99)00104-8). arXiv: [hep-ph/9905481](https://arxiv.org/abs/hep-ph/9905481) [hep-ph].
- [37] John R. Ellis et al. “Supersymmetric Relics from the Big Bang”. In: *Nucl. Phys. B* 238 (1984), pp. 453–476. DOI: [10.1016/0550-3213\(84\)90461-9](https://doi.org/10.1016/0550-3213(84)90461-9).
- [38] Benoit Famaey and Stacy McGaugh. “Modified Newtonian Dynamics (MOND): Observational Phenomenology and Relativistic Extensions”. In: *Living Rev. Rel.* 15 (2012), p. 10. DOI: [10.12942/lrr-2012-10](https://doi.org/10.12942/lrr-2012-10). arXiv: [1112.3960](https://arxiv.org/abs/1112.3960) [astro-ph.CO].
- [39] JiJi Fan and Matthew Reece. “In Wino Veritas? Indirect Searches Shed Light on Neutralino Dark Matter”. In: *JHEP* 10 (2013), p. 124. DOI: [10.1007/JHEP10\(2013\)124](https://doi.org/10.1007/JHEP10(2013)124). arXiv: [1307.4400](https://arxiv.org/abs/1307.4400) [hep-ph].
- [40] Jonathan L. Feng. “Dark Matter Candidates from Particle Physics and Methods of Detection”. In: *Ann. Rev. Astron. Astrophys.* 48 (2010), pp. 495–545. DOI: [10.1146/annurev-astro-082708-101659](https://doi.org/10.1146/annurev-astro-082708-101659). arXiv: [1003.0904](https://arxiv.org/abs/1003.0904) [astro-ph.CO].
- [41] Katherine Freese. “Review of Observational Evidence for Dark Matter in the Universe and in upcoming searches for Dark Stars”. In: *EAS Publ. Ser.* 36 (2009), pp. 113–126. DOI: [10.1051/eas/0936016](https://doi.org/10.1051/eas/0936016). arXiv: [0812.4005](https://arxiv.org/abs/0812.4005) [astro-ph].
- [42] Graciela B. Gelmini. “TASI 2014 Lectures: The Hunt for Dark Matter”. In: *Theoretical Advanced Study Institute in Elementary Particle Physics: Journeys Through the Precision Frontier: Amplitudes for Colliders (TASI 2014) Boulder, Colorado, June 2-27, 2014*. 2015. arXiv: [1502.01320](https://arxiv.org/abs/1502.01320) [hep-ph]. URL: <https://inspirehep.net/record/1342951/files/arXiv:1502.01320.pdf>.
- [43] Paolo Gondolo and Graciela Gelmini. “Cosmic abundances of stable particles: Improved analysis”. In: *Nucl. Phys. B* 360 (1991), pp. 145–179. DOI: [10.1016/0550-3213\(91\)90438-4](https://doi.org/10.1016/0550-3213(91)90438-4).
- [44] Paul Gorenstein and Wallace Tucker. “Astronomical Signatures of Dark Matter”. In: *Adv. High Energy Phys.* 2014 (2014), p. 878203. DOI: [10.1155/2014/878203](https://doi.org/10.1155/2014/878203).
- [45] Kim Griest and David Seckel. “Three exceptions in the calculation of relic abundances”. In: *Phys. Rev. D* 43 (1991), pp. 3191–3203. DOI: [10.1103/PhysRevD.43.3191](https://doi.org/10.1103/PhysRevD.43.3191).
- [46] Rudolf Haag, Jan T. Lopuszanski, and Martin Sohnius. “All Possible Generators of Supersymmetries of the s Matrix”. In: *Nucl. Phys. B* 88 (1975), p. 257. DOI: [10.1016/0550-3213\(75\)90279-5](https://doi.org/10.1016/0550-3213(75)90279-5).
- [47] Howard E. Haber. “Introductory low-energy supersymmetry”. In: *Theoretical Advanced Study Institute (TASI 92): From Black Holes and Strings to Particles Boulder, Colorado, June 3-28, 1992*. 1993. arXiv: [hep-ph/9306207](https://arxiv.org/abs/hep-ph/9306207) [hep-ph].
- [48] Howard E. Haber and Gordon L. Kane. “The Search for Supersymmetry: Probing Physics Beyond the Standard Model”. In: *Phys. Rept.* 117 (1985), pp. 75–263. DOI: [10.1016/0370-1573\(85\)90051-1](https://doi.org/10.1016/0370-1573(85)90051-1).
- [49] Gerard Jungman, Marc Kamionkowski, and Kim Griest. “Supersymmetric dark matter”. In: *Phys. Rept.* 267 (1996), pp. 195–373. DOI: [10.1016/0370-1573\(95\)00058-5](https://doi.org/10.1016/0370-1573(95)00058-5). arXiv: [hep-ph/9506380](https://arxiv.org/abs/hep-ph/9506380) [hep-ph].

- [50] S. F. King and J. P. Roberts. “Natural implementation of neutralino dark matter”. In: *JHEP* 09 (2006), p. 036. DOI: [10.1088/1126-6708/2006/09/036](https://doi.org/10.1088/1126-6708/2006/09/036). arXiv: [hep-ph/0603095](https://arxiv.org/abs/hep-ph/0603095) [[hep-ph](#)].
- [51] Edward W. Kolb and Michael S. Turner, eds. *THE EARLY UNIVERSE. REPRINTS*. 1988.
- [52] DELPHI L3 LEP2 SUSY Working Group ALEPH and note LEPSUSYWG/02-04.1 OPAL experiments. In: (2004). URL: <http://lepsusy.web.cern.ch/lepsusy>.
- [53] J. D. Lewin and P. F. Smith. “Review of mathematics, numerical factors, and corrections for dark matter experiments based on elastic nuclear recoil”. In: *Astropart. Phys.* 6 (1996), pp. 87–112. DOI: [10.1016/S0927-6505\(96\)00047-3](https://doi.org/10.1016/S0927-6505(96)00047-3).
- [54] Stephen P. Martin. “A Supersymmetry primer”. In: (1997). [Adv. Ser. Direct. High Energy Phys.18,1(1998)]. DOI: [10.1142/9789812839657_0001](https://doi.org/10.1142/9789812839657_0001), [10.1142/9789814307505_0001](https://doi.org/10.1142/9789814307505_0001). arXiv: [hep-ph/9709356](https://arxiv.org/abs/hep-ph/9709356) [[hep-ph](#)].
- [55] John McDonald. “Generation of WIMP Miracle-like Densities of Baryons and Dark Matter”. In: (2012). arXiv: [1201.3124](https://arxiv.org/abs/1201.3124) [[hep-ph](#)].
- [56] Satoshi Mizuta and Masahiro Yamaguchi. “Coannihilation effects and relic abundance of Higgsino dominant LSP(s)”. In: *Phys. Lett.* B298 (1993), pp. 120–126. DOI: [10.1016/0370-2693\(93\)91717-2](https://doi.org/10.1016/0370-2693(93)91717-2). arXiv: [hep-ph/9208251](https://arxiv.org/abs/hep-ph/9208251) [[hep-ph](#)].
- [57] Carlos Munoz. “Dark matter detection in the light of recent experimental results”. In: *Int. J. Mod. Phys.* A19 (2004), pp. 3093–3170. DOI: [10.1142/S0217751X04018154](https://doi.org/10.1142/S0217751X04018154). arXiv: [hep-ph/0309346](https://arxiv.org/abs/hep-ph/0309346) [[hep-ph](#)].
- [58] Hitoshi Murayama. “Supersymmetry phenomenology”. In: *Particle physics. Proceedings, Summer School, Trieste, Italy, June 21-July 9, 1999*. 2000, pp. 296–335. arXiv: [hep-ph/0002232](https://arxiv.org/abs/hep-ph/0002232) [[hep-ph](#)]. URL: <http://alice.cern.ch/format/showfull?sysnb=2177492>.
- [59] Yorikiyo Nagashima. *Elementary particle physics: Foundations of the standard model, volume 2*. Weinheim: Wiley-VCH, 2010. ISBN: 9783527409662. URL: <http://www-spires.fnal.gov/spires/find/books/www?cl=QC174.45.N29::2010>.
- [60] K. A. Olive et al. “Review of Particle Physics”. In: *Chin. Phys.* C38 (2014), p. 090001. DOI: [10.1088/1674-1137/38/9/090001](https://doi.org/10.1088/1674-1137/38/9/090001).
- [61] Michael E. Peskin and Daniel V. Schroeder. *An Introduction to quantum field theory*. 1995. ISBN: 9780201503975, 0201503972. URL: <http://www.slac.stanford.edu/spires/find/books/www?cl=QC174.45%3AP4>.
- [62] Stefano Profumo. “Astrophysical Probes of Dark Matter”. In: *Proceedings, Theoretical Advanced Study Institute in Elementary Particle Physics: Searching for New Physics at Small and Large Scales (TASI 2012): Boulder, Colorado, June 4-29, 2012*. 2013, pp. 143–189. DOI: [10.1142/9789814525220_0004](https://doi.org/10.1142/9789814525220_0004). arXiv: [1301.0952](https://arxiv.org/abs/1301.0952) [[hep-ph](#)]. URL: <https://inspirehep.net/record/1209480/files/arXiv:1301.0952.pdf>.
- [63] Janusz Rosiek. “Complete set of Feynman rules for the MSSM: Erratum”. In: (1995). arXiv: [hep-ph/9511250](https://arxiv.org/abs/hep-ph/9511250) [[hep-ph](#)].
- [64] Andi Tan et al. “Dark Matter Results from First 98.7-day Data of PandaX-II Experiment”. In: *Phys. Rev. Lett.* 117.12 (2016), p. 121303. DOI: [10.1103/PhysRevLett.117.121303](https://doi.org/10.1103/PhysRevLett.117.121303). arXiv: [1607.07400](https://arxiv.org/abs/1607.07400) [[hep-ex](#)].
- [65] F. Zwicky. “On the Masses of Nebulae and of Clusters of Nebulae”. In: *Astrophys. J.* 86 (1937), pp. 217–246. DOI: [10.1086/143864](https://doi.org/10.1086/143864).